THE UNIVERSITY
of EDINBURGH

An investigation of inflammatory and oxidative stress mechanisms in the disruption of white matter structure and function following chronic cerebral hypoperfusion

Emma Sigfridsson BSc (Hons)

Doctor of Philosophy
The University of Edinburgh
2019

Table of contents

Declaration ..... **ix**
Acknowledgements ..... **xi**
Abstract ..... **xiii**
Lay Summary ..... **xvii**
List of Figures ..... **xix**
List of Tables ..... **xx**
List of Abbreviations ..... **xxi**

Chapter 1 ..... **1**
Introduction **1**
1.1 Overview **2**
1.2 Importance of the cerebrovascular system **3**
1.3 Vascular cognitive impairment **5**
1.3.1 Vascular risk factors and underlying cerebrovascular causes of VCI 6
1.3.2 Clinical manifestations and diagnostic criteria for VCI 6
1.3.3 Vascular contributions to Alzheimer's dementia 8
1.4 White matter structure and function **8**
1.4.1 Cellular components of white matter 9
1.5 White matter vulnerability in VCI **11**
1.5.1 Chronic cerebral hypoperfusion drives white matter disruption in VCI 11
1.6 Cerebral hypoperfusion models of VCI **13**
1.6.1 Bilateral carotid artery stenosis in mice 13
1.6.2 Alternative models of chronic cerebral hypoperfusion 15
1.7 Inflammation and Oxidative stress **15**
1.7.1 Inflammation 15
1.7.2 Oxidative stress 16
1.7.3 Inflammation and oxidative stress in human VCI 17
1.7.4 Inflammation and oxidative stress in the BCAS model of cerebral hypoperfusion 18
1.8 Targeting inflammatory and oxidative stress mechanisms **19**
1.8.1 Nuclear factor erythroid 2-related factor 2 (Nrf2) 20
1.8.2 Colony-stimulating factor receptor 1 24
1.9 Summary **25**
1.10 Hypothesis **26**
1.11 Aims **26**

Chapter 2 ..... **27**
Materials & Methods **27**
2.1 Animals **28**
2.1.1 Nrf2 knock out mice 28
2.1.2 GFAP-Nrf2.2 mice 29
2.1.3 C57Bl/6J wild type mice 30

2.2 Chronic cerebral hypoperfusion 31
2.3 Laser speckle imaging 32
2.3.1 Laser speckle image analysis 32
2.4 Behavioural testing 32
2.4.1 Radial arm maze 32
2.4.2 Y-maze 33
2.4.3 Barnes maze 34
2.5 Substance administration 37
2.5.1 GW2580 administration 37
2.5.2 5-Bromo-2'-deoxyuridine (BrdU) administration 37
2.6 Tissue collection and processing 37
2.6.1 Transcardial perfusion and brain extraction 37
2.6.2 Brain extraction and white matter dissection 37
2.6.3 Processing for freezing and cryosectioning 38
2.6.4 Automated processing for paraffin embedding 38
2.6.5 Manual processing for paraffin embedding 39
2.6.6 Microtome sectioning 39
2.7 Histology and immunostaining 39
2.7.1 Immunohistochemistry using DAB 39
2.7.2 Immunofluorescent labelling 40
2.7.3 Immunostaining controls 40
2.8 Image acquisition and analysis 42
2.8.1 Image acquisition 42
2.8.2 Image analysis 42
2.8.3 Exclusion criteria 42
2.9 Transcriptomics 43
2.9.1 RNA extraction 43
2.9.2 Reverse transcription (RT)-PCR 44
2.9.3 Quantitative (q)-PCR 44
2.9.4 Exclusion criteria 44
2.10 Statistical analysis 46
2.10.1 Repeated measures ANOVA 46
2.10.2 Two-way ANOVA 46
2.10.3 One-way ANOVA 46
2.10.4 One-sample t-test 46
2.10.5 Pearson's correlation 46
2.10.6 Kruskal-Wallis H test (Non-parametric) 47
2.10.7 Spearman's correlation (Non-parametric) 47

Chapter 3 ..... **49**
Investigating the effect of chronic cerebral hypoperfusion in a mouse model with reduced expression of Nrf2 ..... **49**
3.1 Introduction **50**
3.1.1 Hypothesis 51
3.1.2 Aims 51
3.2 Materials and Methods **52**
3.2.1 Experimental contributions 52
3.2.2 Mice 52
3.2.3 Chronic cerebral hypoperfusion 52
3.2.4 Laser speckle imaging to measure cortical cerebral blood flow 52
3.2.5 Behavioural testing 53
3.2.6 Tissue collection and processing 53
3.2.7 Immunohistochemistry 53
3.2.8 Image analysis 53
3.2.9 Transcriptomics 53
3.2.10 Statistical analysis 54
3.3 Results **56**
3.3.1 Cortical CBF is significantly reduced post-BCAS 56
3.3.2 White matter disruption is more extensive in $Nrf2^{-/-}$ mice compared to wild type and $Nrf2^{+/-}$ post-BCAS 58
3.3.3 The density of microglia is increased post-BCAS to a greater extent in $Nrf2^{-/-}$ mice compared to wild type and $Nrf2^{+/-}$ 60
3.3.4 Astrogliosis in the optic tract is induced to a similar extent in wild type and Nrf2 KO mice post-BCAS 62
3.3.5 *Nrf2* and Nrf2-regulated antioxidant genes are unaltered post-BCAS but pro-inflammatory gene expression is induced 64
3.3.6 Spatial working memory is impaired post-BCAS but is not exacerbated by deficiency of Nrf2 66
3.4 Discussion **69**
3.4.1 Resting cortical CBF is significantly reduced post-BCAS to a similar extent in wild type and $Nrf2^{+/-}$ mice 69
3.4.2 White matter disruption is more severe in $Nrf2^{-/-}$ compared to wild type and $Nrf2^{+/-}$ mice in response to cerebral hypoperfusion 70
3.4.3 Increased microglial density in response to cerebral hypoperfusion is exacerbated in $Nrf2^{-/-}$ compared to wild type and $Nrf2^{+/-}$ mice 72
3.4.4 Cerebral hypoperfusion induces astrogliosis to a similar extent in wild type and Nrf2 KO mice in the optic tract 73
3.4.5 Cerebral hypoperfusion does not affect *Nrf2* or Nrf2-regulated antioxidant gene expression but increases the expression of pro-inflammatory genes 75
3.4.6 Cerebral hypoperfusion causes a subtle impairment in spatial working memory in mice which is not exacerbated by absent or reduced expression of Nrf2 77
3.4.7 Potential mechanisms of white matter disruption 78
3.4.8 Limitations, conclusion and future directions 80

Chapter 4 ..... **83**
Investigating the effect of chronic cerebral hypoperfusion in a mouse model with increased expression of Nrf2 in astrocytes **83**
4.1 Introduction **84**
4.1.1 Hypothesis 85
4.1.2 Aims 85
4.2 Materials and Methods **86**
4.2.1 Experimental contribution 86
4.2.2 Mice 86
4.2.3 Chronic cerebral hypoperfusion 86
4.2.4 Laser speckle imaging to measure cortical cerebral blood flow 86
4.2.5 Behavioural testing 86
4.2.6 Tissue collection and processing 87
4.2.7 Immunohistochemistry 87
4.2.8 Image analysis 87
4.2.9 Transcriptomics 87
4.2.10 Statistical analysis 87
4.3 Results **90**
4.3.1 Cortical cerebral blood flow is significantly reduced post-BCAS 90
4.3.2 Spatial working memory is impaired post-BCAS but is less pronounced in GFAP-Nrf2 mice compared to wild type 91
4.3.3 White matter disruption in the optic tract is less extensive in GFAP-Nrf2 mice compared to wild type post-BCAS 94
4.3.4 The density of microglia is increased post-BCAS in the optic tract 96
4.3.5 Astrogliosis in the optic tract is less in GFAP-Nrf2 mice compared to wild type post-BCAS 98
4.3.6 Pro-inflammatory genes are induced post-BCAS in the optic tract and the level of complement component 4 is reduced in GFAP-Nrf2 mice compared to wild type 100
4.4 Discussion **103**
4.4.1 Resting cortical cerebral blood flow is significantly reduced following bilateral carotid artery stenosis to a similar extent in wild type and GFAP-Nrf2 mice 103
4.4.2 Cerebral hypoperfusion causes an impairment in spatial working memory which is ameliorated in GFAP-Nrf2 mice 103
4.4.3 White matter disruption in the optic tract is less severe in GFAP-Nrf2 compared to wild type mice in response to cerebral hypoperfusion 104
4.4.4 Microglial and astrocyte density is increased in the optic tract in response to cerebral hypoperfusion but only astrogliosis is less severe in GFAP-Nrf2 mice 106
4.4.5 Cerebral hypoperfusion induces pro-inflammatory gene expression in the optic tract and complement component 4 is downregulated in GFAP-Nrf2 mice 107
4.4.6 Alternative mechanisms of Nrf2 pathway activation 109
4.4.7 Limitations, conclusion and future directions 111

Chapter 5 ..... **113**
Investigating the effect of inhibiting microglial proliferation in a mouse model of chronic cerebral hypoperfusion **113**
5.1 Introduction **114**
5.1.1 Hypothesis 115
5.1.2 Aims 115
5.2 Materials and Methods **116**
5.2.1 Experimental contributions 116
5.2.2 Mice 116
5.2.3 Chronic cerebral hypoperfusion 116
5.2.4 Laser speckle imaging to measure cortical cerebral blood flow 116
5.2.5 Study inclusion criteria and group assignment 117
5.2.6 GW2580 administration 117
5.2.7 5-Bromo-2'-deoxyuridine (BrdU) administration 117
5.2.8 Behavioural testing 117
5.2.9 Tissue collection and processing 117
5.2.10 Immunohistochemistry 117
5.2.11 Image analysis 117
5.2.12 Transcriptomics 118
5.2.13 Statistical analysis 118
5.3 Results **120**
5.3.1 GW2580-treatment dampens white matter microglial proliferation and pro-inflammatory signalling one week post-BCAS 120
5.3.2 Resting cortical cerebral blood flow is chronically reduced following bilateral carotid artery stenosis to a similar extent in GW2580- and vehicle-treated animals. 123
5.3.3 GW2580-treatment prevents increases in white matter microglia 6 weeks post-BCAS 125
5.3.4 GW2580-treatment inhibits white matter astrogliosis 6 weeks post-BCAS ... 127
5.3.5 GW2580-treatment protects against white matter disruption 6 weeks post-BCAS 129
5.3.6 GW2580-treatment protects against chronic hypoperfusion-induced impairment in spatial learning 131
5.4 Discussion **133**
5.4.1 Resting cortical cerebral blood flow is acutely and chronically reduced following bilateral carotid artery stenosis to a similar extent in GW2580- and vehicle-treated animals 133
5.4.2 GW2580-treatment dampens microglial proliferation and pro-inflammatory signalling one week following bilateral carotid artery stenosis 133
5.4.3 GW2580-treatment prevents chronic hypoperfusion-induced increases in white matter microglia 134
5.4.4 GW2580-treatment inhibits chronic hypoperfusion-induced white matter astrogliosis 136
5.4.5 GW2580-treatment protects against chronic hypoperfusion-induced white matter disruption 137

5.4.6 GW2580-treatment protects against chronic hypoperfusion-induced impairment in spatial learning 138
5.4.7 Potential mechanisms 140
5.4.8 Limitations, conclusion and future directions 142

Chapter 6 145
General discussion 145
6.1 Implications for future research 146
6.2 Clinical relevance 149
6.2.1 Considerations for targeting CSF1R signalling in humans 149
References 151
Appendix 175

Declaration

I declare that this thesis has been composed solely by myself and has not been submitted for any previous degree or qualification. The work described within this thesis comprises my own original work except where otherwise stated in the text. All external sources of data and information have been specifically referenced.

The study reported in chapter 4 has been published in the journal Scientific Reports under the title “Astrocyte-specific overexpression of Nrf2 protects against optic tract damage and behavioural alterations in a mouse model of cerebral hypoperfusion” (Sigfridsson et al., 2018, see appendix). The author contributions are outlined in chapter 4 and in the manuscript, however the majority of the work was carried out by me with contributions from Dr Martina Marangoni and Prof Karen Horsburgh, and was under the supervision of Prof Karen Horsburgh and Dr Jill Fowler.

Emma Sigfridsson

Date: 24/07/2019

Signature: 

Acknowledgements

Firstly, I want to thank Prof Karen Horsburgh and Dr Jill Fowler for your guidance and support throughout this process. Your experience and scientific integrity was an essential influence in the development of this work and in my own development. Thanks also to the Alzheimer's Society and the RS McDonald Trust for funding this project as part of the Doctoral Training Centre Scotland "Metabolic and Vascular contributors to dementia".

Next I want to thank everybody in the Horsburgh lab who made this journey what it was. Dr Martina Marangoni who was right next to me from the start supporting me until I was confident in myself. Dr Jessica Duncombe, a stable presence with the ability to both challenge and support, with whom I could share both good times and bad, and whom I could always rely on. Thank you both for being amazing role models, teachers and also wonderful friends. I want to thank Joshua Beverley for working alongside me up in the animal unit for hours on end, for always sharing the load and for the assorted topics of conversation that sped up time considerably. I would also like to thank Dr Juraj Koudelka for support in the lab and for providing continuous laughter by absolutely terrible dad jokes. Thanks to Mosi Li, Margaux Aimable and Jemma Pilcher for journeying beside me, I know we didn't always think we would but we made it! There is no way we could have done it without support from the animal unit staff, I especially want to thank Duncan, Keith and Jon, who were always at hand despite their busy schedules.

I also want to thank my family, Mum, Dad, Helena and Lars, Frida and Moa. Trying to explain my research to you in lay terms in Swedish was always a fun challenge. Lars, it still breaks my heart that you aren't here to see me complete this journey. Your perspective on life and your ability to ask just the right question was incredible and I hope to live my life with the same drive and positive attitude that you possessed. Judith and Elis, thank you for your hospitality, your company, for walks along the coast of the East Neuk of Fife and for being my family away from home.

Last but far from least I want to thank Steve. I want to dedicate this work to you. Without your support, your company and your friendship I would not be where I am today. Thank you for always listening and always believing in me even when I didn't. With love, always.

Abstract

Vascular cognitive impairment (VCI) describes a heterogeneous condition caused by cerebrovascular disease and disturbances in cerebral blood flow delivery. It is the second leading form of dementia and vascular factors such as hypertension, diabetes and obesity are associated with an increased risk of developing VCI. White matter alterations are a prominent pathological feature observed in patients with VCI thought to underlie cognitive impairment. Neuroimaging studies show a positive correlation between the burden of white matter alterations and progressive cognitive impairment. Similarly associated both with white matter alterations and cognitive impairment is chronic cerebral hypoperfusion, sustained subtle reductions in cerebral blood flow. Cerebral hypoperfusion is observed before the onset of cognitive decline in humans and reducing cerebral blood flow in animal models replicates important aspects of VCI, suggesting hypoperfusion is an early driver of white matter disruption and VCI. Human neuropathology and preclinical animal models of chronic cerebral hypoperfusion studies have repeatedly identified increased inflammation and oxidative stress. This led to the hypothesis for this thesis; that inflammation and oxidative stress are key drivers of structural and functional white matter disruption when cerebral blood flow is reduced.

The studies reported in this thesis were developed to investigate mechanisms involving inflammation and oxidative stress that can inform future treatments aimed at preventing the disruption of white matter and cognitive impairment in VCI. One such mechanism is the Nrf2 (Nuclear factor erythroid 2-related factor 2) signalling pathway. Nrf2 is a transcription factor that acts to detect and resolve inflammation and oxidative stress via induction of over 200 antioxidant and anti-inflammatory genes. Studies have shown that modulation of Nrf2 alters levels of inflammation and oxidative stress which impact on disease progression in models of Alzheimer's disease, Parkinson's disease and multiple sclerosis. To date, no one has investigated the direct role of Nrf2 in cerebral hypoperfusion-induced white matter disruption. While Nrf2 represents a promising network approach, another targeted mechanism of interest is microglial proliferation. Many neurodegenerative diseases including human VCI demonstrate increases in microglia, a sign of chronic neuroinflammation thought to be detrimental to cells, tissues and synapses. Work by our group has found an association between increasing numbers of microglia and the progressive disruption of white matter structure and function when cerebral blood flow is reduced in a mouse model, however, whether this is cause or consequence has yet to be determined.

The first study of this thesis aimed to test the hypothesis that deficiency of Nrf2 exacerbates white matter pathology and cognitive decline when cerebral blood flow is reduced. Using wild type and Nrf2 knockout mice the study investigated cortical perfusion, white matter disruption and gliosis, cognitive impairment and white matter gene changes following sham or surgically-induced cerebral hypoperfusion (bilateral carotid artery stenosis). There were no differences in the severity of blood flow reductions between genotypes initially, however, wild type mice displayed improved recovery compared to Nrf2 deficient mice. Hypoperfusion induced white matter disruption and microgliosis in the corpus callosum and the optic tract in both genotypes, exacerbated by the absence of Nrf2. Further, hypoperfusion induced white matter astrogliosis and upregulated pro-inflammatory gene signalling in the optic tract and induced an impairment in spatial working memory. However, these measures were not affected by Nrf2 deficiency. The results demonstrate that the absence of Nrf2 exacerbates white matter pathology and microgliosis following cerebral hypoperfusion but does not impact on functional outcome.

The second study aimed to test the hypothesis that enhancing astrocytic Nrf2-signalling preserves white matter structure and cognitive decline when cerebral blood flow is reduced. Astrocytes have larger antioxidant capacity than other cell types in the brain and overexpressing Nrf2 in astrocytes is associated with reduced white matter damage in a model of multiple sclerosis, as well as improved outcome in models of Parkinson's and Huntington's disease. Similar to the first study, wild type mice and mice overexpressing Nrf2 in astrocytes (GFAP-Nrf2) were subjected to bilateral carotid artery stenosis and cortical perfusion, white matter disruption and gliosis, cognitive impairment and white matter gene changes were assessed. There were no differences in the severity of blood flow reductions between genotypes. Akin to the first study, hypoperfusion induced white matter disruption, micro- and astrogliosis and pro-inflammatory gene signalling in the optic tract. The majority of these alterations were ameliorated in GFAP-Nrf2 mice. In addition, the impairment in spatial working memory induced by cerebral hypoperfusion was modestly improved in GFAP-Nrf2 mice compared to wild type controls. These findings support the hypothesis that astrocytic Nrf2 preserves white matter structure and function following cerebral hypoperfusion.

The first two studies identified structural and functional consequences of altered inflammation mediated via alterations in Nrf2 signalling. To thoroughly investigate the Nrf2 signalling pathway following cerebral hypoperfusion the next step would ideally

have been to study microglial Nrf2, however due to the lack of a suitable animal model, the third and final study instead aimed to test the hypothesis that microglial colony-stimulating factor 1 receptor (CSF1R) signalling is a driver of white matter disruption and cognitive decline when cerebral blood flow is reduced. Wild type mice treated with a pharmacological inhibitor of CSF1R (GW2580) or vehicle control, as an oral gavage or in diet, were studied by a similar experimental protocol as the first two studies. There were no differences in the severity of cerebral hypoperfusion between GW2580- or vehicle-treated animals either at one or six weeks following bilateral carotid artery stenosis. One week of GW2580 treatment was shown to modulate microglial proliferation and pro-inflammatory signalling in white matter. Remarkably, treatment with GW2580 for six weeks completely rescued impairments in spatial learning, protected against white matter disruption and prevented increased both white matter micro- and astrogliosis compared to wild type controls. These results suggest that CSF1R signalling in microglia is an important driver of the pathophysiological mechanisms that lead to white matter disruption and cognitive impairment when cerebral blood flow is reduced, and importantly, that targeted inhibition of this improves functional outcome.

In conclusion, the work described in this thesis provides evidence of the contribution of inflammation and oxidative stress to the disruption and functional impairment of cerebral white matter. The results indicate that these mechanisms are amenable to alteration, and that direct microglial inflammatory mechanisms play an important role in the pathogenesis of white matter disruption and cognitive decline. The results demonstrate that targeted inhibition of CSF1R signalling in microglia and increased astrocytic Nrf2 expression leads to improved structural and functional outcome and as such represent a basis for potential treatment which warrants further investigation.

Lay Summary

Dementia is a term used to describe symptoms that disrupt the brain's ability to think, plan and remember. Dementia severely impairs quality of life and always leads to death. In 2018, 50 million people were living with dementia without available disease-modifying treatments. Many mistakenly believe that dementia is an inevitable part of ageing whereas in fact it is caused by a number of different diseases. The second most common cause of dementia is vascular dementia, where the brain doesn't receive a sufficient supply of blood. Animal models where blood flow to the brain is reduced are used to study mechanisms involved. In vascular dementia, cognitive functions such as thinking and planning are the most affected, as a result of damage to the brain's wiring. The wiring is called white matter because of its white appearance under the microscope, and transmits information between different regions necessary for complicated cognitive functions. It is currently unknown how the wiring becomes damaged to cause cognitive impairment in vascular dementia, but studies suggest that inflammation and oxidative stress are involved.

Inflammation is the body's natural response to protect itself against invaders, but uncontrolled inflammation can lead to damage to otherwise healthy cells and tissues such as white matter. Oxidative stress is the result of an imbalance between production and clearance of harmful molecules called reactive oxygen species. Reactive oxygen species are produced as a by-product of cellular energy production and are normally swiftly neutralised by antioxidant defence mechanisms. During disease, production of these molecules increases and if not efficiently cleared these can cause damage. The body possesses defence mechanisms against both oxidative stress and inflammation, one of which is the Nrf2 system. This thesis firstly explores the role of the Nrf2 system in a model of vascular dementia. The results show that reducing brain blood flow in mice without Nrf2 causes more white matter damage and conversely, reducing brain blood flow in mice with higher levels of Nrf2 results in less white matter damage and also less cognitive impairment. The thesis then goes on to study specifically if increased inflammation is an early driver that can be targeted in vascular dementia. The results show that inhibiting the brain's inflammatory cell microglia protects the wiring from damage and prevents learning impairment in mice when brain blood flow is reduced. The work presented in this thesis suggests that enhancing the Nrf2-system and inhibiting inflammation in a cell-specific manner is beneficial, and future studies should explore these mechanism further as potential approaches to treat vascular dementia.

List of Figures

Figure 1.1 Anatomy of the human cerebrovasculature. 5
Figure 1.2 Cerebrovascular diseases associated with vascular cognitive impairment. 7
Figure 1.3 Illustration of the neuro-gliovascular unit. 10
Figure 1.4 Electron micrograph of a central nervous system axon with surrounding myelin. 13
Figure 1.5 Domain structure of Nrf2. 20
Figure 1.6 Molecular basis of the Nrf2-system. 22
Figure 1.7 GW2580 inhibits colony-stimulating factor 1 receptor (CSF1R) signalling. 25
Figure 1.8 Hypothesis and aims. 26

Figure 2.1 Bilateral carotid artery stenosis. 31
Figure 2.2 Schematic diagrams of mazes used for behavioural testing. 36
Figure 2.3 Regions of interest for image analysis of immunostained proteins. 43

Figure 3.1 Cortical cerebral blood flow is reduced post-BCAS. 57
Figure 3.2 White matter disruption is more extensive in $Nr2^{-/-}$ mice compared to wild type and $Nrf2^{+/-}$ post-BCAS. 59
Figure 3.3 The density of microglia is increased post-BCAS to a greater extent in $Nrf2^{-/-}$ mice compared to wild type and $Nrf2^{+/-}$. 61
Figure 3.4 Astrogliosis in the optic tract is induced to a similar extent in wild type and Nrf2 KO mice post-BCAS. 63
Figure 3.5 Nrf2 and Nrf2-regulated antioxidant genes in the optic tract are unaltered post-BCAS but pro-inflammatory genes are induced. 66
Figure 3.6 Spontaneous alternation and mobility are unaltered post-BCAS in wild type and $Nrf2^{+/-/-/-}$ mice. 67
Figure 3.7 Spatial working memory is impaired post-BCAS but is not exacerbated by deficiency in Nrf2. 68

Figure 4.1 Cortical cerebral blood flow is reduced post-BCAS. 91
Figure 4.2 Spontaneous alternation and mobility are unaltered in wild type and GFAP-Nrf2 mice. 92
Figure 4.3 Cerebral hypoperfusion causes an impairment in spatial working memory which is less pronounced in GFAP-Nrf2 mice. 93
Figure 4.4 White matter disruption in the optic tract is less extensive in GFAP-Nrf2 mice compared to wild type post-BCAS. 95
Figure 4.5 The density of microglia is increased post-BCAS in the optic tract. 97
Figure 4.6 Astrogliosis in the optic tract is less in GFAP-Nrf2 mice compared to wild type post-BCAS. 99

Figure 4.7 *Nrf2*, *Slc7a11* and *Gclm* relative gene expression in whole brain is higher in GFAP-Nrf2 animals with no effect of BCAS surgery. 100
Figure 4.8 Pro-inflammatory genes are induced post-BCAS in the optic tract and the level of *C4* is reduced in GFAP-Nrf2 mice. 102

Figure 5.1 Cortical cerebral blood flow is reduced post-BCAS. 121
Figure 5.2 GW2580 treatment dampens white matter microglial proliferation and pro-inflammatory signalling one week post-BCAS. 123
Figure 5.3 Cortical cerebral blood flow is reduced post-BCAS. 124
Figure 5.4 GW2580-treatment prevents increases in white matter microglia 6 weeks post-BCAS. 126
Figure 5.5 GW2580-treatment prevents white matter astrogliosis 6 weeks post-BCAS. 127
Figure 5.6 The extent of astrogliosis in the corpus callosum is positively correlated with increased density of microglia. 128
Figure 5.7 GW2580-treament protects against white matter disruption 6 weeks post-BCAS. 130
Figure 5.8 The severity of white matter disruption in the corpus callosum is positively correlated with increased density of microglia. 130
Figure 5.9 GW2580-treatment protects against hypoperfusion-induced impairment in spatial learning. 132

Figure 6.1 Diagram of alterations observed following reductions in cerebral blood flow. 146

List of Tables

Table 1.1 Subset of Nrf2-regulated genes 21
Table 2.1 Primers used for genotyping 30
Table 2.2 Automatic processing schedule for paraffin embedding 38
Table 2.3 Manual processing for paraffin embedding 39
Table 2.4 Antibodies used for immunohistochemical and immunofluorescent experiments 41
Table 2.5 qPCR primer sequences, cycling conditions and efficiencies 45
Table 3.1 Number of mice in each group and experiment with details of exclusion 55
Table 4.1 Number of mice in each group and experiment with details of exclusion 89
Table 5.1 Number of mice in each group and experiment with details of exclusion 119
Table 6.1 Summary of results of BCAS and BCAS + experimental intervention 147

List of Abbreviations

AD	Alzheimer's disease
Aldh1l1	Aldehyde dehydrogenase 1l1
ANOVA	Analysis of variance
APP/PS1	Amyloid precursor protein/Presenilin 1 (mouse model of AD)
AT-NRF2-KO	Amyloid and tauopathy Nuclear factor erythroid 2-related factor 2 knock out
AT-NRF2-WT	Amyloid and tauopathy Nuclear factor erythroid 2-related factor 2 wild type
ATP	Adenosine triphosphate
BBB	Blood-brain barrier
BCAS	Bilateral carotid artery stenosis
bp	Base pair
C1q	Complement component 1q
C4	Complement component 4
C5	Complement component 5
CBF	Cerebral blood flow
CC	Corpus callosum
CSF	Cerebrospinal fluid
CSF1	Colony-stimulating factor 1
CSF1R	Colony-stimulating factor 1 receptor
DAB	3,3’ diaminobenzidine tetrahydrochloride
DMF	Dimethyl fumarate
DNA	Deoxyribonucleic acid
EAE	Experimental autoimmune encephalomyelitis
fALS	Familial amyotrophic lateral sclerosis
FDA	Food and drug administration
FI	Fimbria
FLAIR	Fluid-attenuated inversion recovery
GFAP	Glial fibrillary acidic protein
GSK3β	Glycogen synthase kinase 3 β
GWAS	Genome wide association studies
HD	Huntington's disease
HIF-1α	Hypoxia inducible factor 1 alpha
Ho1/Hox1	Heme oxygenase 1
Iba1	Ionized calcium binding adapter molecule 1
IC	Internal capsule
IFNγ	Interferon gamma
IL1β	Interleukin 1 beta
IL34	Interleukin 34
IQR	Interquartile range
Keap1	Kelch-like ECH-associated protein-1
LDL	Low-density lipoprotein
MAG	Myelin-associated glycoprotein
MMP	Matrix metalloproteinase
MCP1/Ccl2	Monocyte chemoattractant protein 1/Chemokine (C-C motif) ligand 2
MIP1a/Ccl3	Macrophage inflammatory protein 1 alpha/Chemokine (C-C motif) ligand 3
MPTP	1-methyl-4-phenyl-1,2,3,6-tetrahydropyridine
MRI	Magnetic resonance imaging
mRNA	Messenger ribonucleic acid
MS	Multiple sclerosis

Neh	Nrf2-ECH homology
NF-κB	Nuclear Factor κB
NOX	Nicotinamide adenine dinucleotide phosphate oxidase
Nqo1	NAD(P)H dehydrogenase (quinone)-1
Nrf2	Nuclear factor erythroid 2-related factor 2
OPC	Oligodendrocyte precursor cell
OT	Optic tract
PBS	Phosphate buffered saline
PCR	Polymerase chain reaction
PD	Parkinson's disease
PLP	Proteolipid protein
RNA	Ribonucleic acid
RNS	Reactive nitrogen species
ROS	Reactive oxygen species
SCI	Spinal cord injury
SEM	Standard error of the mean
SOD1	Superoxide dismutase 1
STD	Standard deviation
tBHQ	tert-butyl-hydro-quinone
TLR	Toll-Like Receptors
TNFα	Tumor necrosis factor alpha
TRAP	Translating ribosome affinity purification
VCI	Vascular cognitive impairment
VD	Vascular dementia
VEGFα	Vascular endothelial growth factor alpha
WML	White matter lesion
βTrCP	Beta-transducin repeat containing protein
2VO	Two-vessel occlusion
3VO	Three-vessel occlusion
4VO	Four-vessel occlusion

Chapter 1

Introduction

1.1 Overview

The prevalence of dementia worldwide was in 2018 estimated at 50 million people with a financial cost in excess of US$ 1 trillion (Patterson, 2018). Dementia is a devastating fatal illness that not only affects the individual but also friends and family who have to take greater and greater care responsibilities as the disease progresses. Vascular cognitive impairment (VCI) is the second leading form of dementia (Dichgans and Leys, 2017) and vascular contributions to other dementia subtypes such as Alzheimer's Disease (AD) are becoming increasingly recognised (Kapasi et al., 2017, Iturria-Medina et al., 2016), implicating potentially overlapping pathophysiological mechanisms.

VCI is a heterogeneous disorder resulting from large and small cerebrovascular disease such as large vessel occlusion, bilateral carotid artery stenosis and atherosclerosis (O'Brien et al., 2003, Iadecola, 2013). One major pathological feature observed in VCI patients is alterations to the brain's white matter as detected by *in vivo* imaging (Wardlaw et al., 2015) and post mortem pathological evaluation (Skrobot et al., 2016). Longitudinal neuroimaging studies and neuropathological evidence demonstrate an association between white matter alterations and declining cognition (de Groot et al., 2000, Inzitari et al., 2009, Boyle et al., 2016, Ezzati et al., 2017). Hypoxia and ischaemia are suggested mechanisms underlying white matter pathology (Barker et al., 2013) which may be attributed to chronic cerebral hypoperfusion (Fernando et al., 2006, Schuff et al., 2009, Brickman et al., 2009).

Chronic cerebral hypoperfusion; the modest, sustained reduction of blood flow to the brain, is a cerebrovascular feature observed before the onset of cognitive decline (Ruitenberg et al., 2005). It is not only associated with poorer cognition (Alosco et al., 2013) but also predicts conversion from mild cognitive impairment to dementia (Chao et al., 2010, Hirao et al., 2005). This suggests that chronic cerebral hypoperfusion is an early alteration which may contribute to the onset of VCI and dementia (de la Torre, 2016). Animal models of cerebral hypoperfusion, such as bilateral carotid artery stenosis, recapitulate important features of VCI, including white matter disruption and cognitive impairment (Duncombe et al., 2017). Since the molecular mechanisms underlying VCI are poorly understood, these animal models are essential to investigate hypotheses formed from neuropathology and neuroimaging studies. Increasing evidence suggests that inflammation and oxidative stress are pathophysiological mechanisms contributing to white matter disruption in humans (Simpson et al., 2007b, Al-Mashhadi et al., 2015), and similar changes can be

detected in animal models (Coltman et al., 2011, Reimer et al., 2011, Washida et al., 2010). The transcription factor Nrf2 (Nuclear factor erythroid 2-related factor 2) is a master regulator of anti-inflammatory and antioxidant gene expression which has emerged as a potential therapeutic target for the treatment of neurodegenerative disease (reviewed by Johnson and Johnson, 2015). Nrf2 is critical for maintenance of white matter structure during normal ageing (Hubbs et al., 2007) and pharmacological activation of the Nrf2-pathway via dimethyl fumarate (DMF) is approved by the U.S. Food and Drug Administration for the treatment of multiple sclerosis (reviewed by Suneetha and Raja Rajeswari, 2016). It is currently unknown what the role and therapeutic potential of the Nrf2-pathway is in white matter disruption induced by chronic cerebral hypoperfusion. Further, white matter alterations in humans are associated with increased numbers of microglia (Simpson et al., 2007a, Simpson et al., 2007b) and preclinical studies suggest that expansion of the microglial population via proliferation is detrimental to white matter structure and function when cerebral blood flow (CBF) is reduced (Fowler et al., 2017, Manso et al., 2017). However, a causal relationship remains to be established.

The work described in this thesis was developed to investigate the hypothesis that inflammation and oxidative stress drive the disruption of white matter structure and function following chronic cerebral hypoperfusion. The studies herein are investigating the Nrf2 signalling pathway and microglial proliferation, mechanisms involving inflammation and oxidative stress that may inform future treatments aimed at preventing the disruption of white matter structure and function, utilising the bilateral carotid artery stenosis model of chronic cerebral hypoperfusion in mice.

1.2 Importance of the cerebrovascular system

The brain constitutes ~2% of the body's weight but requires as much as 20% of its total energy supply (Attwell and Laughlin, 2001) making it one of the most energy demanding organs in the body. This energy demand reflects requirements for synaptic transmission in grey matter (Attwell and Laughlin, 2001), as well as the energy required to provide and maintain structural integrity to the neuronal axons that transmit information between distributed neuronal networks and make up the brain's white matter (Harris and Attwell, 2012). Glucose and oxygen are required for the production of the main energy substrate adenosine triphosphate (ATP) (Belanger et al., 2011), and due to a lack of endogenous energy stores the brain is critically dependent on a constant and adequate supply of blood (Kisler et al., 2017). Blood enters the brain through four major arteries, the carotid arteries and the vertebral

arteries (Fig 1.1a, Fig 1.2). Together these join a cerebrovascular structure called the Circle of Willis, found at the base of the brain (Fig 1.1a). This specialised arrangement provides redundancy and redistribution should a feeding artery become occluded or damaged in any way, to maintain the constant supply of blood that the brain requires for normal function (Vrselja et al., 2014). Branching off the Circle of Willis is the anterior, middle and poster cerebral arteries (Fig 1.1a, c), the three major vessels that perfuse the extensive cerebrovascular system (Iadecola, 2013).

The human cerebrovascular system consists of a dense network of blood vessels measuring ~400 miles (Fig 1.1b) with highly specialised functions (Iadecola and Nedergaard, 2007). Autoregulation is a hemodynamic response that keeps CBF constant despite changes in blood pressure via myogenic and metabolic mechanisms altering cerebrovascular resistance (Paulson, 1990). This is an important function that protects the cerebrovasculature from hypertension, however conversely, may leave the brain more vulnerable to hypoperfusion in conditions of systemic hypotension (van Beek et al., 2008). Another specialised function is functional hyperaemia, (or neurovascular coupling) which allows for rapid increases in CBF to accommodate local increases in metabolic demand caused by neuronal activity (Iadecola and Nedergaard, 2007, Attwell et al., 2010). This response is thought to be mediated by neurochemical signalling involving astrocytes, strategically positioned between neurons and the vessels (Iadecola and Nedergaard, 2007, Attwell et al., 2010) (Fig 1.3). Together these functions ensure that CBF remains constant, sufficient and is matched with the current levels of metabolic demand.

It is well known that the interruption of CBF, such as that observed in stroke, leads to brain damage (Hossmann, 2006). However, it has also been demonstrated that subtle reductions in CBF occurring over a longer period of time, referred to as chronic cerebral hypoperfusion, is detrimental to the brain, in particular to the structure and function of the brain's white matter (Brickman et al., 2009). This is thought to be because the normal rate of perfusion in white matter is already roughly half that of grey matter (Chen et al., 2008) and, because the cerebrovasculature is arranged in an outside-in distribution (Fig 1.1c). This renders deep white matter structures more susceptible to reductions in CBF during global chronic cerebral hypoperfusion (Iadecola, 2013).

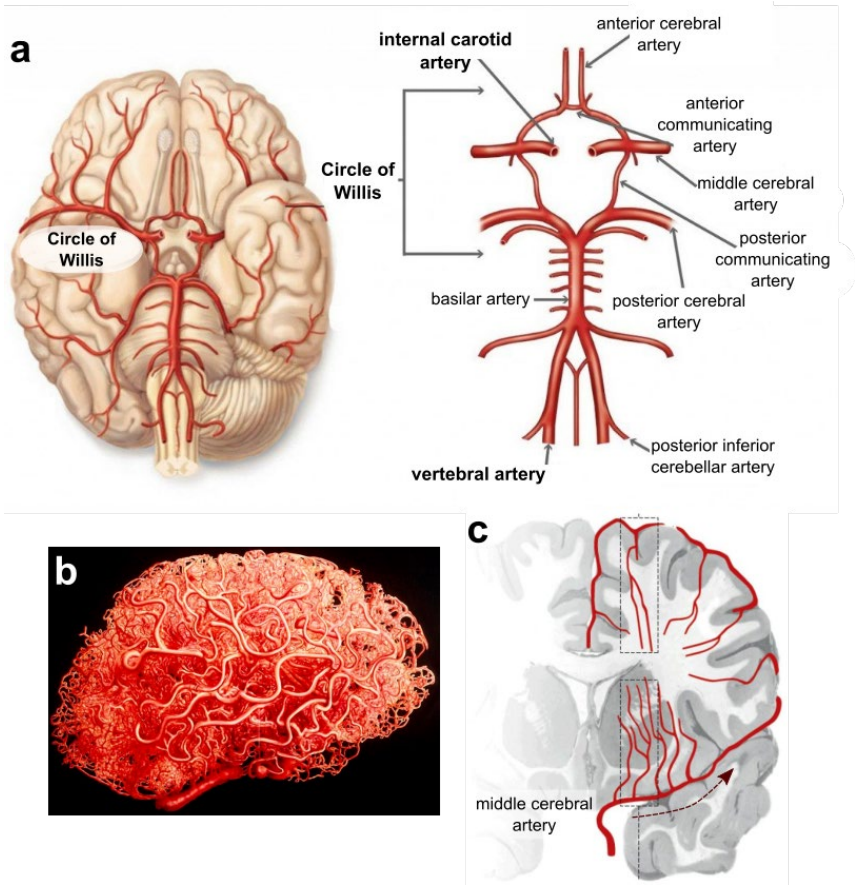

Figure 1.1 Anatomy of the human cerebrovasculature. (a) Cerebrovascular arrangement at the base of the brain including the circle of willis. Blood is supplied through the vertebral and internal carotid arteries and then distributed to the brain via the anterior, middle and posterior cerebral arteries. Adapted from *https://www.scienceabc.com/humans/circle-of-willis-anatomy-diagram-and-functions.html* **(b)** Artwork based on a resin cast showing the blood vessels of the human brain. Credit Francis Leroy, Biocosmos / Science Photo Library, *https://www.sciencephoto.com/media/306297/view/artwork-showing-the-blood-vessels-of-the-brain* **(c)** The outside-in distribution of cerebral blood vessels (adapted from Wardlaw et al., 2013)

1.3 Vascular cognitive impairment

Vascular cognitive impairment (VCI) describes a heterogeneous syndrome caused by cerebrovascular disease and disturbances in CBF delivery (O'Brien et al., 2003, Iadecola, 2013). The term encompasses alterations in cognition ranging from mild, subjective impairment through to severe cognitive impairment culminating in dementia (Dichgans and Leys, 2017, van der Flier et al., 2018).

1.3.1 Vascular risk factors and underlying cerebrovascular causes of VCI

The primary risk factor for developing dementia is age, but vascular risk factors such as hypertension, diabetes, hyperlipidaemia and obesity are all associated with VCI (Iadecola, 2013, Jellinger, 2013, Smith, 2017). These vascular risk factors are thought particularly detrimental if present in midlife, emphasising the early clinically silent changes that are hypothesised to induce cerebrovascular disease and VCI. Some evidence suggests that the incidence of dementia is reducing in high income countries as a result of improved management of vascular risk factors and cerebrovascular disease (Skrobot et al., 2017). However, since vascular changes occur years before the appearance of clinical symptoms, understanding the early pathophysiological mechanisms has proven difficult.

To better understand mechanisms leading to VCI, efforts are being directed towards the cerebrovascular diseases that can be clinically diagnosed (Fig 1.2). Vascular disorders such as atherosclerosis, small vessel disease, and cerebral amyloid angiopathy all contribute to the development of cerebrovascular disruption and ischaemic lesion development (Iadecola, 2013, Jellinger, 2013). Small vessel disease generally leads to multiple smaller infarcts and/or microbleeds and white matter lesions. Cerebrovascular disease of large vessels may lead to chronic cerebral hypoperfusion or stroke caused either by occlusion or rupture of a large vessel. Vessel stiffening, narrowing, occlusion and overall reduced vessel integrity as a result of various vascular pathologies leads to impairments in the delivery and regulation of CBF (Dichgans and Leys, 2017).

1.3.2 Clinical manifestations and diagnostic criteria for VCI

Due to its heterogeneous appearance, VCI has been difficult to diagnose clinically, however a recent consensus study aimed to harmonise VCI classification and diagnostic criteria (Skrobot et al., 2018).

1.3.2.1 Neuropsychological evaluation of VCI

Skrobot et al. (2018) reported that the cognitive domains that should be included for neuropsychological evaluation are executive function, attention, memory, language and visuospatial function. The key distinction between mild and major VCI is the disruption of instrumental activities in daily living which in mild VCI are mild or completely absent despite some impairment in at least one cognitive domain. Major VCI, in contrast, is associated with severe disruption of instrumental activities in daily living and significant deficits in at least one cognitive domain, but often several. The

neuropsychological tests are based on the National Institute of Neurological Disorders and Stroke-Canadian Stroke Network vascular cognitive impairment harmonization standards (Hachinski et al., 2006).

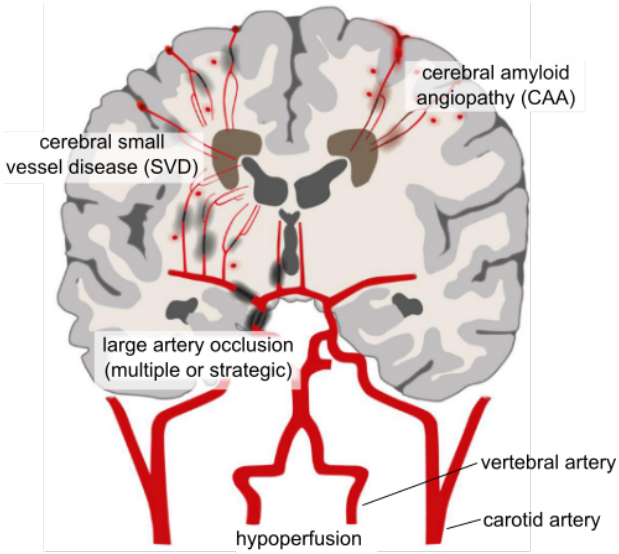

Figure 1.2 Cerebrovascular diseases associated with vascular cognitive impairment. (adapted from Dichgans and Leys, 2017)

1.3.2.2 Neuroimaging features of VCI

Furthermore, the consensus is that imaging evidence is essential for diagnosis of both mild and major VCI, and that magnetic resonance imaging (MRI) is the gold standard (Skrobot et al., 2018). A two-factor approach for diagnosis of VCI is emphasised also in a report by the American Heart Association/American Stroke Association (Gorelick et al., 2011). MRI has been used for a number of years to identify structural alterations associated with neurological disorders. The main neuroimaging features that are considered to contribute to VCI include white matter hyperintensities, brain atrophy; primarily white matter or hippocampal, recent small subcortical infarcts, lacunes (defined as small fluid-filled cavities), perivascular spaces and microbleeds (Wardlaw et al., 2013). Most importantly, alterations to the white matter are considered vital for establishing a diagnosis of VCI (Smith, 2017). Advances in MR technology such as diffusion weighted imaging allows for quantifiable evaluation of white matter integrity, shown to correlate better with cognition than traditional MR modalities such as fluid-attenuated inversion recovery (FLAIR) (Heiss et al., 2016).

1.3.3 Vascular contributions to Alzheimer's dementia

Dementia was originally thought to result from vascular factors and "hardening of the arteries", however following the discovery of the amyloid β peptide in the 1980's, dementia research shifted heavily to the amyloid hypothesis (Iadecola, 2013). In the last couple of decades though, vascular contributions to dementia are receiving resurgent interest due to frequently observed overlap of pathological hallmarks. A comprehensive longitudinal study found that the presence of brain infarcts was associated with poorer cognition and increased prevalence of dementia compared to presence of AD pathology alone (Snowdon et al., 1997). In line with this is a recently published study describing that the effect of genetic risk factors for AD on cognition was partially but significantly mediated by vascular pathologies (Lin et al., 2018). Similarly, a meta-analysis of neuropathological evidence of probable AD identified vascular pathology in over 75% of cases and found that mixed pathologies lowered the threshold for clinical diagnosis of AD (Kapasi et al., 2017). Additional evidence suggests that vascular alterations represent an early event in the disease progression. Iturria-Medina et al. (2016) found that cerebrovascular dysfunction was the earliest detectable feature in patients with late onset AD, and Araque Caballero et al. (2018) observed white matter alterations over a decade before onset of dementia symptoms in patients with autosomal dominant (familial) AD. Together these studies suggest that early vascular alterations drive not only VCI but may also contribute to or even trigger neurodegenerative dementias. More efforts are therefore required to increase our understanding of how cerebrovascular disease induces pathological processes leading to cognitive impairment.

1.4 White matter structure and function

White matter makes up roughly 50% of the human brain (Walhovd et al., 2014) and contains a large proportion of the axons that transmit information between different brain regions (Stassart et al., 2018). Some axons are myelinated, meaning they are enwrapped by the lipid-rich myelin sheath which gives white matter its characteristic colour. Myelination is an evolutionary adaptation seen in vertebrates allowing for much faster conduction of nerve impulses (Aggarwal et al., 2011). The expansion of white matter tracts exceeds that of the neocortex (Filley and Fields, 2016, Paus et al., 2014, Stassart et al., 2018) and since white matter provides the structural connectivity between distributed neural networks involved in complex functions, its role in cognition should not be disregarded.

1.4.1 Cellular components of white matter

The greatest population of cells in the white matter are oligodendrocytes, the glial cell responsible for the production and maintenance of myelin (Walhovd et al., 2014) (Fig 1.3). Oligodendrocytes originate from oligodendrocyte precursor cells (OPCs), which remain in the adult brain and contribute to oligodendrocyte repopulation following injury (McQueen et al., 2014), and aid the restoration of myelin sheaths following demyelination (Stassart et al., 2018). The white matter is perfused by blood vessels, lined by endothelial cells and associated with pericytes and/or smooth muscle cells (Stassart et al., 2018) (Fig 1.3). Together with astrocytes and microglia these components make up what can be referred to as the neuro-gliovascular unit (Fig 1.3), a concept that emphasises the interconnection and communication between different cell types and the need to study these in concert rather than isolation.

1.4.1.1 White matter astrocytes

White matter astrocytes are star-shaped cells primarily involved in maintaining homeostasis (Lundgaard et al., 2014). Astrocytes are, more broadly, essential for maintaining the blood-brain barrier (BBB) with processes covering over 90% of the cerebrovasculature (Lundgaard et al., 2014), and their strategic position between the vasculature and neuronal synapses has led to their proposed involvement in the control of neurovascular coupling (Attwell et al., 2010) (Fig 1.3). Astrocytes are furthermore capable of buffering pH and are the only cell type in the brain with glycogen stores, making them important for homeostatic and metabolic support (Verkhratsky and Nedergaard, 2018). White matter astrocytes directly contact oligodendrocytes through gap junctions and a number of studies support the role for astrocytes in developmental myelination as well as continued support throughout adulthood (Lundgaard et al., 2014, Li et al., 2016a). Lastly, astrocytes also respond to and are capable of modulating the brain's inflammatory response (Sofroniew, 2014a, Sofroniew, 2014b), in conjunction with the brain resident macrophage microglia.

1.4.1.2 White matter microglia

These immune cells are sparser than oligodendrocytes and astrocytes (Walhovd et al., 2014), but as dynamic surveyors and early responders to damage (Nimmerjahn et al., 2005), microglia are important for the innate immune response and also regenerative white matter repair (Lloyd et al., 2017). The functions of microglia include phagocytosis of pathogens and myelin debris, secretion of cytokines, chemokines and growth factors and remodelling of the extracellular matrix (Lloyd et al., 2017, reviewed

by Salter and Stevens, 2017). The heterogeneity between white matter and grey matter microglia is less well known compared to astrocytes. Recent single cell RNA sequencing studies have identified immense heterogeneity of both cell types, much greater than previously thought (Grabert et al., 2016, Boisvert et al., 2018), however the functional consequence of this heterogeneity requires further investigation. More broadly, microglia are thought to be responsible for developmental synaptic pruning (Paolicelli et al., 2011) and to be involved in adult synaptic plasticity important for learning and memory (reviewed by Salter and Stevens, 2017).

It also worth noting that while microglia are the only parenchymal macrophages in the brain, there are other macrophage populations found in very close proximity, for example, perivascular and meningeal macrophages, that are considered important components of the brain-resident immune system (Faraco et al., 2017), and as such should perhaps also be considered part of the neuro-gliovascular unit.

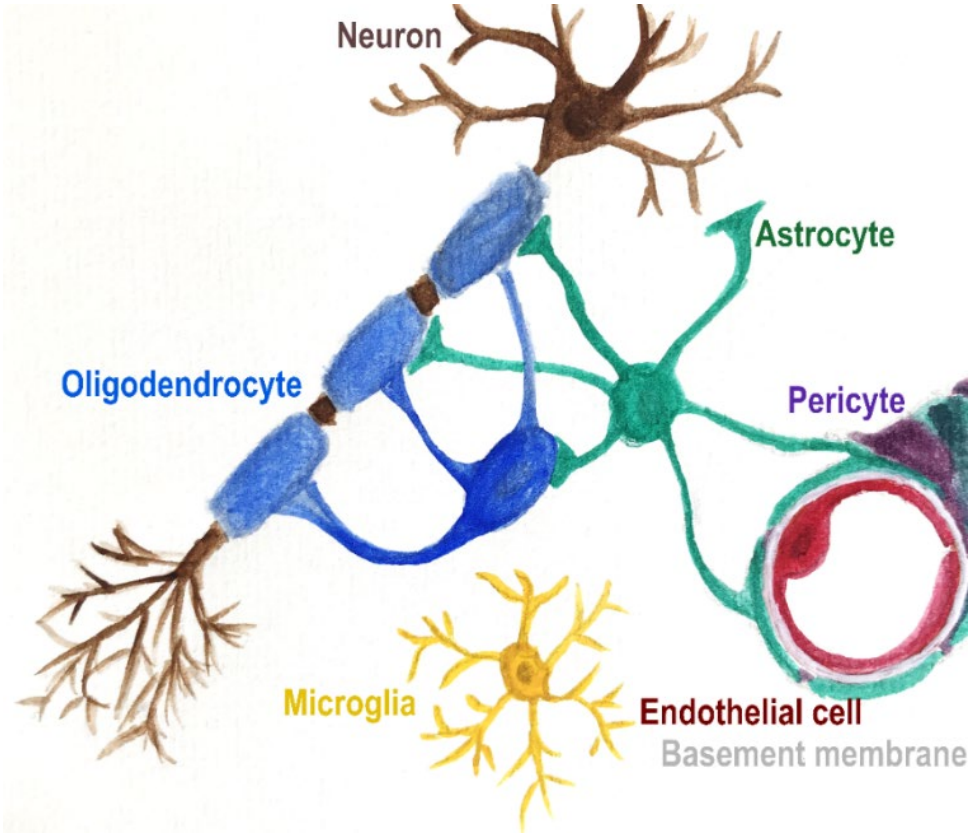

Figure 1.3 Illustration of the neuro-gliovascular unit. The oligodendrocyte (blue) extends processes whose myelin-rich plasma membrane wraps around neuronal axons (brown). Astrocyte processes (green) have end-feet that contact neurons, oligodendrocytes and cover over 90% of cerebral blood vessels. Cerebral blood vessels are lined by endothelial cells (red), basement membrane proteins (white/grey) and contractile cells like pericytes (purple) or smooth muscle cells (not shown). Microglia (yellow) survey the environment and contribute to the inflammatory response essential for host-defence.

1.5 White matter vulnerability in VCI

As previously mentioned, the white matter is essential for relaying information between distributed neuronal networks and as such is critical for cognitive function (Filley and Fields, 2016). White matter disruption leads to a functional disconnect (Lawrence et al., 2013) where information is no longer transmitted efficiently and accurately between different brain regions (Nave, 2010, Chen et al., 2016). Frontal white matter tracts are particularly sensitive to vascular-related disruption, thought to underlie the impairments of the specific cognitive domains affected in VCI (Hachinski et al., 2006) (see 1.3.2.1).

Evidence from a plethora of neuroimaging studies display a clear association between white matter alterations and declining cognition (reviewed by Wardlaw et al., 2015). As an example, The Rotterdam Scan Study found that white matter lesions detected by MRI relate to impaired cognition in a data set of ~1000 individuals. The cognitive impairment chiefly related to tasks that require speed of processing rather than memory, consistent with the cognitive changes reported in VCI (de Groot et al., 2000). These results were corroborated by Bendlin et al. (2010) using more detailed diffusion weighted imaging modalities (see 1.3.2.2). White matter alterations are not only associated with declining cognition, but serve as indicators of the rate of cognitive decline, as the severity of white matter changes detected at the start of a study predicted subsequent rate of global functional and cognitive decline (Inzitari et al., 2009). This was later corroborated by a separate longitudinal study (Boyle et al., 2016). In consort with a large number of additional studies this strongly suggests that white matter alterations drive cognitive decline in ageing and VCI. This is supported also by nineteenth century human post mortem analyses that found that focal white matter lesions result in impaired cognition (reviewed by Filley and Fields, 2016).

1.5.1 Chronic cerebral hypoperfusion drives white matter disruption in VCI

Neuroimaging studies demonstrate that areas of white matter intensities exhibit reduced CBF (Brickman et al., 2009, Schuff et al., 2009) and that perfusion deficits in normal appearing white matter predict future white matter alterations (Promjunyakul et al., 2015, Bernbaum et al., 2015). This suggests that cerebral hypoperfusion may be an important early driver of white matter disruption. Further in support of this are associations identified between impaired cerebral perfusion and cognitive decline (Alosco et al., 2013). Reduced CBF precedes clinical dementia (Ruitenberg et al., 2005) and can, akin to white matter alterations, be used to predict conversion from

mild cognitive impairment to dementia (Chao et al., 2010). Furthermore, individuals with carotid artery stenosis; narrowing of the carotid arteries as a result of atherosclerosis, present with poorer cognition compared to individuals without (Balucani et al., 2012) and a longitudinal study found that intracranial arterial stenosis increases the risk of patients with mild cognitive impairment developing dementia (Zhu et al., 2014).

Chronic cerebral hypoperfusion can be attributed a range of cerebrovascular diseases and risk factors such as atherosclerosis (Barone et al., 2016), small vessel disease (Rosenberg et al., 2015), hypertension (Perrotta et al., 2016) and diabetes (Novak et al., 2006), as well as progressing age (Aanerud et al., 2012). As such, cerebral hypoperfusion may induce common downstream pathophysiological mechanisms which can be targeted for therapeutic intervention in a number of conditions. There is some conflicting evidence suggesting that reduced perfusion may be an effect rather than a cause of white matter alterations as discussed in a recent meta-analysis (Shi et al., 2016b). Although, the authors highlight that most perfusion measures were either global or from grey matter and, as previously indicated, deep white matter structures are more susceptible to reductions in CBF due to the arrangement of the cerebrovasculature (Fig 1.1c), possibly accounting for the discrepancies.

Human neuropathology studies also support cerebral hypoperfusion as a possible cause of white matter alterations in age and VCI. This conclusion is based on immunohistochemical results finding increased hypoxia-inducible factors (HIFs) and matrix metalloproteinases (MMPs) in lesioned white matter (Fernando et al., 2006, Aboul-Enein et al., 2003). These proteins are both known to be regulated by hypoxia and ischaemia and promote vascular inflammation and blood brain barrier breakdown. Similarly, Aboul-Enein et al. (2003) demonstrated in post mortem white matter lesioned tissue, preferential loss of a protein localised at the innermost part of the myelin-sheath; myelin-associated glycoprotein (MAG) (Fig 1.4). MAG is highly susceptible to hypoxia and ischaemia, far more so than other myelin proteins such as proteolipid protein (PLP) (Barker et al., 2013). The ratio of MAG:PLP is used as a post mortem marker of white matter ischaemia, indicative of the previous perfusion status of that tissue (Barker et al., 2014).

Lastly in support of the role of cerebral hypoperfusion in the development of VCI is the incidence of dementia in patients who have suffered strokes. Stroke doubles the risk of dementia and is so closely associated with VCI that it is categorised as its own

sub-type; post-stroke dementia (Smith, 2017). Albeit the reductions in perfusion during a stroke far exceeds those resulting from impaired vessel reactivity and stenosis in cerebral hypoperfusion, pathophysiological features such as inflammation and oxidative stress are observed in both conditions (Raz et al., 2015).

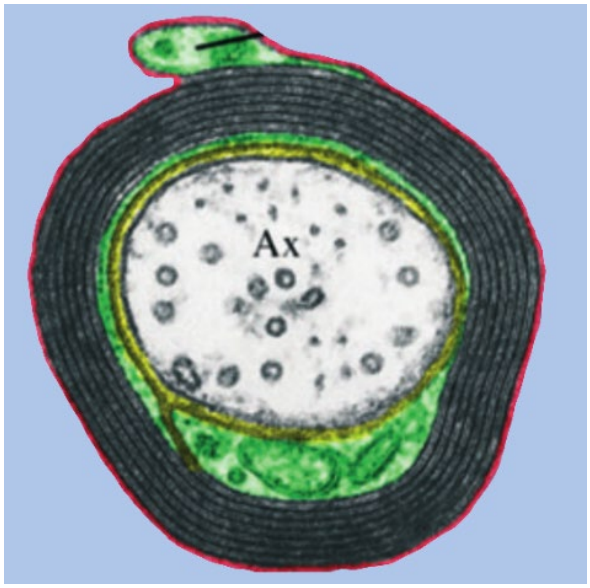

Figure 1.4 Electron micrograph of a central nervous system axon with surrounding myelin. Oligodendrocyte is highlighted in green and myelin sheath can be seen surrounding central axon in black. Yellow indicates location of myelin-associated glycoprotein (MAG) and outside the myelin sheath in red is myelin-oligodendrocyte glycoprotein (MOG). (adapted from Quarles, 2007)

1.6 Cerebral hypoperfusion models of VCI

Rodent models of cerebral hypoperfusion provide an excellent tool for investigating flow-related pathophysiological mechanisms involved in white matter disruption relevant to VCI. Cerebral blood flow is reduced in rats and mice by occlusion or stenosis primarily of the carotid arteries (Fig 1.1, 1.2). Mouse models provide advantages as a mammalian system with a genome amenable to genetic modification that is also highly analogous with the human genome.

1.6.1 Bilateral carotid artery stenosis in mice

Originally developed by Shibata et al. (2004), bilateral carotid artery stenosis (BCAS) is achieved by application of microcoils to the carotid arteries, thereby reducing their lumen and the flow of blood to the Circle of Willis. Extensive characterisation by our group and others show that BCAS in mice induces modest, chronic reductions in CBF (20-50%) leading to diffuse evolving white matter pathology

and cognitive impairment (Ihara and Tomimoto, 2011, Coltman et al., 2011, McQueen et al., 2014, Hattori et al., 2016). At 1 month following BCAS surgery the white matter is selectively disrupted as detected by MRI (Holland et al., 2011) and histology or immunohistochemistry (Shibata et al., 2004, Coltman et al., 2011). Further, 1 month of BCAS induces an impairment in spatial working memory, attributed to disrupted frontal-subcortical circuitry, whereas reference memory is still intact (Shibata et al., 2007, Coltman et al., 2011) consistent with VCI in humans. Longer-term BCAS (3-8 months) induces additional cerebrovascular disruption including stroke lesions, blood brain barrier disruption and microhaemorrhages, resembling small vessel disease pathology, which coincide with more extensive cognitive impairment including impaired reference memory, (Kitamura et al., 2017, Holland et al., 2015, Nishio et al., 2010). These studies demonstrate that BCAS-induced chronic cerebral hypoperfusion in mice is a relevant and suitable experimental model of VCI. Importantly, CBF reductions following BCAS in mice are sub ischaemic (<70%) but induce hypoxic conditions in the white matter from 3 days onwards (Duncombe et al., 2017) consistent with human neuropathology (Fernando et al., 2006, Aboul-Enein et al., 2003, Barker et al., 2013).

1.6.1.1 Considerations for the study of BCAS

The cerebrovascular arrangement has been shown to differ between mouse strains (Yang et al., 1997) and CBF may recover following BCAS, particularly in young mice over time due to vascular remodelling (Shibata et al., 2004). Longitudinal CBF measurements are therefore important tools for assessing and comparing experimental results. This is also of particular importance as the extent of CBF reduction following BCAS can vary considerably between animals of same strain and age.

Additionally, criticism of the model is that blood flow reductions following BCAS occur acute which is not representative of chronic hypoperfusion in humans which arises gradually. An alternative model has been developed using an ameroid constrictor device which by absorption of extracellular fluid slowly induces stenosis of the carotid arteries. This approach has been employed in rats (Kitamura et al., 2012) and mice (Hattori et al., 2015) demonstrating similar results as those seen in the BCAS model. In rats the gradual occlusion model resulted in slower and less severe reductions in CBF (~30%) and selective disruption of white matter while still producing cognitive impairment (Kitamura et al., 2012). In mice, the CBF reduction was induced gradually, however, by 28 days the ameroid constrictor device had absorbed enough

fluid to completely occlude the carotid artery and the resulting pathology was therefore more severe than that produced by BCAS (Hattori et al., 2015).

1.6.2 Alternative models of chronic cerebral hypoperfusion

The two-vessel occlusion model (2VO) in rats was initially established to study VCI and did reproduce white matter disruption and cognitive imapairment (Ohta et al., 1997, Wakita et al., 2002, Farkas et al., 2004). However, acute blood flow reductions following 2VO surgery are severe (>70%) and concomitant grey matter damage is frequently observed (Tomimoto et al., 1997). Similarly severe reductions in perfusion are observed when occluding three or even four arteries (3VO/4VO) (reviewed by Jiwa et al., 2010) and occlusion models in rats should therefore be considered models of global ischaemia. Results discussed from these models will be clearly stated in the text. Occlusion of the carotid arteries in C57Bl/6J mice can only be performed transiently, as the lack of collateral blood supply means that permanent occlusion results in death (Yang et al., 1997). Unilateral common carotid artery occlusion in mice produces reductions in cerebral blood flow more representative of chronic cerebral hypoperfusion in humans (Scheff et al., 2016) and selective white matter pathology relevant to VCI (Yoshizaki et al., 2008). However, a limitation of this model is that perfusion recovers substantially over time and in one study was reported to have recovered completely by 15 days (Guo et al., 2011).

Altogether, the BCAS model in mice is well characterised and induces both pathological and behavioural features relevant to human VCI. As such it is the most suitable model at present to study pathophysiological mechanisms of chronic cerebral hypoperfusion-induced white matter disruption and cognitive impairment.

1.7 Inflammation and Oxidative stress

Potential pathophysiological mechanisms underlying white matter disruption and cognitive impairment

1.7.1 Inflammation

Inflammation is an endogenous protective response mediated primarily by microglia to prevent infection and tissue damage caused by invading pathogens, dying cells or debris (Salter and Stevens, 2017). The inflammatory response by microglia is commonly referred to as microgliosis. Microglia are capable of phagocytosis; engulfment of inflammatory stimuli, and can neutralise immune threats by generating an oxidative burst, in which free radicals in large quantities attack and destroy pathogens (Mahad et al., 2015). Further, microglia are secretory cells that

release a number of pro-inflammatory mediators aimed at recruiting and activating additional inflammatory cells (Sasaki, 2016). In the same way, astrocytes can undergo reactive astrogliosis in response to inflammatory stimuli, contributing to the secretion of inflammatory mediators and free radicals (Sofroniew, 2014b). Inflammation is a tightly regulated process, although many disease states are characterised by dysregulated and uncontrolled inflammation leading to damage of otherwise healthy tissues.

1.7.1.1 Inflammatory mechanisms detrimental to white matter

The presence of myelin debris and/or white matter hypoxia may induce gliosis of microglia and astrocytes. HIFs released in response to hypoxia enhance activity of the pro-inflammatory transcription factor Nuclear Factor κB (NF-κB) by increasing signalling and expression of Toll-Like Receptors (TLRs); proteins involved in immune cell activation (Eltzschig and Carmeliet, 2011). Further, endothelial cells express TLRs and are also activated by hypoxia/ischaemia (Anrather and Iadecola, 2016), and have therefore been suggested to induce pro-inflammatory signalling in brain-endogenous microglia, thereby contributing to a neuroinflammatory response (Liao, 2013). In addition, hypoxia (Fernando et al., 2006), endothelial cells (Liao, 2013) and innate immune cells (Rosenberg, 2017) are all capable of secreting and/or activating MMPs. These enzymes are responsible for degradation of the extracellular matrix during normal remodelling, but may aberrantly cause BBB opening and/or myelin disruption (Rosenberg, 2009), further exacerbating neuroinflammation.

1.7.2 Oxidative stress

Oxidative stress is the result of an imbalance between the production and clearance of harmful molecules called free radicals. Free radicals are molecules such as reactive oxygen or nitrogen species (ROS/RNS), produced primarily as by-products of cellular respiration in mitochondria. As previously mentioned, free radicals are also produced by inflammatory cells and through enzymes such as nicotinamide adenine dinucleotide phosphate oxidases (NAPDH-oxidases/NOXs) (Bennett et al., 2009) to combat invading pathogens. Free radicals are important cell signalling molecules but due to their high reactivity can be detrimental to lipids, proteins and DNA (Thannickal and Fanburg, 2000). Under normal conditions, antioxidant mechanisms are sufficient to prevent tissue damage by free radicals, but under pathological conditions where generation of ROS increases, antioxidant defences become overwhelmed and oxidative stress ensues (Bennett et al., 2009).

1.7.2.1 Oxidative stress mechanisms detrimental to white matter

In hypoxic white matter, oxidative stress may result from mitochondrial dysfunction which increases the production of free radicals and/or from inhibition of protein synthesis which leads to reduced antioxidant production (Liu and Zhang, 2012). As previously mentioned, an additional source of free radicals is the NOXs, recognised as major contributors to oxidative stress in vascular disease (Drummond et al., 2011). Vascular oxidative stress, in addition, disrupts cerebrovascular functions such as neurovascular coupling and endothelial-dependent vasodilation (Toth et al., 2017), potentially exacerbating hypoxia-inducing cerebral hypoperfusion and creating a vicious cycle potentiating further oxidative stress.

1.7.3 Inflammation and oxidative stress in human VCI

Neuropathological and neuroimaging studies of human VCI find markers of both inflammation (Akiguchi et al., 1997, Rosenberg et al., 2001, Cagnin et al., 2001, Olsson et al., 2013) and oxidative stress (Gackowski et al., 2008, Gustaw-Rothenberg et al., 2010, Li et al., 2010, Back et al., 2011).

A post mortem microarray study found that gene expression related to the immune response was altered in white matter lesions (Simpson et al., 2009), and microglial responses in particular are observed (Akiguchi et al., 1997, Simpson et al., 2007a, Simpson et al., 2007b). Rather than reactive astrogliosis, human VCI studies more commonly exhibit astrocyte degeneration, referred to as clasmatodendrosis (Akiguchi et al., 1997, Simpson et al., 2007a, Chen et al., 2016). This is a process of irreversible astrocyte damage thought to result from acidosis and energy failure induced by mitochondrial inhibition (Hase et al., 2017). However, studies show that astrogliosis occurs in response to ischaemia and in other inflammatory white matter diseases such as multiple sclerosis (Sofroniew and Vinters, 2010), and it is possible that clasmatodendrosis observed in human VCI post mortem tissue represents end-stage of disease.

Markers of oxidative DNA damage can be detected in CSF of humans with mixed VCI/AD (Gackowski et al., 2008) and markers of oxidative lipid damage are higher in the plasma of patients with VCI compared to both AD and control (Gustaw-Rothenberg et al., 2010), perhaps indicating the higher burden of white matter disruption. Similarly, low-density lipoprotein cholesterol (LDL) in plasma of VCI patients was found to show greater oxidative modification compared to AD and control LDL, which was also correlated to the level of cognitive impairment (Li et al., 2010). Finally, free radical injury of axonal membranes and myelin measured in post mortem

tissue was found to be increased independent of AD (Back et al., 2011), suggesting it is a more important mechanism in VCI.

Evidence from human studies clearly implicate inflammation and oxidative stress in VCI suggesting these are potential pathophysiological mechanisms whereby white matter disruption occurs. To investigate if these mechanisms are causal or secondary to the observed pathology and cognitive impairment, preclinical models of VCI such as the BCAS model of cerebral hypoperfusion in mice are invaluable.

1.7.4 Inflammation and oxidative stress in the BCAS model of cerebral hypoperfusion

Our group has demonstrated using the BCAS model in mice, that pro-inflammatory gene signalling in white matter is increased as early as 3 days post-surgery (Reimer et al., 2011), likely in response to the reduced tissue oxygen tension indicative of hypoxia (Duncombe et al., 2017). Furthermore, increases in the number of white matter microglia can be detected between 7-30 days post-BCAS (Fowler et al., 2017, Coltman et al., 2011, McQueen et al., 2014). We find that only microglia are significantly increased at 1 month in the corpus callosum, whereas the number of astrocytes is unchanged (McQueen et al., 2014). Reactive astrogliosis (density of astrocytes) is significant in the corpus callosum at 3 months post-BCAS (Kitamura et al., 2017), and in subcortical grey matter at 6 months (Holland et al., 2015). This is in contrast to the original study describing the model that found microgliosis paralleled by astrogliosis as early as 14 days (Shibata et al., 2004). Microglial changes were detected at 7 days when astrocytes were still unchanged suggesting that the microglial response occurs initially. Additional studies report increases in both micro- and astrogliosis at 7 days (Saggu et al., 2016) and 3 weeks post-BCAS (Dong et al., 2011) suggesting that both cell types are involved in the inflammatory response when CBF is reduced. The discrepancies between our group and others may be due to differences in the severity of hypoperfusion or bregma levels studied.

Studies show that inflammation in the BCAS model can be modulated using MMP inhibitors (Nakaji et al., 2006) or hypotensive agents (Washida et al., 2010, Dong et al., 2011), as well as generic immunosuppressant approaches (Qin et al., 2017, Manso et al., 2017, Fowler et al., 2017). These are associated with improved white matter structure and cognitive function and show a reduction in both micro- and astrogliosis. This highlights the contribution of inflammation to disease progression, and suggests it may play an important role in the induction of pathology. The study by Liu et al. (2013) found that absence of complement component 5 (C5); an important

inflammatory mediator, abolished white matter disruption and micro- and astrogliosis following BCAS. Another study saw that inhibition of the pro-inflammatory transcription factor NF-κB in astrocytes greatly reduced white matter disruption, microgliosis and cognitive impairment (Saggu et al., 2016). Two separate studies by our group find associations between increasing number of white matter microglia and reduced white matter structure and function (Manso et al., 2017, Fowler et al., 2017, Kitamura et al., 2017). Furthermore, anti-inflammatory pharmacological treatment that reduced the number of microglia was associated with improved function (Manso et al., 2017, Fowler et al., 2017), suggesting that microglia may drive the progressive disruption of white matter function. Astrogliosis was not evaluated in these studies though and since microglia and astrocytes both produce and respond to many of the same molecular mediators, evaluating cell-specific contributions is difficult.

Using the BCAS model in mice, Miyamoto et al. (2013) demonstrated that oxidative stress induces oligodendrocyte and OPC cell death and inhibits OPC renewal, processes which could be inhibited by the radical scavenger Edaravone. In a similar study, Dong et al. (2011) showed that oxidative stress could also be reduced by inhibition of the renin-angiotensin system using a drug previously approved for the treatment of hypertension (Aliskiren). Further, Washida et al. (2010) found that another hypotensive drug (Telmisartan) had antioxidative and anti-inflammatory effects, but only at non-hypotensive levels. The renin-angiotensin system increases expression and activity of the superoxide-producing enzyme NOX2 (Kim et al., 2012), and these studies demonstrate that inhibiting oxidative stress is associated with reduced white matter damage and gliosis.

In summary, evidence from both human and animal studies suggest that inflammation and oxidative stress may drive white matter disruption and cognitive impairment in cerebral hypoperfusion and VCI. The studies in this thesis will build on the existing literature and interrogate the role of inflammation and oxidative stress in white matter structural and functional disruption using the BCAS model of chronic cerebral hypoperfusion, by studying regulatory mechanisms that may inform future treatment.

1.8 Targeting inflammatory and oxidative stress mechanisms To prevent the disruption of white matter structure and function

Inflammation and oxidative stress are interrelated mechanisms that share triggers and are involved in many of the same pathologies, ultimately aggravating one another and subsequent damage. As such the therapeutic potential of targeting both together

may exceed that which has been achieved by previous separate approaches. With the development of highly specific transgenic models and pharmacological agents, cell-specific contributions to inflammation and oxidative stress in white matter disruption can begin to be addressed.

1.8.1 Nuclear factor erythroid 2-related factor 2 (Nrf2)

Both brain and body possess endogenous regulatory mechanisms to prevent chronic inflammation and oxidative stress. One such mechanism is mediated via Nuclear factor erythroid 2-related factor (Nrf2), also called the master regulator of anti-inflammatory and antioxidant defences. Nrf2 is a basic leucine zipper transcription factor (Moi et al., 1994) consisting of 7 Nrf2-ECH homology domains (Neh) (Itoh et al., 1999, Dinkova-Kostova et al., 2018) (Fig 1.5), first isolated and described in the early 1990's (Andrews et al., 1993, Moi et al., 1994). Nrf2 has been shown to regulate the expression of over 200 cytoprotective genes (Ishii et al., 2000, Lee et al., 2003), and is important not only for cellular protection against oxidants and pro-inflammatory molecules, but also to maintain mitochondrial function and protein homeostasis (Dinkova-Kostova et al., 2018).

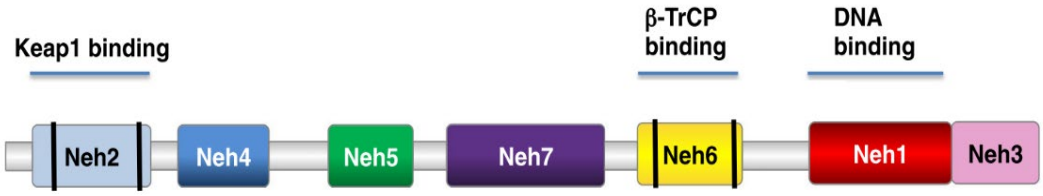

Figure 1.5 Domain structure of Nrf2. The Neh2 domain binds to Keap1, Neh6 to β-TrCP and Neh1 binds to ARE on target genes. Adapted from (Dinkova-Kostova et al., 2018).

Nrf2 acts primarily by binding to the highly conserved antioxidant response element (ARE) found in the promoter region of antioxidant, detoxifying and anti-inflammatory genes (Rushmore et al., 1991, Venugopal and Jaiswal, 1996, Itoh et al., 1997, Piantadosi et al., 2011, reviewed by Raghunath et al., 2018), but has also been shown to inhibit the activity of NF-κB (Thimmulappa et al., 2006, Cuadrado et al., 2014), and directly inhibit the expression of pro-inflammatory genes in a non-ARE-dependent manner (Kobayashi et al., 2016) (Table 1.1).

1.8.1.1 Molecular basis of the Nrf2 system

Nrf2 is a cytoplasmic protein which under normal conditions is rapidly turned over through proteosomal degradation mediated by the ubiquitin ligase adaptors Keap1 (Kelch-like ECH-associated protein-1) (Itoh et al., 1999, Itoh et al., 2003) and βTrCP

(beta-transducin repeat containing protein), the latter dependent on GSK3β (glycogen synthase kinase 3β)-dependent phosphorylation of Nrf2 (Rada et al., 2012) (Fig 1.6). In response to cellular stressors such as oxidative stress and inflammation, conformational change of cysteine residues on Keap1 or direct inhibition of Nrf2-binding sites on Keap1 (Yamazaki et al., 2015) or GSK3β (Gameiro et al., 2017) leads to the disruption of Nrf2-degradation. As a result, newly synthesised Nrf2 is free to translocate to the nucleus where it binds to AREs (mediated by small Maf proteins (Itoh et al., 1997)) and thereby activates the transcription of cytoprotective genes (Fig 1.6) (Table 1.1). As the cellular stress is resolved through antioxidant, detoxifying or anti-inflammatory mechanisms, Keap1 and GSK3β/TrCP-dependent degradation resumes, completing the negative feedback loop which regulates the Nrf2 system (Yamazaki et al., 2015, Cuadrado, 2016).

Further mechanisms of Nrf2 regulation have been described, including phosphorylation of Nrf2 by stress-sensing kinases promoting the dissociation of Nrf2 from Keap1 and subsequent nuclear translocation (Kobayashi and Yamamoto, 2006) as well as epigenetic repression and modification of Nrf2 (Bell et al., 2015, Guo et al., 2015). Finally, it has also been demonstrated that NF-κB activation induces Nrf2 activation in a negative feedback loop, and the crosstalk between the two transcription factors is considered an important mechanism for regulating inflammation (Cuadrado et al., 2014).

Table 1.1 Subset of Nrf2-regulated genes

Gene	Accession no.	ARE-regulated	Function	Citation
Induced				
Gclm	U95053	Yes	Antioxidant/reducing potential	(Lee et al., 2003)
Gclc	U85414	Yes	Antioxidant/reducing potential	(Lee et al., 2003)
Ho1	X56824	Yes	Antioxidant/reducing potential	(Lee et al., 2003)
Trdx	X77585	Yes	Antioxidant/reducing potential	(Lee et al., 2003)
Gpx4	D87896	Yes	Antioxidant/reducing potential	(Lee et al., 2003)
Slc7a11	AI451155	Yes	Detoxification	(Shi et al., 2016a)
Nqo-1	U12961	Yes	Detoxification	(Lee et al., 2003)
Gsta4	L06047	Yes	Detoxification	(Lee et al., 2003)
Gstp1	X53451	Yes	Detoxification	(Lee et al., 2003)
Clec4d	AF061272	Yes	Defense/immune/inflammation	(Lee et al., 2003)
Pla2g7	U34277	Yes	Defense/immune/inflammation	(Lee et al., 2003)
Mmp12	M82831	Yes	Defense/immune/inflammation	(Lee et al., 2003)
Il10	NP_034678	Yes	Defense/immune/inflammation	(Piantadosi et al., 2011)
Inhibited				
Il6	NM_031168	No	Pro-inflammatory	(Kobayashi et al., 2016)
Il1β	NM_008361	No	Pro-inflammatory	(Kobayashi et al., 2016)

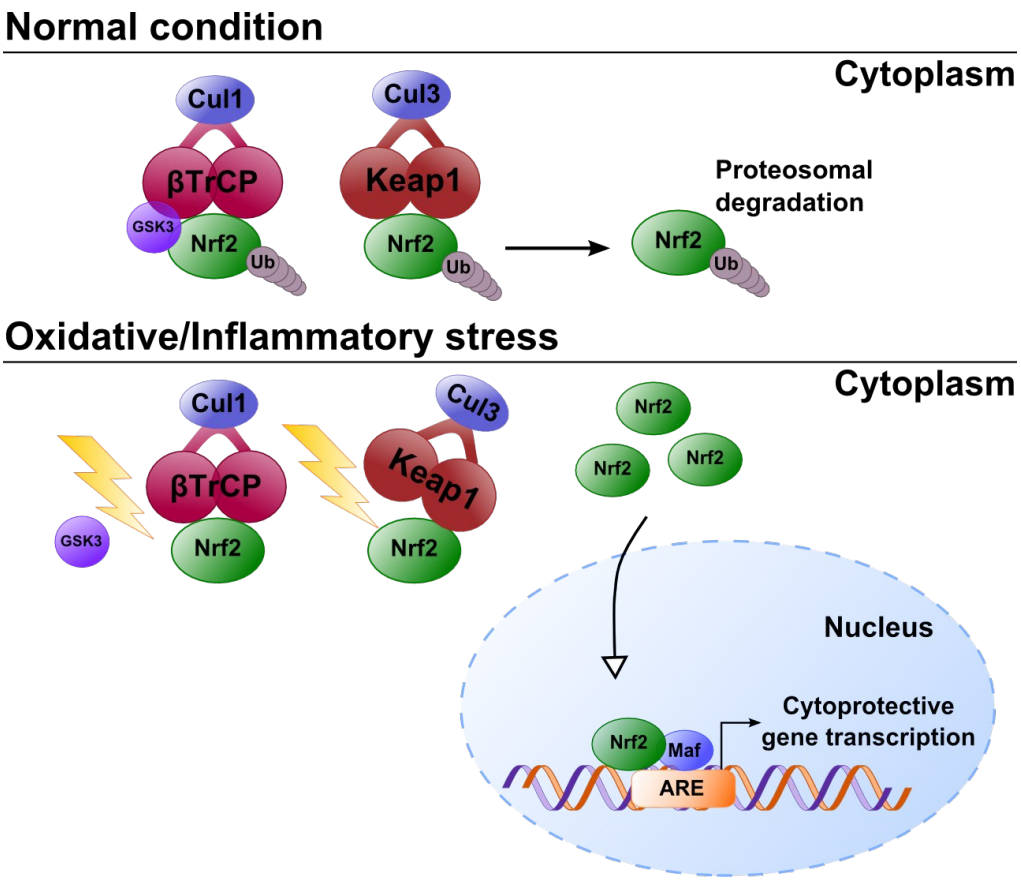

Figure 1.6 Molecular basis of the Nrf2-system. In the normal condition, Nrf2 is rapidly turned over by proteosomal degradation mediated by ubiquitin ligase adaptors Keap1 and βTrCP. Oxidative and inflammatory stress disrupts Keap1/ βTrCP-Nrf2 interactions which allows newly synthesised Nrf2 to translocate to the nucleus where it binds antioxidant response elements (AREs) found in the promoter region of cytoprotective genes, inducing their transcription to combat the cellular stress.

1.8.1.2 Nrf2 is highly expressed by astrocytes in the central nervous system

Astrocytes have been shown to express Nrf2 at levels greatly exceeding that of neurons (Zhang et al., 2016), and neuronal antioxidant defences are intrinsically weak to permit redox-sensitive signalling necessary during development (Bell et al., 2015). *In vitro* studies demonstrate that astrocytes are necessary for Nrf2-mediated neuroprotection against oxidative stress (Lee et al., 2003, Shih et al., 2003, Kraft et al., 2004), and are thought to provide the antioxidant support that neurons themselves lack. A mouse model overexpressing Nrf2 specifically in astrocytes (GFAP-Nrf2) was therefore developed to investigate the therapeutic potential of boosting astrocytic Nrf2-signalling *in vivo* (Vargas et al., 2008).

1.8.1.3 Nrf2 in neurodegenerative and white matter disease

Because inflammation and oxidative stress are characteristic of most neurodegenerative diseases, the therapeutic potential of the Nrf2 pathway has been under investigation for almost a decade (reviewed by Joshi and Johnson, 2012, Cuadrado, 2016, Dinkova-Kostova et al., 2018). Interestingly, Nrf2 expression and transcriptional activity declines with age (Ungvari et al., 2011a, Ungvari et al., 2011b, Valcarcel-Ares et al., 2012, reviewed bySchmidlin et al., 2019), perhaps explaining age-related increased in inflammation and oxidative stress.

Nrf2 knockout studies demonstrate exacerbation of neurodegenerative pathologies *in vivo* in models of Parkinson's disease (PD) (Jakel et al., 2007, Innamorato et al., 2010, Lastres-Becker et al., 2012), familial amyotrophic lateral sclerosis (fALS) (Vargas et al., 2013) and AD (Joshi et al., 2015, Branca et al., 2017, Rojo et al., 2017, Rojo et al., 2018). Conversely, pharmacological Nrf2-activators or GFAP-Nrf2 mice, has been shown to confer neuroprotection *in vivo* in models of fALS (Vargas et al., 2008), Huntington's disease (HD) (Calkins et al., 2010), PD (Chen et al., 2009, Gan et al., 2012, Ahuja et al., 2016) and AD (Cui et al., 2017). Nrf2-activation is also protective against focal ischaemia (Zhao et al., 2006), and interestingly is endogenously activated by ischaemic preconditioning thought to underlie the resulting neuroprotection to subsequent ischaemic insults, specifically through upregulation of glutathione-related genes *Gclc, Gclm* and *Slc7a11* (*xCT*) (Bell et al., 2011a, Bell et al., 2011b) (Table 1).

Further, Nrf2 knockout mice have been shown to develop vacuolar white matter degeneration and widespread astrogliosis with advancing age. The absence of Nrf2 exacerbates demyelination in a model of the inflammatory white matter disease multiple sclerosis (experimental autoimmune encephalomyelitis (EAE)) (Johnson et al., 2010), and impairs remyelination in a model of peripheral nerve injury (Zhang et al., 2013). Together these studies indicate an important role for Nrf2 in white matter maintenance and repair similar to its role of antioxidant support for neurons. Comparable to studies activating Nrf2 in neurodegenerative disease models, pharmacological activation of Nrf2 in EAE using DMF (dimethyl fumarate) protects white matter and improves clinical scores (Linker et al., 2011), and DMF has been approved by the U.S. Food and Drug Administration (FDA) for treatment of relapsing forms of multiple sclerosis (Gopal et al., 2017). Pharmacological activation of Nrf2 using DMF or an alternative drug sulforaphane, is associated with improved white matter structure following experimental hypoperfusion (Fowler et al., 2017, Mao et al.,

2018). Genetic approaches of modulating the Nrf2-pathway more specifically have yet to be applied in cerebral hypoperfusion models and the study of the specific contributions of Nrf2-deficiency and astrocytic Nrf2 to white matter pathology in the BCAS model is entirely novel.

1.8.2 Colony-stimulating factor receptor 1

As previously mentioned, increased number of microglia is detected in human VCI (Akiguchi et al., 1997, Simpson et al., 2007a, Simpson et al., 2007b) and microglial proliferation is seen in the BCAS model of cerebral hypoperfusion, which when targeted by generic anti-inflammatory agents was associated with improved function (Manso et al., 2017, Fowler et al., 2017). However, to effectively interrogate the cell-specific contribution that microglial proliferation plays in white matter disruption a more targeted approach is required.

Microglial proliferation is dependent on signalling via the colony-stimulating factor 1 receptor (CSF1R) which is expressed on macrophage lineage cells (Pixley and Stanley, 2004). The two known ligands for the CSF1R are the cytokines colony-stimulating factor 1 (CSF1) and interleukin 34 (IL34) (Chitu et al., 2016), which upon binding the CSF1R induce autophosphorylation of the tyrosine kinase and a subsequent intracellular signalling cascade which induces gene transcription promoting survival, chemotaxis and proliferation (Conway et al., 2005). Some available pharmacological agents that target the CSF1R (e.g. PLX3397, PLX5622, Plexxikon, Ink) result in complete/partial ablation of the existing microglial population. Although studies have shown beneficial effects of ablating microglia on memory in models of AD (Dagher et al., 2015, Spangenberg et al., 2016) and on myelin integrity in EAE (Nissen et al., 2018), in different disease models such as stroke and ALS, microglial ablation is associated with worse outcome (Jin et al., 2017, Spiller et al., 2018).

As an alternative, the tyrosine kinase inhibitor GW2580, highly selective for the CSF1R, is reported to prevent the expansion of microglia without affecting the stable microglial population (Conway et al., 2005, Gomez-Nicola et al., 2013) (Fig 1.7). Inhibiting CSF1R using GW2580 treatment has proven advantageous in disease models of AD (Olmos-Alonso et al., 2016), prion disease (Gomez-Nicola et al., 2013) and multiple sclerosis (Crespo et al., 2011), although the role of CSF1R signalling following cerebral hypoperfusion remains to be determined. GW2580 treatment provides a cell-specific approach to investigate the effect of CSF1R signalling in microglia on white matter disruption and cognitive impairment.

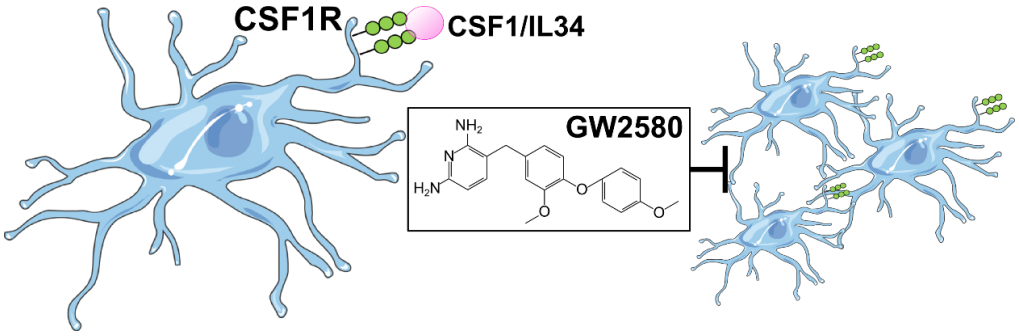

Figure 1.7 GW2580 inhibits colony-stimulating factor 1 receptor (CSF1R) signalling. Binding of colony-stimulating factor 1 (CSF1) or interleukin 34 (IL34) induces proliferation, survival, chemotaxis and gene transcription of microglia. The pharmacological agent GW2580 inhibits CSF1R signalling and is reported to inhibit microglial proliferation without affecting the stable microglial population (Gomez-Nicola et al., 2013).

1.9 Summary

Vascular cognitive impairment is a heterogeneous disorder with a tremendous unmet need for mechanistic understanding and development of successful therapies. Bilateral carotid artery stenosis-induced cerebral hypoperfusion is an experimental model of VCI which replicates important aspects of pathology and cognitive impairment and as such represents a highly appropriate tool for preclinical studies. Inflammation and oxidative stress have been associated with disease progression in both VCI and experimental hypoperfusion and this thesis will assess to what extent these mechanisms are key drivers of white matter disruption that may be targeted therapeutically. The Nrf2 pathway represents a promising therapeutic approach for the treatment of VCI with the potential to reduce both inflammation and oxidative stress simultaneously to preserve white matter structure and function. Using sophisticated genetic tools the studies herein aim to investigate the role of Nrf2 in the maintenance of white matter and cognitive function in the bilateral carotid artery stenosis model of VCI. Further, increases in microglia is commonly observed in human VCI and microglial proliferation is closely associated with white matter structural and functional disruption in the animal model. The final aim is therefore to investigate whether CSF1R signalling in microglial specifically drive the disruption of white matter structure and function in the bilateral carotid artery stenosis model of VCI, using highly selective pharmacological inhibition (GW2580).

1.10 Hypothesis

The hypothesis of the present thesis is that oxidative stress and inflammatory mechanisms drive structural and functional white matter disruption induced by bilateral carotid artery stenosis in mice (Fig 1.8).

1.11 Aims

The following aims were investigated to address the above hypothesis (Fig 1.8):

1. Assess the effect of Nrf2 deficiency on white matter pathology and cognitive alterations in the BCAS model in mice.
2. Assess the effect of astrocytic overexpression of Nrf2 on white matter pathology and cognitive alterations in the BCAS model in mice.
3. Assess the effect of inhibiting CSF1R signalling in microglia on white matter pathology and cognitive alterations in the BCAS model in mice.

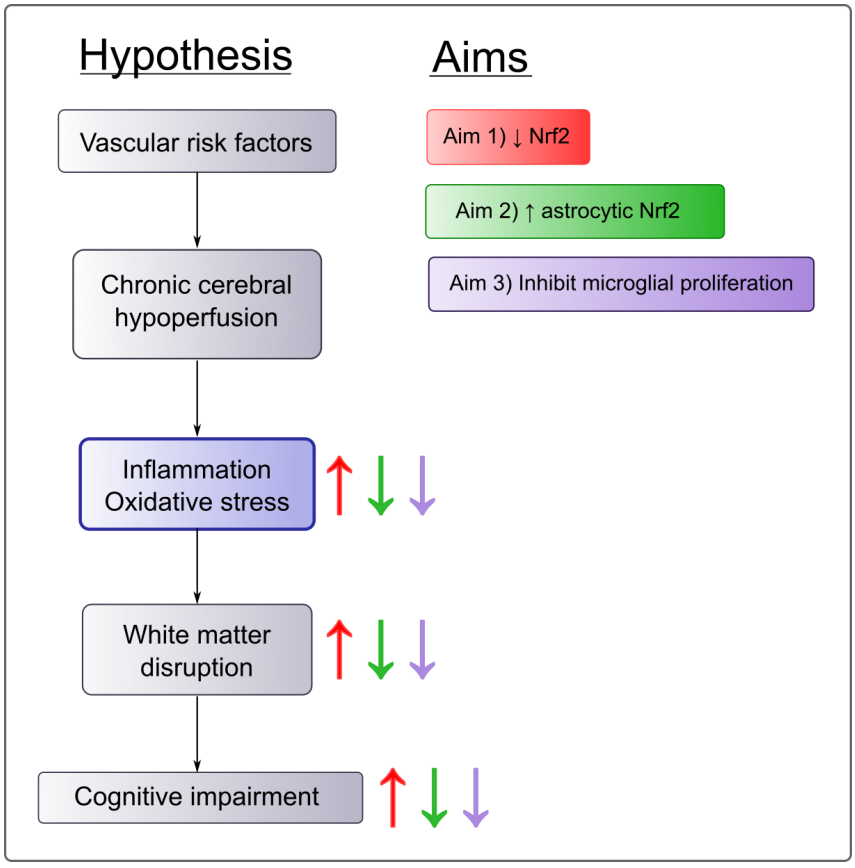

Figure 1.8 Hypothesis and aims. Red arrow indicates the prediction that reduced Nrf2 (Aim 1) will increase inflammation and oxidative stress and result in exacerbated white matter disruption and cognitive impairment. The green and purple arrow indicates the prediction that increased astrocytic Nrf2 (Aim 2) or inhibition of CSF1R signalling in microglial (Aim 3) will reduce inflammation and oxidative stress and result in ameliorated white matter disruption and cognitive impairment.

Chapter 2

Materials & Methods

2.1 Animals

All animals were group housed on a 12-hour light/dark cycle with *ad libitum* access to food and water unless otherwise stated due to experimental requirements. All experiments were conducted in accordance with the Animal (Scientific Procedures) Act 1986 and local ethical approval at the University of Edinburgh, and were performed under personal and project licences granted by the Home Office. Experimenters were blinded to genotype and surgery status of all animals throughout data collection and analysis in accordance with ARRIVE guidelines (Kilkenny et al., 2010).

2.1.1 Nrf2 knock out mice

The Nrf2 knock out (KO) line was originally developed by Yuet Wai Kan at University of California in San Francisco. The Nrf2 gene was knocked out it in embryonic stem cells (129X1/SvJ) by homologous recombination and used to derive the line, of which homozygotes were found to develop normally and were fertile (Chan et al., 1996). Adult male Nrf2 KO mice were obtained from The Jackson Laboratory (strain name = B6.129X1-Nfe2l2tm1Ywk/J; backcrossed onto C57Bl/6 mice for at least 10 generations) and re-derived in house. Imported homozygous $Nrf2^{-/-}$ mice were crossed onto wild type C57Bl/6J and heterozygous progeny was further crossed to generate the experimental animals utilised in chapter 3.

2.1.1.1 Genotyping of Nrf2 knock out mice

DNA was extracted from tail biopsies using ethanol precipitation. Each biopsy was incubated overnight in 20 µl PCR buffer (10X; Tris·Cl, KCl, $(NH_4)_2SO_4$, 15 mM $MgCl_2$, QIAGEN), 4 µl Proteinase K (ThermoFisher) and 164 µl nuclease-free H_2O (QIAGEN) at 55^0C followed by heat inactivation at 95°C for 15 min after which samples were placed on ice for 10 min. Samples were then vortexed and centrifuged at 18,000 x g for 10 min at room temperature and supernatant transferred to a chilled Eppendorf tube. The volume was made up to 200 µl with nuclease-free H_2O and 20 µl of 3M Sodium Acetate (pH 5.2, Sigma-Aldrich) was added and mixed by inverting the tube. 440 µl of cold (-20°C) absolute ethanol (VWR) was added and the tube inverted several times before incubating at -20°C for >3 hours. Samples were then centrifuged at 18,000 g for 15 min at 4°C and supernatant carefully discarded leaving the DNA pellet at the bottom of the tube. The DNA pellet was washed with 400 µl of cold (-20°C) 70% Ethanol and vortexed well. A final centrifugation at 18,000 x g for 15 min at 4°C was performed before discarding ethanol and allowing the DNA pellet to air

dry. DNA was then resuspended in 20 µl nuclease-free H_2O and incubated at 37°C overnight then stored at -20°C until PCR.

Polymerase chain reaction (PCR) was performed using QIAGEN HotStarTaq; 10 µl added to 3.2 µl of each sample along with 5.3 µl PCR grade H_2O and 0.5 µl of each of three primers (Sigma-Aldrich, Table 2.1) for a final primer concentration of 0.25 µM. The PCR program was as follows; 95°C for 15 min followed by 10 cycles of 20 sec at 94°C, 45 sec at 65°C, 45 sec at 68°C; then 28 cycles of 15 sec at 94°C, 45 sec at 50°C, 45 sec at 72°C; finished with 2 min at 72°C and 5 min at 10°C.

Samples were then run (with 4 µl of loading dye (6X, Promega)) on a 3% agarose gel (Agarose, Promega; in Tris/Borate/EDTA buffer, Sigma-Aldrich) with 15 µl Invitrogen™ SYBR™ Safe stain (ThermoFisher Scientific) at 100 V for 1 hours. Wild type animals displayed one band of 262 base pairs (bp; Nrf2), $Nrf2^{+/-}$ animals displayed two bands, one at 262 bp and another and 400 bp (mutant band) and $Nrf2^{-/-}$ one band at 400 bp (no Nrf2 band).

All animals were re-genotyped at the end of the study to verify genetic status.

2.1.2 GFAP-Nrf2.2 mice

GFAP-Nrf2.2 mice were imported from Professor JA Johnson, University of Wisconsin, and developed as previously described (Vargas et al., 2008). Briefly, a human GFAP-Nrf2 transgene was introduced into mice through pronuclear microinjection using fertilised eggs of the FVB/N strain. Imported GFAP-Nrf2 mice were crossed with wild type C57Bl/6J mice in-house, and first generation crosses (FVB/C57Bl/6J F1) were utilised for experiments in chapter 4.

2.1.2.1 Genotyping of GFAP-Nrf2 mice

DNA was extracted from ear clips using 100 µl 50mM sodium hydroxide. Ear clips with sodium hydroxide were centrifuged for 90 sec at 12,000 x g. Samples were then incubated in a water bath at 100°C for 7 min and then kept on ice for 10 min and were then ready for PCR.

PCR was performed using GoTaq® Green Master Mix (Promega); 12.5 µl added to 1 µl of each sample along with 10.5 µl PCR grade H_2O and 0.25 µl of each of four primers (Sigma-Aldrich, Table 2.1) for a final primer concentration of 25 mM. The PCR program was as follows; 95°C for 5 min followed by 35 cycles of 30 sec at 95°C, 30 sec at 54°C, 30 sec at 72°C; finalised by 5 min at 72°C and held at 4°C.

Samples were then run on a 3% agarose gel (Agarose, Promega; in Tris/Borate/EDTA buffer, Sigma-Aldrich) with 15 µl Invitrogen™ SYBR™ Safe stain (ThermoFisher Scientific) at 100 V for 1 hours. Wild type animals displayed one band

of 262 bp (Nrf2) and GFAP-Nrf2 animals displayed two bands, one at 262 bp (Nrf2) and one at 400 bp (human GFAP).

All animals were re-genotyped at the end of the study to verify genetic status.

Table 2.1 Primers used for genotyping

Nrf2 knock out primers	Sequence (5' → 3')
Common forward (13444)	GCC TGA GAG CTG TAG GCC C
Wild type reverse (13445)	GGA ATG GAA AAT AGC TCC TGC C
Mutant reverse (oIMR8495)	GAC AGT ATC GGC CTC AGG AA
GFAP-Nrf2 primers	
Nrf2 forward	GCC TGA GAG CTG TAG GCC C
Nrf2 reverse	GGA ATG GAA AAT AGC TCC TGC C
GFAP forward	CTT CAT AAA GCC CTC GCA TC
GFAP reverse	TCT TGC CTC CAA AGG ATG TC

2.1.3 C57Bl/6J wild type mice

Wild type C57Bl/6J were purchased from Charles River Laboratories (JAX^{TM-} C57BL/6J) and utilised for experiments in chapter 5.

2.2 Chronic cerebral hypoperfusion

Bilateral carotid artery stenosis (BCAS) surgery (as previously described by Coltman et al., 2011, and as developed by Shibata et al., 2004) was used to induce chronic cerebral hypoperfusion. In brief, a small cervical midline incision was made and the common carotid arteries were exposed by careful dissection and displacement of the superficial muscles, surrounding connective tissue and the vagus nerve. A 0.16 or 0.18 mm internal diameter microcoil (Sawane Spring Co, Japan. Fig 2.1b) was placed around one common carotid artery (Fig 2.1a), the animal was allowed to recover and was 30 min later re-anesthetised for the placement of the second microcoil (0.18 mm). Sham surgery was performed in the same manner excluding the placement of the microcoils. The incision was sutured and animals were allowed to recover in a heated incubator. All surgical procedures were conducted using aseptic techniques while under isoflurane anaesthesia (5% induction, 1.5% maintenance), and animals were closely monitored 72 hours post-surgery. Surgeries were performed by Prof Karen Horsburgh or Dr Jessica Duncombe (specified in relevant chapters).

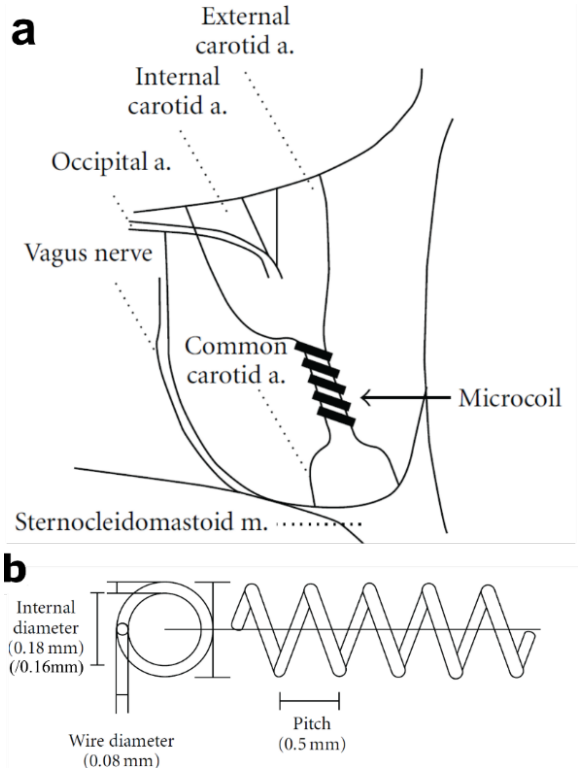

Figure 2.1 Bilateral carotid artery stenosis. (a) Schematic diagram of microcoil around the common carotid artery below the carotid bifurcation. **(b)** Schematic diagram of the microcoil. (Adapted from Ihara and Tomimoto, 2011)

2.3 Laser speckle imaging

Laser speckle imaging is a technique that generates semi-quantitative measurements of superficial cortical perfusion through the intact mouse skull. A speckle contrast imager with a laser source and a camera is mounted above a stereotactic frame. The camera detects the reflected laser light which has a characteristic speckle pattern depending on the velocity of the underlying particles which is then converts to an arbitrary unit by computer software.

Superficial cortical perfusion was measured at rest under isoflurane anaesthesia prior to, 24 hours and 6 weeks post-BCAS surgery, using a moorFLPI2 speckle contrast imager (Moor Instruments, UK). The animal's head was held in position using a stereotactic frame and body temperature was monitored and maintained at 37°C using a heated pad. The skull was exposed by a midline incision and reflection of the scalp. Water-based gel was evenly spread on the exposed skull and a 2 min baseline perfusion recording was acquired. The scalp was then sutured, and local analgesic applied to reduce any pain or discomfort to the animals which were recovered in a heated incubator.

2.3.1 Laser speckle image analysis

An arbitrary flux measure was obtained by manually placing regions of interest in the same place on consecutive scans using large vessels as landmarks (moorFLPI-2 V1.0 software). Due to biological variation, the cortical cerebral blood flow (CBF) of each animal was normalised to its own baseline measurement which was obtained prior to surgery and data were then expressed as percentage CBF of baseline.

2.4 Behavioural testing

Animals were handled extensively, every day for 1-2 weeks, prior to the start of each behavioural test to habituate the animals to the experimenters and to facilitate the avoidance of anxious behaviour which may influence performance.

2.4.1 Radial arm maze

Spatial working memory in chapter 3 and 4 (Nrf2 studies) was assessed using the 8-arm radial arm maze. Animals were singly housed and food restricted (maintained at 85-90% of initial body weight) one week prior to, and throughout the radial arm maze test, to promote motivation (12-hour light/dark cycle, *ad libitum* access to water). Following the last trial animals were provided food *ad libitum*. The radial arm maze test was commenced four weeks post-BCAS.

The radial arm maze comprises a central platform (20 cm in diameter) surrounded by 8 arms (47 cm long by 7 cm wide with 20 cm Plexiglas walls) (Fig 2.2a). Each arm has a 2 cm deep plastic well for placement of a sugar pellet and all arms can be isolated from the central platform by Plexiglas doors (remotely controlled using Any-Maze software, Stoelting, UK). Large brightly coloured, high contrast spatial cues were placed on each of the four walls surrounding the maze, and a camera mounted on the ceiling was used for data acquisition connected to Any-Maze tracking software (v4.99, Stoelting Europe, Ireland).

The aim of the radial arm maze is to assess the animals' ability to remember arms entered during each trial in order to retrieval all eight pellets (enter all eight arms) with as few revisiting errors as possible.

2.4.1.1 Acclimatisation phase

Pre-training is required to acclimatise the animals to the test and environment to reduce stress and anxiety. This consisted of one 5 min trial of free exploration with sugar pellets scattered at random, and another where each animal was allowed to walk down each arm from the central platform to retrieve sugar pellets from the plastic wells. These two trials were performed on two consecutive days.

2.4.1.2 Learning phase

The behavioural test was carried out on 16 consecutive days (1 trial/day). Each arm was baited with a sugar pellet and the animal was placed in the central platform at the start of the trial. The animal was confined to the central platform for 5 sec between each arm choice and the trial finished when the animal had retrieved all 8 pellets or when 25 min had elapsed. The number of revisiting errors (visits into unbaited arms) during each trial were recorded and analysed as a measure of spatial learning and working memory.

2.4.1.3 Inclusion criteria

Animals needed to explore more than 75% of the maze during 2 of the first 4 trials to be included in the behavioural analysis of the radial arm maze as less implies a lack of motivation which results in a skewed learning profile. Details of exclusions are described in relevant chapters.

2.4.2 Y-maze

Animals were placed in the centre of a standard Y-maze (3 arms; 49.5 cm long, 11 cm wide, walls 10 cm high) (Fig 2.2b) and allowed to freely explore the three arms for 5 min. The percentage of spontaneous alternation and total number of arm entries were recorded and analysed as a measure of innate exploratory behaviour and overall

mobility. The Y-maze test was performed after the radial arm maze in the same room using the same spatial cues and data acquisition system described in 2.4.1 (Any-Maze tracking software (v4.99, Stoelting Europe, Ireland)).

2.4.3 Barnes maze

Spatial learning and reference memory in chapter 5 was assessed using the Barnes maze (Barnes, 1979). The maze is a simple circular white platform (115 cm high x 91.5 cm wide) with 20 “escape holes” evenly situated around the edge (San Diego Instruments) (Fig 2.2c). A small, black escape chamber was placed under one of the holes; position alternated for consecutive animals to avoid olfactory cues influencing behaviour, and a holding cylinder (10.5 cm in diameter) was used to place the animals in the maze before each trial. The maze was brightly lit, and an aversive noise was played to motivate animals to escape. The same spatial cues and data acquisition system described in 2.4.1 were used for animals to navigate the environment and to record mouse behaviour (Any-Maze tracking software (v4.99, Stoelting Europe, Ireland)). The Barnes maze was commenced four weeks post-BCAS.

The aim of the Barnes maze is to assess the animals’ ability to learn and remember the location of the escape chamber. Spatial learning was assessed during an initial learning phase and reference memory in a 72 hour probe test. Executive function and cognitive flexibility were tested in a reversal learning phase and an additional 72 hour probe test.

2.4.3.1 Acclimatisation phase

In order to prevent stress and anxiety associated with a novel environment, animals were acclimatised to the Barnes maze and the behavioural room. During acclimatisation there were no bright lights or aversive noise. For two consecutive days, animals were placed in the holding cylinder for 10 sec, and then returned to their home cage. On the third day, animals were again placed in the holding cylinder for 10 sec but this time the cylinder was removed, and the animals were allowed to freely explore the maze for 3 min. Following the 3 min, animals were gently guided into the escape chamber where they were kept for 1 min before being returned to their home cage.

2.4.3.2 Learning phase

The day after the acclimatisation phase was the start of the learning phase. Animals were trained during two trials every day, with a 1 hour trial interval, over 6 consecutive days. Briefly, animals were placed in the holding cylinder for 10 sec, the

cylinder was removed, and an aversive noise started playing (85db) while animals were allowed 3 min to locate and enter the escape chamber. If animals were unable to locate the escape chamber during the 3 min they were gently guided to it and kept in the chamber for 1 min before being returned to their home cage. As soon as the mouse entered the escape chamber the aversive noise ceased. All maze equipment was cleaned with 70% ethanol between each animal, and the escape chamber was carefully cleaned with ethanol and rinsed with water to avoid aversive alcohol vapours building up. Latency to escape was recorded and analysed as a measure of spatial learning.

2.4.3.3 72 hour probe

Long-term spatial memory was assessed using a probe test 72 hours after the final trial of the learning phase. Conditions were kept constant with the learning phase, however the escape chamber was removed, and the animals were only allowed to explore the maze for 90 sec. Memory was assessed as the proportion of time spent in the target quadrant, i.e. where the escape chamber was located during the learning phase. Because a large proportion of animals spent some time in the target quadrant but then re-commence exploring as there was no escape chamber, the probe test analysed the proportion of time spent in the target quadrant during the first 60 sec.

2.4.3.4 Reminder phase

Animals were subjected to two additional trials with the escape chamber returned to the original position to re-establish the chamber location memory following the probe trial. Conditions and trial duration were kept constant with the learning phase.

2.4.3.5 Reversal learning phase

To test executive function and cognitive flexibility, the chamber location was shifted 180° to the opposite side of the maze, with spatial cues remaining in the same positions. Conditions and trial duration were kept constant with the learning phase, and the reversal learning phase was performed twice a day for 3 days (1 hour trial interval). Latency to escape was again recorded and analysed as a measure of re-learning, i.e. cognitive flexibility.

2.4.3.6 Reversal 72 hour probe

Performed exactly like the 72 hour probe, the escape chamber was removed and animals were allowed to explore the maze for 90 sec. Similarly, the proportion of time spent in the new target quadrant was used to assess long-term memory of the reversal learning phase chamber location. Because a large proportion of animals spent some time in the target quadrant but then re-commence exploring as there was

no escape chamber, the probe test was analysed as a proportion of time spent in the target quadrant during the first 60 sec.

2.4.3.7 Inclusion criteria

Animals need to be motivated to actively explore the maze in order to locate the escape chamber, and they need to learn that the task is to locate and enter the escape chamber. Inclusion criteria were therefore as follows; animals must enter a minimum of 3 quadrants in 2 of the first 5 learning phase trials and animals must voluntarily enter the escape chamber at least 3 out of the final 6 trials to demonstrate that they have learned the task objective. Details of exclusions are detailed in the relevant chapter.

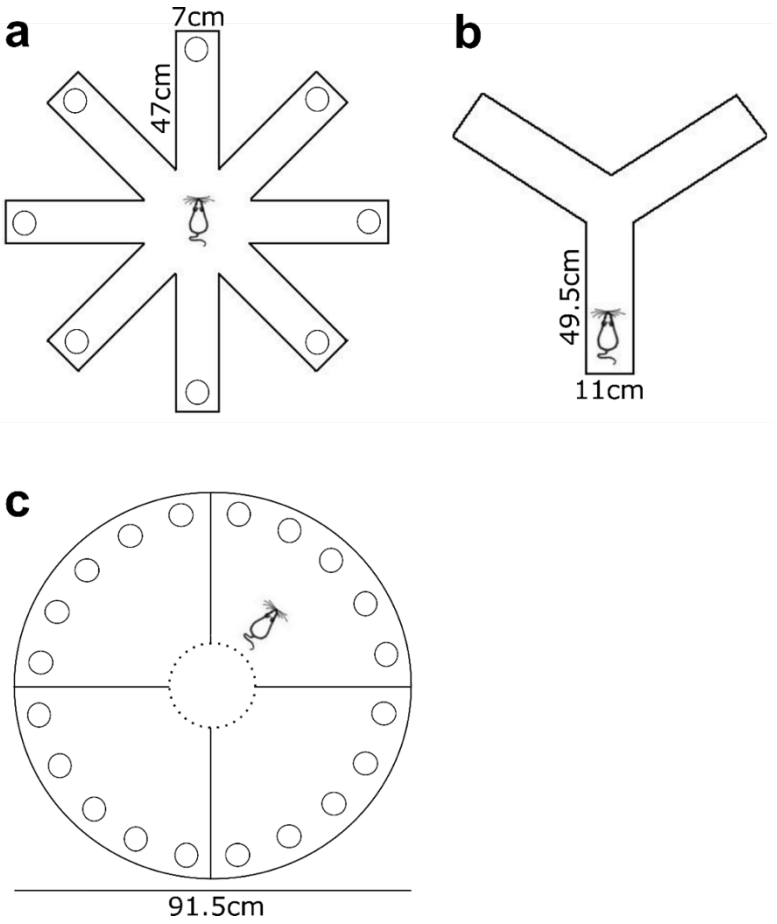

Figure 2.2 Schematic diagrams of mazes used for behavioural testing. (a) 8-arm radial arm maze with central platform that measures 20 cm in diameter, each of the 8 arms measures 47 cm by 7 cm and have 20 cm tall Plexiglas walls. The plastic wells at the end of each arm are 2 cm deep. **(b)** Y-maze with 3 arms measuring 49.5cm by 11cm with solid white walls 10cm high. **(c)** Barnes maze sits 115 cm above ground and is 91.5cm in diameter. 20 escape holes are situated along the edge of the maze, and the escape chamber is positioned under one of those holes. The dotted line represents the position of the holding cylinder at the start of each trial.

2.5 Substance administration

2.5.1 GW2580 administration

GW2580 is a pharmacological tyrosine kinase inhibitor for the CSF1 receptor (CSF1R) found on macrophage lineage cells including brain resident microglia.

GW2580 (LC Laboratories, PKC Pharmaceuticals Inc., USA) was administered by oral gavage (Chapter 5 acute study) at a concentration of 75mg/kg in 0.5% Hypromellose (H3785, Sigma-Aldrich) and 0.1% Tween®80 (P1754, Sigma-Aldrich), once daily starting 24 hours post-BCAS. The vehicle solution was prepared with the same reagents and administered in an identical manner to drug administration. Alternatively GW2580 was administered at 0.1% concentration in diet (LC Laboratories, PKC Pharmaceuticals Inc., USA and Test Diet Europe) (Chapter 5 chronic study) *ad libitum* starting 24 hours post-BCAS.

2.5.2 5-Bromo-2'-deoxyuridine (BrdU) administration

5-Bromo-2-'-deoxyuridine (BrdU, B5002, Sigma-Aldrich) was administered orally at 50mg/kg for the final three days (of the acute and chronic study in Chapter 5) to label actively proliferating cells. For the GW2580-treated animals in the acute study, BrdU was added to the GW2580 gavage solution as described in 2.5.1. For all other animals, BrdU was prepared in vehicle solution as described in 2.5.1.

2.6 Tissue collection and processing

2.6.1 Transcardial perfusion and brain extraction

Animals from the studies described in chapter 3 and 4 were sacrificed under deep anaesthesia (induction at 5% isoflurane, maintenance at 3%) by transcardiac perfusion with 40 ml of 0.9% heparinised (0.002%) phosphate buffered saline. The heart was exposed through a midline incision, a needle was inserted into the left ventricle and the right atrium was opened with scissors. Perfusions were performed at 2 ml/min until blood and tissues cleared.

Brain tissue was then removed and separated into hemi brains down the midline using a blade. One hemi brain was snap frozen in liquid nitrogen. The other was fixed in 4% paraformaldehyde for 24 hours and further processed automatically for paraffin embedding or manually for freezing.

2.6.2 Brain extraction and white matter dissection

Animals from the study in chapter 5 were sacrificed by dislocation of the neck by Dr Edel Hennessy/Dr Juraj Koudelka. Brains were rapidly removed and transferred to ice-cold artificial cerebrospinal fluid. Dr Hennessy/Koudelka sectioned 2 mm of the

forebrain from which corpus callosum was isolated under a dissecting microscope and snap frozen in liquid nitrogen (by ES). Dr Hennessy/Koudelka sectioned the brain further using a vibratome (Hyrax V50) and a 1.6 mm slice was collected at -1.65 mm posterior of bregma (according to Paxinos and Franklin, 2001) in a Cellsafe+ Biopsy Capsule (Cell Path) for fixation in 4% paraformaldehyde for 24 hours and further processed manually for paraffin embedding.

2.6.3 Processing for freezing and cryosectioning

For the study in chapter 3, hemi brains were transferred from 4% paraformaldehyde to 30% sucrose for 72 hours, then frozen in isopentane chilled to -42°C using dry ice. 10 µm coronal sections were collected onto superfrost plus slides (VWR International) at -1.70 mm posterior of bregma (according to Paxinos and Franklin, 2001) using a cryostat (Leica CM1950), and the rest of the hemi brain cut at 30 µm coronal sections and stored in cryoprotective medium at -20°C.

2.6.4 Automated processing for paraffin embedding

For the study in chapter 4, hemi brains were transferred from 4% paraformaldehyde to phosphate buffered saline and sectioned into two 3 mm coronal blocks at either side of bregma using a mouse matrix. Tissue blocks were processed on an automated Tissue Tek VIP 2 (Sakura) at the Shared University Research Facility as described in Table 2.2 and then manually embedded in paraffin.

Table 2.2 Automatic processing schedule for paraffin embedding

Solution	Duration (min)	Temperature (°C)
70% Ethanol	60	35
90% Ethanol	60	35
100% Ethanol	60	35
100% Ethanol	90	35
100% Ethanol	120	35
100% Ethanol	60	35
Xylene	60	35
Xylene	60	35
Xylene	60	35
Paraffin wax	60	60
Paraffin wax	60	60
Paraffin wax	60	60
Paraffin wax	60	60

2.6.5 Manual processing for paraffin embedding

For the study in chapter 5, fixed brain tissue slices were transferred to phosphate buffered saline and maintained in cell sure tissue cassettes throughout manual processing as described in Table 2.3 and then embedded in paraffin.

Table 2.3 Manual processing for paraffin embedding

Solution	Duration (min)	Temperature (°C)
Tap water	30	RT
70% Ethanol	30	RT
70% Ethanol	30	RT
90% Ethanol	30	RT
90% Ethanol	30	RT
100% Ethanol	60	RT
100% Ethanol	90	RT
Xylene	60	RT
Xylene	60	RT
Paraffin wax	60	60
Paraffin wax	60	60
Paraffin wax	60	60
Paraffin wax	60	60

2.6.6 Microtome sectioning

Paraffin embedded tissues were cut to 6 µm coronal tissue sections at -1.70 mm posterior of bregma (according to Paxinos and Franklin, 2001) (Fig 2.3) using a rotary microtome (Leica RM2135, Leica Microsystems, Germany) and mounted on superfrost plus slides (VWR International).

2.7 Histology and immunostaining

Standard laboratory procedures were utilised for histology and immunostaining. Paraffin sections were deparaffinised for 30 min at 60°C followed by 2 x 15 min in xylene. Frozen sections were air dried for 30 min, washed in phosphate-buffered saline (PBS) then dehydrated through a series of alcohols (70%, 90%, 100%), followed by 10 min in xylene. Paraffin and frozen sections were following these initial steps treated identically for histology and immunohistochemistry.

2.7.1 Immunohistochemistry using DAB

Sections were returned to 100% ethanol and endogenous peroxidases were then quenched using 3% hydrogen peroxide in methanol. Antigen retrieval was carried out when required (Iba1 and GFAP). For citric acid retrieval, sections were incubated in 10 mM citric acid (pH6) and placed in a Decloaking chamber (Biocare Medical), heated to 95°C for 10 min. Sections were then washed in PBS and blocked at room

temperature for 1 hour with 10% normal serum and 0.5% bovine serum albumin before overnight primary antibody incubation at 4°C. Sections were then washed in PBS and biotinylated secondary antibodies were applied for 1 hour (room temperature) and further amplified using the Vector ABC Elite Kit (Vector Labs, UK) before visualisation of peroxidase activity using 3,3' diaminobenzidine tetrahydrochloride (DAB, Vector Labs, UK) for 3 min. Sections were then washed in running water and dehydrated through a series of alcohols (70%, 90%, 100%) before 15 min in xylene and mounting with DPX (Sigma, UK). Primary antibodies and concentrations are found in the Table 2.4.

2.7.2 Immunofluorescent labelling

Sections were rehydrated through a series of alcohols (100%, 90%, 70%) and rinsed in running water. Antigen retrieval was carried out as described above (Methods section 2.6.2). Sections were then washed in PBS and blocked at room temperature for 1 hour (10% normal serum, 0.5% bovine serum albumin in PBS) before overnight primary incubation at 4°C. Primary antibodies were diluted in blocking solution made up in 0.3% Triton-X PBS, concentrations found in Table 2.4. On the second day, sections were washed PBS and incubated in biotinylated secondary antibodies for 1 hour (room temperature) if amplification was required. This was followed by another PBS wash and then application of the fluorescent secondary antibodies for 1 hour (room temperature) protected from light. Sections were then again washed in PBS, followed by Tris-buffer and then allowed to air dry for 30 min before mounting with Vectashield Hardset with DAPI (Vector, UK).

2.7.3 Immunostaining controls

Prior to large immunostaining experiments, antibody conditions and concentrations were carefully optimised. To ensure consistency, a section with a known level of staining was included as a positive control and closely examined alongside the tissue of interest. To ensure antibody specificity, all immunostaining experiments included a negative control where the primary antibody was not applied but all other steps were kept identical. Antibody staining was only analysed if this negative control was clear, and repeated if not. To prevent batch variation, all sections from one study were stained for individual proteins in single experiments.

Table 2.4 Antibodies used for immunohistochemical and immunofluorescent experiments

Primary antibody	Target	Dilution	Retrieval	Supplier	Secondary antibody	Dilution	Supplier
Anti-Iba1	Microglia/ macrophages	1:1000 (DAB) 1:250 (IF)	Citrate/ 95°C	Menarini, MP290-CR05	Biotinylated anti-rabbit Anti-rabbit Alexa Fluor 555	1:100 1:200	Vector BA1100 Invitrogen A31572
Anti-GFAP	Astrocytes	1:1000	Citrate/ 95°C	Life technologies 13-0300	Biotinylated anti-rat	1:100	Vector BA4001
Anti-MAG	Myelin associated glycoprotein	1:15000	No	Abcam ab89780	Biotinylated anti-mouse	1:100	Vector BA2001
Anti-BrdU	Bromodeoxy-uridine	1:50	Citrate/ 95°C	Abcam, ab6326	Biotinylated anti-rat Streptavidin Alexa Fluor 488	1:100 1:100	Vector BA4900 Invitrogen S11223

2.8 Image acquisition and analysis

2.8.1 Image acquisition

DAB-labelled sections were imaged using a BX51 microscope (x20, Olympus, UK) or an Axio Scan.Z1 slide scanner (x20, Zeiss, Germany) (specified in the relevant chapter). Joshua Beverley performed all slide scanner imaging. Immunofluorescent labelling for Iba1/BrdU was imaged using a Zeiss 710 confocal microscope (x20, Zeiss, Germany), or a Leica TCS SP5 confocal microscope (x20, Leica Microsystems, Germany) by Dr Jessica Duncombe, who also delineated the corpus callosum regions for Iba1/BrdU analysis.

2.8.2 Image analysis

All image analysis was performed using ImageJ software (v1.46, NIH, Bethesda, MD, USA). Iba1/BrdU was manually assessed for cell counts of single and double labelled cells in the corpus callosum, using DAPI as a positive cell marker. DAB-labelled sections were evaluated in the corpus callosum (CC), the internal capsule (IC) and the optic tract (OT) or fimbria (FI) which were manually delineated by the experimenter (Fig. 2.3). Iba1, GFAP and MAG was analysed by percentage area measured after subtracting background and applying a global manual threshold. For MAG staining where this was not possible due to increased background, sections were instead graded on a scale from 0-3 depending on presence and extent of aberrantly accumulated MAG (indicative of axon-glial disruption) (Olympus BX51 microscope, Olympus, UK), and grades for each side of the brain were summed giving a total scale of disruption of 0-6. All analysis was performed on two sections from each animal and results averaged to represent a single data point. Details of stains and analyses used can be found in relevant chapters.

2.8.3 Exclusion criteria

Due to minor variation in the anatomical level of sections stained, some animals had to be excluded from immunohistochemical analysis where particular regions of interest were absent. Details of exclusions are specified in relevant chapters.

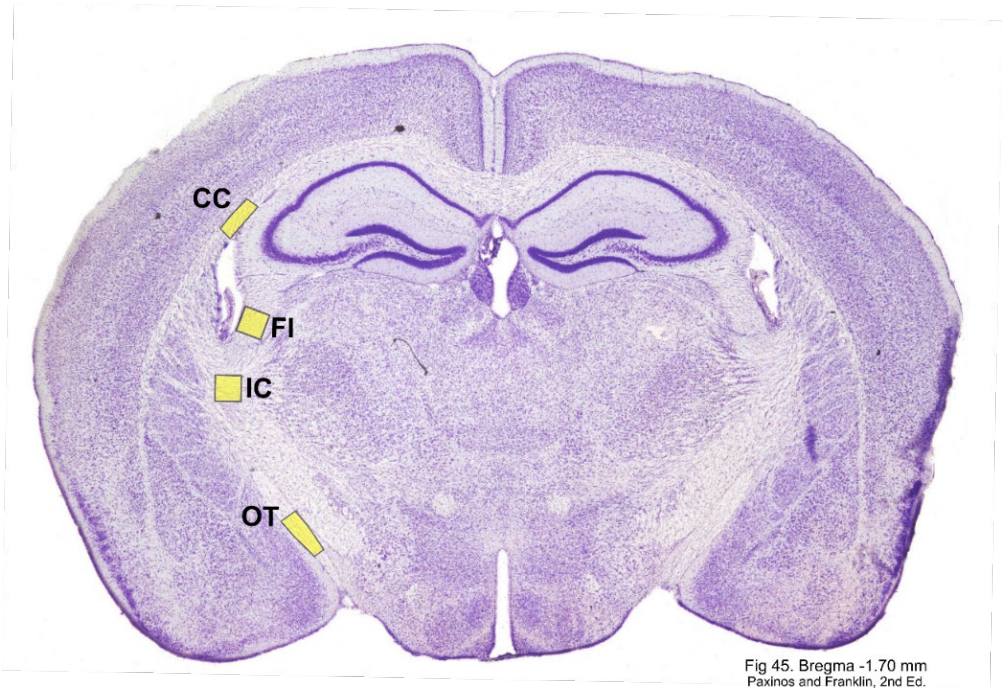

Figure 2.3 Regions of interest for image analysis of immunostained proteins. CC, corpus callosum; FI, fimbria; IC, internal capsule; OT, optic tract were manually delineated using ImageJ software. Figure 45, Bregma -1.70 mm (Paxinos and Franklin, 2001)

2.9 Transcriptomics

RNA was isolated from optic tract-enriched samples or a slice of whole brain dissected from snap-frozen hemi brains, or from freshly dissected white matter as described in 2.6.3.

2.9.1 RNA extraction

RNA was extracted using the QIAGEN RNeasy Lipid Tissue Mini Kit according to manufacturer's instruction. Briefly, <100mg fresh frozen tissue was homogenised in 1ml QIAzol® lysis reagent using the Qiagen automated tissue lyser system and metal beads. The homogenate was transferred to fresh Rnase/Dnase free tubes and incubated for a couple of minutes at room temperature with 200µl chloroform. The upper aqueous phase was collected following 15 min centrifugation at 4°C (12,000 x *g*), and RNA was subsequently purified in mini spin columns and washed with a series of buffers before it was eluted in Rnase free water. Rnase-free Dnase I (Thermo Scientific/QIAGEN) was used to remove genomic DNA according to manufacturer's instruction.

2.9.2 Reverse transcription (RT)-PCR

cDNA was synthesised from 1-3 µg RNA using the Roche Transcriptor First Strand cDNA Synthesis Kit, according to manufacturer's instruction. Briefly, RNA was added to reverse transcriptase reaction mix and cycled through 10 min 25°C; 30 min 55°C; 5 min 85°C. NoRT control was run alongside and cDNA was diluted to the equivalent of 3 ng initial RNA per 15 µl qPCR reaction.

2.9.3 Quantitative (q)-PCR

The CFX96 Real-Time PCR Machine (Bio Rad) was used with the DyNAmo ColorFlash SYBR Green qPCR kit according to manufacturer's instructions (Thermo Scientific). cDNA template was mixed with SYBR green master mix, water and forward and reverse primer (200 nM each final concentration). Samples were run in duplicates alongside no template and no RT negative controls. Primer sequences are listed in Table 2.5. The qPCR cycling programme was 7-10 min at 95°C for denaturing; 40 cycles of 10 sec at 95°C, primer-specific annealing/extension conditions (listed in Table 2.5) with detection of fluorescence; followed by 1 cycle (for dissociation curve) at 65°C with a ramp up of 0.5°C every 30 sec at 95°C with continuous detection of fluorescence. Data was normalised to *Gapdh* or *18S* expression as a reference gene (specified in each graph) and expressed as fold change of sham expression. Neither reference gene was significantly altered as a result of surgery or genotype.

2.9.4 Exclusion criteria

Samples where reference gene expression was detected >2STD (standard deviation) away from the mean were excluded from analysis. Samples were also excluded if gene of interest expression was >3 interquartile ranges (IQR) below the first quartile or >3 IQR above the third quartile for each group. Details of exclusions are specified in relevant chapters.

Table 2.5 qPCR primer sequences, cycling conditions and efficiencies

Gene of interest	Forward primer sequence	Reverse Primer sequence	Annealing/extension conditions	Primer efficiency
Gapdh	5'-GGGTGTAACCACGAGAAAT-3'	5'-CCTTCCACAATGCCAAAGTT-3'	62.5°C 30s	97.4%
			65°C 30s	97.5%
			60°C 40s / 72°C 30s	92.8%
			62.5°C 30s / 72°C 30s	101.1%
			65°C 30s / 72°C 30s	99.2%
18S	5'- CCCAGTAAGTGCGGGTCAT-3'	5'- CCGAGGGCCTCACTAAACC-3'	62.5°C 30s	96.6%
			65°C 30s	96.8%
			60°C / 72°C 30s	93.8%
			62.5°C 30s / 72°C 30s	102.1
			65°C 30s / 72°C 30s	102.1%
Nrf2	5'-CAGCTCAAGGGCACAGTGC-3'	5'-GTGGCCCAAGTCTTGCTCC-3'	65°C 30s / 72°C 30s	106.3%
Slc7a11	5'-ATACTCCAGAACACGGGCAG-3'	5'-AGTTCCACCCAGACTCGAAC-3'	65°C 30s / 72°C 30s	95.6%
Gclm	5'-GCACAGCGAGGAGCTTC-3'	5'-GAGCATGCCATGTCAACTG-3'	60°C 30s / 72°C 30s	92%
			60°C 40s / 72°C 30s	92.4%
C4	5'- ACAACAAGGGAGACCCCCAG-3'	5'-GCTCAGAGAGCCAGAGTCCTA-3'	65°C 30s	91.1%
C1q a	5'- CAAGGACTGAAGGGCGTGAA-3'	5'- CAAGCGTCATTGGGTTCTGC-3'	62.5°C 30s	93%
			62.5°C 30s / 72°C 30s	94.7%
Ccl3	5'- GCCAGGTGTCATTTTCCTGACT-3'	5'- TCAGGCATTCAGTTCCAGGTC-3'	62.5°C 30s	91.5%
Ccl2	5'- TCCCAAAGAAGCTGTAGTTTTTGTC-3'	5'- CCCATTCCTTCTTGGGGTCA-3'	62.5°C 30s / 72°C 30s	90.1%

2.10 Statistical analysis

Statistical analysis was performed using SPSS (v22, IBM Corp.) and Graphpad Prism (v5, GraphPad Software Inc, La Jolla, USA). Significance was determined at $p<0.05$. Analysis of variance (ANOVA) was the a priori statistical approach, with Bonferroni adjustment for multiple comparisons for *post hoc* analysis. Where semi-quantitative data was considered, non-parametric statistical tests were utilised.

2.10.1 Repeated measures ANOVA

Repeated measures ANOVA with Bonferroni adjustment for *post hoc* analysis and Greenhouse-Geisser correction for violation of sphericity was used to investigate the effect of BCAS surgery and genotype (between-subjects factors) on cerebral blood flow over time (within-subjects factor) (Chapter 3-5), revisiting errors over consecutive trials (within-subjects factor) in the radial arm maze (Chapter 3-4) and the effect of group (between-subjects factor) and escape latency over consecutive trials (within-subjects factor) in the learning and reversal phase of the Barnes maze (Chapter 5).

2.10.2 Two-way ANOVA

Two-way ANOVA with Bonferroni adjustment for *post hoc* analysis was used to investigate the effect of BCAS surgery and genotype on spontaneous alternation and total entries in the Y-maze and Iba1, GFAP and MAG positive percentage area in white matter tracts and gene expression (Chapter 3-4).

2.10.3 One-way ANOVA

One-way ANOVA with Bonferroni adjustment for *post hoc* analysis was used to investigate a group effect on percentage of proliferating Iba1 positive cells, *C4* gene expression, number and density of Iba1 positive cells, density of GFAP and percentage time spent in the target quadrant during Barnes Maze probe tests (Chapter 5).

2.10.4 One-sample t-test

One-sample t-test was used to analyse Y-maze spontaneous alternation for each group against chance (50%) (Chapter 3-4) and to test each group against chance (25%) during probe tests in the Barnes Maze (Chapter 5).

2.10.5 Pearson's correlation

Pearson's correlation was used to investigate the relationship between density of Iba1 and GFAP (Chapter 5).

2.10.6 Kruskal-Wallis H test (Non-parametric)

Kruskal-Wallis H test with Dunn's *post hoc* test with Bonferroni adjustment for multiple comparisons was used to analyse the MAG grade for white matter disruption as this data set is semi-quantitative (Chapter 5).

2.10.7 Spearman's correlation (Non-parametric)

Spearman's correlation was used to investigate the relationship between density of Iba1 and MAG grade in the corpus callosum (Chapter 5).

Chapter 3

Investigating the effect of chronic cerebral hypoperfusion in a mouse model with reduced expression of Nrf2

3.1 Introduction

Vascular risk factors may lead to the development of vascular cognitive impairment (VCI) and dementia by promoting cerebral hypoperfusion (de la Torre, 2012). Cerebral hypoperfusion is observed before the onset of cognitive decline (Ruitenberg et al., 2005) and the severity of hypoperfusion predicts conversion from mild cognitive impairment to dementia (Chao et al., 2010, Hirao et al., 2005). One of the primary pathological features of VCI and dementia is white matter disruption (Dichgans and Leys, 2017) and previous work demonstrates that bilateral carotid artery stenosis (BCAS) in mice induces cerebral hypoperfusion which reproduces important features of VCI, including white matter disruption and cognitive impairment (Coltman et al., 2011, Holland et al., 2011, Shibata et al., 2004, Shibata et al., 2007). VCI and dementia are both commonly associated with increased levels of inflammation (Rosenberg, 2009, Raz et al., 2015) and oxidative stress (Gackowski et al., 2008, Bennett et al., 2009), which led to the hypothesis that these are important pathophysiological mechanisms whereby white matter structure and function is disrupted. To address this hypothesis, this study is investigating the transcription factor Nrf2 (Nuclear factor erythroid 2-related factor 2), an important regulator of endogenous antioxidant and anti-inflammatory genes. Nrf2 has been shown to play a role in maintaining white matter structural integrity under normal physiological conditions as Nrf2 knock out mice display age-related white matter disruption (Hubbs et al., 2007). In models of white matter disease (sciatic nerve injury and EAE), the lack of Nrf2 impairs remyelination and functional recovery (Zhang et al., 2013, Johnson et al., 2010) indicating that Nrf2 is also involved in maintaining white matter during pathological conditions, and in promoting white matter recovery and repair following injury. Hypoperfusion-induced white matter disruption is likewise associated with inflammation (Coltman et al., 2011, Reimer et al., 2011, Saggu et al., 2016) and oxidative stress (Washida et al., 2010, Dong et al., 2011, Miyamoto et al., 2013) however it is currently unknown what role the Nrf2 system plays. By investigating the effects of bilateral carotid artery stenosis in transgenic mice with reduced or absent expression of Nrf2 this study is interrogating the role of this transcription factor in the disruption of white matter structure and function following chronic cerebral hypoperfusion.

3.1.1 Hypothesis

This study tests the hypothesis that deficiency of the transcription factor Nrf2 exacerbates white matter disruption and cognitive impairment following BCAS-induced chronic cerebral hypoperfusion.

3.1.2 Aims

In wild type,$Nrf2^{+/-}$ and $Nrf2^{-/-}$ mice the aims are to:

1. Assess cerebral blood flow to determine the extent of BCAS-induced cerebral hypoperfusion
2. Assess the structural integrity of white matter
3. Assess white matter micro- and astrogliosis
4. Assess oxidative stress and inflammatory genes
5. Asses spatial working memory
6. For the above measures determine whether deficiency of Nrf2 exacerbates the effects of BCAS

3.2 Materials and Methods

3.2.1 Experimental contributions

The study presented in this chapter was carried out by myself, Dr Martina Marangoni, Professor Karen Horsburgh and Dr Jill Fowler. I performed laser speckle imaging, behavioural testing, and tissue collection/processing/sectioning with assistance from Dr Martina Marangoni. I performed immunostaining and imaging for MAG and Iba1, RNA extractions, quantitative PCR and all data analysis presented in this chapter. Professor Karen Horsburgh performed BCAS surgery and Dr Jill Fowler performed immunostaining and imaging for GFAP.

3.2.2 Mice

Genetic details of Nrf2 knock out (KO) mice are described in 2.1.1. Due to difficulties in breeding sufficient numbers of homozygous mice, some measures only included data from heterozygotes or combined data from both heterozygotes and homozygotes. Wild type littermates were also not generated at sufficient numbers and were therefore complemented with separately purchased C57Bl/6J, genetically identical to the Nrf2 KO line's background strain according to supplier. Adult male mice, mean age 6 m 17 d (4 to 9 m), weighing on average 33.4 g (25.4-43.8 g) (n=37) were randomly assigned surgical intervention as detailed in Table 3.1. The experimenters were blinded to genotype and surgery status of animals throughout data collection and analysis in accordance with ARRIVE guidelines (Kilkenny et al., 2010).

3.2.3 Chronic cerebral hypoperfusion

Mice underwent bilateral carotid artery stenosis (BCAS) or sham surgery, as described in 2.2. BCAS surgery was performed to induce chronic cerebral hypoperfusion, using two 0.18 mm in diameter microcoils. Recovery following surgery was closely monitored for 72 hours and animals showing poor recovery were culled. Three animals tolerated surgery poorly (two wild type, one $Nrf2^{+/-}$) and were humanely culled by cervical dislocation (see Table 3.1).

3.2.4 Laser speckle imaging to measure cortical cerebral blood flow

Cortical cerebral blood flow (CBF) was measured at rest prior to, 24 hours and 6 weeks post-BCAS as described in 2.3 in a subset of mice, detailed in Table 3.1 and the relevant figure. Because no $Nrf2^{-/-}$ BCAS animals were imaged, data from blood flow analysis may only be compared between wild type and $Nrf2^{+/-}$ sham and BCAS groups.

3.2.5 Behavioural testing

Animals were singly housed and food restricted for the behavioural tests which were performed as described in 2.4.1-2.4.2. Spatial working memory was assessed by the 8-arm radial arm maze (2.4.1) and spontaneous alternation and mobility was assessed in the Y-maze (2.4.2). Behavioural testing commenced four weeks post-BCAS. Inclusion criteria described in 2.4.1.3 was applied excluding two animals (one wild type BCAS and one Nrf2 KO sham) from behavioural analysis. Due to the limited n-numbers of the $Nrf2^{-/-}$ groups all Nrf2 KO animals were grouped together for the behavioural analysis. Final numbers for each group are detailed in Table 3.1 and relevant figures.

3.2.6 Tissue collection and processing

Animals were sacrificed 6 weeks post-BCAS as described in 2.6.1. The tissue was further processed for freezing and cryosectioning as described in 2.6.3.

3.2.7 Immunohistochemistry

Performed according to 2.7.1. Details of antibodies used (anti-MAG, anti-Iba1, anti-GFAP) can be found in Table 2.4. Immunohistochemistry was performed on 30 µm coronal sections from all animals.

3.2.8 Image analysis

Images for MAG and Iba1 were acquired using a BX51 microscope (x20, Olympus, UK) and GFAP images were acquired by Dr Jill Fowler using Zeiss Axio Scope.A1 (x5, Zeiss, UK). Images were analysed for percentage area of MAG, Iba1 and GFAP as described in 2.8.2 in the corpus callosum (CC), internal capsule (IC) and optic tract (OT) (Fig 2.3). Briefly, ImageJ software (v1.46, NIH, Bethesda, MD, USA) was used to apply a global manual threshold followed by quantification of the positive signal detected above the selected threshold. Applying exclusion criteria outlined in 2.8.3 resulted in one animal in the wild type BCAS group and one in the $Nrf2^{+/-}$ BCAS group being excluded from the internal capsule and optic tract analysis of Iba1. Similarly, one wild type BCAS animal was excluded from GFAP analysis in the internal capsule. Final numbers for each region and stain are detailed in Table 3.1 and relevant figures.

3.2.9 Transcriptomics

Performed according to 2.9 using optic tract-enriched samples. Details of primers used (*Gapdh, Nrf2, Slc7a11, Gclm, Ccl3, C1q, C4*) can be found in Table 2.5. Exclusion criteria outlined in 2.9.4 was applied excluding one wild type sham from *Gclm* and one $Nrf2^{+/-}$ BCAS animal from *Slc7a11* analysis. Final numbers detailed in

Table 3.1 and the relevant figure also containing reference gene used for each experiment.

3.2.10 Statistical analysis

Repeated measures ANOVA was used to analyse cerebral blood flow and behaviour as described in 2.10.1. The radial arm maze was analysed separately for the first and second half of the test as the first half primarily represents a learning phase. Two-way ANOVA was used to investigate the effect of BCAS surgery and genotype in the Y-maze and Iba1, GFAP and MAG positive percentage area in white matter tracts and gene expression (2.10.2). One-sample t-test was used to analyse Y-maze spontaneous alternation (2.10.4). Data are presented as mean ± standard error of the mean (SEM). Statistical significance was determined at $p<0.05$.

Table 3.1 Number of mice in each group and experiment with details of exclusion

BCAS surgery	**Wild type**	**Nrf2$^{+/-}$**	**Nrf2$^{-/-}$**
Sham	7	7	3
BCAS	8	6	3
Details of exclusion			
Poor recovery from BCAS surgery	2 (Hypo)	1 (Hypo)	0
Laser speckle imaging	**Wild type**	**Nrf2$^{+/-}$**	**Nrf2$^{-/-}$**
Sham	4	4	1
BCAS	5	3	0
Behavioural testing	**Wild type**	**Nrf2$^{+/-}$**	**Nrf2$^{-/-}$**
Sham	7	7	2
BCAS	7	6	3
Details of exclusion			
Initial lack of motivation	1 (Hypo)	0	1 (sham)
Immunohistochemistry (CC, IC, OT)	**Wild type**	**Nrf2$^{+/-}$**	**Nrf2$^{-/-}$**
MAG			
Sham	7, 7, 7	7, 7, 7	3, 3, 3
BCAS	8, 8, 8	6, 6, 6	3, 3, 3
Iba1			
Sham	7, 7, 7	7, 7, 7	3, 3, 3
BCAS	8, 7, 7	6, 5, 5	3, 3, 3
Details of exclusion			
Anatomical area missing from slide	0	1 (IC/OT)	0
GFAP			
Sham	7, 7, 7	7, 7, 7	3, 3, 3
BCAS	8, 7, 8	6, 6, 6	3, 3, 3
Details of exclusion			
Anatomical area missing from slide	1 (IC)	0	0
qPCR (*Nrf2, Ccl3, C1q, C4, Gclm, Slc7a11*)	**Wild type**	**Nrf2$^{+/-}$**	**Nrf2$^{-/-}$**
Sham	7, 7, 7, 7, 6, 7	7, 7, 7, 7, 7, 7	3, 3, 3, 3, 3, 3
BCAS	8, 8, 8, 8, 8, 8	6, 6, 6, 6, 6, 5	3, 3, 3, 3, 3, 3
Details of exclusion			
3IQR<Q1 / 3IQR>Q3 (outlier)	1 (*Gclm*)	1 (*Slc7a11*)	0

3.3 Results

3.3.1 Cortical CBF is significantly reduced post-BCAS

CBF was evaluated using laser speckle imaging prior to, 24 hours, and 6 weeks post-BCAS surgery in a subset of animals to assess the extent of cerebral hypoperfusion and to determine if this differed between wild type and $Nrf2^{+/-}$ groups. Resting CBF over time was calculated as a percentage of each animal's baseline flux (arbitrary unit).

BCAS reduced CBF between 40-50%, whereas CBF in sham mice was relatively unchanged from baseline (Fig 3.1). There was a significant effect of time ($F_{(2,26)}$=36.9, p<0.0001) and surgery ($F_{(1,13)}$=22.3, p<0.0001) and a significant interaction between time and surgery ($F_{(2,26)}$=14.7, p<0.0001) (Fig 3.1b). There was no overall effect of genotype ($F_{(1,13)}$=0.72, p=0.41) though *post hoc* tests found a significant CBF reduction in wild type and $Nrf2^{+/-}$ mice at 24 hours (WT; p=0.001, $Nrf2^{+/-}$, p=0.002) but at 6 weeks in the $Nrf2^{+/-}$ only (WT; p=0.18, $Nrf2^{+/-}$; p=0.02), indicating some CBF recovery in wild type mice (Fig 3.1b).

Since CBF measurements were only performed on a subset of animals which did not include $Nrf2^{-/-}$ BCAS, we are unable to determine if the reduction of cerebral blood flow following BCAS surgery is more severe when Nrf2 is completely absent. On the other hand, the available data show that wild type animals display greater CBF recovery (~10%) than $Nrf2^{+/-}$ animals (~5%), although the initial cerebral hypoperfusion is comparable.

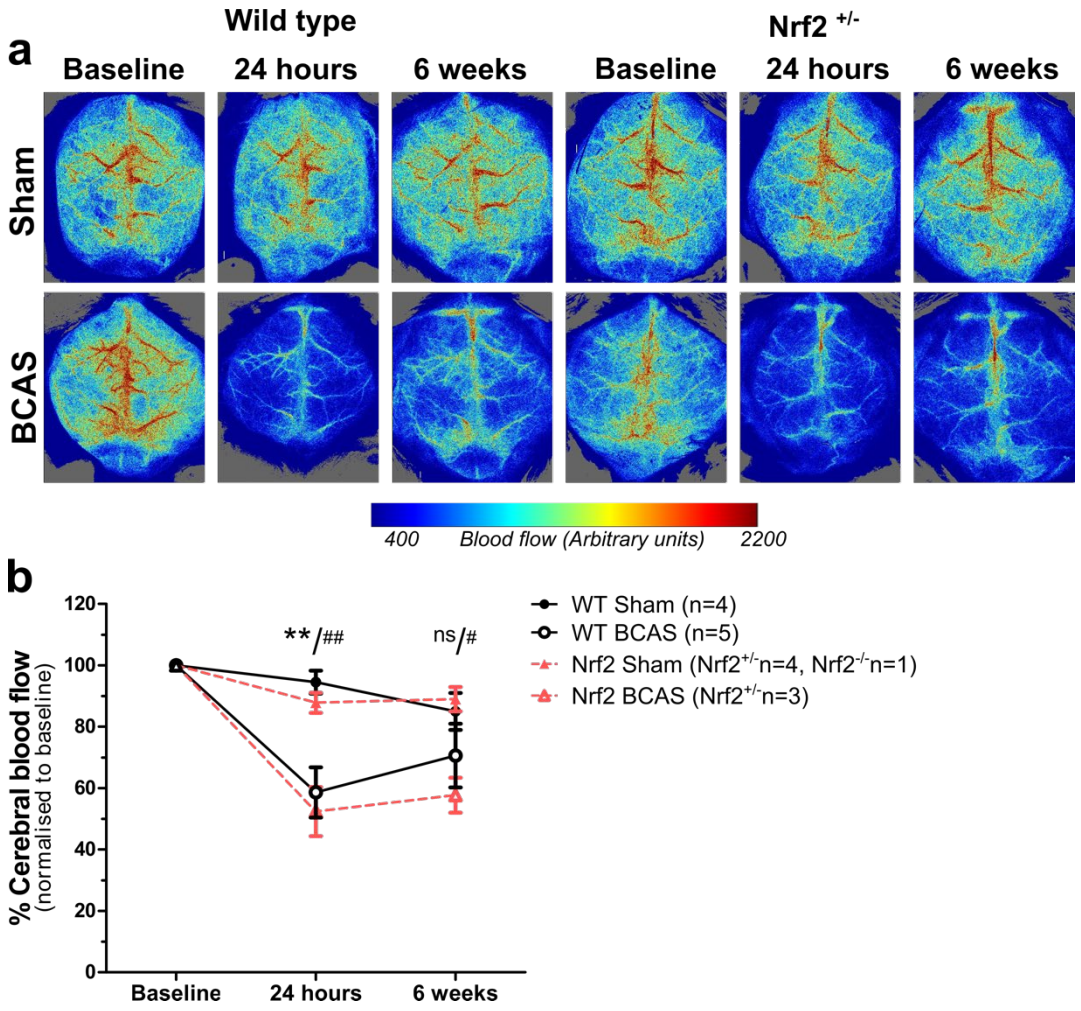

Figure 3.1 Cortical cerebral blood flow is reduced post-BCAS. (a) Representative images of laser speckle flowmetry in sham and BCAS, wild type and Nrf2$^{+/-}$ animals at baseline, 24 hours and 6 weeks. **(b)** BCAS surgery reduced CBF at 24 hours to a similar extent in both genotypes with some recovery in wild type BCAS at 6 weeks. Mean±SEM. **p<0.01 (* indicates *post hoc* differences between wild type sham and BCAS), #p<0.05, ##p<0.01 (# indicates *post hoc* differences between Nrf2$^{+/-}$ sham and BCAS).

3.3.2 White matter disruption is more extensive in Nrf2$^{-/-}$ mice compared to wild type and Nrf2$^{+/-}$ post-BCAS

White matter disruption was evaluated to corroborate previous results in wild type mice (Coltman et al., 2011, Holland et al., 2011) and to determine if this was exacerbated by a reduction or absence of Nrf2. The initially selective white matter disruption observed in the BCAS model is hypothesised to underlie the accompanying cognitive impairment. Alterations in immunostaining for myelin associated glycoprotein (MAG), present at the axon-glial interface, can be detected as aberrant accumulations.

The percentage area of MAG positive immunostaining was quantified in key white matter tracts: corpus callosum (CC), internal capsule (IC) and optic tract (OT). There was significant white matter disruption in the corpus callosum post-BCAS ($F_{(1,28)}$=6.04, p=0.02) with an additional effect of genotype ($F_{(2,28)}$=4.47, p=0.02), but no interaction or significant *post hoc* effects (Fig 3.2a). There was no significant white matter disruption in the internal capsule as a result of BCAS surgery or genotype ($F_{(1,28)}$=2.99, p=0.09, $F_{(2,28)}$=1.89, p=0.17 respectively) (Fig 3.2b). Notably in the optic tract, there was prominent white matter disruption post-BCAS ($F_{(1,28)}$=35.84, p<0.0001) with a further effect of genotype ($F_{(2,28)}$=3.96, p=0.03) and a significant interaction between the two variables ($F_{(2,28)}$=3.87, p=0.03) (Fig 3.2c). *Post hoc* analysis found significant differences between all BCAS groups and their respective sham controls (WT p=0.04, Nrf2$^{+/-}$ p=0.004, Nrf2$^{-/-}$ p<0.001). Furthermore, there was significantly greater white matter disruption in the Nrf2$^{-/-}$ BCAS group compared to both Nrf2$^{+/-}$ (p=0.02) and wild type BCAS (p=0.001) (Fig 3.2c). Collectively, these data show that cerebral hypoperfusion induced by BCAS surgery causes white matter disruption in two major white matter tracts and that, principally in the optic tract, this disruption is exacerbated in the absence of Nrf2.

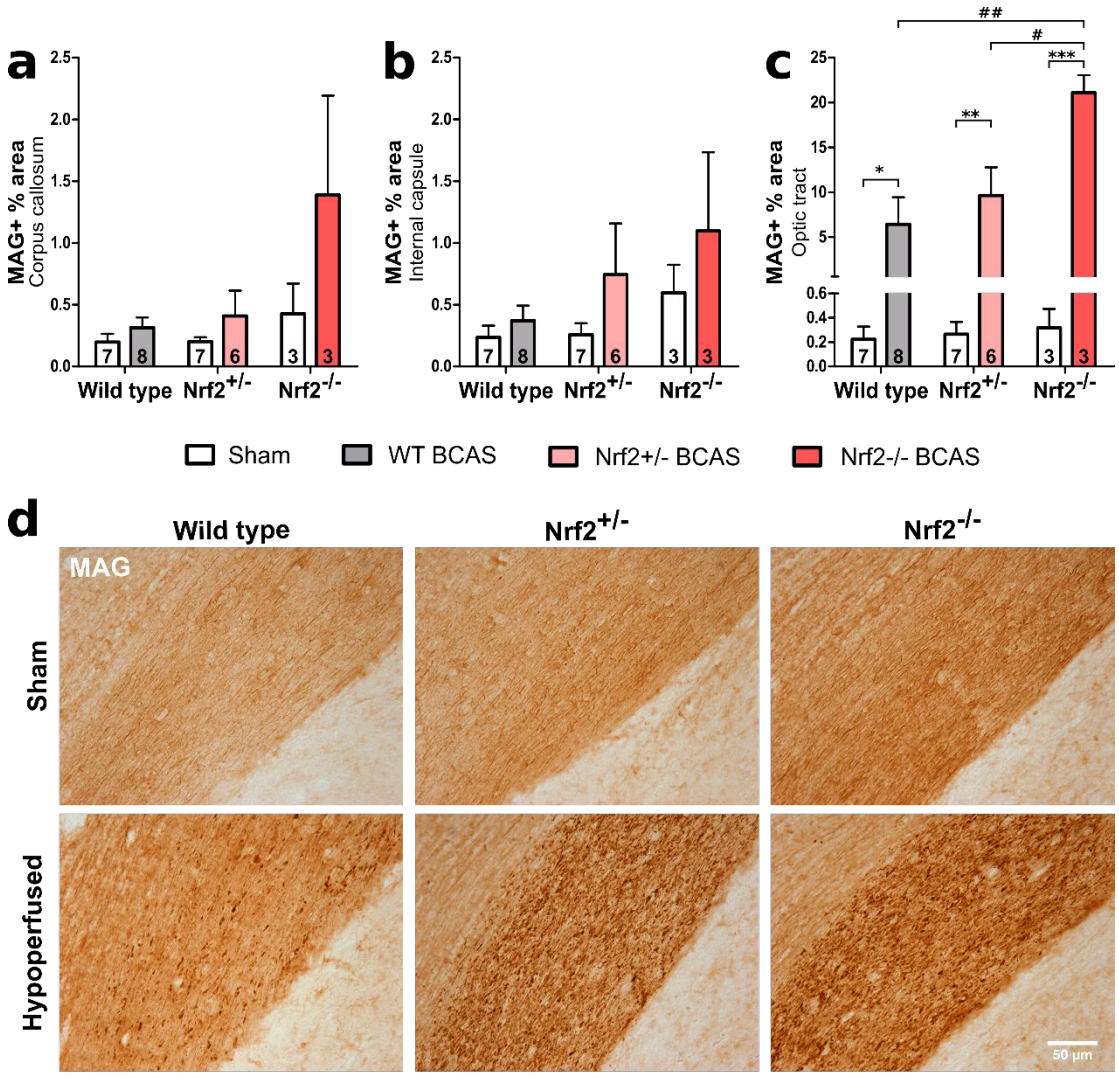

Figure 3.2 White matter disruption is more extensive in Nr2$^{-/-}$ mice compared to wild type and Nrf2$^{+/-}$ post-BCAS. (a) White matter disruption was detected post-BCAS in the corpus callosum, with a significant effect of genotype (no *post hoc* differences). **(b)** White matter disruption in the internal capsule was not significant. **(c)** The optic tract displayed prominent white matter disruption post-BCAS with a further effect of genotype, with the Nrf2$^{-/-}$ group displaying the most severe disruption. Mean±SEM. n-number presented in each bar. *p<0.05, **p<0.01, ***p<0.001 (* indicates *post hoc* differences between sham and BCAS), #p<0.05, ##p<0.01 (# indicates *post hoc* differences between BCAS groups). **(d)** Representative images of MAG staining in the optic tract. Scale bar 50 µm.

3.3.3 The density of microglia is increased post-BCAS to a greater extent in Nrf2$^{-/-}$ mice compared to wild type and Nrf2$^{+/-}$

White matter disruption in the BCAS model has been reported in parallel with acute inflammatory signalling (Reimer et al., 2011) and increased density of the inflammatory cell microglia (Coltman et al., 2011, McQueen et al., 2014). Similarly, Nrf2$^{-/-}$ mice have been reported to have increased number of microglia at baseline (Rojo et al., 2010) and an exacerbated microglial response in disease models such as Alzheimer's disease (Joshi et al., 2015, Branca et al., 2017, Rojo et al., 2018). This study therefore went on to assess the microglial inflammatory response, to determine if this was consistent with previous results and whether it was exacerbated by a reduction or absence of Nrf2.

Immunohistochemistry for ionized calcium binding adapter molecule 1 (Iba1) was used and quantified as positive percentage area in key white matter tracts: corpus callosum, internal capsule and optic tract. There was a significant increase in density of microglia post-BCAS in the corpus callosum ($F_{(1,28)}$=7.63, p=0.01) with a further effect of genotype ($F_{(2,28)}$=4.25, p=0.02) but no interaction (Fig 3.3a). *Post hoc* analysis identified significantly greater density in the Nrf2$^{-/-}$ BCAS group compared to sham controls (p=0.004), and other BCAS groups (Nrf2$^{+/-}$ p=0.005 and wild types p=0.003 respectively) (Fig 3.3a). The effect of BCAS surgery and genotype narrowly missed accepted levels of statistical significance in the internal capsule ($F_{(1,26)}$=3.66, p=0.07, $F_{(2,26)}$=3.15, p=0.06 respectively) (Fig 3.3b), but similar to the white matter disruption, there was a profound microglial response in the optic tract post-BCAS (Fig 3.3c). There was a significant effect of both BCAS surgery and genotype ($F_{(1,26)}$=61.12, p<0.0001, ($F_{(2,26)}$=7.21, p=0.003 respectively), and a significant interaction ($F_{(2,26)}$=5.8, p=0.008). *Post hoc* analysis found significantly greater density of microglia in all BCAS groups compared to their sham controls (WT p=0.005, Nrf2$^{+/-}$ p<0.001, Nrf2$^{-/-}$ p<0.001) and in the Nrf2$^{-/-}$ BCAS group compared to both Nrf2$^{+/-}$ (p=0.002) and wild type BCAS (p<0.001) (Fig. 3.3c). These data show that cerebral hypoperfusion induced by BCAS surgery causes an increased density of microglia in two major white matter tracts which exhibit white matter pathology, and that this increase is exacerbated in the absence of Nrf2.

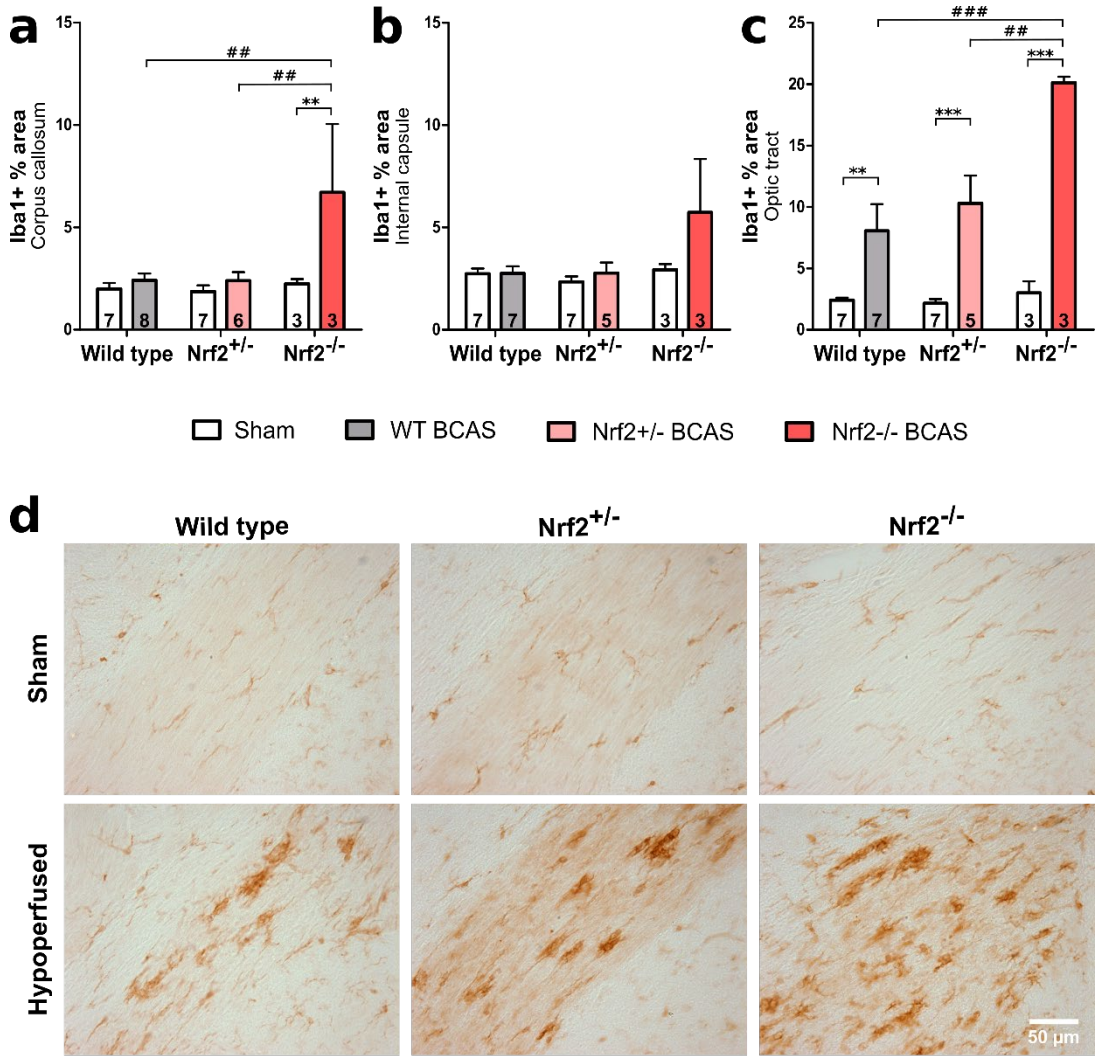

Figure 3.3 The density of microglia is increased post-BCAS to a greater extent in Nrf2$^{-/-}$ mice compared to wild type and Nrf2$^{+/-}$. (a) There was an effect of BCAS surgery and genotype on density of Iba1 in the corpus callosum, with the Nrf2$^{-/-}$ BCAS group displaying the highest density. **(b)** The effect of BCAS and genotype narrowly missed accepted levels of statistical significance in the internal capsule. **(c)** The optic tract displayed an increased density of Iba1 post-BCAS, with a further effect of genotype, again with the Nrf2$^{-/-}$ BCAS group displaying the highest density. Mean±SEM. n-number presented in each bar. **p<0.01, ***p<0.001 (* indicates *post hoc* differences between sham and BCAS), #p<0.05, ##p<0.01, ###p<0.001 (# indicates *post hoc* differences between BCAS groups). **(d)** Representative images of Iba1 staining in the optic tract. Scale bar 50 µm.

3.3.4 Astrogliosis in the optic tract is induced to a similar extent in wild type and Nrf2 KO mice post-BCAS

Aged Nrf2 KO mice display widespread astrogliosis in both grey and white matter (Hubbs et al., 2007) and astrocytes have been reported to actively contribute to chronic neuroinflammation (Sofroniew, 2014a). Previous work by the group find no alterations in the number of astrocytes in the corpus callosum at 4 weeks post-BCAS in wild type mice (McQueen et al., 2014) although other groups do (Saggu et al., 2016). To thoroughly evaluate the inflammatory response, glial fibrillary acidic protein (GFAP) immunohistochemistry was used to assess astrogliosis. The aim was to determine if the current study was consistent with previous results by us or others and to investigate if astrogliosis was exacerbated by a reduction or absence of Nrf2, similar to the microglial response.

Reactive astrogliosis was quantified as GFAP positive percentage area in the main white matter tracts: corpus callosum, internal capsule and optic tract. BCAS surgery did not affect the percentage area of GFAP in the corpus callosum or the internal capsule ($F_{(1,28)}$=1.08, p=0.31; $F_{(1,27)}$=0.30, p=0.59 respectively) (Fig 3.4a-b). However, there was an effect of genotype in the corpus callosum ($F_{(2,28)}$=3.96, p=0.03) and *post hoc* analysis found that GFAP expression in $Nrf2^{-/-}$ animals was overall higher than wild types (p=0.03). This genotype effect was not present in the internal capsule ($F_{(2,27)}$=1.52, p=0.24). Consistent with the white matter disruption and the microglial response, there was a significant effect of BCAS surgery in the optic tract ($F_{(1,28)}$=43.61, p<0.0001), although the effect of genotype narrowly missed accepted levels of statistical significance ($F_{(2,28)}$=3.26, p=0.053) (Fig 3.4c). *Post hoc* analysis found significant astrogliosis in all three BCAS groups compared to their sham controls (WT p=0.005, $Nrf2^{+/-}$ p<0.001, $Nrf2^{-/-}$ p<0.001). These data show that cerebral hypoperfusion induced by BCAS surgery causes astrogliosis in the optic tract and there is a trend towards this effect being more pronounced in the absence of Nrf2.

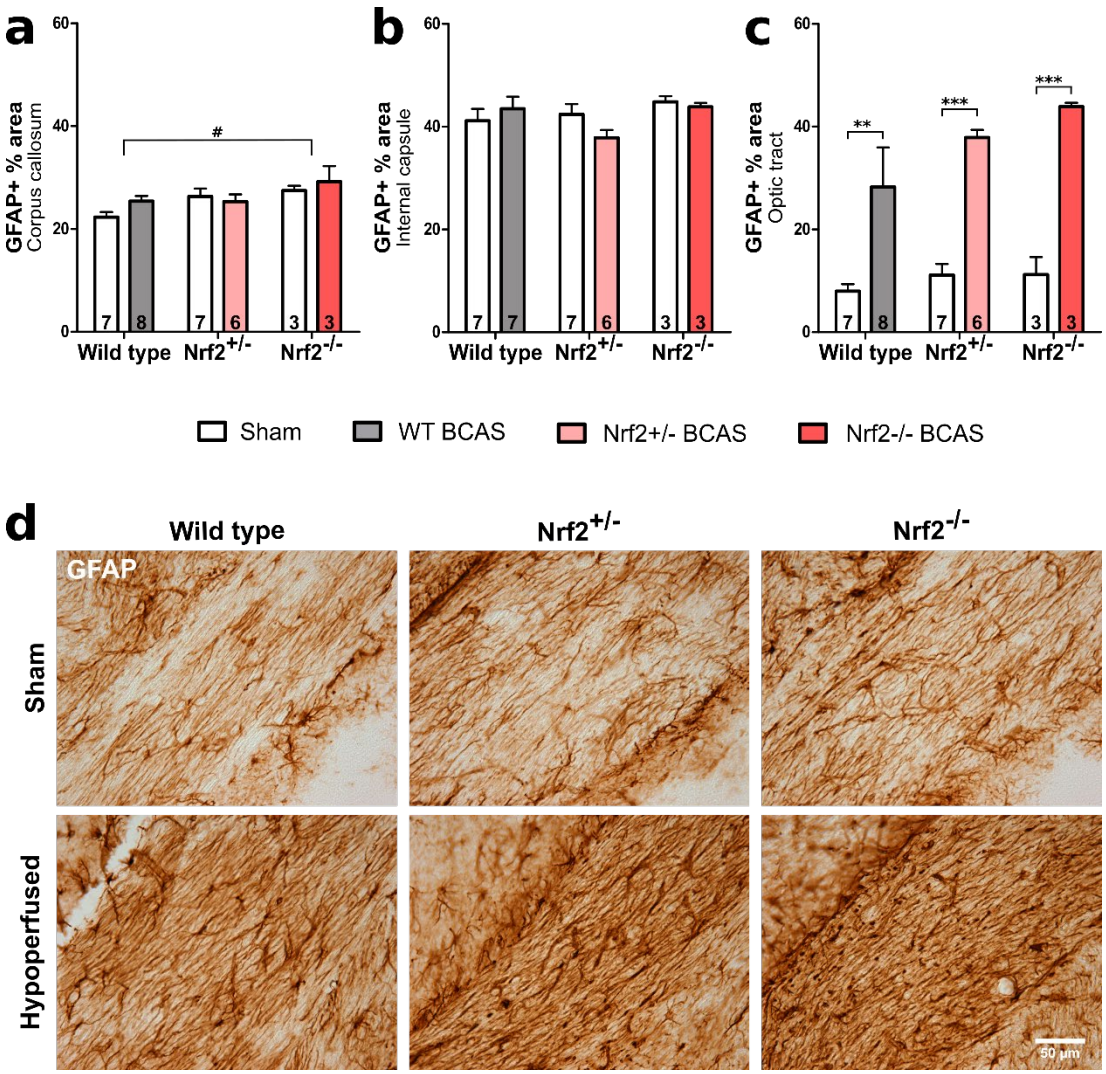

Figure 3.4 Astrogliosis in the optic tract is induced to a similar extent in wild type and Nrf2 KO mice post-BCAS. (a) There was a significant effect of genotype on % Area of GFAP in the corpus callosum but there was no effect of BCAS surgery. **(b)** % Area of GFAP was unchanged in the internal capsule. **(c)** There was a significant effect of BCAS surgery on % area of GFAP in the optic tract but the effect of genotype just missed accepted levels of statistical significance. Mean±SEM. **p<0.01, ***p<0.001 (* indicates *post hoc* differences between sham and BCAS), #p<0.05 (# indicates *post hoc* differences between wild type and Nrf2$^{-/-}$). n-number presented in each bar. **(d)** Representative images of GFAP staining in the optic tract. Scale bar 50 µm. (Stained and imaged by Dr Jill Fowler.)

3.3.5 *Nrf2* and Nrf2-regulated antioxidant genes are unaltered post-BCAS but pro-inflammatory gene expression is induced

The results presented in this chapter thus far demonstrate that BCAS surgery induces cerebral hypoperfusion in wild type and Nrf2 KO mice causing white matter disruption and increased density of both microglia and astrocytes. Since pathological and cellular inflammatory changes are exacerbated in $Nrf2^{-/-}$ mice post-BCAS the next aim was to assess antioxidant and inflammatory gene changes to investigate if they are altered post-BCAS, and to determine if these are differentially regulated in the absence of Nrf2.

Quantitative PCR analysis was used to assess gene expression levels in optic tract-enriched samples as this was the area with most prominent pathology. *Nrf2* levels were significantly reduced to about 50% in $Nrf2^{+/-}$ mice ($p<0.001$) and nearly undetectable in $Nrf2^{-/-}$ compared to wild type mice ($p<0.001$) (genotype effect; $F_{(2,28)}=29.6$, $p<0.0001$) (Fig. 3.5a). BCAS surgery did not alter the expression of *Nrf2* ($F_{(1,28)}=0.01$, $p=0.91$) (Fig 3.5a) so to further investigate the effect of BCAS surgery on Nrf2-mediated signalling two known Nrf2-regulated antioxidant genes involved in glutathione synthesis were measured: *Slc7a11* (*xCT*; encoding the glutamate/cystine antiporter) and *Gclm*, (glutamate-cysteine ligase enzyme subunit) (Fig 3.5b-c). These genes were selected for investigation as they have previously been reported to increase along with Nrf2 following ischaemic preconditioning suggesting the glutathione system may be an important for Nrf2-mediated neuroprotection against ischaemia and hypoxia (Bell et al., 2011b) as well as oxidative stress (Shih et al., 2003).

Contrary to expectations, there was no effect of BCAS surgery or genotype on *Slc7a11* ($F_{(1,27)}=0.23$, $p=0.63$, $F_{(1,27)}=2.25$, $p=0.13$ respectively) or *Gclm* expression ($F_{(1,27)}=0.39$, $p=0.54$, $F_{(1,27)}=0.24$ $p=0.79$ respectively) (Fig 3.5b-c). Instead, as the pathological assessment identified inflammatory cell changes, and because inflammatory protein and gene changes have been observed in previous hypoperfusion studies (Fowler et al., 2017, Reimer et al., 2011), three pro-inflammatory genes were examined next. Two complement components, *C4* and *C1q*, and chemokine ligand 3 (*Ccl3*) were measured also by qPCR. The expression of *Ccl3* and *C1q* was increased post-BCAS ($F_{(1,28)}=7.96$, $p=0.009$, $F_{(1,28)}=4.61$, $p=0.04$ respectively), whereas the effect of BCAS surgery on *C4* expression narrowly missed accepted levels of statistical significance ($F_{(1,28)}=3.9$, $p=0.058$) (Fig 3.5d-f). Pro-inflammatory gene expression appears to increase in $Nrf2^{+/-/-/-}$ animals, but no

significant effect of genotype was detected for any of the markers (*Ccl3*-$F_{(2,28)}$=0.68, p=0.52, *C1q*-$F_{(2,28)}$=0.28, p=0.76, *C4*-$F_{(2,28)}$=0.48, p=0.63) (Fig 3.5d-f), though *post hoc* analysis identified significantly increased expression of *Ccl3* in the Nrf2$^{-/-}$ BCAS group compared to sham controls (p=0.048) (Fig 3.5c).

These data show that the expression of *Nrf2* is reduced/absent to the expected levels in Nrf2$^{+/-}$/Nrf2$^{-/-}$ animals, with no effect of BCAS surgery. There was no effect of BCAS surgery or genotype on Nrf2-regulated antioxidant expression but BCAS-induced cerebral hypoperfusion minimally, but significantly increased the expression of three pro-inflammatory genes in both wild type and Nrf2$^{+/-/-/-}$ animals.

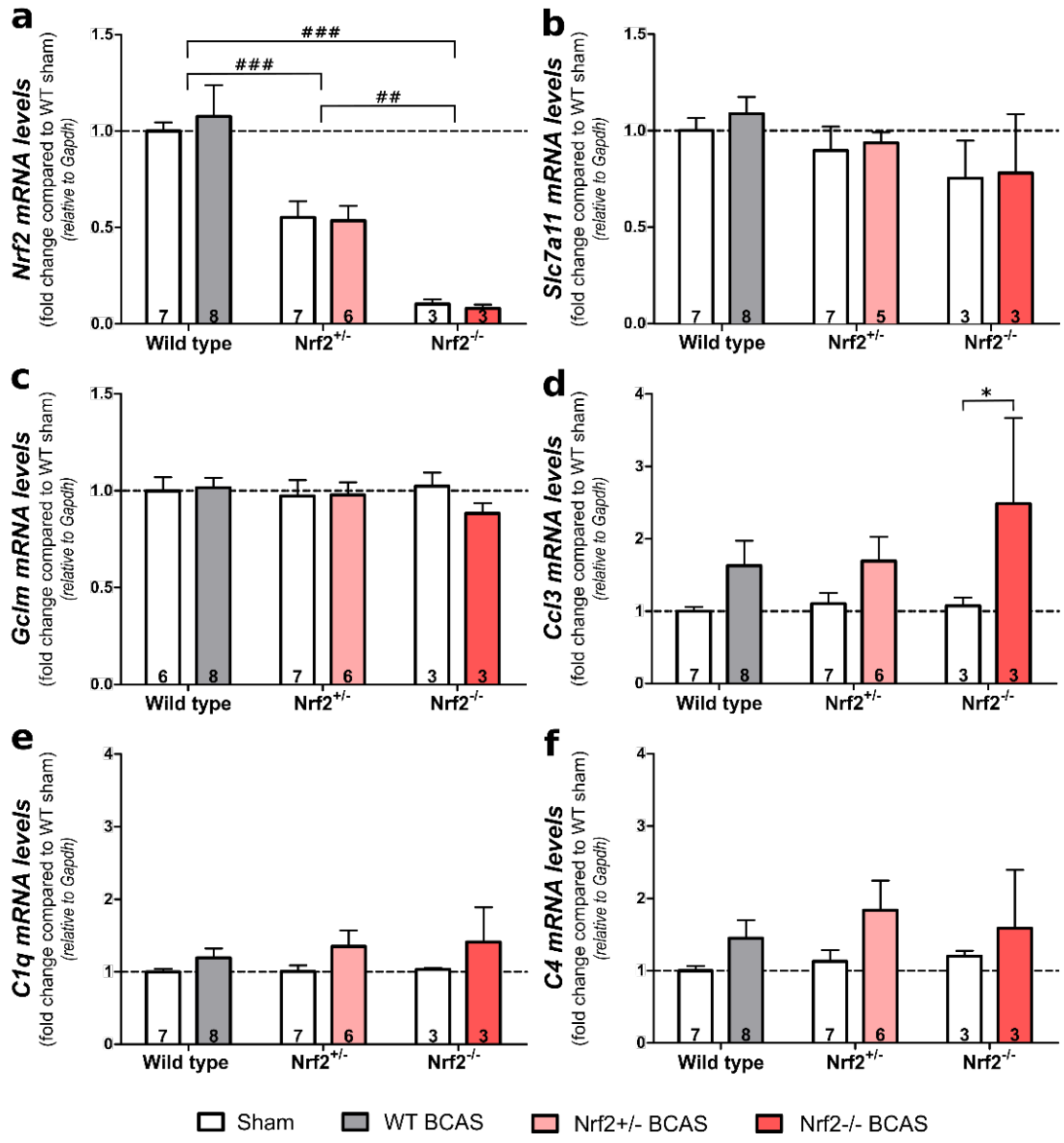

◄Figure 3.5 Nrf2 and Nrf2-regulated antioxidant genes in the optic tract are unaltered post-BCAS but pro-inflammatory genes are induced. (a) There was an effect of genotype on Nrf2 expression but no effect of BCAS surgery. Nrf2 was reduced by ~50% in $Nrf2^{+/-}$ mice and almost undetectable in $Nrf2^{-/-}$ mice. **(b)** There was no effect of BCAS surgery or genotype on Slc7a11 **(c)** or Gclm expression, **(d)** however, BCAS surgery increased the expression of Ccl3 and (e) C1q. **(f)** The effect of BCAS surgery just missed accepted levels of statistical significance for C4 expression and there was no genotype effect on any gene. Gene expression was normalised to Gapdh and expressed as fold change compared to wild type shams. Mean±SEM. n-number presented in each bar. Dashed line indicates WT sham mean. *p<0.05 (* indicates *post hoc* differences between sham and BCAS groups), ##p<0.01, ###p<0.001 (# indicates differences between genotypes).

3.3.6 Spatial working memory is impaired post-BCAS but is not exacerbated by deficiency of Nrf2

As previously mentioned, white matter disruption is hypothesised to underlie impairments in cognition. The 8-arm radial arm maze was used in the current study to assess spatial working memory as it has previously been demonstrated to be sensitive to hypoperfusion-induced disruption of frontocortical circuitry (by us and others Coltman et al., 2011, Shibata et al., 2007). Since white matter pathology is exacerbated in $Nrf2^{-/-}$ BCAS mice, the next was to determine if this was associated with more severe cognitive impairment. Spatial working memory was quantified as number of revisiting errors before entry into all 8 arms and cognitively healthy animals display a progressive reduction in revisiting errors over consecutive trials as they learn the task. Regretfully, due to the low numbers of $Nrf2^{-/-}$ animals they were grouped with $Nrf2^{+/-}$ animals for the behavioural analysis, however it is noted that since there was no difference in pathology between wild type and $Nrf2^{+/-}$ BCAS groups functional effects are likely difficult to detect in this manner. Statistical analysis was performed on the first and second half of the test separately because the first half is primarily a learning phase (Fig 3.7).

Spontaneous alternation and total entries in the Y-maze were recorded and compared across groups as they represent potential confounds to performance in the radial arm maze. Wild type and $Nrf2^{+/-}/^{-/-}$ groups all spontaneously alternated above chance level (WT sham p=0.007, WT BCAS p=0.02, $Nrf2^{+/-}/^{-/-}$ sham p=0.02, $Nrf2^{+/-}/^{-/-}$ BCAS p=0.02) and there was no effect of BCAS surgery ($F_{(1,28)}$=0.07, p=0.8) or genotype ($F_{(1,28)}$=1.37, p=0.25) on spontaneous alternation (Fig 3.6a). There was also no effect of BCAS surgery ($F_{(1,28)}$=1.26, p=0.27) or genotype ($F_{(1,28)}$=1.66, p=0.21) on total entries (Fig 3.6b).

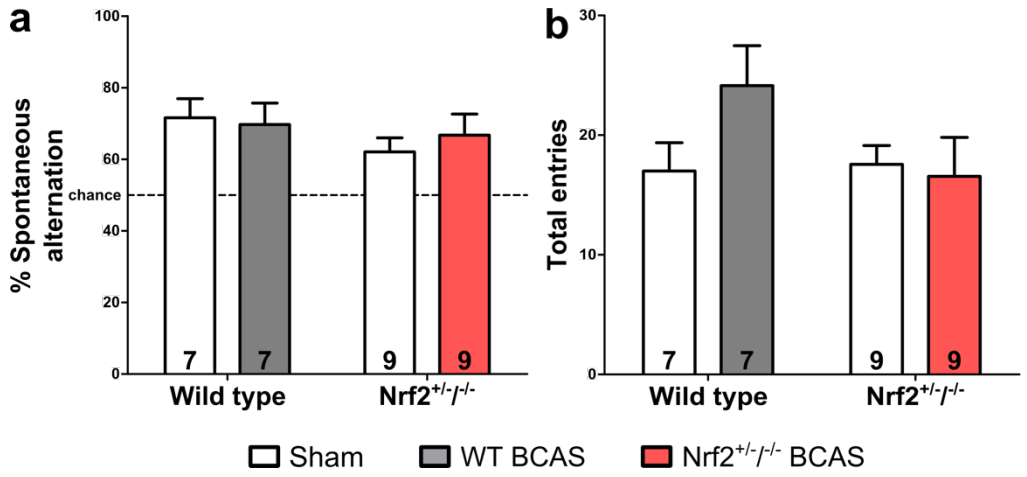

Figure 3.6 Spontaneous alternation and mobility are unaltered post-BCAS in wild type and Nrf2$^{+/-/-/-}$ mice. (a) Wild type and Nrf2 KO groups all spontaneously alternated above chance level in the Y-maze task, and there was no effect of BCAS surgery or genotype. **(b)** There was no effect of BCAS surgery or genotype on total entries in the Y-maze task. Mean±SEM. n-number presented in each bar.

For the radial arm maze, there was a significant effect of trial during both the first and second half of the test ($F_{(1,84)}$=7.03, p<0.0001, $F_{(3,84)}$=3.62, p=0.02 respectively) indicating that mice were able to learn the task successfully (Fig 3.7a-d). The effect of BCAS surgery was not significant during the first half of the test ($F_{(1,28)}$=0.10, p=0.76) but was significant during the second half ($F_{(1,28)}$=4.21, p=0.049) (Fig 3.7a-b). This indicates that while both sham and BCAS groups were learning the task initially, the BCAS groups' learning plateaus and they commit significantly more revisiting errors than sham groups during the second half of the test. However, there was no effect of genotype on spatial working memory (first half, $F_{(1,28)}$=0.07, p=0.79; second half, $F_{(1,28)}$=0.001, p=0.98) (Fig 3.7c-d), which contests the hypothesis that reductions in Nrf2 exacerbates cognitive deficits caused by BCAS-induced cerebral hypoperfusion, however due to the low n-number we are unable to determine if the absence of Nrf2 has a detrimental effect on spatial working memory post-BCAS.

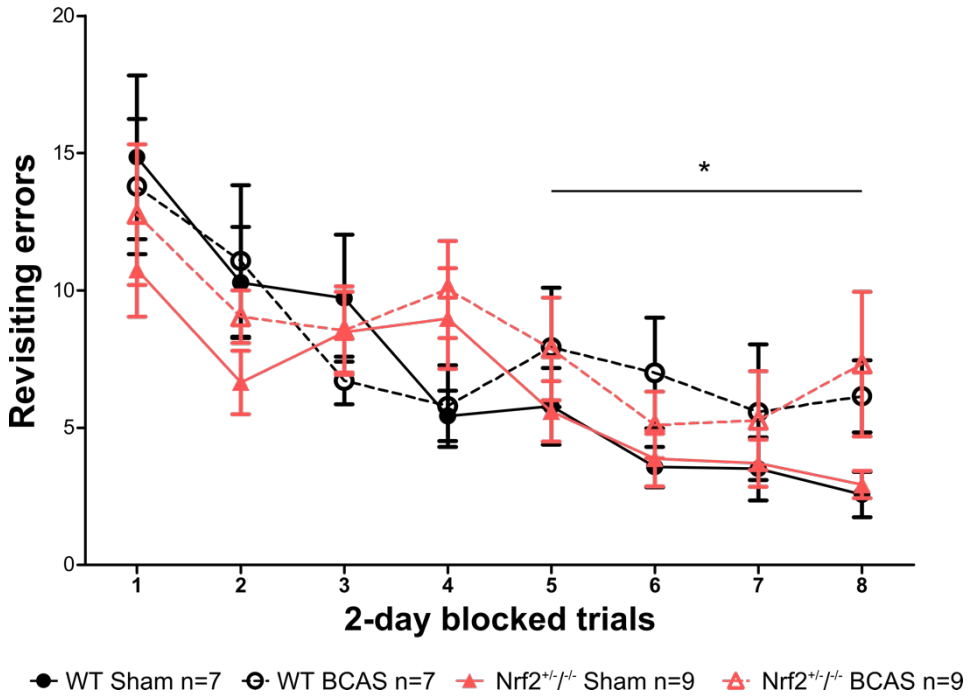

Figure 3.7 Spatial working memory is impaired post-BCAS but is not exacerbated by deficiency in Nrf2. There was an effect of trial during both first and second half of the test indicating learning over time. During the second half of the test, revisiting errors were significantly higher post-BCAS demonstrating impaired spatial working memory. However, there was no effect of genotype on revisiting errors during either the first or second part of the test. *Post hoc* analyses identified no further significant differences. Mean±SEM. *p<0.05 (* indicates main effect of BCAS surgery during second half of test).

3.4 Discussion

Previous studies of the BCAS model in mice demonstrate increased inflammation (Coltman et al., 2011, Reimer et al., 2011, Saggu et al., 2016) and oxidative stress (Washida et al., 2010, Dong et al., 2011, Miyamoto et al., 2013), indicating these may be pathophysiological mechanisms whereby white matter disruption occurs when cerebral blood flow is reduced. The current study was designed to test the hypothesis that deficiency of the anti-inflammatory/antioxidant regulating transcription factor Nrf2 exacerbates white matter disruption and cognitive impairment following BCAS-surgery. The results show that absence but not reduction of Nrf2 aggravates white matter disruption and gliosis, but with the available data no conclusion can be drawn as to whether this is associated with functional deficits in spatial working memory following 6 weeks of mild cerebral hypoperfusion.

3.4.1 Resting cortical CBF is significantly reduced post-BCAS to a similar extent in wild type and Nrf2$^{+/-}$ mice

The first aim of the study was to examine the extent of CBF reductions post-BCAS. The CBF alterations were able to be determined only in a subset of animals and this included no hypoperfused Nrf2$^{-/-}$ animals. Using laser speckle imaging, CBF was found to be reduced by 40-50% at 24 hours. This is more severe than the original characterisation which reported a 25% reduction in CBF at 24 hours (Shibata et al., 2004). Previous work by the group saw slightly less severe reduction in CBF of 36% at 3 days post-BCAS (McQueen et al., 2014). This discrepancy is likely due to CBF recovery which has been demonstrated to occur almost immediately following surgery (Shibata et al., 2004). Importantly, the extent of CBF reduction seen in the current study is not sufficient to induce ischaemia which would elicit a different pathophysiological response and while laser speckle imaging is only able to measure the superficial cortical circulation previous work by the lab has demonstrated that it is reflective of both deep white matter and subcortical perfusion as measured by arterial spin labelling MRI (Duncombe et al., 2017). It was noted that CBF recovered slightly but persisted at 6 weeks and that CBF recovery was comparably greater in wild types. This is consistent with previous studies by us (McQueen et al., 2014) and others (Shibata et al., 2004) reporting 10-15% CBF recovery in wild type mice at 1 month. The data also suggest that Nrf2 deficiency may impair CBF recovery following BCAS surgery.

Impaired CBF recovery in Nrf2$^{+/-}$ animals may be explained by studies that have found that absence of Nrf2 impairs angiogenic capacity *in vitro* (Valcarcel-Ares et al., 2012, Zhao et al., 2016, Gremmels et al., 2017, Huang et al., 2018) and inhibits upregulation of angiogenic vascular endothelial growth factor (VEGF) *in vivo* in a model of venous hypertension (Li et al., 2016b). This also suggests that the capacity of blood flow recovery following BCAS surgery may be even more inferior in Nrf2$^{-/-}$ compared to wild type mice however additional studies would be required to determine the effect of BCAS on blood flow in Nrf2$^{-/-}$ mice. With the available data we conclude that BCAS surgery reduces CBF chronically and reductions are comparable between wild type and Nrf2$^{+/-}$ mice acutely but CBF recovery occurs to a greater extent in wild type.

3.4.2 White matter disruption is more severe in Nrf2$^{-/-}$ compared to wild type and Nrf2$^{+/-}$ mice in response to cerebral hypoperfusion

The BCAS model has been well-characterised by our group and others and white matter pathology has been demonstrated (Coltman et al., 2011, Holland et al., 2011, Shibata et al., 2004). In this study white matter disruption was detected in the corpus callosum and optic tract following 6 weeks of mild cerebral hypoperfusion, evident by increased density of MAG positive debris. MAG is expressed at the axon-glial interface and is sensitive to hypoxia-induced injury (Aboul-Enein et al., 2003). Human post mortem studies identify loss of MAG, in particular its ratio to the more stable PLP, as a measure of white matter ischaemia (Barker et al., 2013). Cerebral hypoperfusion in mice exhibits this feature as early as 3 days post-surgery, and at least initially affects MAG without influencing other markers of myelin such as myelin basic protein and Fluoromyelin (Reimer et al., 2011, McQueen et al., 2014), consistent with hypoxia-induced white matter injury in humans (Aboul-Enein et al., 2003).

The current study saw more prominent white matter disruption in the optic tract than in the corpus callosum, areas which in previous studies have been reported collectively (Coltman et al., 2011, Holland et al., 2011). These reports have therefore not commented on potential reasons for regional susceptibility of different areas; which may be due to differences in vascular supply to the two tracts. The ophthalmic artery supplying the optic nerve and tract, branches off the internal carotid artery prior to it joining the circle of Willis (Ruberte et al., 2017). The corpus callosum in contrast, despite being a deep white matter structure, has a slightly better collateral blood supply and may therefore benefit from some compensatory redistribution (Ruberte et al., 2017). Studies in rats require complete occlusion of both common carotid arteries

due to a richer collateral blood supply, however this induces CBF reductions and white matter disruption in the optic tract (Wakita et al., 2002, Farkas et al., 2004). Other studies using the BCAS model in mice demonstrate more pronounced disruption of the corpus callosum compared to the current study (Shibata et al., 2004, Nakaji et al., 2006, Washida et al., 2010), although utilisation of different markers (commonly used histological stain Klüver-Barrera) measured at a different Bregma level (0.50 mm; striatum) may account for the observed differences. Because C57Bl/6 mice often display an incomplete circle of Willis, the forebrain is expected to exhibit greater cerebral hypoperfusion post-BCAS (Yang et al., 1997), potentially explaining greater disruption of the corpus callosum at the level of the striatum as opposed to the hippocampus.

Further, it is important to note that MAG only represents a single protein and while aberrant accumulations of this indicates a disruption of the axon-glial interface present in the white matter suggesting impaired function it does not report on the overall state or integrity of the myelin. Some early studies identified disrupted myelin using immunostaining for degraded myelin basic protein (dMBP) (Coltman et al., 2011, Holland et al., 2011), whereas others found no effect of BCAS on myelin basic protein, fluoromyelin or markers of axonal damage (Reimer et al., 2011, McQueen et al., 2014) following 1 month of mild cerebral hypoperfusion. Further unpublished data of overall myelin basic protein levels as measured using western blotting has led to the hypothesis that myelin and axons at least initially remain intact while alterations in MAG can be observed, indicating impaired communication which is also relevant to changes observed in human VaD (Aboul-Enein et al., 2003).

As such, the current study finds that cerebral hypoperfusion induces white matter axon-glial disruption which is exacerbated in the absence of Nrf2 in both the corpus callosum and the optic tract. This supports the hypothesis that Nrf2, present in wild type and $Nrf2^{+/-}$ mice, acts to limit whiter matter disruption following hypoperfusion. This is consistent with earlier studies investigating the role of Nrf2 in the maintenance of white matter integrity. Hubbs et al. (2007) found that the absence of Nrf2 in aged mice (>10 months) is associated with vacuolar white matter degeneration, extensive astrogliosis and myelin-specific oxidative injury. In the EAE model of multiple sclerosis, previous studies show that absence of Nrf2 results in more demyelination and worse clinical scores, associated with more extensive microglial and inflammatory gene responses compared to wild type controls (Johnson et al., 2010).

3.4.3 Increased microglial density in response to cerebral hypoperfusion is exacerbated in Nrf2$^{-/-}$ compared to wild type and Nrf2$^{+/-}$ mice

White matter disruption has previously been shown to be paralleled by cellular inflammation primarily characterised by a microglial response (Shibata et al., 2004, McQueen et al., 2014, Miki et al., 2009, Saggu et al., 2016). White matter inflammation is proposed to contribute to age and disease-related white matter pathology through excessive pro-inflammatory signalling, phagocytosis and oxidative stress (Raj et al., 2017). The data presented in the current study are consistent with previous work displaying increased density of microglia in the corpus callosum and optic tract, correlating with area and severity of white matter disruption. The results also demonstrate that hypoperfusion-induced increases in microglial density are further increased in the absence of Nrf2, suggesting that signalling through Nrf2 normally acts to limit upregulation of microglia post-BCAS.

Microglial density was assessed using immunohistochemistry for Iba1. Iba1 is a marker common of both microglia and macrophages, although, recently published data by our group identified all Iba1 positive cells in the corpus callosum co-labelled for the microglia-specific marker TMEM119 (Manso et al., 2017). This indicates that there is little to no infiltration of peripheral macrophages following mild cerebral hypoperfusion. Further, associations between number of Iba1 positive microglia and white matter function suggests microglia may be important contributors to the disease process through secretion of cytokines and chemokines (Manso et al., 2017, Fowler et al., 2017). It is noted that Iba1 is a pan-marker for microglia/macrophages providing no more than morphological information about activation state and sub-population of said cells. Utilising alternative markers such as major histocompatibility complex II, cluster of differentiation 40 and 68 associated with antigen presentation and phagocytosis which are upregulated on the surface of microglia upon activation (Simpson et al., 2007b) may increase our understanding of the disease process and the involvement of Nrf2. Recent studies have shown that there is tremendous regional heterogeneity of naïve microglia which changes with advancing age (Grabert et al., 2016, Soreq et al., 2017), highlighting the possibility of huge variation in microglial responses across the brain and lifespan which may need to be considered in future studies.

Microglia, in white matter, are important for myelin repair both through phagocytosis of myelin degradation products which are neurotoxic and prevent

recovery if not cleared (Aboul-Enein et al., 2003), and through release of growth factors (Lloyd et al., 2017). A study of peripheral nerve crush injury found that Nrf2$^{-/-}$ mice had a reduced ability to clear myelin debris (Zhang et al., 2013), a mechanism by which white matter disruption may be exacerbated in Nrf2$^{-/-}$ mice also in the current study. Additional work suggest that Nrf2 is a regulator of microglial dynamics, for example, microglia isolated from Nrf2$^{-/-}$ mice display an exacerbated inflammatory response in response to exogenously applied α-synuclein (Lastres-Becker et al., 2012). *In vivo* in an experimental model of Parkinson's disease (chronic MPTP injections), authors report increased microglia numbers in Nrf2$^{-/-}$ mice in control conditions (saline injection) (Rojo et al., 2010), indicating that Nrf2 may regulate microglial number. In contrast, the current study did not detect an increase in microglial density in Nrf2$^{-/-}$ animals that were not subjected to BCAS, although this may be a result of studying younger animals compared to Rojo et al. (2010). Further, Rojo et al. (2010) identified reduced levels of phagocytosis in Nrf2$^{-/-}$ mice in line with the study by Zhang et al. (2013) where clearance of myelin debris peripherally was impaired. Increased microglial gene (Iba1/cluster of differentiation 11b) and protein expression (Iba1) has also been reported in several models of Alzheimer's disease lacking Nrf2 (Joshi et al., 2015, Branca et al., 2017, Rojo et al., 2018), further implicating Nrf2 in the regulation of microglial dynamics.

3.4.4 Cerebral hypoperfusion induces astrogliosis to a similar extent in wild type and Nrf2 KO mice in the optic tract

The next aim of the study was to investigate the extent of astrogliosis to determine if this was influenced post-BCAS and altered by Nrf2 deficiency. The data showed that there was no effect of cerebral hypoperfusion in the corpus callosum or the internal capsule, however astrogliosis was detected post-BCAS in the optic tract, reflective of the magnitude of white matter disruption and microgliosis in the same area. There was also a trend suggesting that this response was more severe in Nrf2$^{-/-}$ mice. Previous work by the group in wild type mice detected no alterations in the number of GFAP positive astrocytes at 1 month (McQueen et al., 2014) but found increased density of GFAP in the corpus callosum and the thalamus at 3 and 6 months respectively (Kitamura et al., 2017, Holland et al., 2015), considerably later than the microglial response. The results from the current study finds astrogliosis in the optic tract at an earlier time point that previously observed, although astrogliosis has not been assessed to the same extent as microglia and never in the optic tract. Other groups show white matter astrogliosis alongside the microglial response in the corpus

callosum and internal capsule (Shibata et al., 2004, Nakaji et al., 2006, Dong et al., 2011). This suggests that both astrocytes and microglia contribute to the inflammatory response triggered by BCAS-induced cerebral hypoperfusion, which may be responsible for the disruption of white matter. The results demonstrated in the current study are in support of this.

Interestingly, there was a slight increase in the density of GFAP positive astrocytes in both sham and hypoperfused Nrf2$^{-/-}$ mice in the corpus callosum. The report by Hubbs et al. (2007) found that aged Nrf2$^{-/-}$ mice display widespread astrogliosis, suggesting that Nrf2 contributes to the regulation of astroglial activation state. Previous studies using Nrf2$^{-/-}$ mice in models of neurodegeneration show increases in GFAP protein (Rojo et al., 2018, Branca et al., 2017), mRNA (Granado et al., 2011) or both (Joshi et al., 2015), leading to the prediction that a greater response would be seen in the current study. Although, Johnson et al. (2010) report that absence of Nrf2 in the EAE model of multiple sclerosis resulted in similar levels of astrogliosis compared to wild type mice, highlighting that Nrf2 may regulate astrogliosis differently in different disease models. Importantly, a lack of significant astrogliosis does not inform on the antioxidant and pro/anti-inflammatory capacity of those astrocytes, which may differ between genotypes. Transcriptomic analysis of isolated astrocytes display a different profile based on the activating insult, suggested to indicate the functional phenotype of that population of reactive astrocytes (Zamanian et al., 2012). Microarray analysis may therefore provide far more information than immunohistochemistry. Similar to the discussion of Iba1 as a marker for microglia, GFAP is known to label only a subset of resting astrocytes (Cahoy et al., 2008). During reactive astrogliosis GFAP is massively upregulated (Sofroniew, 2014a) making it an acceptable marker for astrogliosis but may be inadequate to study the distribution and morphology of alternative astrocyte sub-populations. Alternative markers such as Aldh1l1 (Aldehyde dehydrogenase 1l1) have been identified, and shown to cover a much greater proportion of the entire astrocyte population (Cahoy et al., 2008), albeit still not all of it. Again similar to the studies performed on microglia, astrocytes have also been shown to display both regional and age-dependent heterogeneity (Morel et al., 2017, Boisvert et al., 2018).

Isolated astrocytes from Nrf2$^{-/-}$ mice do not respond to endogenously applied α-synuclein (Lastres-Becker et al., 2012) whilst in wild type astrocytes α-synuclein induces the expression of Nrf2-regulated antioxidant and detoxifying genes *Heme oxygenase 1* (*Hmox1*) and *NAD(P)H dehydrogenase 1* (*Nqo1*). *In vitro* studies have

identified astrocytes as the primary cell type for Nrf2-activation (Shih et al., 2003, Kraft et al., 2004) and astrocytes have been shown to mediate neuroprotection through increased synthesis of the antioxidant glutathione (Shih et al., 2003). Oligodendrocytes, which are highly metabolically active cells also receive antioxidant support from astrocytes (Lundgaard et al., 2014), highlighting the possibility that, at least initially, a loss of astrocyte antioxidant function rather than pronounced astrocyte-mediated inflammation may contribute to white matter disruption following hypoperfusion in $Nrf2^{-/-}$ mice.

3.4.5 Cerebral hypoperfusion does not affect *Nrf2* or Nrf2-regulated antioxidant gene expression but increases the expression of pro-inflammatory genes

As the previous results demonstrate exacerbated white matter disruption in $Nrf2^{-/-}$ mice associated with increases in microgliosis the next aim was to investigate the gene alterations which may underlie this, as well as determine the expression levels of *Nrf2* in wild type and transgenic mice. Quantitative PCR (qPCR) analysis was used to determine *Nrf2* expression of wild type, heterozygous ($Nrf2^{+/-}$) and homozygous Nrf2 ($Nrf2^{-/-}$) knockout mice used in the current study. There was a 50% reduction of *Nrf2* in $Nrf2^{+/-}$ mice and *Nrf2* expression was nearly undetectable in $Nrf2^{-/-}$ mice compared to wild type controls. Contrary to expectations, cerebral hypoperfusion did not alter the expression of *Nrf2*. The prediction was that hypoperfusion would increase expression of *Nrf2* in wild type mice since previous hypoperfusion studies identify increased inflammation (Fowler et al., 2017, Saggu et al., 2016) and oxidative stress (Dong et al., 2011, Miyamoto et al., 2013). However, this may be due to previous studies inducing more severe reductions in cerebral blood flow, using 0.17 mm microcoils (Saggu et al., 2016) or 0.16/0.18 mm microcoils (Fowler et al., 2017), in particular as a similar study by our group found that, despite increases in white matter disruption and microglial numbers, a battery of pro-inflammatory genes were unaltered at 12 weeks following mild hypoperfusion using 0.18 mm microcoils (Manso et al., 2017).

Another possibility is that the *Nrf2* expression may have increased acutely following the reduction of CBF, such as that observed following middle cerebral artery occlusion where *Nrf2* peaks between 8 hours (Tanaka et al., 2011) and 24 hours (Srivastava et al., 2013) but is reduced again at 72 hours. This response is also observed following traumatic brain injury (Miller et al., 2014) and indicates that regulatory mechanisms of the Nrf2 system may prevent it from being chronically

activated. This suggests that if Nrf2 activation did occur in the following study it is likely to have been detectable more acutely following BCAS surgery. A more detailed time course study following BCAS surgery would be required to determine if this is the case, which could be further strengthened by measuring Nrf2 protein levels and/or Nrf2/ARE DNA binding ability assays. Nonetheless, the results show that $Nrf2^{+/-}$/$Nrf2^{-/-}$ mice display the expected reductions of *Nrf2* compared to wild type mice.

Two antioxidant genes were assessed next, *Slc7a11* and *Gclm*, as these are known to be regulated by Nrf2 and are important for the synthesis of glutathione (Bell et al., 2011b). The glutathione system has been shown to be a major pathway mediating neuroprotection against oxidative stress by Nrf2 (Shih et al., 2003). *Gclm*/GCLm is decreased in $Nrf2^{-/-}$ compared to wild type mice in a model of Parkinson's disease (Innamorato et al., 2010) and following methamphetamine-induced axonal damage (Granado et al., 2011). The prediction was that these genes would be reduced in $Nrf2^{+/-}$/$Nrf2^{-/-}$ mice, however there was no effect of genotype nor cerebral hypoperfusion. The results suggest that these genes are not constitutively downregulated in $Nrf2^{+/-}$/$Nrf2^{-/-}$ mice, and the lack of a hypoperfusion effect prevents conclusions to be drawn as to whether the induction/expression of these genes is inferior to wild type mice as seen in other disease models.

Pro-inflammatory gene signalling has been reported to be exacerbated in $Nrf2^{-/-}$ mice in models of Parkinson's disease (Rojo et al., 2010) and Alzheimer's disease (Rojo et al., 2017). Hypoperfusion studies in mice identify significant increases of the chemokine Ccl3 (MIP1α) (Fowler et al., 2017) and increased expression of the pro-inflammatory complement pathway (Reimer et al., 2011), and so the next aim was to measure the expression of *Ccl3*, complement component 1q (*C1q)* and 4 (*C4)*. *Ccl3* was significantly increased by cerebral hypoperfusion, although there was no overall genotype effect present CCL3 is a pro-inflammatory chemotactic protein involved in the recruitment of pro-inflammatory cells (Maurer and von Stebut, 2004), and it has also been shown to impair cognition through impairment of hippocampal synaptic transmission (Marciniak et al., 2015). Had *Ccl3* been significantly increased in all $Nrf2^{-/-}$ mice following cerebral hypoperfusion this may have been a mechanisms whereby microglial density was increased. Hypoperfusion induced a significant increase in *C1q, C4* expression just missed accepted levels of significance, although there was no genotype effect. Activation of the complement pathway has been suggested to potentiate chronic inflammation and neurodegeneration (Stevens et al., 2007), and *C1q* specifically has been suggested to mediate astrocyte activation by microglia in

conjunction with tumour necrosis factor (TNF) and interleukin 1β (IL1β) (Liddelow et al., 2017). Interestingly, the complement cascade has also been shown to be activated by myelin-associated products (Johns and Bernard, 1997), suggesting that white matter disruption in itself may potentiate inflammatory changes observed following cerebral hypoperfusion.

Considering the exacerbated pathology in Nrf2$^{-/-}$ mice in the current study the prediction was reduced antioxidant and/or increased pro-inflammatory gene signalling. However, as previously discussed, the Nrf2-regulated response manifests differently in different disease models and greater effects may have been detected if measuring alternative markers, such as the canonical Nrf2 genes *Heme oxygenase 1* (*Hox1*) and *NAD(P)H dehydrogenase (quinone)-1 (Nqo1)* (Dowell and Johnson, 2013) which are generally not induced in Nrf2$^{-/-}$ mice (Lastres-Becker et al., 2012, Rojo et al., 2010). Alternative classical pro-inflammatory markers such as *TNFα* and *IL1β* are shown to be increased in Nrf2$^{-/-}$ mice (Rojo et al., 2010), however, the hypoperfusion model is more subtle than many of the reported models and pro-inflammatory markers have previously been difficult to detect several weeks after surgery (Manso et al., 2017). Another reason gene changes were unaltered in Nrf2$^{-/-}$ mice may be due to a lack of sensitivity as a result of analysing white matter homogenates containing a collection of different cell types. A recent study identified rather striking differences in gene expression in response to peripheral LPS injection and in a model of Alzheimer's disease when comparing whole brain to cell-specific populations from the same animal (Swartzlander et al., 2018). Alternatively, due to the current mouse model where Nrf2 is globally reduced or absent from the moment of conception and throughout development, it is possible that compensatory mechanisms are at play.

Nonetheless, the qPCR results identify an increase in pro-inflammatory genes following cerebral hypoperfusion consistent with previous reports (Fowler et al., 2017, Reimer et al., 2011), and there is some indication that this is slightly increased in Nrf2$^{-/-}$ mice.

3.4.6 Cerebral hypoperfusion causes a subtle impairment in spatial working memory in mice which is not exacerbated by absent or reduced expression of Nrf2

Cerebral hypoperfusion has previously been shown to cause an impairment in spatial working memory (Shibata et al., 2007, Coltman et al., 2011) attributed to disruption of frontal-subcortical circuitry, and because we saw exacerbated white

matter pathology in $Nrf2^{-/-}$ mice the next aim was to investigate spatial working memory. Consistent with previous reports, the current study demonstrated that cerebral hypoperfusion impairs working memory both in wild type and Nrf2 KO mice ($Nrf2^{+/-}$/$Nrf2^{-/-}$). However, in contrast to the hypothesis and the pathology results, the reduction/absence of Nrf2 did not exacerbate this impairment. One possibility is that this may be due to technical limitations. The low number of $Nrf2^{-/-}$ mice available for the study prevented analysis of $Nrf2^{+/-}$ and $Nrf2^{-/-}$ groups separately as this analysis would be underpowered. It is likely that the results from the $Nrf2^{+/-}$ mice are masking any effects present in the $Nrf2^{-/-}$ mice, in particular as the pathology revealed that $Nrf2^{+/-}$ mice overall displayed similar white matter disruption and gliosis compared to wild type mice. Another explanation is that the increased magnitude of white matter disruption in $Nrf2^{-/-}$ mice is insufficient to impair spatial working memory further at this time point. Longer duration of hypoperfusion would be expected to intensify the pathological differences between wild type and Nrf2 deficient animals, and a later time point may have identified functional effects of Nrf2-deficiency, in spite of the low n-numbers. To the best of our knowledge, there are no previous reports on cognitive function in Nrf2-deficient mice. With the existing data a conclusion cannot be drawn as to whether the absence of Nrf2 exacerbates spatial working memory impairment following cerebral hypoperfusion, albeit the pathological data is consistent with similar spatial working memory impairment between $Nrf2^{+/-}$ and wild type mice.

3.4.7 Potential mechanisms of white matter disruption

White matter lesions (WML) have been suggested to occur as a result of hypoxia as human post mortem studies find associations between WML and hypoxia-inducible factors (Fernando et al., 2006), and between the loss of MAG and increased HIF-1α (Aboul-Enein et al., 2003). Cerebral hypoperfusion induces white matter hypoxia, as demonstrated by reduced tissue oxygen tension in the corpus callosum 3 days post-surgery, persisting at least 6 weeks (Duncombe et al., 2017). The initial disruption of white matter following hypoperfusion is therefore likely caused by hypoxia as loss of MAG is detectable at similar time points (Reimer et al., 2011, McQueen et al., 2014). Hypoxia leads to disrupted mitochondrial oxidative phosphorylation which in turn leads to generation of reactive oxygen species (ROS) and oxidative stress (Toth and Warfel, 2017). Oxidative damage is observed in human post mortem tissue with WML indicating that oxidative stress is detrimental to the integrity of white matter (Al-Mashhadi et al., 2015). The primary molecular response to hypoxia is the stabilisation of the transcription factor HIF-1, which induces downstream gene changes that

promote angiogenesis and alterations in cellular metabolism to improve tissue oxygenation (Toth and Warfel, 2017). Nrf2 is also activated by hypoxia (Toth and Warfel, 2017), and it has been shown that knockdown of Nrf2 inhibits hypoxia-induced activation and secretion of HIF-1α (Ji et al., 2014, Zhao et al., 2016, Huang et al., 2018). This means that hypoxia may be exacerbated in $Nrf2^{-/-}$ mice following hypoperfusion, which would be expected to potentiate oxidative stress indirectly, in addition to direct effects from potential lack of Nrf2-mediated antioxidant signalling.

Direct measures of hypoxia or oxidative stress were not included in the current study but have been previously reported following hypoperfusion in mice (Duncombe et al., 2017), and pharmacological inhibition of oxidative stress is associated with improved white matter integrity in the BCAS model in mice (Dong et al., 2011, Miyamoto et al., 2013). Unpublished work by our group find free radicals in the brains of aged hypoperfused mice, providing support of oxidative stress as a pathological feature. However, without direct measures of free radical production or oxidative stress from the current study no conclusions can be drawn as to whether this is exacerbated in $Nrf2^{-/-}$ mice. Nrf2 deficiency in the context of oxidative stress alongside white matter integrity has not been described in the literature, however oxidative damage to proteins and lipids is increased in $Nrf2^{-/-}$ mice with both amyloid and tauopathy (AT-NRF2-KO) compared to mice with amyloid and tauopathy alone (AT-NRF2-WT) (Rojo et al., 2017). Oxidative stress may result from increased ROS production which was shown by *in vitro* work to be aggravated in the absence of Nrf2 through upregulation of the enzyme NOX2 (Kovac et al., 2015), whose activity is also shown to increase following hypoperfusion (Dong et al., 2011). In addition, oxidative stress is exacerbated by reduced antioxidant support, observed in $Nrf2^{-/-}$ mice in response to methamphetamine-induced axonal damage (Granado et al., 2011) and in a mouse model of Alzheimer's disease (AT-NRF2-KO) (Rojo et al., 2017). Therefore, hypoxia and oxidative stress are probable mechanisms whereby white matter disruption is exacerbated in $Nrf2^{-/-}$ mice in the current study. However, both may interact with and potentiate the reported inflammatory response also suggested to contribute to white matter disruption (Simpson et al., 2007a, Raj et al., 2017).

Nrf2 under normal conditions acts to limit inflammation through crosstalk with the NF-κB regulated signalling pathway (Cuadrado et al., 2014). Activation of NF-κB potentiates pro-inflammatory signalling (Lawrence, 2009) and is followed by activation of Nrf2 which acts by way of negative feedback to prevent further activation of NF-κB (Cuadrado et al., 2014). It is therefore possible that absence of Nrf2 results in

increased microglial number/density through uncontrolled NF-κB activation. Reactive oxygen species can also directly activate the NF-κB pathway (Cuadrado et al., 2014) and so the absence of Nrf2 may further potentiate inflammation indirectly through dysfunctional redox regulation and oxidative stress. Nrf2 furthermore acts to resolve inflammation through induction of anti-inflammatory genes (Lee et al., 2003), and through direct inhibition of pro-inflammatory genes in a non-ARE dependent manner (Kobayashi et al., 2016), which in addition may explain why microglial density is increased following hypoperfusion in $Nrf2^{-/-}$ mice.

3.4.8 Limitations, conclusion and future directions

The study would have been improved by an increased number of $Nrf2^{-/-}$ mice to adequately interrogate the role of Nrf2 in CBF regulation and cognition following hypoperfusion. A major shortcoming of the study is the lack of CBF measurements in $Nrf2^{-/-}$ mice, which if different from wild types may underlie the results.

There are also a number of technical limitations of laser speckle imaging which may influence the results. As mentioned previously, this technique only records superficial cortical perfusion and while previous data demonstrates that this reflects the magnitude of hypoperfusion in subcortical and deep white matter a measured using MRI (Duncombe et al., 2017) there is a possibility that this is differentially affected in wild type and $Nrf2^{-/-}$ mice. A recently developed alternative approach to laser speckle is 3-photon imaging which has recently been reported to allow a depth of imaging of 500-1000μm from the surface of the cortex (Wang et al., 2018, Koizumi et al., 2018).

An important factor that affects CBF is blood pressure. While basal blood pressure is reported not to differ between wild type and $Nrf2^{-/-}$ mice (Li et al., 2011), one study finds that selective inhibition of the Nrf2 gene in the rostral ventrolateral medulla in mice induces hypertension (Gao et al., 2017) and another study investigating Nrf2 in diabetic mice finds that Nrf2 deficiency exacerbates hypertension in this pre-existing condition (Zhao et al., 2018). Together these studies highlight that differences in blood pressure between genotypes may arise, in particular perhaps following BCAS surgery, however this cannot be commented on as it was not measured in the current study. Similar, and relevant to blood pressure and subsequent CBF regulation is blood gas content. In particular the partial pressure of CO_2 (Payne et al., 2011) which was also not recorded during the laser speckle imaging but has a significant impact on cerebral autoregulation. Future experiments would be improved by monitoring blood pressure and blood gases during CBF laser speckle recordings using an intra-arterial

catheter or blood pressure using a tail cuff as a catheter limits the repeatability of the experiment.

Further, wild type animals had to be imported as enough wild type littermates were not generated during the in-house breeding, which resulted in an imbalance of ages between experimental groups, representing a major limitation for interpretation of the results. The wild type groups average ages were 6 months with a few animals as young as 4 months old and $Nrf2^{+/-}$ groups average ages were 7 months and $Nrf2^{-/-}$ 8 months respectively. As Wolf et al., (2017) reports, age impacts not only on cerebral blood flow following BCAS, with more severe reductions in aged animals compared to young, but also on subsequent white matter disruption and microglial activation. It is hence a possibility that the results observed in the current study are influenced by age as opposed to or in combination with the reduced expression of Nrf2. Hubbs et al., (2007) report that $Nrf2^{-/-}$ animals display white matter pathology and astroglial activation with advancing age only, and hence a combinatory effect of both is plausible.

In addition, an understanding of the mechanisms involved in the disruption of white matter would have been improved by measures of hypoxia and/or oxidative stress. Attempts were made to measure different types of oxidative stress in fixed tissue using immunohistochemistry to no avail. Quantitative analysis of hypoxia and oxidative stress proteins could be performed using western or dot blot analysis using the collected snap frozen tissue. Alternatively, *in vivo* methods of measuring tissue oxygen tension and reactive oxygen species production are available using probes or injected fluorescent ligands but are experimentally challenging, particularly in the central nervous system. These types of experiments would typically require additional cohorts of mice which would greatly increase time and costs. Further, transcriptomic analysis of cell-specific populations including more Nrf2-regulated genes would allow for a greater understanding of Nrf2 signalling in response to cerebral hypoperfusion. Nrf2 signalling in the vasculature has been shown to decline with age (Ungvari et al., 2011a) and may explain why age is a major risk factor for VCI. However, preserving Nrf2 signalling throughout development and adulthood in mice would better model the human condition. Inducible, cell-specific transgenic drivers are now available that could be used to knock out the Nrf2 gene in an individual cell type at a suitable time. This would ensure that compensatory mechanisms that may occur as a result of Nrf2 being absent during development can be circumvented.

Finally, while this model of cerebral hypoperfusion has been demonstrated to selectively disrupt white matter initially (4 weeks) (Shibata et al., 2004, Coltman et al., 2011), progressive damage also to grey matter (3-6 months) (Holland et al., 2015) may influence results observed following BCAS in mice. While limited, (Miki et al., 2009) demonstrate that at 35 days following mild cerebral hypoperfusion there is some evidence of neuronal cell loss in the cortex and the hippocampus and at 5-6 months after BCAS hippocampal atrophy is evident (Nishio et al., 2010). This suggests that grey matter damage may be secondary to the observed white matter disruption which is likely why it is rarely studied following BCAS in mice. Nonetheless, grey matter pathology would be expected to likewise contribute to cognitive impairment and in conjunction with white matter disruption resembles pathological alterations observed in small vessel disease and further may contribute to worsening of other dementias such as Alzheimer's disease (Snowdon et al., 1997, Iturria-Medina et al., 2016, Kapasi et al., 2017, Lin et al., 2018). However, histological analysis of the mice from the current study found only minimal ischaemic neuronal pathology (2/17 hypoperfused animals: 1 wild type, 1 $Nrf2^{-/-}$) suggesting this is not greatly impacting on the results in this chapter although it is worth noting that microglial increases can also be observed in the hippocampus, contradicting the reports of a selective white matter response to hypoperfusion.

In conclusion, the current study determined that white matter disruption and microgliosis following cerebral hypoperfusion is exacerbated in mice lacking the transcription factor Nrf2, in support of the hypothesis. Contrary to the hypothesis there was no effect of Nrf2-deficiency on cognitive performance, although this may be due to technical limitations of insufficient power. As a final point, the current study implicates inflammation and/or oxidative stress as contributors to hypoperfusion-induced white matter pathology, altered by the absence of Nrf2 signalling.

Additional hypoperfusion studies utilising $Nrf2^{-/-}$ mice with novel cell-isolation and transcriptional experimental approaches could be informative, however the potential of exploiting the Nrf2 pathway to reduce or prevent white matter pathology and cognitive impairment is of superior value and will therefore be investigated in the next chapter of this thesis.

Chapter 4

Investigating the effect of chronic cerebral hypoperfusion in a mouse model with increased expression of Nrf2 in astrocytes

4.1 Introduction

The previous chapter of this thesis demonstrates that lack of the transcription factor Nrf2 exacerbates white matter disruption and gliosis compared to wild type mice following cerebral hypoperfusion. Another recently published study found that DMF treatment, an anti-inflammatory drug thought to act primarily via activation of the Nrf2 pathway, ameliorates white matter impairment and microgliosis following severe cerebral hypoperfusion (Fowler et al., 2017). Further exploration of the involvement of Nrf2 in response to hypoperfusion was thus of interest, and in particular, the potential of Nrf2 to limit or prevent white matter pathology and cognitive impairment. *In vitro* experiments of neuronal/glial co-cultures show that Nrf2 is expressed several fold higher in astrocytes compared to neurons (Shih et al., 2003), and that Nrf2 activation occurs preferentially in astrocytes (Kraft et al., 2004). Mice overexpressing Nrf2 specifically in astrocytes were therefore developed (GFAP-Nrf2 mice, Vargas et al., 2008) to investigate the therapeutic potential of boosting Nrf2 signalling in neurodegenerative disease (reviewed by Johnson and Johnson, 2015). GFAP-Nrf2 mice display improved outcomes in models of familial amyotrophic lateral sclerosis, Huntington's and Parkinson's disease (Vargas et al., 2008, Calkins et al., 2010, Gan et al., 2012, Chen et al., 2009). Relevant to the study of cerebrovascular disease and vascular cognitive impairment is the ability of Nrf2 to preserve white matter integrity. Pharmacological activation of Nrf2 using DMF is now an approved treatment of multiple sclerosis (Gopal et al., 2017), and pharmacological Nrf2 activation is associated with improved white matter integrity in models of hypoperfusion (Fowler et al., 2017, Mao et al., 2018). This study was developed to build on previous work by interrogating the effects of increased Nrf2 expression specifically in astrocytes following cerebral hypoperfusion. The advantage of this approach is the ability to selectively investigate the effect of astrocytic Nrf2 using transgenic GFAP-Nrf2 mice (Vargas et al., 2008), unlike previous studies which have used pharmacological approaches to indirectly assess the effect of Nrf2-activation of white matter structure and function (Jin et al., 2014, Liu et al., 2015, Zhang et al., 2017, Fowler et al., 2017, Mao et al., 2018).

4.1.1 Hypothesis

This study tests the hypothesis that increased expression of Nrf2 in astrocytes prevents white matter disruption and cognitive impairment following BCAS-induced chronic cerebral hypoperfusion.

4.1.2 Aims

In wild type and GFAP-Nrf2 mice the aims are to:

1. Assess cerebral blood flow to determine the extent of BCAS-induced cerebral hypoperfusion
2. Assess spatial working memory
3. Assess the structural integrity of white matter
4. Assess white matter micro- and astrogliosis
5. Assess oxidative stress and inflammatory genes
6. For the above measures determine whether astrocytic overexpression of Nrf2 ameliorates the effects of BCAS

4.2 Materials and Methods

4.2.1 Experimental contribution

The study presented in this chapter was carried out by myself, Dr Martina Marangoni and Professor Karen Horsburgh. I performed laser speckle imaging, behavioural testing, and tissue collection/processing/sectioning with assistance from Dr Martina Marangoni. I performed immunostaining and imaging for MAG, Iba1 and GFAP, RNA extractions, quantitative PCR and all data analysis presented in this chapter. Professor Karen Horsburgh performed BCAS surgery.

4.2.2 Mice

Genetic details of GFAP-Nrf2 mice are described in 2.1.2. Adult male GFAP-Nrf2 and wild type littermates, mean age 4 m 23 d (4 to 5 m), weighing on average 35.4 g (27.6-41.4 g), were used for the following experiments. Animals (n=40) were randomly assigned surgical intervention as detailed in Table 4.1. The experimenters were blinded to genotype and surgery status of animals throughout data collection and analysis throughout data collection and analysis in accordance with ARRIVE guidelines (Kilkenny et al., 2010).

4.2.3 Chronic cerebral hypoperfusion

Mice underwent bilateral carotid artery stenosis (BCAS) or sham surgery, as described in 2.2. BCAS surgery was performed to induce chronic cerebral hypoperfusion, using two 0.18 mm in diameter microcoils. Recovery following surgery is closely monitored for 72 hours and animals showing poor recovery are culled. Four animals tolerated surgery poorly (two wild types and two GFAP-Nrf2 mice) and were humanely culled by cervical dislocation (see Table 4.1).

4.2.4 Laser speckle imaging to measure cortical cerebral blood flow

Cortical cerebral blood flow (CBF) was measured at rest prior to, 24 hours and 6 weeks post-BCAS as described in 2.3. Laser speckle imaging was performed on all animals.

4.2.5 Behavioural testing

Animals were singly housed and food restricted for the behavioural tests which were performed as described in 2.4.1-2.4.2. Spatial working memory was assessed by the 8-arm radial arm maze (2.4.1) and spontaneous alternation and mobility was assessed in the Y-maze (2.4.2). Behavioural testing commenced four weeks post-BCAS. Inclusion criteria described in 2.4.1.3 was applied excluding six animals (three

wild type shams, two wild type BCAS and one GFAP-Nrf2 BCAS animal) from behavioural analysis. Final numbers for each group are detailed in Table 4.1 and relevant figures.

4.2.6 Tissue collection and processing

Animals were sacrificed 6 weeks post-BCAS as described in 2.6.1. The tissue was further automatically processed for paraffin embedding as described in 2.6.4 and Table 2.2 and sectioned as described in 2.6.6.

4.2.7 Immunohistochemistry

Performed according to 2.7.1. Details of antibodies used (anti-MAG, anti-Iba1, anti-GFAP) can be found in Table 2.4. Immunohistochemistry was performed on 6µm coronal sections from all animals.

4.2.8 Image analysis

Images were acquired using a BX51 microscope (x20, Olympus, UK). Images were analysed for percentage area of MAG, Iba1 and GFAP as described in 2.8.2 in the CC, IC and OT (Fig 2.3). Briefly, ImageJ software (v1.46, NIH, Bethesda, MD, USA) was used to apply a global manual threshold followed by quantification of the positive signal detected above the selected threshold. Applying exclusion criteria outlined in 2.8.3 resulted in one GFAP-Nrf2 sham animal being excluded from the optic tract analysis of MAG. Final numbers for each region and stain are detailed in Table 4.1 and relevant figures.

4.2.9 Transcriptomics

Performed according to 2.9 using whole brain and optic tract-enriched samples. Details of primers used (*Gapdh, 18s, Nrf2, Slc7a11, Gclm, Ccl3, Ccl2, C1q,* C4) can be found in Table 2.5. Exclusion criteria were applied as described in 2.9.4, resulting in no exclusion from whole brain samples but from optic tract-enriched samples exclusion of one wild type sham animal from *Gclm* analysis, one wild type sham, one wild type BCAS and one GFAP-Nrf2 BCAS animal from *Ccl3* analysis and one wild type BCAS animals from *Ccl2* analysis. Final numbers are detailed in Table 4.1 and the relevant figure also containing reference gene used for each experiment.

4.2.10 Statistical analysis

Repeated measures ANOVA was used to analyse cerebral blood flow and behaviour as described in 2.10.1. The radial arm maze was analysed separately for the first and second half of the test as the first half primarily represents a learning

phase. Two-way ANOVA was used to investigate the effect of BCAS surgery and genotype in the Y-maze and Iba1, GFAP and MAG positive percentage area in white matter tracts and gene expression (2.10.2). One-sample t-test was used to analyse Y-maze spontaneous alternation (2.10.4). Unpaired one-tailed t-test was used to investigate the fold change of white matter disruption (2.10.5). Data is presented as mean ± standard error of the mean (SEM). Statistical significance was determined at $p<0.05$.

Table 4.1 Number of mice in each group and experiment with details of exclusion

BCAS surgery	**Wild type**	**GFAP-Nrf2**
Sham	8	10
BCAS	8	10
Details of exclusion		
Poor recovery from BCAS surgery	2 (Hypo)	2 (Hypo)
Laser speckle imaging	**Wild type**	**GFAP-Nrf2**
Sham	8	10
BCAS	8	10
Behavioural testing	**Wild type**	**GFAP-Nrf2**
Sham	5	10
BCAS	6	9
Details of exclusion		
Initial lack of motivation	5	1
Immunohistochemistry (CC, IC, OT)	**Wild type**	**GFAP-Nrf2**
MAG		
Sham	8, 8, 8	10, 10, 9
BCAS	8, 8, 8	10, 10, 10
Details of exclusion		
Anatomical area missing from slide	0	1 (OT)
Iba1		
Sham	8, 8, 8	10, 10, 10
BCAS	8, 8, 8	10, 10, 10
GFAP		
Sham	8, 8, 8	10, 10, 10
BCAS	8, 8, 8	10, 10, 10
qPCR whole brain (*Nrf2, Slc7a11, Gclm*)	**Wild type**	**GFAP-Nrf2**
Sham	8, 8, 8	10, 10, 10
BCAS	8, 8, 8	10, 10, 10
qPCR optic tract (*Nrf2, Gclm, C4, C1q, Ccl3, Ccl2*)	**Wild type**	**GFAP-Nrf2**
Sham	8, 7, 8, 8, 7, 8	10, 10, 10, 10, 10, 10
BCAS	8, 8, 8, 8, 7, 7	10, 10, 10, 10, 9, 10
Details of exclusion		
3IQR<Q1 / 3IQR>Q3 (outlier)	2 (*Ccl3, Ccl2*)	1 (*Ccl3*)
Reference gene >2STD from mean	2 (*Gclm, Ccl3*)	0

4.3 Results

4.3.1 Cortical cerebral blood flow is significantly reduced post-BCAS

CBF was evaluated using laser speckle imaging prior to, 24 hours and 6 weeks post-BCAS surgery to determine the extent of cerebral hypoperfusion and to determine if this differed between genotypes. Resting CBF over time was calculated as a percentage of each animal's baseline flux (arbitrary unit).

BCAS surgery induced reductions in CBF between 30-40%, whereas CBF in the sham group remained relatively stable over time (Fig 4.1). There was a significant effect of time ($F_{(2,64)}$=57.02, p<0.0001) and BCAS surgery ($F_{(1,32)}$=55.2, p<0.0001) and a significant interaction between time and surgery ($F_{(2,64)}$=32.63, p<0.0001) (Fig. 4.1b). *Post hoc* tests found that BCAS surgery reduced CBF in wild type and GFAP-Nrf2 groups at 24 hours (p<0.001) and 6 weeks (WT; p<0.001, GFAP-Nrf2 p=0.03). No effect of genotype was detected ($F_{(1,32)}$=0.03, p=0.86), indicating that overexpression of Nrf2 does not affect resting CBF in sham or BCAS groups (Fig 4.1a-b).

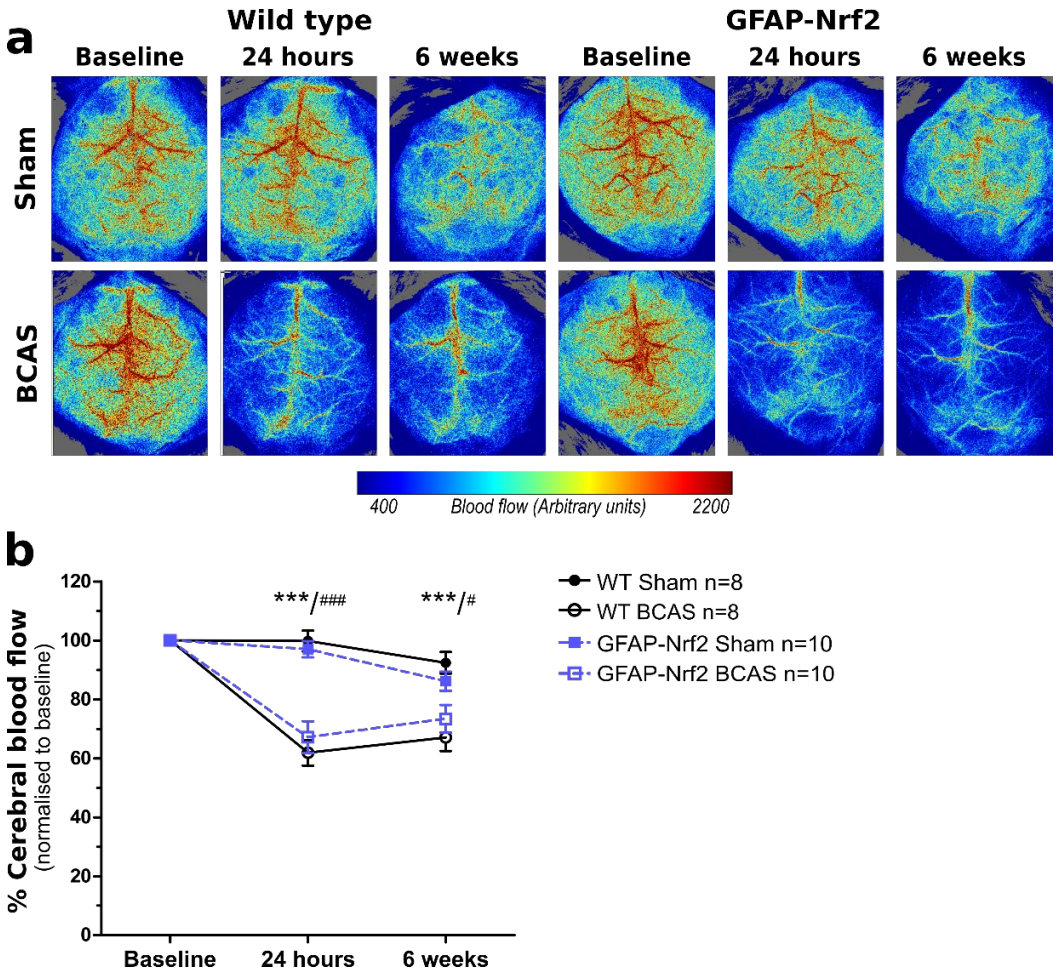

◄**Figure 4.1 Cortical cerebral blood flow is reduced post-BCAS. (a)** Representative images of laser speckle flowmetry in sham and BCAS, wild type and GFAP-Nrf2 animals at baseline, 24 hours and 6 weeks. **(b)** BCAS surgery reduced CBF to a similar extent in both genotypes. Mean±SEM. ***p<0.001 (* indicates *post hoc* differences between wild type sham and BCAS), #p<0.05, ###p<0.001 (# indicates *post hoc* differences between GFAP-Nrf2 sham and BCAS.

4.3.2 Spatial working memory is impaired post-BCAS but is less pronounced in GFAP-Nrf2 mice compared to wild type

The previous chapter of this thesis demonstrates that even though the absence of Nrf2 exacerbates white matter pathology and gliosis, the cognitive impairment was comparable between wild type and Nrf2 KO mice. Because the overarching hypothesis is that oxidative stress and inflammation drive both structural *and* functional white matter disruption in the current study we next sought to determine if astrocytic overexpression of Nrf2 protects against BCAS-induced cognitive impairment before assessing structural alterations. The 8-arm radial arm maze was used to assess spatial working memory as described in the previous chapter (3.3.6) and published work (Coltman et al., 2011), to corroborate previous results in wild type mice and to determine if there was a difference between genotypes. Due to differences in the learning profile of wild type and GFAP-Nrf2 sham groups (Fig 4.3a), the effect of BCAS surgery was initially investigated for each genotype separately, and similar to the previous chapter, because the first half of the test represents a learning phase, statistical analysis was performed on the first and second half of the test separately (Fig 4.3b-c).

Again, as a control measure, spontaneous alternation and total entries in the Y-maze were recorded and compared across groups (potential confounds to performance in the radial arm maze). Wild type and GFAP-Nrf2 groups all spontaneously alternated above chance level (WT sham p=0.047, WT BCAS p=0.03, GFAP-Nrf2 sham p<0.001, GFAP-Nrf2 BCAS p=0.0002), and there was no effect of BCAS surgery ($F_{(1,26)}$=0.88, p=0.36) or genotype ($F_{(1,26)}$=2.37, p=0.14) on spontaneous alternation (Fig 4.2a). There was also no effect of BCAS surgery ($F_{(1,26)}$=3.96, p=0.06) or genotype ($F_{(1,26)}$=2.57, p=0.12) on total entries (Fig 4.2b).

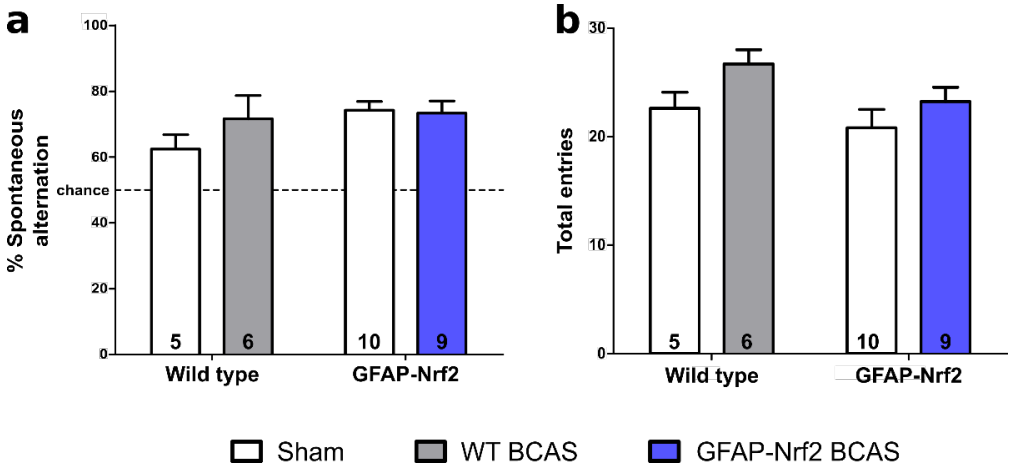

Figure 4.2 Spontaneous alternation and mobility are unaltered in wild type and GFAP-Nrf2 mice. (a) Wild type and GFAP-Nrf2 groups all spontaneously alternated above chance level in the Y-maze task, and there was no effect of BCAS surgery or genotype. **(b)** There was also no effect of BCAS surgery or genotype on total entries in the Y-maze task. Mean±SEM. n-number presented in each bar.

For the radial arm maze, there was an overall effect of trial for both wild type ($F_{(2.9,25.9)}$=3.39, p=0.04) and GFAP-Nrf2 mice ($F_{(4,68.3)}$=9.47, p<0.0001) (Fig 4.3b-c), indicative of learning. There was no difference in revisiting errors between wild type sham and BCAS groups in the first half of the test ($F_{(1,9)}$=1.51, p=0.25) but in the second half the wild type BCAS group made significantly more revisiting errors than sham controls ($F_{(1,9)}$=6.56, p=0.03) indicative of impaired spatial working memory (Fig 4.3b). *Post hoc* analysis found significant differences at block 5, 6 and 7 (p=0.01, 0.04, 0.04 respectively). In contrast, the GFAP-Nrf2 sham group was not significantly different from BCAS in the first half of the test ($F_{(1,17)}$=0.33, p=0.57) and in the second half the effect of BCAS surgery missed the accepted levels of statistical significance ($F_{(1,17)}$=3.81, p=0.07) indicating only a trend of impaired spatial working memory in the GFAP-Nrf2 BCAS group (Fig 4.3c). To investigate whether there may be a genotype difference, the fold change of revisiting errors of BCAS groups compared to respective sham controls was calculated as a measure of magnitude of cognitive impairment. There was an overall genotype effect ($F_{(1,13)}$=4.79, p=0.048), a significant effect of trial ($F_{(2.5,32.4)}$=8.70, p<0.0001) and a significant interaction between trial and genotype ($F_{(2.5,32.4)}$=3.36, p=0.04) (Fig 4.3d). *Post hoc* analysis identified significant differences between wild type and GFAP-Nrf2 groups at blocks 4, 5 and 6 (p=0.046, 0.02, 0.03 respectively) (Fig 4.3d). Overall these data suggest a modest protective effect of astrocytic Nrf2 overexpression on spatial working memory impairment caused by BCAS-induced hypoperfusion.

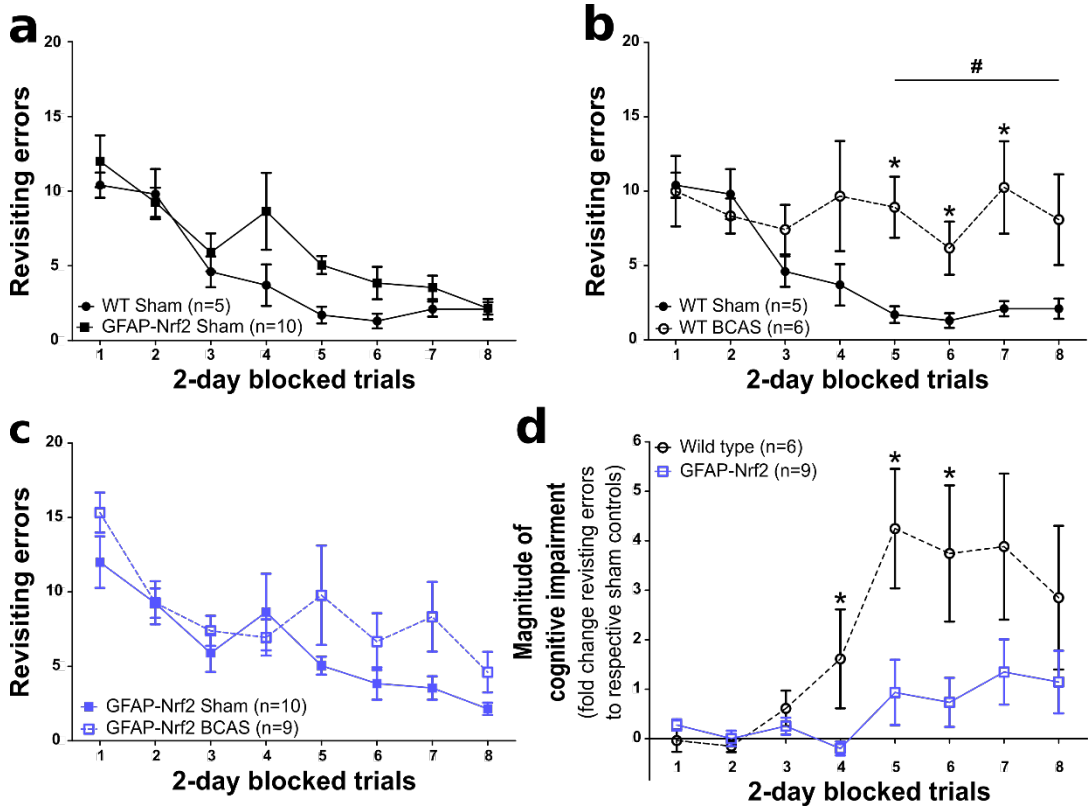

Figure 4.3 Cerebral hypoperfusion causes an impairment in spatial working memory which is less pronounced in GFAP-Nrf2 mice. (a) The learning profile for wild type and GFAP-Nrf2 sham groups displayed a different pattern, however was not significantly different from each other. **(b)** The wild type BCAS group committed significantly more revisiting errors than wild type shams during the second half of the test. **(c)** The GFAP-Nrf2 BCAS group trended towards committing more revisiting errors than GFAP-Nrf2 shams. **(d)** The magnitude of cognitive impairment was greater in wild types compared to GFAP-Nrf2. Mean±SEM. *p<0.05 (* indicates *post hoc* differences between groups), #p<0.05 (# indicates main effect of BCAS surgery during second half of test).

4.3.3 White matter disruption in the optic tract is less extensive in GFAP-Nrf2 mice compared to wild type post-BCAS

Behavioural performance in the radial arm maze is dependent on the integrity of myelinated axons within the white matter for efficient communication. Alterations in immunostaining for myelin associated glycoprotein (MAG) was used to assess white matter disruption as previously described in Chapter 3 (3.3.2) to evaluate the pathological response to BCAS compared to the previous chapter and studies and to determine if this differed between genotypes.

The percentage area of MAG positive immunostaining was quantified in key white matter tracts: corpus callosum, internal capsule and optic tract. There was no significant white matter disruption post-BCAS in the corpus callosum ($F_{(1,32)}$=2.63, p=0.12) or the internal capsule ($F_{(1,32)}$=0.08, p=0.78), and no effect of genotype ($F_{(1,32)}$=0.82, p=0.37; $F_{(1,32)}$=0.17, p=0.68 respectively) (Fig 4.4a-b). Similar to the study presented in chapter 3, there was a prominent white matter disruption post-BCAS in the optic tract ($F_{(1,31)}$=13.57, p=0.001) albeit no significant effect of genotype ($F_{(1,32)}$=0.6, p=0.44) (Fig 4.4c). *Post hoc* analysis of the effect of BCAS revealed significant white matter disruption in the wild type BCAS group compared to sham controls (p=0.004), but the difference between GFAP-Nrf2 BCAS and sham controls missed accepted levels of statistical significance (p=0.054) (Fig. 4.4c). To investigate whether the magnitude of white matter disruption in the optic tract differs between genotypes, the fold difference of MAG positive percentage area compared to controls was calculated and compared between wild type and GFAP-Nrf2 mice (Fig. 4.4d). There was a significantly higher magnitude of white matter disruption in wild type mice (p=0.03) (Fig 4.4d), indicating a modest protective effect of Nrf2 overexpression on optic tract white matter integrity following BCAS-induced cerebral hypoperfusion.

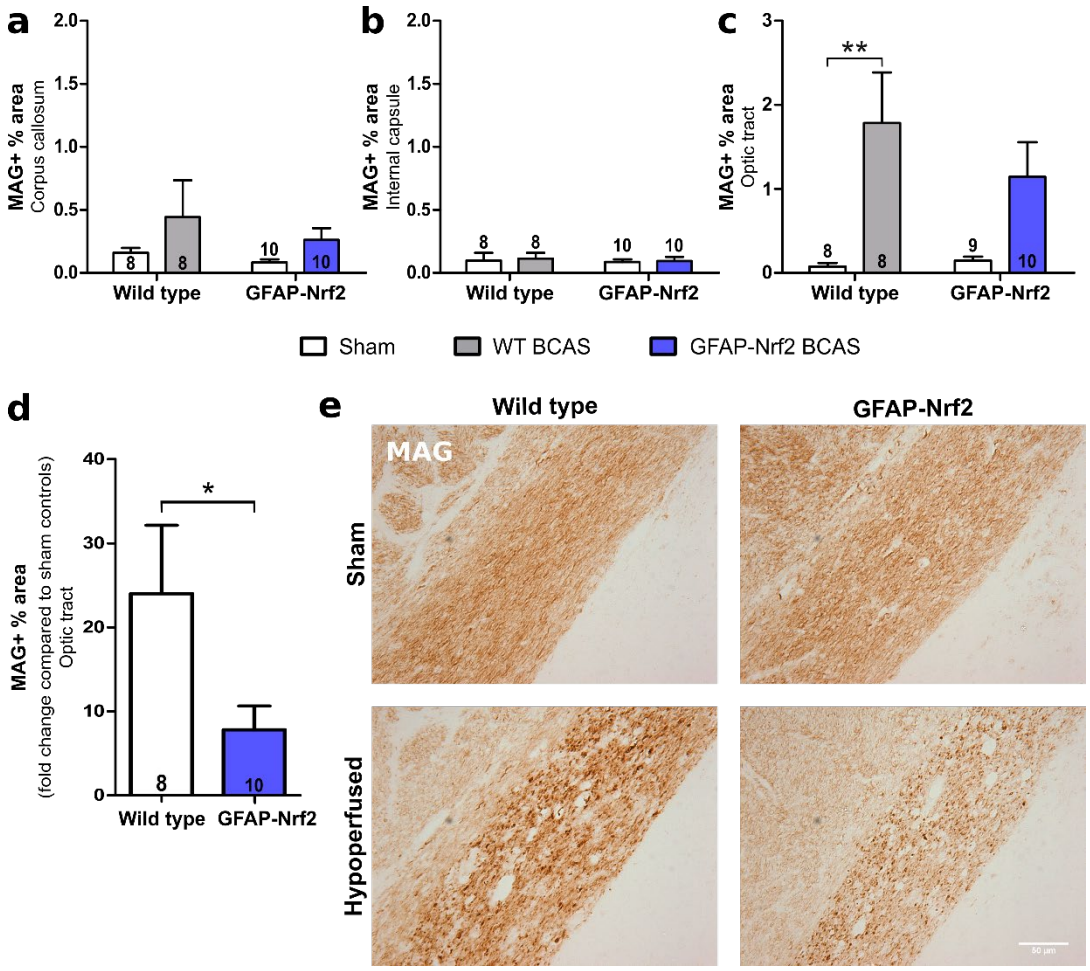

Figure 4.4 White matter disruption in the optic tract is less extensive in GFAP-Nrf2 mice compared to wild type post-BCAS. (a) There was no effect of BCAS surgery or genotype in the corpus callosum, (b) nor in the internal capsule. **(c)** In the optic tract, there was an effect of BCAS albeit no overall effect of genotype. **(d)** Fold change of white matter disruption compared to respective sham controls in the optic tract was significantly increased in wild type animals. Mean±SEM. n-number presented in each bar. *p<0.05, **p<0.01. **(e)** Representative images of MAG staining in the optic tract. Scale bar 50 µm.

4.3.4 The density of microglia is increased post-BCAS in the optic tract

To assess the inflammatory response associated with white matter disruption as observed in the previous chapter and studies (Coltman et al., 2011, McQueen et al., 2014), immunohistochemistry for ionized calcium binding adapter molecule 1 (Iba1) was used as previously described in Chapter 3 (3.3.3). Further, Iba1 positive percentage area was used to determine if astrocytic overexpression of Nrf2 influences the inflammatory response of microglia post-BCAS.

Iba1 was evaluated in key white matter tracts: corpus callosum, internal capsule and optic tract. Consistent with the absence of white matter disruption, there was no significant increase in density of microglia post-BCAS in the corpus callosum ($F_{(1,32)}$=2.41, p=0.13) nor in the internal capsule ($F_{(1,32)}$=2.75, p=0.11), and there was no effect of genotype ($F_{(1,32)}$=3.12, p=0.09; $F_{(1,32)}$=2.23, p=0.14 respectively) (Fig 4.5a-b). The white matter disruption in the optic tract was paralleled by an increased density of microglia post-BCAS ($F_{(1,32)}$=14.74, p=0.001), and *post hoc* analysis detected significantly higher densities in wild type and GFAP-Nrf2 BCAS groups compared to their sham controls (p=0.007, p=0.02 respectively) (Fig 4.5c). There was no effect of genotype on microglial density ($F_{(1,32)}$=0.29, p=0.59) (Fig 4.5c). These data show that cerebral hypoperfusion induced by BCAS surgery causes an increased density of microglia in the optic tract which also exhibits white matter pathology, but that this is not reduced by astrocytic overexpression of Nrf2.

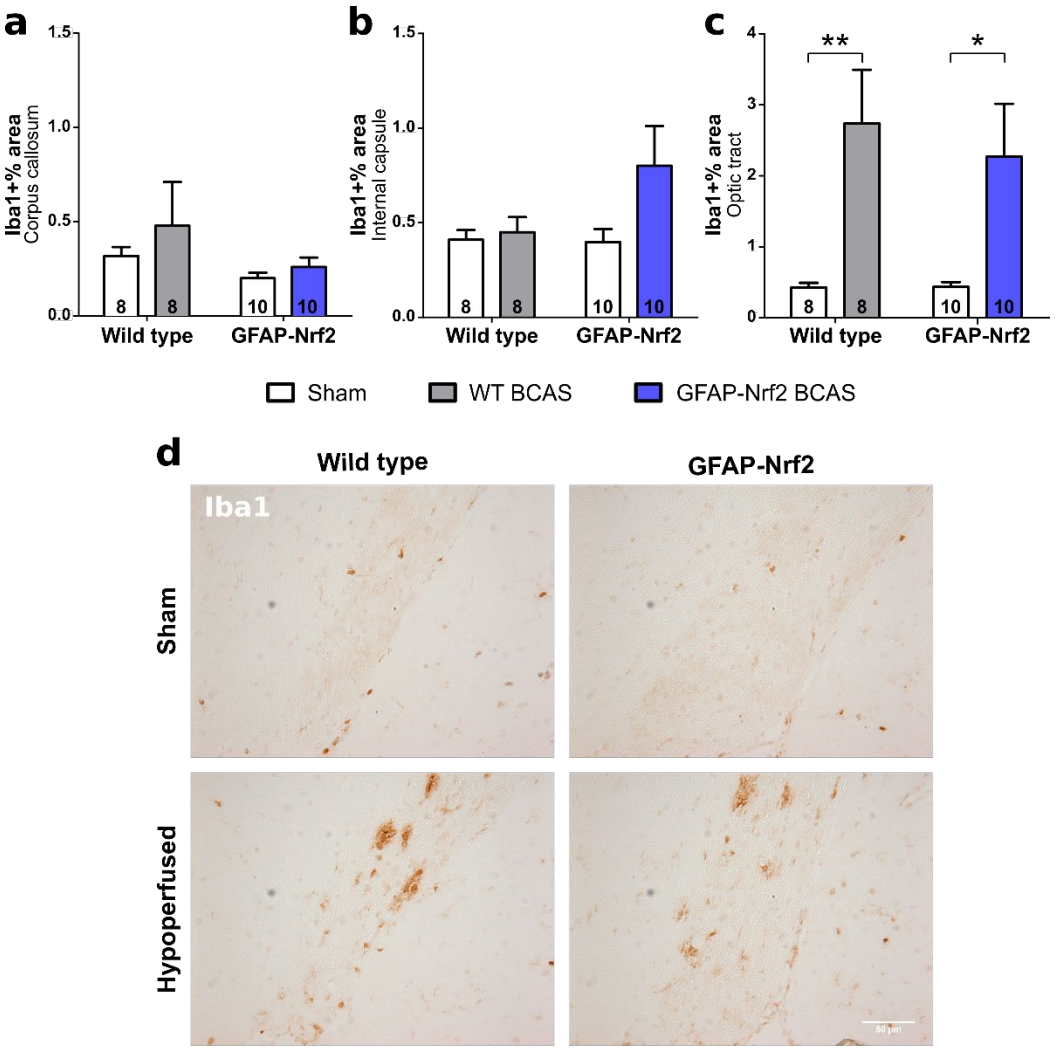

Figure 4.5 The density of microglia is increased post-BCAS in the optic tract. (a) There was no effect of BCAS or genotype on % area of Iba1 in the corpus callosum **(b)** nor the internal capsule. **(c)** There was an effect of BCAS in the optic tract, with no further effect of genotype. Mean±SEM. n-number presented in each bar. *p<0.05, **p<0.01. **(d)** Representative images of Iba1 staining in the optic tract. Scale bar 50 µm.

4.3.5 Astrogliosis in the optic tract is less in GFAP-Nrf2 mice compared to wild type post-BCAS

Despite seeing no genotype effect on the microglial inflammatory response post-BCAS, the next aim was to assess astrogliosis since Nrf2 is specifically overexpressed in astrocytes, and because the previous chapter of this thesis detected significant astrogliosis in both wild type and Nrf2 KO animals post-BCAS (3.3.4).

Glial fibrillary acidic protein (GFAP) immunohistochemistry: quantified as GFAP positive percentage area was evaluated in the main white matter tracts: corpus callosum, internal capsule and optic tract. BCAS surgery induced reactive astrogliosis in the optic tract ($F_{(1,32)}$=38.87, p<0.0001) (Fig 4.6c) but, similar to Iba1 expression and white matter disruption, not in the corpus callosum or the internal capsule ($F_{(1,32)}$=1.43, p=0.24, $F_{(1,32)}$=2.01, p=0.17 respectively) (Fig 4.6a-b). There was also no effect of genotype in these regions ($F_{(1,32)}$=1.95, p=0.17, $F_{(1,32)}$=3.34, p=0.08 respectively) (Fig 4.6a-b). However, there was a significant effect of genotype in the optic tract ($F_{(1,32)}$=7.45, p=0.01) and a significant interaction between BCAS surgery and genotype ($F_{(1,32)}$=7.05, p=0.01). *Post hoc* tests identified significant reactive astrogliosis in wild type (p<0.001) and GFAP-Nrf2 BCAS groups (p=0.01), but also a significant reduction in the GFAP-Nrf2 BCAS group compared to wild type BCAS (p=0.001) (Fig 4.6c). These data illustrate that cerebral hypoperfusion induced by BCAS surgery causes reactive astrogliosis in the optic tract, and that the extent of astrogliosis is reduced by astrocytic overexpression of Nrf2.

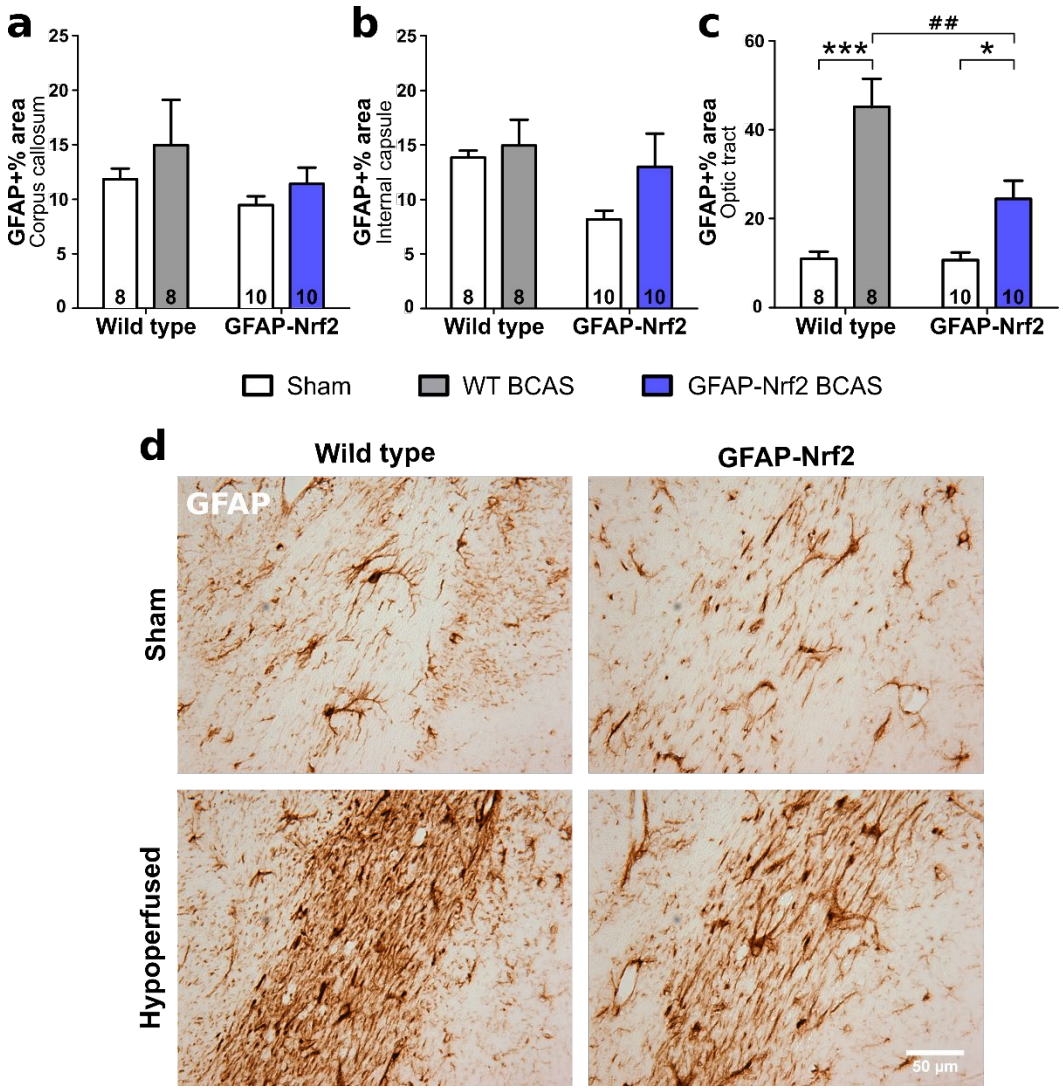

Figure 4.6 Astrogliosis in the optic tract is less in GFAP-Nrf2 mice compared to wild type post-BCAS. (a) % Area of GFAP in the corpus callosum and **(b)** internal capsule was unchanged post-BCAS with no effect of genotype. **(c)** % Area of GFAP in the optic tract was increased post-BCAS with a significant effect of genotype and the GFAP-Nrf2 BCAS group displayed less astrogliosis compared to wild type BCAS. Mean±SEM. n-number presented in each bar. *p<0.05, ***p<0.001 (* indicates *post hoc* differences between sham and BCAS), ##p<0.01 (# indicates *post hoc* differences between BCAS groups). **(d)** Representative images of GFAP staining in the optic tract. Scale bar 50µm.

4.3.6 Pro-inflammatory genes are induced post-BCAS in the optic tract and the level of complement component 4 is reduced in GFAP-Nrf2 mice compared to wild type

The results presented in this chapter demonstrate that BCAS surgery induces cerebral hypoperfusion in wild type and GFAP-Nrf2 mice which causes white matter disruption and increased density of both microglia and astrocytes in parallel with impaired spatial working memory. The data indicates that GFAP-Nrf2 provides modest protection of white matter structure and function and reduces the astroglial response post-BCAS. We therefore went on to assess antioxidant and inflammatory gene changes as described in the previous chapter (3.3.5), to determine if there were differences between wild type and GFAP-Nrf2 mice that underlie the protective effects observed.

Relative gene expression of *Nrf2*, *Scl7a11* (*xCT*; encoding the glutamate/cystine antiporter) and *Gclm*, (glutamate-cysteine ligase enzyme subunit), two Nrf2-regulated genes involved in glutathione synthesis were initially measured in a whole brain slice corresponding to the level of pathological assessment using qPCR and compared across groups (Fig 4.7-a-c). There was a 3.5-fold increase in *Nrf2* and an accompanied 2-fold increase in *Slc7a11* and *Gclm* ($F_{(1,32)}$=298, p<0.0001, $F_{(1,32)}$=74.05, p<0.0001, $F_{(1,32)}$=737.5, p<0.0001 respectively), however there was no effect of BCAS surgery ($F_{(1,32)}$=*0.16, p=0.69,* $F_{(1,32)}$=0.26, p=0.61, $F_{(1,32)}$=0.08, p=0.79 respectively).

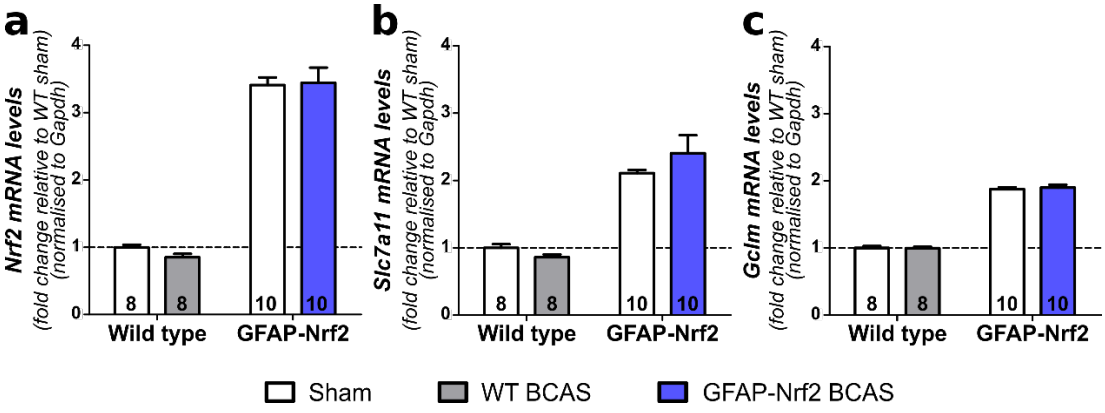

Figure 4.7 *Nrf2*, *Slc7a11* and *Gclm* relative gene expression in whole brain is higher in GFAP-Nrf2 animals with no effect of BCAS surgery. (a) *Nrf2*, **(b)** *Slc7a11* and **(c)** *Gclm* expression was significantly higher in GFAP-Nrf2 animals but this was not altered post-BCAS. Gene expression was normalised to *Gapdh* and expressed relative to WT sham. Mean±SEM. n-number presented in each bar. Dashed line indicates WT sham mean.

Alterations in gene expression were further investigated instead in optic tract enriched samples since the previous results demonstrate disruption and glial alterations in this region. *Nrf2* expression in the optic tract was similar to that of the whole brain sample with a 4-fold increase in GFAP-Nrf2 animals compared to wild type ($F_{(1,32)}$=116.4, p<0.0001) and no further effect of BCAS surgery ($F_{(1,32)}$=0.47, p=0.5) (Fig 4.8a). To investigate the involvement of the glutathione antioxidant system *Gclm* expression was measured in optic tract enriched samples, but similarly found an effect of genotype ($F_{(1,31)}$=49.83, p<0.0001) but not BCAS surgery ($F_{(1,31)}$=0.22, p=0.65) (Fig 4.8b). Collectively the results suggest that antioxidant gene alterations cannot explain the white matter protection conferred in the GFAP-Nrf2 BCAS group at this time. Instead, the inflammatory milieu beyond the cellular responses was explored as an alternative mechanism whereby Nrf2 may confer protection following BCAS-induced hypoperfusion. Gene expression of complement component 4 and 1q (*C4, C1q)* and two chemokines; *Ccl3 (Mip-1α)* and *Ccl2 (Mcp-1)*, which have previously been detected in the BCAS-model (Fowler et al., 2017, Reimer et al., 2011) were measured.

BCAS surgery significantly increased the expression of *C4, C1q,* and *Ccl3* expression ($F_{(1,32)}$=8.07, p=0.008, $F_{(1,32)}$=7.92, p=0.008, $F_{(1,29)}$=8.68, p=0.006; respectively) (Fig 4.8c-e), whereas *Ccl2* expression was reduced ($F_{(1,31)}$=6.09, p=0.02) (Fig 4.8f). *C4* expression was also significantly different in GFAP-Nrf2 animals ($F_{(1,32)}$=5.66, p=0.02) and *post hoc* analysis found significant upregulation in the wild type BCAS (p=0.005) but not the GFAP-Nrf2 BCAS group (p=0.39), and further that *C4* expression was significantly lower in GFAP-Nrf2 BCAS compared to the wild type BCAS group (p=0.007) (Fig 4.8c). *C1q* expression followed a similar pattern, however there was no overall genotype effect ($F_{(1,32)}$=0.*05, p*=0.83). *Post hoc* tests found a significant increase of *C1q* in wild type BCAS compared to shams (p=0.02) but found no significant difference between GFAP-Nrf2 groups (p=0.13) (Fig 4.8d). No effect of genotype was detected on *Ccl3* and *Ccl2* expression ($F_{(1,29)}$=0.12, p=0.73, $F_{(1,31)}$=1.62, p=0.21; respectively), and *post hoc* analysis identified significant differences between GFAP-Nrf2 groups (p=0.03, p=0.01; respectively), but not between wild type groups (p=0.07, p=0.35; respectively) (Fig 4.8e-f). Together the data indicates that BCAS-induced cerebral hypoperfusion increases the expression of specific pro-inflammatory genes and that Nrf2-overexpression in astrocytes may protect white matter integrity and behavioural performance by selectively suppressing aspects of this inflammatory response.

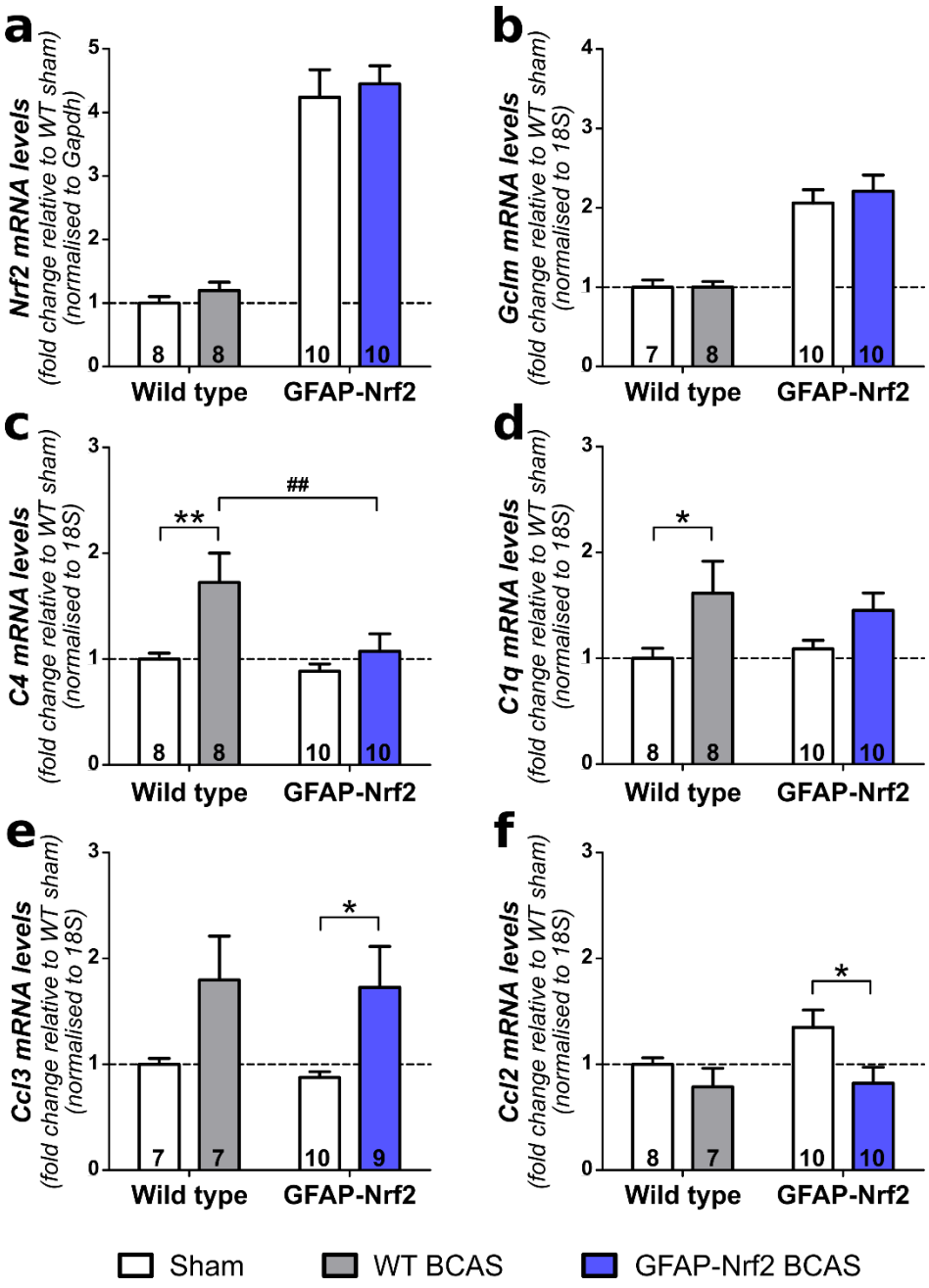

Figure 4.8 Pro-inflammatory genes are induced post-BCAS in the optic tract and the level of *C4* is reduced in GFAP-Nrf2 mice. (a) *Nrf2* and **(b)** *Gclm* expression in the optic tract was increased in GFAP-Nrf2 animals, but was not altered post-BCAS. **(c)** *C4* expression in the optic tract was increased post-BCAS with an effect of genotype and the GFAP-Nrf2 BCAS group displaying levels of expression similar to both sham groups. **(d)** BCAS surgery increased *C1q* and **(e)** *Ccl3* expression in the optic tract, but reduced the expression of *Ccl2*. There was no effect of genotype on the expression of *C1q*, *Ccl3* or *Ccl2*. Gene expression was normalised to *Gapdh* or *18S* and expressed relative to WT sham. Mean±SEM. n-number presented in each bar. Dashed line indicates WT sham mean. *p<0.05, **p<0.01 (* indicates *post hoc* differences between sham and BCAS), ##p<0.01 (# indicates *post hoc* differences between BCAS groups.

4.4 Discussion

The present study was designed to test the hypothesis that overexpression of the transcription factor Nrf2 specifically in astrocytes limits cerebral hypoperfusion-induced white matter disruption and spatial working memory impairment. The results demonstrate that white matter disruption and astrogliosis was alleviated in the optic tract, in parallel with modestly improved spatial working memory. These protective effects appear to be mediated via repression of specific inflammatory genes.

4.4.1 Resting cortical cerebral blood flow is significantly reduced following bilateral carotid artery stenosis to a similar extent in wild type and GFAP-Nrf2 mice

In agreement with previous work, this study finds that bilateral carotid artery stenosis induces mild, sustained cerebral hypoperfusion in wild type mice, which is similar in Nrf2-overexpressing mice. The extent of CBF reduction (~30-40% at 24 hours) and modest restoration at 6 weeks (~5%) is comparable to those previously published (McQueen et al., 2014, Shibata et al., 2004, Nishio et al., 2010, Maki et al., 2011). Importantly, no difference was found in the extent of CBF reduction between wild type and GFAP-Nrf2 mice. As discussed in the previous chapter, absence of Nrf2 has previously been shown to have vascular related effects acting to impair angiogenic capacity *in vitro* (Valcarcel-Ares et al., 2012, Gremmels et al., 2017, Zhao et al., 2016) and inhibits the upregulation of VEGF in an *in vivo* model of venous hypertension (Li et al., 2016b). The prediction may therefore have been to observe greater recovery of CBF in GFAP-Nrf2 mice, in particular because increased VEGFα expression and other angiogenic genes are detected 3 days following hypoperfusion (Reimer et al., 2011). Promoting these endogenous processes to improve CBF is currently explored in models of hypoperfusion to establish its potential in the treatment of vascular dementia (as discussed in Du et al., 2016). Nevertheless, the current study found that overexpression of Nrf2 in astrocytes does not alter CBF responses following BCAS surgery, which therefore allowed the effects of Nrf2 to be investigated without confounding flow-related differences.

4.4.2 Cerebral hypoperfusion causes an impairment in spatial working memory which is ameliorated in GFAP-Nrf2 mice

Consistent with the previous chapter and published studies, the results demonstrate that hypoperfusion induces impairments in spatial working memory in wild type mice as measured by the radial arm maze (Coltman et al., 2011, Shibata et

al., 2007). Wild type and GFAP-Nrf2 sham mice were able to learn the task with increasing trial duration but the hypoperfused mice in both cohorts were impaired compared to their controls. It was noted that the baseline learning pattern was different in the wild type and GFAP-Nrf2 sham mice. To the best of our knowledge no previously published studies using this transgenic mouse line have investigated cognitive changes, and no reports of altered cognition at baseline in models of Nrf2-overexpression/activation have been identified. One potential explanation may be a disruption in redox balance. Reactive oxygen species (ROS), albeit detrimental in excess, are cell signalling molecules (Thannickal and Fanburg, 2000) important for synaptic plasticity (Massaad and Klann, 2011, De Pasquale et al., 2014), and it is possible that Nrf2-overexpression affects spatial behaviour by excessive ROS depletion. Despite this different baseline learning pattern, GFAP-Nrf2 sham mice successfully learned the task by trial block 8 and the extent of impairment in spatial working memory in GFAP-Nrf2 hypoperfused mice was modestly, but significantly less pronounced as compared to wild type mice. Thus the data supports the hypothesis that increased expression of Nrf2 may protect against hypoperfusion induced functional impairment.

4.4.3 White matter disruption in the optic tract is less severe in GFAP-Nrf2 compared to wild type mice in response to cerebral hypoperfusion

Since the impairment in spatial working memory was less pronounced in hypoperfused GFAP-Nrf2 mice this suggested that there may be fewer pathological alterations. The previous chapter of this thesis and earlier studies demonstrate that white matter is particularly vulnerable to cerebral hypoperfusion (3.3.2, Coltman et al., 2011, Holland et al., 2011, Shibata et al., 2004, Ihara and Tomimoto, 2011), similar to ischaemic and hypoxic white matter damage in human VCI (Barker et al., 2013, Aboul-Enein et al., 2003). The current study agrees with previous findings of hypoperfusion-induced white matter disruption, however only in the optic tract where the extent of pathology is more severe than previously reported, with the exception of the previous chapter of this thesis. As discussed, the vascular supply to the two tracts differs and may account for this optic tract vulnerability. An alternative explanation is that this study utilised mice on a different background strain compared to previous studies (FVB/C57Bl/6J F1 mice in this study compared to pure C57Bl/6J in previous studies). It is reported that the cerebral vasculature of different strains is differently organised and may therefore present with different spatial distribution and severity of

hypoperfusion (Yang et al., 1997). There is also a possibility that the optic tract in FVB/C57Bl/6J F1 mice is more vulnerable to hypoperfusion than C57Bl/6J mice due to genetic differences, as pure FVB/N mice are known to be visually impaired from an early age due to a mutation causing retinal degeneration (Brown and Wong, 2007). However, it is unlikely that the mice were visually impaired since our FVB/C57 first generation cross successfully learned the visual-dependent radial arm maze task and we observed no altered behaviour indicating visual impairment in any of the mice and because the previous chapter displayed a similar pattern of pathology. However, with the available data, we cannot discount that disruption of the optic tract in hypoperfused mice resulted in impaired visual acuity underlying the impaired performance on the radial arm maze task.

Even so, the results indicate that astrocyte-specific overexpression of Nrf2 modestly reduces white matter disruption in the optic tract. GFAP-Nrf2 mice, to the best of our knowledge, have not previously been studied in the context of white matter injury and repair, but, overexpression of astrocytic Nrf2 by GFAP-specific Keap1-deletion reduced demyelination and oligodendrocyte cell loss in the cuprizone model of multiple sclerosis (Draheim et al., 2016). Similarly, Nrf2-activating pharmacological compounds have been reported to protect white matter both in models of multiple sclerosis (Linker et al., 2011) and cerebral hypoperfusion (Fowler et al., 2017, Mao et al., 2018). The compound DMF was recently approved for the treatment of multiple sclerosis in humans (Gopal et al., 2017), and although one study using $Nrf2^{-/-}$ mice indicates that DMF can be beneficial in the absence of Nrf2 (Schulze-Topphoff et al., 2016), there is a large body of evidence highlighting downstream activation of the Nrf2 signalling pathway as a mechanisms of action (Linker et al., 2011, Ahuja et al., 2016, Gopal et al., 2017). The subtle pathology observed in this study, compared to previously published hypoperfusion studies (Reimer et al., 2011, Coltman et al., 2011, Holland et al., 2011, McQueen et al., 2014) and models of multiple sclerosis, may have limited the ability to investigate the effect of Nrf2-overexpression completely. There is also a possibility that mechanisms other than hypoxia, oxidative stress and inflammation contribute to white matter disruption, such as reduced trophic support or increased blood brain barrier permeability (Iadecola, 2013), which Nrf2-overexpression may not influence. Nevertheless, the subtle reduction in the severity of white matter disruption in Nrf2-overexpressing mice was associated with modest improvements in spatial working memory compared to wild type mice, in agreement with the hypothesis.

4.4.4 Microglial and astrocyte density is increased in the optic tract in response to cerebral hypoperfusion but only astrogliosis is less severe in GFAP-Nrf2 mice

As previously introduced, earlier reports indicate that microgliosis precedes significant increases in astrogliosis following cerebral hypoperfusion, and associations between microgliosis and impaired white matter function suggest that microglia are important contributors to the disease process (Fowler et al., 2017, Manso et al., 2017). However, in the studies reported in this thesis, both microglial and astrocyte density in the optic tract were increased after 6 weeks of mild hypoperfusion. Other studies have identified associations between astrogliosis and impaired white matter integrity following cerebral hypoperfusion in mice (Saggu et al., 2016) and astrogliosis and impaired spatial working memory following 2VO in rats (Vicente et al., 2009). Similar to the proposed microglial contribution this is suggested to occur through increased inflammation (Saggu et al., 2016) but may also result from astrocyte dysfunction such as reduced astroglial glutamate uptake resulting in excitotoxicity (Vicente et al., 2009).

The current study found that overexpression of Nrf2 in astrocytes reduced the extent of astrogliosis but did not have an effect on microglial density after hypoperfusion. This was somewhat unexpected as GFAP-Nrf2 mice have previously been demonstrated to have reduced astro- and microgliosis in models of Parkinson's Disease (Gan et al., 2012, Chen et al., 2009), and as discussed in the previous chapter (3.4.3), considering the role Nrf2 is suggested to play in regulating microglial dynamics (Rojo et al., 2010, Joshi et al., 2015, Branca et al., 2017, Rojo et al., 2018). However, there is some conflicting evidence of the effect of Nrf2 on gliosis, for example in a transgenic mouse model of Alzheimer's disease (APP/PS1). One study found that only astrogliosis was reduced by increasing Nrf2 (Kanninen et al., 2009), while another found that both astro- and microgliosis were affected (Fragoulis et al., 2017), though both were associated with improved cognition. These differences may be accounted for by different means of Nrf2-activation; lentiviral-Nrf2 hippocampal injection (Kanninen et al., 2009), oral administration of the Nrf2-activating compound methysticin (Fragoulis et al., 2017) or transgenic overexpression of Nrf2 in astrocytes (Gan et al., 2012, Chen et al., 2009). The contrasting results from previous studies in GFAP-Nrf2 mice may be explained by different experimental models, and perhaps particularly by the comparably more subtle pathology in the current study. Together,

these studies highlight the complexity of glial responses in different disease models and suggest that the benefit of Nrf2-activation may be context-dependent.

Despite the above discrepancies, the study by Saggu et al. (2016) implicates astrocyte-specific activation of pro-inflammatory NF-κB in the disruption of white matter structure and function following cerebral hypoperfusion in mice. It is possible that GFAP-Nrf2 mice in the current study, Nrf2 being a negative regulator of NF-κB, downregulate pro-inflammatory signalling specifically in astrocytes, without significantly affecting microgliosis. It is worth noting that the immunohistochemical results presented in this study are merely morphological and do not reveal anything about the inflammatory state of individual cells or the overall inflammatory milieu. Nonetheless, these results demonstrate that increased Nrf2 expression in astrocytes alone can have downstream beneficial effects on optic tract white matter integrity and spatial working memory.

4.4.5 Cerebral hypoperfusion induces pro-inflammatory gene expression in the optic tract and complement component 4 is downregulated in GFAP-Nrf2 mice

To probe mechanisms by which Nrf2 overexpression in astrocytes mediates these protective effects, the levels of two glutathione-related genes; *Slc7a11* (*xCT*) and *Gclm* were measured in a whole brain sample. As previously mentioned, the glutathione system forms an important part of cellular antioxidant capacity (Dringen, 2000) and has been shown previously to be upregulated by ischaemic preconditioning in an Nrf2-dependent manner (Bell et al., 2011b), as well as in GFAP-Nrf2 mice in several models of neurodegenerative disease (Vargas et al., 2008, Calkins et al., 2010, Gan et al., 2012). We found an increase in both *Slc7a11* and *Gclm* in GFAP-Nrf2 compared to wild type mice, however contrary to expectations there were no further increases in expression of these genes with hypoperfusion. Given that hypoperfusion induces oxidative damage (Dong et al., 2011, Miyamoto et al., 2013), the prediction was that antioxidant gene expression would be increased also in wild type hypoperfused animals indicative of Nrf2 pathway activation. Instead, antioxidant enzymes were increased only in GFAP-Nrf2 animals; in line with a study in a transgenic model of Parkinson's disease (Gan et al., 2012). The current results, consistent with those reported in the previous chapter, suggest that hypoperfusion in wild type mice may be insufficient to induce Nrf2 expression and activation directly but, considering the current experimental design, it is impossible to rule out acute changes that may have occurred following hypoperfusion surgery. It would be

plausible to assume that transient activation of antioxidant genes induced by hypoperfusion would be superior in GFAP-Nrf2 compared to wild type mice although a time-course study would be required to verify this assumption. On a similar note, the constitutively higher glutathione-related gene expression in the GFAP-Nrf2 animals may indicate a higher capacity of glutathione synthesis perhaps providing some protection to white matter following hypoperfusion, however, direct measures of glutathione would be required to draw that conclusion. A model of Alexander disease, a white matter disease caused by aberrant accumulation of GFAP, found glutathione-independent protective effects of GFAP-Nrf2 expression (LaPash Daniels et al., 2012). Similarly, a proteomic study of Nrf2-overexpressing astrocytes found important roles of detoxifying and anti-inflammatory enzymes catalase, peroxiredoxin-6 and prostaglandin reductase 1 (Dowell and Johnson, 2013) which could alternatively be implicated following hypoperfusion.

The speculation was that since no alterations in glutathione-related genes were observed, the protective effect seen in the study could be mediated by modulation of the inflammatory environment rather than by antioxidant mechanisms. This was investigated by further qPCR analysis of optic tract-enriched samples of pro-inflammatory genes; *C4* and *C1q*; complement component 4 and 1q, and *Ccl3 (MIP-1α)* and *Ccl2 (MCP-1);* chemokine (C-C motif) ligand 3 and 2. The complement system is an important part of the innate immune system, aiding early responses to infection or injury. It also contributes to the adaptive immune system by interacting with antigen/antibody complexes eliciting a cascade of proteolytic events which ultimately boost phagocytosis and inflammation by the recruitment of more inflammatory cells (Janeway et al., 2001). *Ccl3/Ccl2* encode pro-inflammatory chemokines involved in the recruitment of microglia and astrocytes as well as peripheral monocytes and macrophages (Bose and Cho, 2013, Maurer and von Stebut, 2004). Increased expression of complement components as well as pro-inflammatory chemokines has long been recognised as an indication of chronic inflammation for example in Alzheimer's disease (Bennett et al., 2009, Eikelenboom and Stam, 1982, Azizi et al., 2014). Previous work finds increased expression of *C4* and a putative receptor for *C1q* in white matter at 72 hours post-hypoperfusion (Reimer et al., 2011) and in whole brain at 4 weeks following mild hypoperfusion in wild type mice (*unpublished obeservations*) using microarray analysis, as well as increased protein levels of Ccl3 and Ccl2 following severe hypoperfusion (Fowler et al., 2017). The previous chapter reports increased *Ccl3* and *C1q* (and *C4* trend) with

cerebral hypoperfusion. In the current study, an increase in *C4, C1q* and *Ccl3* expression following hypoperfusion was determined in wild type mice, indicative of ongoing inflammation. In contrast to previous work where Ccl2 protein was increased at 1 week after severe hypoperfusion (Fowler et al., 2017) and 2 weeks after mild hypoperfusion (Yuan et al., 2017), *Ccl2* expression was determined to be downregulated in the current study. The discrepancy may be due to differences in anatomical areas sampled and/or different extent of hypoperfusion. Overall, the differential change in inflammatory gene expression likely reflects the spatial and temporal heterogeneity of inflammatory responses to hypoperfusion which is likely highly dynamic.

In Nrf2 overexpressing mice the increase in complement related genes was dampened. Complement activation has been suggested to potentiate chronic inflammation and neurodegeneration (Liddelow et al., 2017, Stevens et al., 2007), and has been demonstrated to trigger neuroinflammation following traumatic brain injury (Alawieh et al., 2018). Since direct inhibition of complement has been neuroprotective in mouse models of Alzheimer's disease (Shi et al., 2017) and cerebral ischaemia (Yang et al., 2013, Ducruet et al., 2012), reduced complement activation may be a mechanism whereby Nrf2 overexpression is protective following hypoperfusion. Recent evidence has also demonstrated that Nrf2 not only induces the expression of cytoprotective genes but is also able to suppress expression of pro-inflammatory genes directly (Kobayashi et al., 2016). Since the Nrf2 overexpression is selectively in astrocytes, one possibility is that these are more resistant to microglia-driven pro-inflammatory signalling. Isolation and transcriptomic analysis of astrocytes and microglia separately would have allowed more detailed information regarding the protective mechanisms involved. And as previously mentioned, recent work has highlighted how transcriptomic analysis of mixed cell populations may be misleading as gene signalling is differentially regulated in different cell types (Swartzlander et al., 2018). Nevertheless, the results demonstrate that astrocyte-specific overexpression of Nrf2 alters the inflammatory milieu by dampening aspects of the pro-inflammatory response following cerebral hypoperfusion.

4.4.6 Alternative mechanisms of Nrf2 pathway activation

Despite the experimental evidence of astrocytes role in antioxidant and anti-inflammatory defence, GFAP-Nrf2 mice may not be the most efficient method to boost Nrf2 activity. It is unknown if the molecular mechanisms controlling Nrf2 become altered by the constitutively increased expression of Nrf2 throughout development

and adulthood. An alternative approach is transgenic mouse models which instead downregulate Keap1, the main repressor of Nrf2, that have been shown to efficiently increase Nrf2 signalling (Draheim et al., 2016). Cell-specific downregulation of Keap1 combined with a diet-inducible transgenic driver would provide a highly specific model to investigate the therapeutic potential of boosting Nrf2 in disease without confounds of it being upregulated throughout development. Further, this represents a highly plausible therapeutic approach where pharmacological inhibition of Keap1 may boost Nrf2 as and when required.

Alternatively, pharmacological activation of Nrf2 can be utilised to achieve a more global response, and of course represents a more clinically relevant approach. Compounds such as Sulforaphane, Methysticin, Curcumin and Resveratrol are naturally occurring Nrf2-activators (Liddell, 2017). Further, synthetic Nrf2 activators such as *tert*-butyl-hydro-quinone (tBHQ) are available, with Dimethyl fumarate (DMF) approved for treatment of relapsing form of MS (Dinkova-Kostova et al., 2018) and Edaravone for the treatment of ALS (Liddell, 2017). The precise mechanisms of how these compounds activate Nrf2 is not completely known, but they are thought to disrupt Keap1 or Keap1/Nrf2 interactions (Dinkova-Kostova et al., 2018). Further, compounds inhibiting GSK3β are able to activate Nrf2 and may be beneficial in treatment of mixed dementias since GSK3β is an important contributor to the hyperphosphorylation of tau, responsible for forming neurofibrillary tangles, one of the characteristic AD hallmarks (Gameiro et al., 2017).

Relevant to the study of hypoperfusion/ischaemia, a recent study utilising the 2VO model in rats, find that Nrf2 activation using Sulforaphane ameliorates but, similar to the results in the current study, does not completely rescue cognitive impairment and white matter disruption (Mao et al., 2018). Similar cognitive results are seen in a 2VO study instead using Edaravone, although white matter integrity was not assessed (Zhang et al., 2017). Previous work in the BCAS model in mice, find that Nrf2 activation using DMF improves white matter function, however without significantly improving white matter structure (Fowler et al., 2017). The specificity of these compounds for activation of Nrf2 has been disputed, and the development of more specific and effective pharmacological activators may prove more favourable. Although, the greater beneficial effects of already available Nrf2 activators in other disease models, such as Sulforaphane reducing infarct volume in experimental stroke (Zhao et al., 2006), or DMF in MS (Linker et al., 2011), suggests that alternative

therapeutic approaches should perhaps be explored in the context of cerebral hypoperfusion and VCI.

4.4.7 Limitations, conclusion and future directions

A limitation of the current study is the comparably more subtle pathology observed compared to previous studies and other models. To overcome this, carotid artery stenosis could be induced with one of the microcoils having a smaller diameter, hence producing slightly more severe reductions in cerebral blood flow. Alternatively, as the BCAS model is progressive, extending the time course would exacerbate pathology and perhaps reveal greater differences between wild type and GFAP-Nrf2 animals.

Further, and as discussed in the previous chapter, transcriptomic analysis of mixed cell populations, albeit white matter-enriched samples, could be masking subtle and cell-specific changes (Swartzlander et al., 2018). Cell-isolation studies and more detailed analyses of a greater number of genes would provide more information than the current approach. A relatively recent approach called translating ribosome affinity purification (TRAP), utilises cell-specific ribosomal tags to isolate translating mRNA and thereby getting as close to a functional readout as currently possible using transcriptomic analysis (Heiman et al., 2014). Crossing these mice with mice overexpressing Nrf2 or repressing Keap1 could be used to investigate Nrf2 signalling following cerebral hypoperfusion in much greater detail.

An additional consideration is whether GFAP is an appropriate promoter of Nrf2 in astrocytes. A novel astrocyte marker Aldh1l1 has been identified (Cahoy et al., 2008), frequently used as it is expressed by a much larger proportion of the astrocyte population. Aldh1l1 has already been used for astrocyte-specific targeting of the TRAP transgene described above (Morel et al., 2017) and may provide a better target for transgenic overexpression of Nrf2. Alternatively, Nrf2 despite being expressed at low levels in neurons, is abundant not only in astrocytes but endothelial cells and microglia too (Zhang et al., 2014), and global overexpression/activation of Nrf2 may result in increased protection of white matter and cognitive function when cerebral blood flow is reduced.

Of further interest, both in terms of cerebral hypoperfusion and in particular as Nrf2 is overexpressed specifically in astrocytes is the effect on astrocyte-blood vessel signalling. As previously introduced, astrocytes are considered essential to relay information about increased neuronal activity to the blood vessels to mediate activity-depend increases in blood flow, also called neurovascular coupling (Iadecola and Nedergaard, 2007). Our group has previously demonstrated that age-related deficits

in neurovascular coupling can be detected using Laser speckle imaging during whisker stimulation (Duncombe et al., 2016) and unpublished data show that this can also be detected following 3 months of cerebral hypoperfusion. This technique was employed also in the current study but is technically very challenging and did not identify a difference in neurovascular function between groups. Hypoperfusion is hypothesised to induce vascular dysfunction via mechanisms of oxidative stress, as reactive oxygen species can reduce the bioavailability of the vascular tone regulator nitric oxide, as well as impair its function and ability to be produced (Pierini and Bryan, 2015). Increased antioxidant and anti-inflammatory potential of astrocytes through increased Nrf2-signalling is therefore subsequently hypothesised to protect against hypoperfusion-induced neurovascular coupling deficits and future studies should aim to incorporate and refine this technique.

Additionally worth noting, as briefly discussed in the previous chapter, is the potential influence of grey matter damage or neuronal dysfunction. Similar to the previous chapter, minimal ischaemic neuronal damage was observed in the hypoperfused animals (3/18: 2 wild type, 1 GFAP-Nrf2), however that does not reflect neuronal function such as synaptic plasticity, which to the best of our knowledge has not been investigated in mice following BCAS. However in rats it was recently reported that synaptic plasticity is perturbed by hypoperfusion (2VO) as measured by electrophysiology (long-term potentiation) and western blotting of synaptic proteins (Yao et al., 2019), indicating that this is a measure worth studied in the future.

In conclusion, the results indicate that Nrf2 overexpression in astrocytes dampens hypoperfusion-induced astrogliosis and pro-inflammatory signalling in the optic tract and modestly reduces white matter disruption and cognitive impairment. This supports the hypothesis that astrocytic Nrf2 reduces pathology and subsequent cognitive impairment following cerebral hypoperfusion, however, since the effects of hypoperfusion aren't completely abolished, additional mechanisms must be involved. Hypoperfusion studies find associations between increasing numbers of microglia and impaired white matter function and cognition (Fowler et al., 2017, Manso et al., 2017, Kitamura et al., 2017). Since these represent early changes there is a possibility that microglial proliferation drives white matter pathology when cerebral blood flow is compromised. The final chapter of this thesis will hence go on to investigate this hypothesis and the therapeutic potential of inhibiting microglial proliferation to improve white matter structure and cognitive function following BCAS-induced cerebral hypoperfusion.

Chapter 5

Investigating the effect of inhibiting microglial proliferation in a mouse model of chronic cerebral hypoperfusion

5.1 Introduction

The studies in chapter 3-4 highlight that inflammation and oxidative stress contribute to the loss of white matter integrity and cognitive impairment following BCAS-induced cerebral hypoperfusion, as altered expression of the antioxidant and anti-inflammatory transcription factor Nrf2 impacted on structural and functional outcome. It would be of interest to next investigate the role of Nrf2 in microglia, as this cell type is largely implicated in the inflammatory response following BCAS. However, due to the lack of an available mouse model this thesis instead goes on to interrogate the role of microglial colony-stimulating factor 1 receptor (CSF1R) signalling to determine if modulating the microglial inflammatory response impacts on disease progression.

Microglial numbers increase progressively following cerebral hypoperfusion, resulting from proliferation rather than migration or infiltration of peripheral macrophages (Manso et al., 2017). The extent of white matter dysfunction (as measured by electrophysiology) is closely associated with increasing microglial numbers, and white matter function is improved when the numbers of microglia are reduced (Manso et al., 2017, Fowler et al., 2017). Further, increasing number of microglia have also been associated with cognitive impairment following mild hypoperfusion (Kitamura et al., 2017). This suggests that microglia may drive the progressive disruption and dysfunction of myelinated axons following hypoperfusion, ultimately leading to cognitive impairment. Previous studies have used non-specific pharmacological anti-inflammatory approaches (minocycline (Manso et al., 2017) and DMF (Fowler et al., 2017)), but in order to specifically test the hypothesis that microglia drive the pathological changes more specific inhibition of microglia is required. The drug GW2580 is a kinase inhibitor which is highly selective for CSF1R, which when bound by its ligands stimulates survival, differentiation and proliferation of microglia (Conway et al., 2005). This drug is advantageous as it is reported not to affect the stable microglial population but inhibits its expansion (Gomez-Nicola et al., 2013). GW2580 treatment has been shown to improve/slow down both grey and white matter degenerative diseases such as prion disease (Gomez-Nicola et al., 2013), Alzheimer's disease (Olmos-Alonso et al., 2016) and multiple sclerosis (Crespo et al., 2011), however it has yet to be investigated in the context of chronic cerebral hypoperfusion.

5.1.1 Hypothesis

This study tests the hypothesis that microglial CSF1R signalling causes white matter disruption and cognitive impairment following BCAS-induced chronic cerebral hypoperfusion.

5.1.2 Aims

In wild type mice treated with vehicle or GW2580 the aims are to:

1. Assess cerebral blood flow to determine the extent of BCAS-induced cerebral hypoperfusion
2. Assess white matter microglial proliferation and pro-inflammatory signalling one week post-BCAS and determine whether GW2580-treatment inhibits these
3. Assess white matter microglia and astrogliosis 6 weeks post-BCAS
4. Assess white matter disruption 6 weeks post-BCAS
5. Assess spatial learning and memory 6 weeks post-BCAS
6. For the above measures determine whether chronic GW2580-treatment reduces the effects of BCAS

5.2 Materials and Methods

5.2.1 Experimental contributions

The studies presented in this chapter were carried out by myself, Dr Jessica Duncombe and Joshua Beverley, Dr Edel Hennessey and Dr Juraj Koudelka. I performed laser speckle imaging, behavioural testing, white matter dissections, tissue processing/sectioning, immunostaining for GFAP and MAG, RNA extractions, quantitative PCR and all data analysis presented in this chapter. Dr Jessica Duncombe performed BCAS surgery, administered oral gavages, processed tissue, stained tissue from the chronic study for Iba1/BrdU and imaged all fluorescently stained sections. Joshua Beverley performed laser speckle imaging, behavioural testing, tissue sectioning, immunostaining for Iba1, slide scanner imaging and assisted with RNA extractions. Dr Edel Hennessey administered oral gavages, collected and processed tissue and stained tissue from the acute study for Iba1/BrdU. Dr Juraj Koudelka collected tissue for the chronic study.

5.2.2 Mice

Wild type mice (C57Bl6/J) (n=106) were purchased from Charles River Laboratories (JAX^{TM-} C57BL/6J) and randomly assigned surgical intervention as detailed in Table 5.1. Mean age 3 m 9 d (3 m 2d to 3 m 23 d), weighing on average 29 g (23.1 – 33.8 g). Mice were studied acutely (1 week) and chronically (6 weeks) following BCAS or sham surgery.

5.2.3 Chronic cerebral hypoperfusion

Mice underwent bilateral carotid artery stenosis (BCAS) or sham surgery, as described in 2.2. BCAS surgery was performed to induce chronic cerebral hypoperfusion, using one 0.16 mm and one 0.18 mm in diameter microcoil. Recovery following surgery is closely monitored for 72 hours and animals showing poor recovery are culled. Six animals in the first study and seven animals in the second study tolerated surgery poorly and were humanely culled by cervical dislocation (see Table 5.1)

5.2.4 Laser speckle imaging to measure cortical cerebral blood flow

Cortical cerebral blood flow (CBF) was measured at baseline, 24 hours and 6 days post-BCAS for the acute study and baseline, 24 hours and 6 weeks post-BCAS for the chronic study as described in 2.3. Laser speckle imaging was performed on all animals.

5.2.5 Study inclusion criteria and group assignment

Laser speckle imaging was analysed after the second imaging session (baseline and 24 hour measurements) as described in 2.3.1, and animals displaying an average CBF reduction exceeding 35% from baseline were included in the final study. This excluded twelve animals from the acute study and nine animals from the chronic study. BCAS animals were then randomly assigned experimental treatment, balanced for magnitude of 24 hour CBF reduction as detailed in Table 5.1 and relevant figures.

5.2.6 GW2580 administration

GW2580 (LC Laboratories, PKC Pharmaceuticals Inc., USA) was administered by oral gavage or in diet as described in 2.5.1. For the chronic study where GW2580 was administered in diet, food intake was monitored and determined not to be different between treatment groups.

5.2.7 5-Bromo-2'-deoxyuridine (BrdU) administration

5-Bromo-2'-deoxyuridine (BrdU, B5002, Sigma-Aldrich) was administered by oral gavage during the final three days as described in 2.5.2.

5.2.8 Behavioural testing

The Barnes maze was used to assess spatial learning and memory in the chronic study as described in 2.4.3. Behavioural testing commenced four weeks post-BCAS. Inclusion criteria described in 2.4.3.7 was applied highlighting one sham animal that was subsequently excluded from the study (Final numbers in Table 5.1 and relevant figure).

5.2.9 Tissue collection and processing

Animals were sacrificed by cervical dislocation and white matter was isolated as described in 2.6.2. The tissue was further processed manually for paraffin embedding as described in 2.6.5 and Table 2.3 and sectioned as described in 2.6.6.

5.2.10 Immunohistochemistry

Performed according to 2.7.1-2.7.2. Details of antibodies used (anti-MAG, anti-Iba1, anti-GFAP, anti-BrdU) can be found in Table 2.4. Immunohistochemistry was performed on 6µm coronal sections from all animals as detailed in Table 5.1 and relevant figures.

5.2.11 Image analysis

DAB-stained sections (Iba1/GFAP) were imaged using an Axio Scan.Z1 slide scanner (x20, Zeiss, Germany). Fluorescently stained sections were as described in

2.8.1 and analysed by manual counting as described in 2.8.2. DAB-labelled images were analysed for percentage area of Iba1 and GFAP, and MAG was analysed by manual grading as described in 2.8.2 in the CC, IC and FI (Fig 2.3). Briefly, ImageJ software (v1.46, NIH, Bethesda, MD, USA) was used to apply a global manual threshold followed by quantification of the positive signal detected above the selected threshold. Applying exclusion criteria outlined in 2.8.3 resulted in no exclusions. Final numbers for each region and stain are detailed in Table 5.1 and relevant figures.

5.2.12 Transcriptomics

Quantitative-PCR was performed on animals from the acute study (see Table 5.1). RNA extraction was performed as described in 2.9.1 using white matter enriched samples and RT-PCR and qPCR experiments as described in 2.9.2-2.9.3. Details of primers used (*18s, C4*) can be found in Table 2.5. Animal numbers and reference gene used are specified in the relevant figure.

5.2.13 Statistical analysis

Repeated measures ANOVA was used to investigate group effects on CBF and escape latency in the learning and reversal phase of the Barnes maze (2.10.1). One-sample t-test was used to test each group against chance (25%) during probe tests (2.10.4) and one-way ANOVA was used to investigate a group effect in all other data sets apart from MAG grade (2.10.3). Pearson's correlation was used to investigate the relationship between Iba1 and GFAP (2.10.5). Kruskal-Wallis H test was used to analyse the MAG grade for white matter disruption (2.10.6). Spearman's correlation was used to investigate the relationship between Iba1 and MAG (2.10.7). Data are presented as mean ± standard error of the mean (SEM) or as median with errors bars representing interquartile range (IQR) where non-parametric statistical analysis was used (specified in relevant figure legend). Statistical significance was determined at $p<0.05$.

Table 5.1 Number of mice in each group and experiment with details of exclusion

BCAS Surgery	**Acute (1 week)**	**Chronic (6 weeks)**
Sham	13	10
BCAS	45	38
Final group assignments		
Sham (Vehicle)	13	10
BCAS vehicle	14	12
BCAS GW2580	13	10
Details of exclusion		
Poor recovery from BCAS surgery	6 (3 veh/3 GW)	7 (veh)
<35% CBF reduction	12 (6 veh/6 GW)	9 (4 veh/5 GW)
Behavioural testing		**Chronic (6 weeks)**
Sham (Vehicle)		9
BCAS vehicle		12
BCAS GW2580		10
Details of exclusion		
Non-completion of task >50%/trials		1
Immunohistochemistry All stains/regions	**Acute (1 week)**	**Chronic (6 weeks)**
Sham (Vehicle)	13	9
BCAS vehicle	14	12
BCAS GW2580	13	10
qPCR	**Acute (1 week)**	
Sham (Vehicle)	13	
BCAS vehicle	14	
BCAS GW2580	13	

5.3 Results

5.3.1 GW2580-treatment dampens white matter microglial proliferation and pro-inflammatory signalling one week post-BCAS

The first aim of the study was to assess the extent of microglial proliferation and to determine if GW2580 could alter this response one week post-BCAS. Initially CBF was measured using laser speckle imaging prior to, 24 hours and 6 days post-BCAS as previously described (3.3.1/4.3.1), to ensure that the extent of reduction was sufficient (>35%) to model cerebral hypoperfusion.

BCAS surgery using one 0.18 and one 0.16 mm microcoil induced reductions in CBF of ~60%, whereas sham mice displayed relatively stable CBF over time (Fig 5.1). There was a significant effect of time ($F_{(2,74)}$=217.6, p<0.0001) and group ($F_{(2,74)}$=37.66, p<0.0001) and a significant interaction ($F_{(2,74)}$=42.87, p<0.0001) (Fig 5.1b). *Post hoc* tests found that BCAS reduced CBF in vehicle- and GW2580-treated animals both at 24 hours (p<0.001) and at 6 days (p<0.001) and there was no difference between groups at any time (p=1.00) (Fig 5.1b). This demonstrates that treatment with GW2580 does not influence resting CBF one week post-BCAS and that the effect of drug treatment can be assessed without confounding flow-related differences between groups.

Immunofluorescent labelling of Iba1 and BrdU was used to assess the percentage of proliferating microglia in the corpus callosum one week post-BCAS (Fig 5.2a). The results show that the percentage of proliferating microglia was significantly different between the groups ($F_{(2,37)}$=5.08, p=0.01), and *post hoc* analysis found that the BCAS vehicle group has significantly more proliferating microglia compared to shams (p=0.02). In contrast, the proportion of microglia proliferating in the BCAS GW2580 group compared to shams missed accepted levels of statistical significance (p=0.06) (Fig 5.2b). The data indicate that GW2580-treatment reduces but does not completely inhibit microglial proliferation following one week of BCAS-induced cerebral hypoperfusion.

Furthermore, because previous studies using GW2580 has reported a shift in inflammatory profiles following drug treatment (Gomez-Nicola et al., 2013, Olmos-Alonso et al., 2016), we next measured the expression of the pro-inflammatory marker complement component 4 (*C4*), as this was demonstrated to increase following BCAS-surgery in the previous chapter of this thesis (see Results 4.3.6, Fig. 4.8).

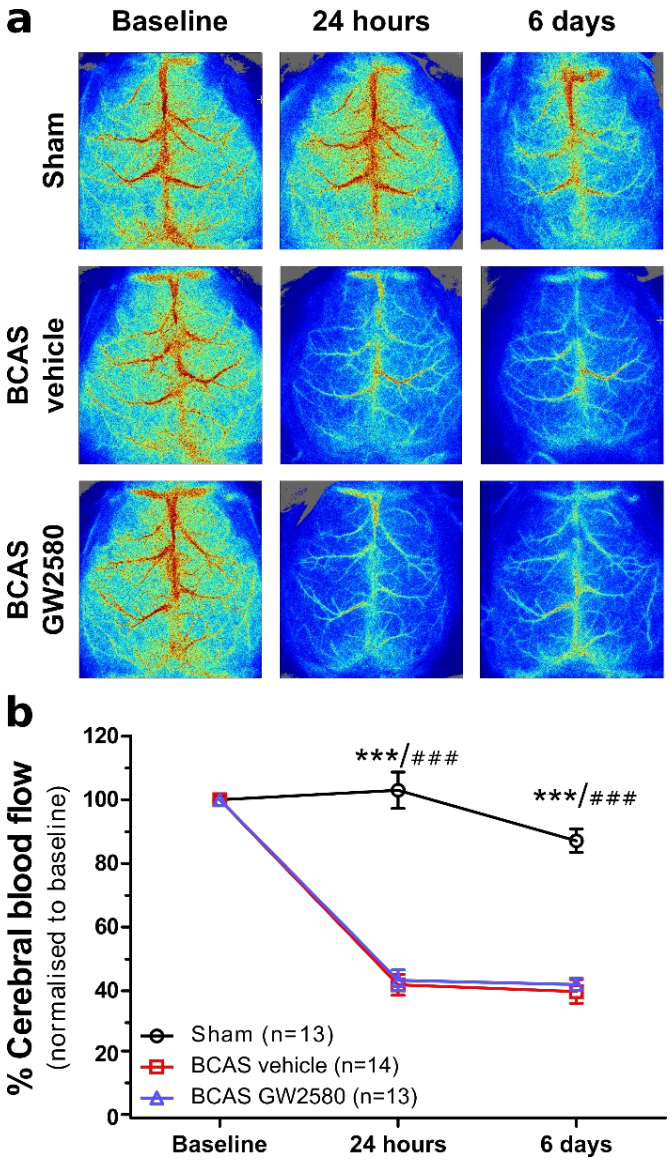

Figure 5.1 Cortical cerebral blood flow is reduced post-BCAS. (a) Representative images of laser speckle flowmetry in sham, BCAS vehicle and BCAS GW2580 animals at baseline, 24 hours and 6 days. **(b)** BCAS surgery reduced CBF to a similar extent in both vehicle and GW2580 groups. Mean±SEM. ***p<0.001 (* indicates *post hoc* differences between sham and BCAS vehicle), ###p<0.001 (# indicates *post hoc* differences between sham and BCAS GW2580).

C4 was shown to be significantly different between groups ($F_{(2,37)}$=5.65, p=0.007) and *post hoc* analysis found significantly increased *C4* in the BCAS vehicle group compared to shams (p=0.005) but not between the BCAS GW2580 group and shams (p=0.38) (Fig 5.2c). Together these data indicate that GW2580-treatment reduces microglial proliferation, and modestly dampens pro-inflammatory signalling compared to vehicle-treatment one week following moderate cerebral hypoperfusion.

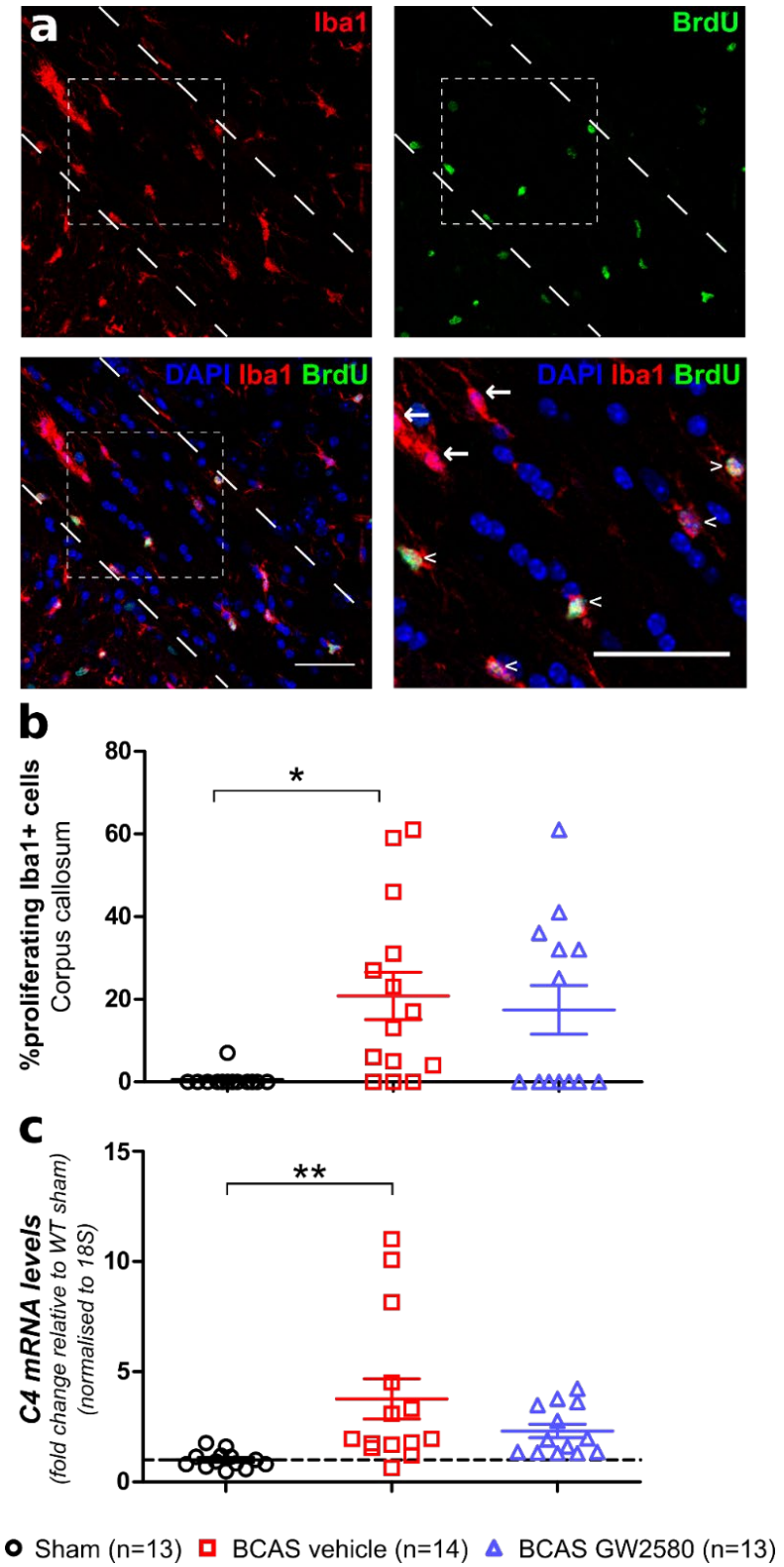
a
Iba1
BrdU
DAPI Iba1 BrdU
DAPI Iba1 BrdU
b
%proliferating Iba1+ cells
Corpus callosum
80
60
40
20
0
*
c
C4 mRNA levels
(fold change relative to WT sham)
(normalised to 18S)
15
10
5
0
**
Sham (n=13)
BCAS vehicle (n=14)
BCAS GW2580 (n=13)

◄Figure 5.2 GW2580 treatment dampens white matter microglial proliferation and pro-inflammatory signalling one week post-BCAS. (a) Representative images of Iba1/BrdU positive staining. Arrow represents Iba1 positive cells and arrowhead represents Iba1/BrdU double positive cells. Scale bar 50 µm. **(b)** Percentage of proliferating Iba1 positive cells in the corpus callosum is increased in the BCAS vehicle group compared to shams whereas the BCAS GW2580 group missed accepted levels of statistical significance. **(c)** Pro-inflammatory marker *C4* is increased in the BCAS vehicle group compared to shams but not in the BCAS GW2580 group. Dashed line indicated WT sham mean. Mean±SEM. *p<0.05, **p<0.01.

5.3.2 Resting cortical cerebral blood flow is chronically reduced following bilateral carotid artery stenosis to a similar extent in GW2580- and vehicle-treated animals

The acute study demonstrated that microglial proliferation and pro-inflammatory signalling was modestly modulated one week following moderate hypoperfusion using GW2580-treatment. The next aim was to undertake a chronic study over 6 weeks to investigate the long-term pathological and cognitive changes following moderate hypoperfusion and the ability to modulate these using GW2580 in diet. The extent of cerebral hypoperfusion was evaluated using laser speckle flowmetry prior to, 24 hours and 6 weeks following BCAS surgery as previously described (3.3.1/4.3.1). BCAS surgery (0.18 mm/0.16 mm microcoils) reduced CBF by ~50%, and sham mice displayed stable CBF over time (Fig 5.3). There was a significant effect of time ($F_{(1.56,43.6)}$=164.85, p<0.0001) and group ($F_{(2,28)}$=110.15, p<0.0001) and a significant interaction ($F_{(3.11,43.6)}$=32.51, p<0.0001) (Fig 5.3b). *Post hoc* tests found that BCAS surgery reduced CBF in vehicle- and GW2580-treated animals at 24 hours (p<0.001) and at 6 weeks (p<0.001) post-surgery, but there was no difference between these groups (24 hours p=1.00, 6 weeks p=0.77) (Fig 5.3b). This demonstrates that treatment with GW2580 does not influence resting CBF following BCAS either acutely or chronically, and that the following results can be interpreted without confounding flow-related differences between groups.

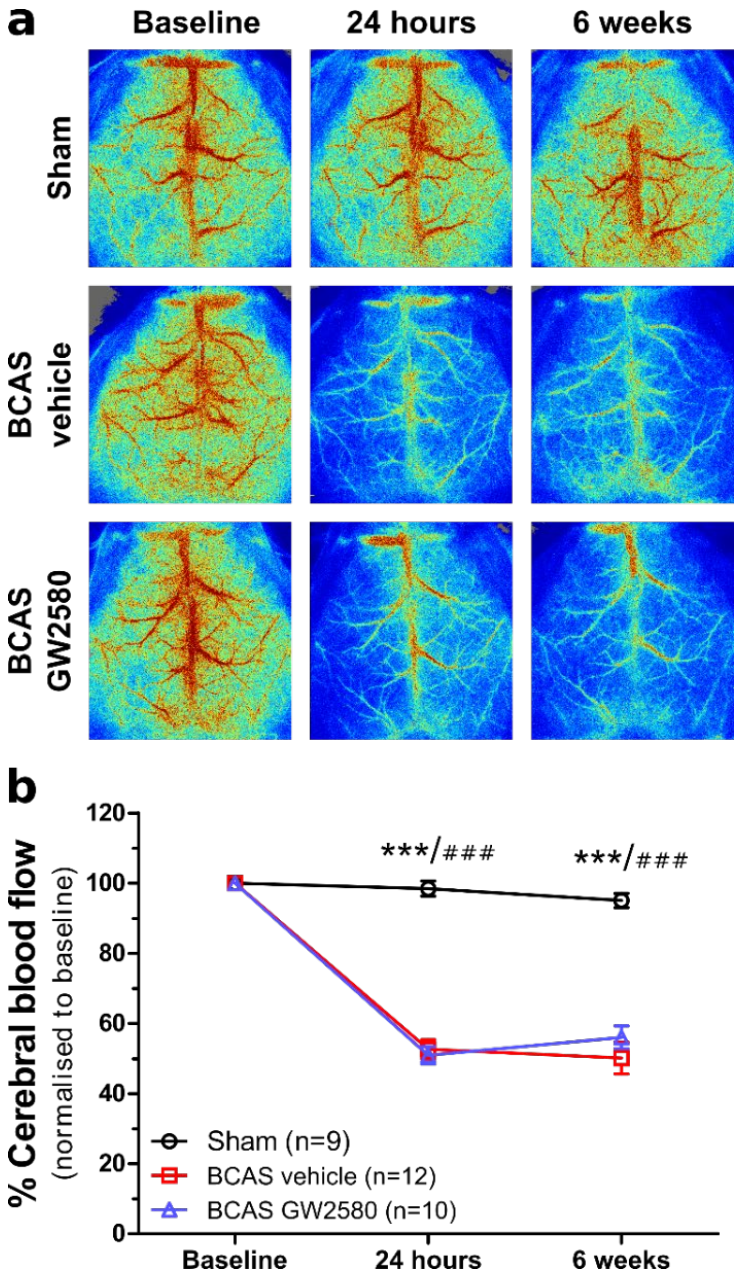

Figure 5.3 Cortical cerebral blood flow is reduced post-BCAS. (a) Representative images of laser speckle flowmetry in sham, BCAS vehicle and BCAS GW2580 animals at baseline, 24 hours and 6 days. **(b)** BCAS surgery reduced CBF to a similar extent in both vehicle and GW2580 groups. Mean±SEM. ***p<0.001 (* indicates *post hoc* differences between sham and BCAS vehicle), ###p<0.001 (# indicates *post hoc* differences between sham and BCAS GW2580).

5.3.3 GW2580-treatment prevents increases in white matter microglia 6 weeks post-BCAS

To determine whether GW2580-treatment was effectively inhibiting increases in white matter microglia, immunofluorescent and DAB staining of Iba1 was evaluated in the corpus callosum, fimbria and the internal capsule. Immunofluorescent staining was used to quantify the number of microglia/0.1mm^2 as these could be corroborated by the nuclear DAPI label and DAB staining was quantified as percentage area (density) to include more information about activation state as activated microglia are reported to occupy a larger area than quiescent ones (Nayak et al., 2014).

There was an overall group effect on the number of Iba1 positive cells/0.1mm^2 in the corpus callosum ($F_{(2,28)}$=5.19, p=0.01) and *post hoc* analysis identified a significant increase in microglia in the BCAS vehicle group compared to BCAS GW250 (p=0.01) (Fig 5.4a). Similarly, there was an overall group effect on the density of microglia in the corpus callosum ($F_{(2,28)}$=5.42, p=0.01) and *post hoc* analysis found a significant increase in the BCAS vehicle group compared to both sham (p=0.03) and BCAS GW2580 groups (p=0.03) (Fig 5.4b). The density of microglia in the fimbria and internal capsule was not significantly altered in any group ($F_{(2,28)}$=2.28, p=0.12, $F_{(2,28)}$=1.74, p=0.19 respectively) (Fig 5.4c-d). These results demonstrate that microglia in the corpus callosum are increased in response to BCAS-induced chronic cerebral hypoperfusion, and that GW2580-treatment successfully prevents this upregulation.

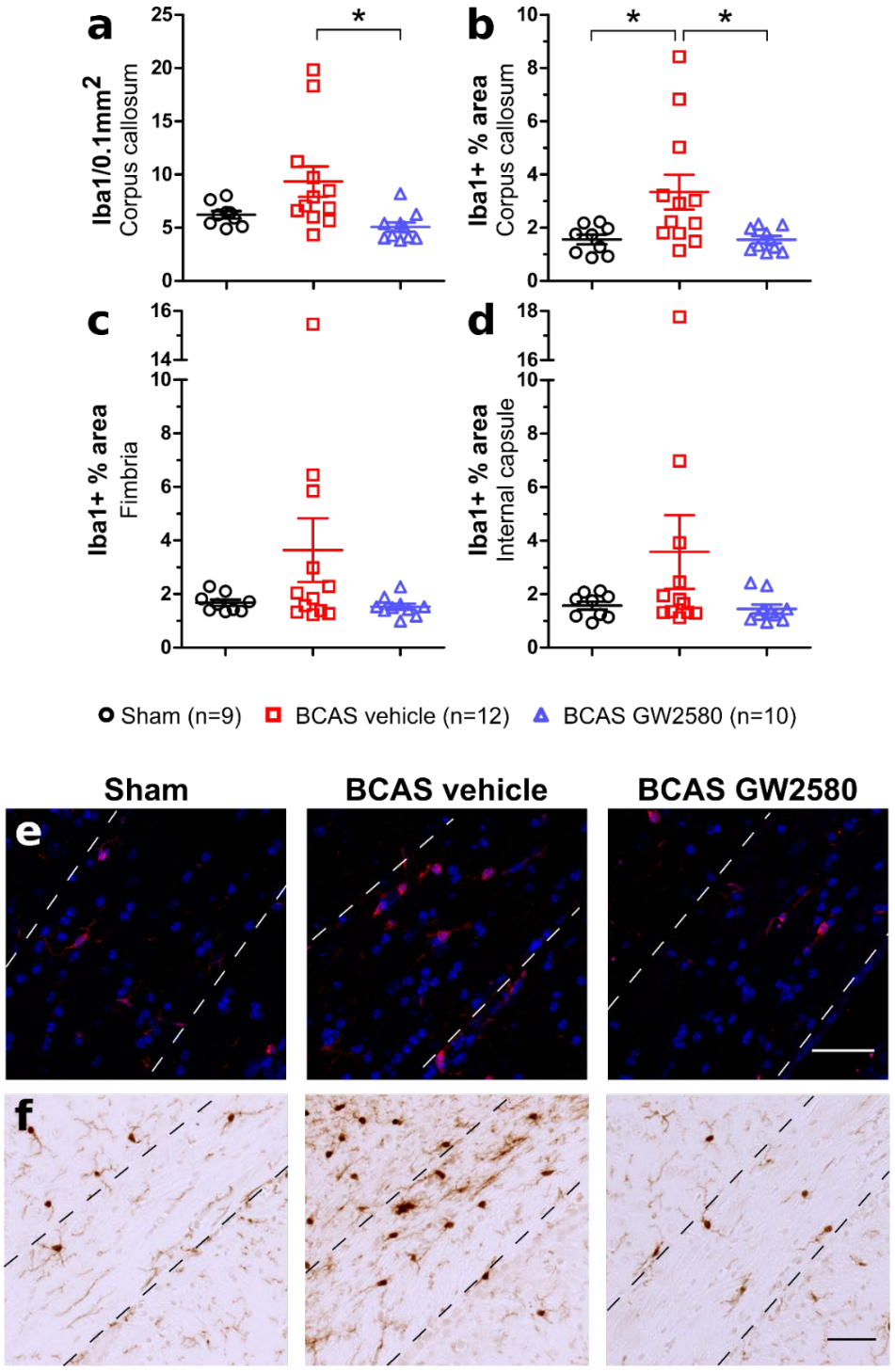

Figure 5.4 GW2580-treatment prevents increases in white matter microglia 6 weeks post-BCAS. (a) Iba1/0.1mm^2 in the corpus callosum is increased in the BCAS vehicle group but not the BCAS GW2580 group. **(b)** Iba1 percentage area in the corpus callosum in the BCAS vehicle group is increase compared to both sham and BCAS GW2580 **(c)(d)** Iba1 percentage area is not significantly altered in the fimbria and the internal capsule. Mean±SEM. *p<0.05. **(e)** Representative images of fluorescent Iba1/DAPI in the corpus callosum **(f)** Representative images of DAB Iba1 in the corpus callosum. Scale bar 50 µm. Dashed line indicates boundary of the corpus callosum.

5.3.4 GW2580-treatment inhibits white matter astrogliosis 6 weeks post-BCAS

Glial fibrillary acidic protein (GFAP) was used to determine if inhibiting increases in microglia altered the extent of astrogliosis; quantified as percentage area in the corpus callosum, fimbria and internal capsule. There was a significant effect of group in the corpus callosum ($F_{(2,28)}$=6.09, p=0.006) and *post hoc* tests found that the BCAS vehicle group displays significant astrogliosis compared to shams (p=0.01) and the BCAS GW2580 group (p=0.04) (Fig 5.5a). Similar to the microglial response, there was no significant difference between groups in the fimbria or the internal capsule ($F_{(2,28)}$=1.81, p=0.18, $F_{(2,28)}$=0.68, p=0.52 respectively) (Fig 5.5b-c).

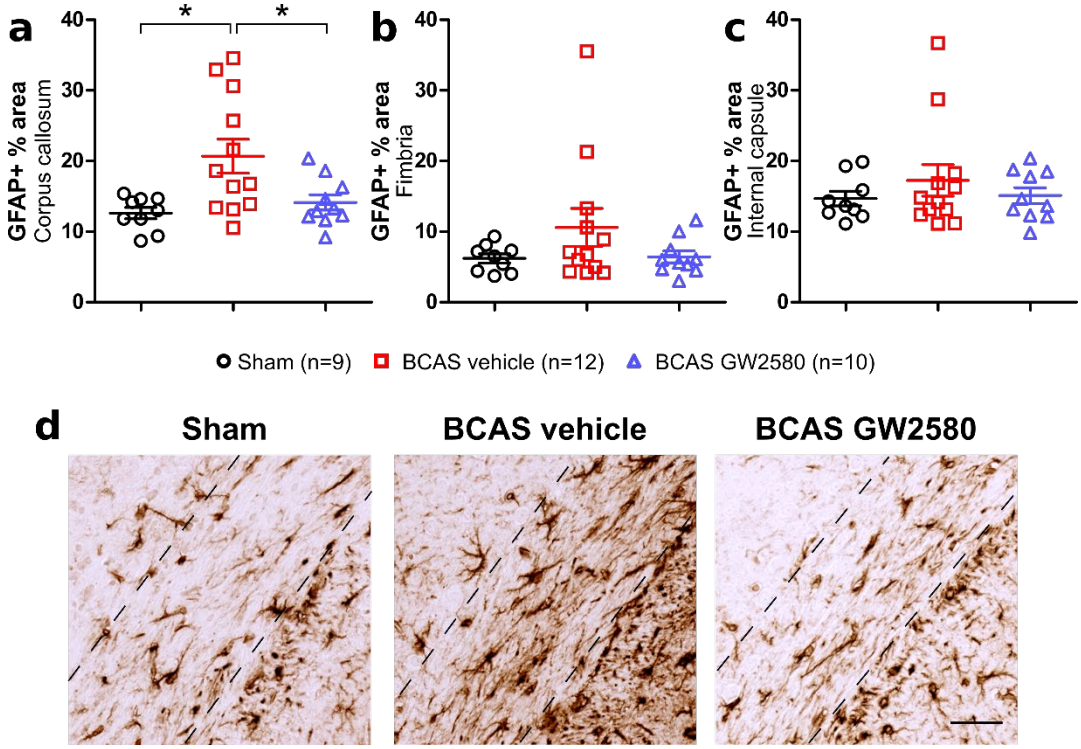

Figure 5.5 GW2580-treatment prevents white matter astrogliosis 6 weeks post-BCAS. (a) Astrogliosis was increased in the BCAS vehicle group compared to shams and the BCAS GW2580 group. **(b)(c)** Astrogliosis is not significantly altered in the fimbria and the internal capsule. Mean±SEM. *p<0.05. **(d)** Representative images of GFAP in the corpus callosum. Scale bar 50 µm.

In addition, the extent of astrogliosis in the corpus callosum had a strong positive correlation with increasing density of microglia in the same area (r=0.88, n=31, p<0.0001) (Fig 5.6). Together, these data demonstrate that BCAS-induced hypoperfusion causes astrogliosis in the corpus callosum, associated with increases in microglia, and that treatment with GW2580 successfully inhibits both.

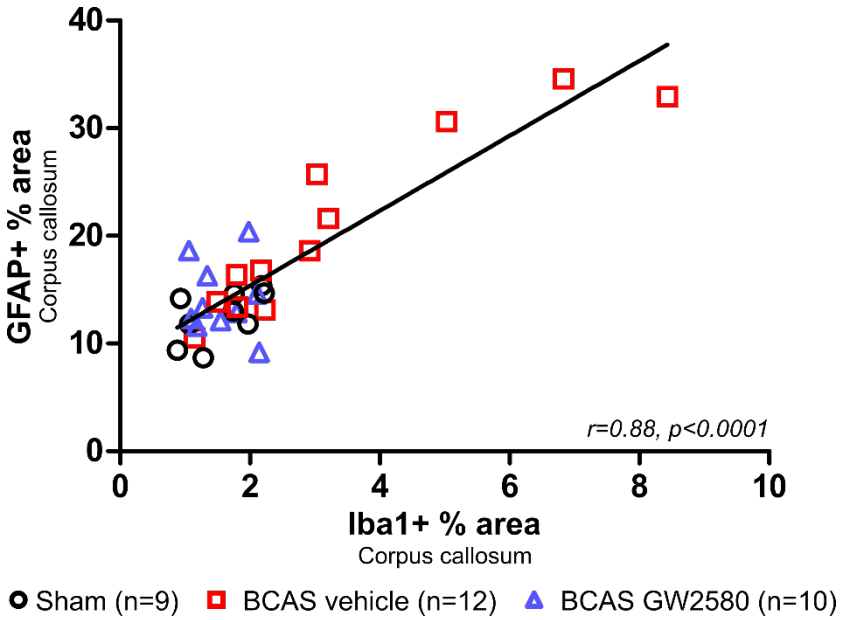

Figure 5.6 The extent of astrogliosis in the corpus callosum is positively correlated with increased density of microglia. The extent of astrogliosis (percentage area of GFAP) is positively correlated with increased density of microglia (percentage area of Iba1) in the corpus callosum. Mean, n=31.

5.3.5 GW2580-treatment protects against white matter disruption 6 weeks post-BCAS

Myelin associated glycoprotein (MAG) was used to asses white matter disruption as previously described in Chapter 3 (3.3.2) but due to increased background the severity of white matter disruption was quantified by a grading score between 0-3 (none to extensive aberrantly accumulated MAG) for each side of the brain and summed to get a total scale of 0-6 for the corpus callosum, the fimbria and the internal capsule. There was a significant effect of group in the corpus callosum ($X^2(2)=8.62$, p=0.01) and *post hoc* test found that the BCAS vehicle group displayed significant white matter disruption compared to shams (p=0.02) which was not detected between BCAS GW2580 and shams (p=0.72) (Fig 5.7a). Similarly, there was a significant effect of group in the fimbria ($X^2(2)=9.05$, p=0.01) and *post hoc* tests found significant white matter disruption in the BCAS vehicle group compared to shams (p=0.04) and the BCAS GW2580 group (p=0.03) (Fig 5.7b). There was also a group effect in the internal capsule ($X^2(2)=7.98$, p=0.02) where *post hoc* test again found significant white matter disruption in the BCAS vehicle group compared to shams (p=0.03) (5.7c).

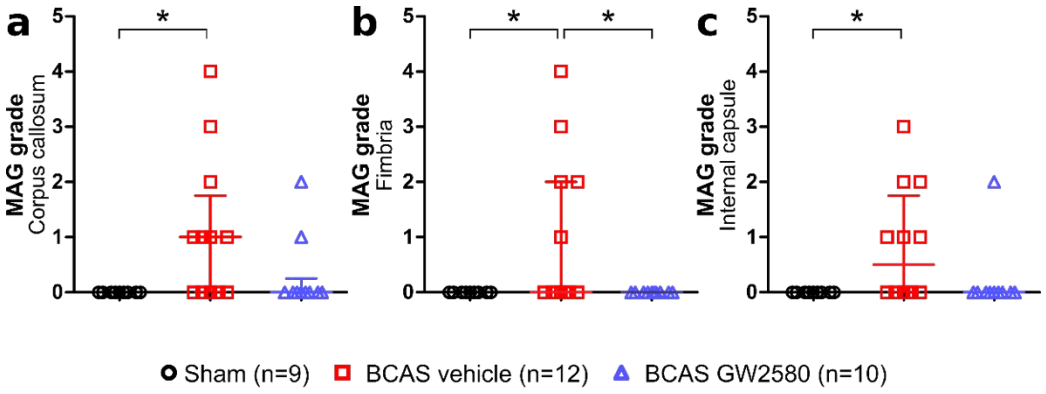

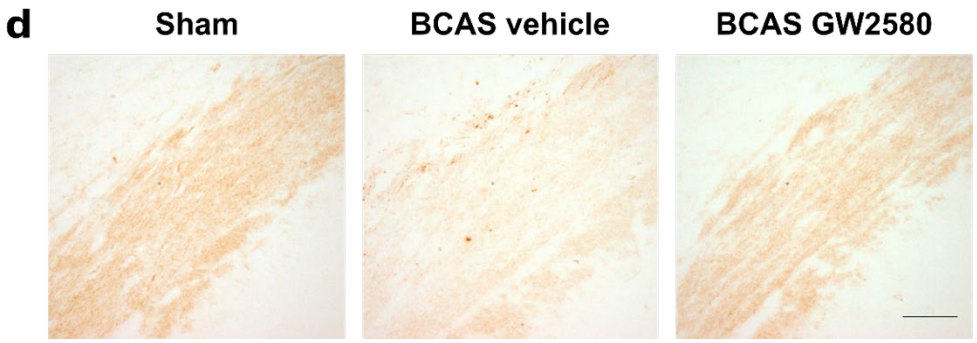

◄**Figure 5.7 GW2580-treament protects against white matter disruption 6 weeks post-BCAS. (a)** White matter disruption in the corpus callosum was evident in the BCAS vehicle group. **(b)** The fimbria was similarly disrupted in the BCAS vehicle group as well as the **(c)** the internal capsule. There was no white matter disruption in the BCAS GW2580 group in any region. Median**, bars represent** IQR. *p<0.05. **(d)** Representative images of MAG in the corpus callosum. Scale bar 50 µm.

Further, the extent of white matter disruption in the corpus callosum was positively correlated with increased density of microglia in the same area (r=55, n=31, p=0.001) (Fig 5.8). Collectively, these results demonstrate that treatment with GW2580 protects against white matter disruption resulting from BCAS-induced hypoperfusion, and that the extent of disruption is associated with increased density of microglia.

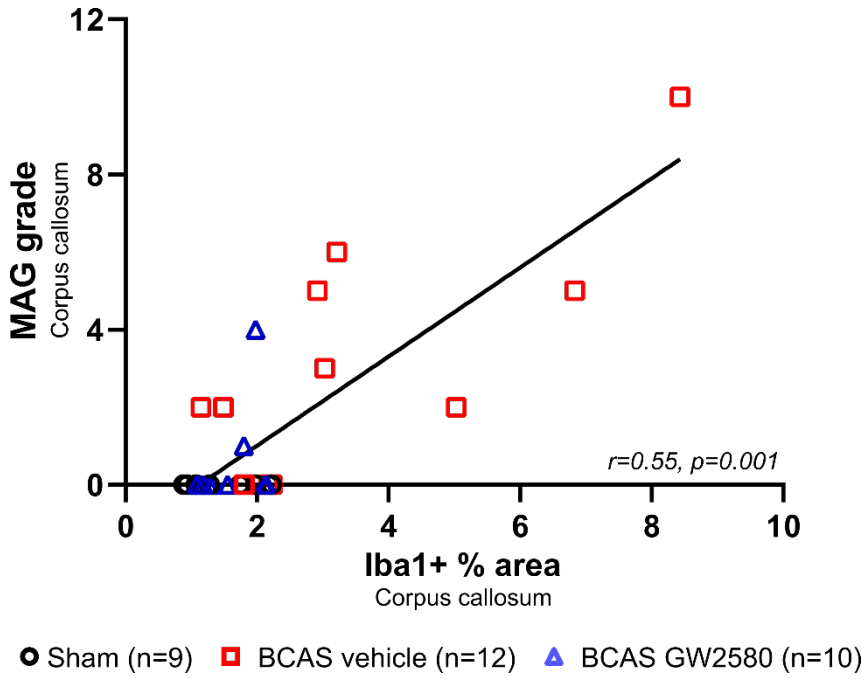

Figure 5.8 The severity of white matter disruption in the corpus callosum is positively correlated with increased density of microglia. The severity of white matter disruption (MAG grade) is positively correlated with increased density of microglia (percentage area of Iba1) in the corpus callosum. Mean, n=31.

5.3.6 GW2580-treatment protects against chronic hypoperfusion-induced impairment in spatial learning

Spatial learning and memory and cognitive flexibility was assessed using the Barnes maze after four weeks of cerebral hypoperfusion. Spatial learning was quantified as the time taken for the animal to find the correct hole and enter the escape chamber, i.e. escape latency, and plotted over consecutive trials. There was a significant effect of time ($F_{(3.34,93.51)}$=65.08, p<0.0001) indicative of learning (Fig 5.9a). There was also an overall significant effect of group ($F_{(2,28)}$=13.12, p<0.0001) and *post hoc* tests identified overall significantly greater escape latency in the BCAS vehicle group compared to shams (p<0.001) (Fig 5.9a) demonstrating an impairment in spatial learning induced by hypoperfusion. Remarkably, the BCAS GW2580 group displayed very similar escape latency compared to shams, which was significantly lower than the BCAS vehicle group (p=0.001) (Fig 5.9a), indicating that GW2580 protects against hypoperfusion-induced impairment in spatial learning.

Spatial reference memory was quantified as proportion of time spent in the quadrant where the escape chamber was previously located (probe test). The sham group spent significantly more time than chance in the target quadrant (p<0.001), whereas the BCAS vehicle group narrowly missed accepted levels of statistical significance (p=0.06) (Fig 5.9b), indicating a trend of impairment in spatial memory. The BCAS GW2580 group spent significantly more time than chance in the target quadrant (p=0.049), however performance was similar between both BCAS groups and there was no overall difference between any of the groups ($F_{(2,28)}$=2.41, p=0.11) (Fig 5.9b).

Cognitive flexibility was assessed similar to spatial learning and memory with reversed location of the escape chamber (180º), training animals for an additional 3 days (2 trials/day). There was a significant effect of time ($F_{(2,56)}$=31.98, p<0.0001) during the reversal phase indicative of learning (Fig 5.9c). The BCAS vehicle group appears to perform worse than sham and BCAS GW2580 groups, however the effect of group narrowly misses accepted level of statistical significance ($F_{(2,28)}$=3.28, p=0.053) (Fig 5.9c). During the reversal probe only the sham group spend significantly more time than chance in the target quadrant (p=0.02, BCAS vehicle p=0.08, BCAS GW2580 p=0.18) (Fig 5.9d), although performance of the sham group compared to the initial probe is worse, indicating the increased complexity of the reversal task. There was no overall difference between groups in the reversal probe ($F_{(2,28)}$=0.49, p=0.62). Collectively the results demonstrate that GW2580-treatment effectively

protects against hypoperfusion-induced impairment in spatial learning, whereas spatial reference memory was similar between vehicle and GW2580-treated groups. There are indications that cognitive flexibility is improved by GW2580 treatment but there was no effect of the drug on reference memory following the reversal phase.

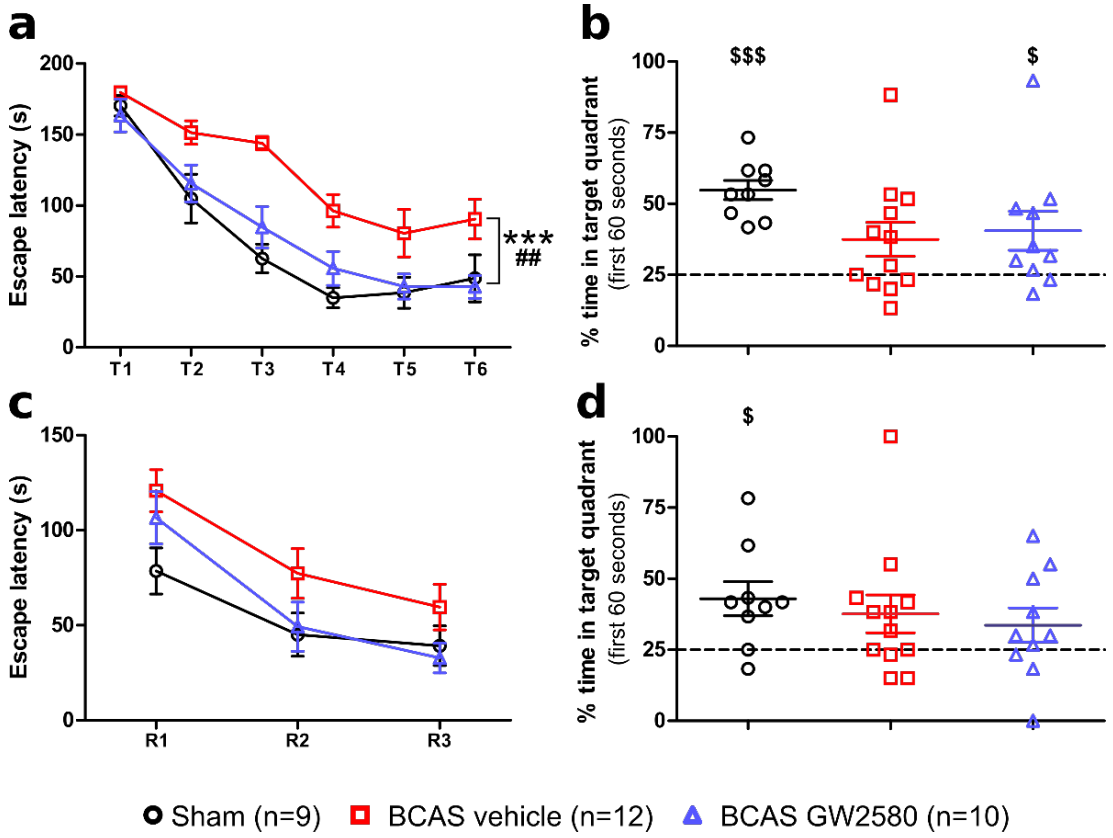

Figure 5.9 GW2580-treatment protects against hypoperfusion-induced impairment in spatial learning. (a) There was an overall effect of time indicating learning and the BCAS vehicle group had increased escape latency compared to shams indicating impaired spatial learning. Escape latency was similar between BCAS GW2580 and shams indicating that GW2580 protects against spatial learning impairment. **(b)** Sham and BCAS GW2580 groups spent more time than chance in the target quadrant whereas the BCAS vehicle group missed accepted levels of statistical significance. There was no overall difference between groups. **(c)** There was an overall effect of time on escape latency during the reversal phase but no group effect. **(d)** Only the sham group spent more time than chance in target quadrant during the reversal probe test and there was no overall difference between the groups. Dashed line indicates chance level (25%). Mean±SEM. ***p<0.001 (* indicates *post hoc* differences between BCAS vehicle and sham groups), ##p<0.01 (# indicates *post hoc* differences between BCAS vehicle and BCAS GW2580 groups), $p<0.05, $$$p<0.001 ($ indicates difference between each group and chance level).

5.4 Discussion

The current study was designed to investigate whether microglial CSF1R signalling contributes to white matter disruption and cognitive impairment following cerebral hypoperfusion. The results demonstrate that treatment with GW2580 following BCAS acutely reduced microglial proliferation and pro-inflammatory signalling modestly and chronically inhibited increases in white matter microglia and astrogliosis, preserved white matter structure and protected against hypoperfusion-induced impairment in spatial learning.

5.4.1 Resting cortical cerebral blood flow is acutely and chronically reduced following bilateral carotid artery stenosis to a similar extent in GW2580- and vehicle-treated animals

The overarching aim of the study was to assess the effect of inhibiting microglial CSF1R signalling on white matter disease progression and cognition. In order to test this a robust increase in microglia was warranted. To ensure this, the BCAS model was modified (compared to chapter 3/4) to utilise a mixed coil strategy (0.16/0.18 mm) and strict inclusion criteria of >35% CBF reduction at 24 hours post-BCAS. Consistent with previous reports (Fowler et al., 2017, Miki et al., 2009), this produced a reduction in CBF of 50-60% at 24 hours which persisted over the one and the six week time points measured. Importantly, the results demonstrate comparable CBF reduction between GW2580- and vehicle-treated BCAS groups indicating that GW2580 treatment does not affect the CBF response to BCAS surgery and hence allowing subsequent results to be assessed without confounding flow-related differences.

5.4.2 GW2580-treatment dampens microglial proliferation and pro-inflammatory signalling one week following bilateral carotid artery stenosis

After BCAS had been determined to induce sufficient reductions in CBF the next aim was to evaluate the microglial response and whether GW2580 treatment inhibited microglial proliferation. Consistent with previous studies (Fowler et al., 2017), the current study saw an increase in white matter microglia in the corpus callosum one week post-BCAS, and to determine the effect of GW2580 treatment on microglial proliferation, BrdU was administered during the final 3 days (incorporates into DNA of actively proliferating cells).

The data demonstrates that treatment with GW2580 does not inhibit microglial proliferation in the corpus callosum one week post-BCAS in all animals, however there

was statistically no difference between the sham and GW2580-treated group. These results suggest that treatment with GW2580 in the current study induced an all-or-nothing inhibitory response on microglial proliferation. This is in contrast with previous studies administering GW2580 where microglial proliferation was reduced by ~50% in models of prion disease (Gomez-Nicola et al., 2013) and AD (Olmos-Alonso et al., 2016) using the same dose (75mg/kg), although only mean±SEM was reported without individual data points and hence the distribution of this response across the group is impossible to interpret.

Further, these studies demonstrate that GW2580 shifts the overall inflammatory profile from pro- to anti-inflammatory (Gomez-Nicola et al., 2013, Olmos-Alonso et al., 2016) and the pro-inflammatory marker *C4* was therefore measured using qPCR. While *C4* was significantly upregulated only in the vehicle-treated hypoperfused group compared to the sham this result was driven by a small number of animals with considerably higher expression. Additional inflammatory markers would need to be investigated to determine if the GW2580 at one week following moderate hypoperfusion alters the inflammatory profile consistent with the published literature. Nonetheless, it was determined that since GW2580 inhibited microglial proliferation in a subset of animals, the effect of GW2580 would be studied longer term (6 weeks) to interrogate the effect of chronic CSF1R inhibition on white matter pathology and cognition post-BCAS.

5.4.3 GW2580-treatment prevents chronic hypoperfusion-induced increases in white matter microglia

Consistent with previous studies of acute severe (Fowler et al., 2017) and chronic mild cerebral hypoperfusion (Manso et al., 2017, Kitamura et al., 2017) there was a significant increase in microglia in the corpus callosum in vehicle-treated animals 6 weeks post-BCAS. The next aim was therefore to determine the efficacy of GW2580 administration in diet over the same period. Similar to the acute study, BrdU was administered during the last 3 days but there was no evidence of proliferating microglia at this time in any group, suggesting that the rate of proliferation is higher acutely following BCAS surgery. Instead number and density of Iba1 positive cells in the corpus callosum was assessed, and density of Iba1 positive cells in the fimbria and internal capsule. Remarkably, chronic treatment with GW2580 completely inhibited hypoperfusion-induced increases in both microglial number and density in the corpus callosum.

Compared to previous studies administering GW2580 chronically (1-3 months) at the same doses, either by daily oral gavage (75mg/kg) or *ad libitum* in chow (0.1%), the results in the current study demonstrate more successful inhibition of microglial upregulation, however without further experiments this cannot be attributed to an inhibition of proliferation. In models of prion disease, AD, ALS and spinal cord injury (SCI), GW2580 treatment reduced microglial proliferation by ~50% but was compared to wild type controls still elevated (about 2-fold), shown using BrdU/ErdU (Gomez-Nicola et al., 2013, Olmos-Alonso et al., 2016, Martinez-Muriana et al., 2016, Gerber et al., 2018). It was also noted that the extent of inhibition following GW2580-treatment in the current study was more effective chronically vs acute. There may be explanations for this.

Firstly, the models that GW2580 has been previously studied in are all far more severe than chronic cerebral hypoperfusion. That would be expected to induce a greater release of inflammatory molecules such as CSF1 and IL34 which bind to CSF1R to induce proliferation of microglia. GW2580 acts as a competitive inhibitor at the ATP pocket of CSF1R and as many tyrosine kinases have similar structure it is possible that it would show nonspecific kinase inhibition, however, (Conway et al., 2005) showed that at least *in vitro* GW2580 was inactive against 26 kinases. One possibility is that the bioavailability of GW2580 following the current treatment paradigms is insufficient to completely inhibit the binding of CSF1/IL34 to its receptor due to its action as a competitive antagonist. In the cerebral hypoperfusion model, a large initial microglial proliferative event may be necessary to perpetuate the chronic inflammation which in turn is detrimental to white matter structure and function. In contrast, prions, amyloid, SOD1 (superoxide dismutase) deficiency and SCI may by different means induce continuous production of inflammatory mediators that compete with GW2580. That would explain why GW2580 is unable to completely inhibit microglial proliferation in these models as well as acutely following BCAS, but that by 6 weeks post-BCAS GW2580-treated animals display levels of microglia similar to wild type controls. Experimental evidence in support of this includes early detectably increases in a battery of pro-inflammatory genes in white matter in the hypoperfusion model (72 hours post-BCAS) (Reimer et al., 2011), which are demonstrably more difficult to detect at later time points (6 weeks) (Manso et al., 2017). In contrast, the prion model displays robust increases in pro-inflammatory genes such as IL1β, CSF1 and IL34 at 18 weeks post-inoculation (Gomez-Nicola et al., 2013), similarly observed in 9 month old AD mice (Olmos-Alonso et al., 2016).

However, of note, the levels of CSF1 and IL34 have not been measured following BCAS which would be required before this explanation can be verified.

Secondly, an alternative explanation may be that microglial apoptosis in the GW2580-treated group accounts for the apparent greater efficacy in the chronic compared to the acute study. It was recently shown that the microglial population self-renews by coupled proliferation and apoptosis at a rate estimated to replace the entire population in about 3 months (Askew et al., 2017). An experiment administering GW2580 to wild type animals for 3 months found reduced number of microglia (Askew et al., 2017) suggesting that CSF1R is involved in this homeostatic proliferative mechanism. The proliferation/apoptosis dynamics of the microglial population following cerebral hypoperfusion has not been investigated, and there may be hypoperfusion-driven alterations in the rate of apoptosis which go undetected by comparably greater rates of proliferation. This could be tested by a time course study employing BrdU administration and a TUNEL assay.

Even so, the data demonstrates successful inhibition of the hypoperfusion-induced white matter microglial response using GW2580, and so the next aim was to assess the effect of this inhibition on the wider inflammatory response and on white matter disruption and cognition.

5.4.4 GW2580-treatment inhibits chronic hypoperfusion-induced white matter astrogliosis

Because the previous chapters of this thesis detects significant astrogliosis following mild chronic hypoperfusion the effect of inhibiting CSF1R signalling in microglia on white matter astrocytes was interrogated post-BCAS. The results demonstrate that astrogliosis is increased in the corpus callosum post-BCAS and that this is inhibited by treatment with GW2580, and that this response is positively correlated with increasing density of microglia. Following treatment with GW2580, only one previous study reported the effects on astrocytes. Gerber et al. (2018) found reduced astrocytosis in several parts of the spinal cord following GW2580 administration in SCI, however due to lack of uninjured controls it is impossible to say if this reduction was comparable to that observed in the current study.

These data, and the fact that astrocytes have been shown not to express CSF1R (Gomez-Nicola et al., 2013), indicates that CSF1R-mediated microglial upregulation likely resulting from proliferation following cerebral hypoperfusion may be required to induce reactive astrogliosis. This would be consistent with a recent study by Liddelow et al. (2017) that proposes that secreted microglial factors are responsible for the

induction of astrogliosis. Interestingly they argue that the type of stimuli that induces the microgliosis (e.g. ischaemia/systemic inflammation) determines if the reactive astrocytes will assume a harmful or protective phenotype (Liddelow et al., 2017, Zamanian et al., 2012). Alternatively, in the current study, the effect on astrogliosis may be indirectly mediated via an overall reduction in pro-inflammatory signalling since astrocytes, similar to microglia, are known to be dynamic responders to their environment (Sofroniew and Vinters, 2010). Teasing out the specific cell-to-cell interactions is difficult with the current experimental paradigm but could be addressed using cell isolation studies and transcriptomics as previously discussed. The inflammatory response of both cell types is incredibly complex as they respond to and produce many of the same molecules (Sofroniew, 2014b), however recent studies are beginning to shed some light on signals mediating microglia/astrocyte crosstalk (Rothhammer et al., 2018, Liddelow et al., 2017, Yun et al., 2018). The converse of the current experiment would be to specifically inhibit astrogliosis and study the effect on microglia. However, because astrocyte reactivity can be induced by such a vast number of triggers; pro-inflammatory molecules (TNFα, IL1β), cell damage, death and ischaemia (ATP, ROS, RNS) and neuronal hyperactivity (Glutamate) (Sofroniew and Vinters, 2010), finding one such agent may prove problematic.

Regardless, the data demonstrate that inhibiting increases in white matter microglia following BCAS using a microglia-specific drug efficiently inhibits increases in white matter astrogliosis, ultimately blocking the cellular inflammatory response observed when cerebral perfusion is reduced. The next question is what effect does this have on white matter pathology and cognition.

5.4.5 GW2580-treatment protects against chronic hypoperfusion-induced white matter disruption

The next aim was to determine the effect of GW280 on white matter disruption post-BCAS. Consistent with previous studies (Coltman et al., 2011, Holland et al., 2011, Reimer et al., 2011, McQueen et al., 2014, Kitamura et al., 2017), BCAS induced white matter disruption in the corpus callosum, fimbria and internal capsule and treatment with GW2580 protected against hypoperfusion-induced white matter disruption in all regions studied. Increasing density of microglia in the corpus callosum was positively correlated with progressive white matter disruption in the same area. This indicates that upregulation and activation of white matter microglia is actively contributing to the pathological disruption of myelinated axons following chronic hypoperfusion. This is consistent with previous work that find close associations

between number of microglia and impaired white matter structure and function (Manso et al., 2017, Fowler et al., 2017, Kitamura et al., 2017). This is the first line of evidence demonstrating the direct contribution of microglia to white matter disruption following chronic cerebral hypoperfusion using highly selective pharmacological inhibition of microglial proliferation.

The study by Fowler et al. (2017) reported that treatment with the Nrf2-activating compound DMF following severe hypoperfusion reduced microglial number and improved white matter function (measured by electrophysiology) but surprisingly did not reduce white matter disruption. This may be because white matter microglia were not restored to sham levels as observed in the current study. Manso et al. (2017) demonstrated that increasing numbers of microglia following mild hypoperfusion was associated with increasing white matter disruption, reduced axonal node length and impaired white matter function. Using the generic anti-inflammatory drug Minocycline, microglial proliferation was reduced (almost to sham levels) and white matter function was restored to sham levels, however white matter structure following drug treatment was not assessed.

Microglia are thought to be detrimental to white matter and oligodendrocytes by releasing cytokines and free radicals, and by sustaining inflammation through antigen-presentation (Howell et al., 2010). Treatment with the drug fingolimod which shifts microglia toward an anti-inflammatory phenotype saw partially improved spatial working memory and white matter structure following hypoperfusion (Qin et al., 2017), suggesting pro-inflammatory signalling by microglia contributes to white matter disruption. GW2580 treatment has similarly been demonstrated to shift microglia from a pro- to an anti-inflammatory phenotype in models of prion disease and AD (Gomez-Nicola et al., 2013, Olmos-Alonso et al., 2016). Proteomic or transcriptomic analysis of the inflammatory milieu in the current study could be used to investigate if GW2580 is similarly shifting microglial phenotype in addition to inhibiting their upregulation.

There are a number of mechanisms whereby inhibiting microglial upregulation using GW2580 may protect white matter following cerebral hypoperfusion. The current study went on to assess the effect of microglial CSF1R signalling on cognition.

5.4.6 GW2580-treatment protects against chronic hypoperfusion-induced impairment in spatial learning

Because white matter disruption is thought to underlie cognitive impairment the next aim was to assess spatial learning and memory, to determine the effect of microglial CSF1R signalling on cognition. The data demonstrate that cerebral

hypoperfusion induced an impairment in spatial learning and reference memory. This is firstly consistent with the impairment in spatial working memory detected in the first two chapters of this thesis and previous studies using the radial arm maze (Shibata et al., 2007, Coltman et al., 2011). Secondly, impairments in reference memory following mild cerebral hypoperfusion has previously not been detected until 5-6 months post-BCAS (Holland et al., 2015, Nishio et al., 2010). This suggests that by increasing the severity of cerebral hypoperfusion this also induces progressively more severe cognitive deficits, however different behavioural tests were utilised and as such cannot be reliably compared.

In agreement with the hypothesis, treatment with GW2580 protected against hypoperfusion-induced impaired spatial learning, but only displayed modest protection of spatial reference memory. The advantage of using the Barnes maze is that spatial learning, also referred to as learning working memory, could be assessed alongside spatial reference memory (Sharma et al., 2010). The observed protection is likely a result of the preservation of white matter structure as spatial learning and working memory is dependent on the integrity of the white matter circuitry to ensure efficient communication between different brain regions (Shibata et al., 2007, Coltman et al., 2011). Spatial reference memory on the other hand is suggested to be more hippocampal-dependent (Nishio et al., 2010, Sharma et al., 2010). The hippocampus, being connected via myelinated axons, is also dependent on good white matter integrity but there may be alternative mechanisms influencing cognition in this study, for example neuronal functions required for memory. As discussed in previous chapters, longer term hypoperfusion results in hippocampal neuronal damage and atrophy and it is a possibility that neuronal alterations that influence memory are changing alongside the detected white matter disruption. For example, if synaptic plasticity is impaired such as in rats following 2VO (Yao et al., 2019), this would be expected to influence the ability to remember the position of the escape chamber during the probe test and it may be possible that treatment with GW2580 preserves white matter structure more efficiently than neuronal function. Olmos-Alonso et al., (2016) found using a T-maze that short term memory, very similar to spatial learning (learning working memory) in this context, was improved following treatment of GW2580 in APP/PS1 mice, which is consistent with the current results. Further, Luo et al. (2013) report expression of CSF1R on a small subset of hippocampal and cortical neurons, and find that activation of the receptor is associated with protection against excitotoxic insult and increased neuronal survival. GW2580-treatment

following cerebral hypoperfusion may therefore inhibit CSF1R signalling on hippocampal neurons causing dysfunction and/or damage. Minimal neuronal damage was observed using haematoxylin and eosin (5/22 hypoperfused animals), but interestingly only occurred in vehicle-treated animals. This suggests that GW2580 may be neuroprotective following BCAS although the results from the probe test suggests that this may not have subsequently protected function. However, it does highlight the importance of considering potential non-microglial effects of inhibiting the activity of CSF1R using GW2580. Future studies incorporating electrophysiology to measure long-term potentiation may shed more light on the role of synaptic plasticity/neuronal function following spatial learning and memory following BCAS with and without GW2580 treatment.

A similar pattern of performance was observed during the reversal phase which tests cognitive flexibility and executive function (O'Leary and Brown, 2013). There was an indication that hypoperfusion induced an impairment in learning the new position of the escape chamber, whereas drug-treated animals performed similar to shams. Only shams displayed intact memory of the new position, possibly indicating more beneficial effects of the drug on learning rather than memory.

Selective protection of spatial learning as opposed to reference memory may be of clinical importance. VCI is characterised by impairments in cognitive function depending on good white matter integrity, e.g. such as speed of processing (de Groot et al., 2000), however as the disease progresses memory is also known to be impaired (Skrobot et al., 2017). It is therefore important to understand how inhibiting microglial upregulation via CSF1R may influence cognition early versus late in the disease progression and if there are mechanisms involved in memory impairment in VCI beyond the disruption of white matter a combination of treatments may be required.

Nonetheless, the data demonstrate complete protection against hypoperfusion-induced spatial learning impairment, consistent with the preservation of white matter structure and relevant to human VCI. This is in support of the hypothesis that microglial upregulation via CSF1R signalling causes white matter disruption and cognitive impairment following BCAS-induced chronic cerebral hypoperfusion.

5.4.7 Potential mechanisms

Excessive phagocytosis of white matter components may directly contribute to white matter disruption in age and following hypoperfusion (Raj et al., 2017), but reduced phagocytosis may also be detrimental to white matter integrity indirectly via

increased burden of neurotoxic products such as myelin debris which may exacerbate further inflammation (Chitu et al., 2016). GW2580 has previously been reported to be beneficial in models of multiple sclerosis (Crespo et al., 2011, Borjini et al., 2016). While both studies saw improved clinical scores with the drug treatment, and Crespo et al. (2011) attributed this to reduced macrophage infiltration and proinflammatory signalling, neither quantified the extent of white matter disruption nor investigated mechanisms beyond the inflammatory response. It is currently unknown how GW2580 affects alternative microglial functions such as phagocytosis, though *in vitro* application of CSF1 stimulates phagocytosis of amyloid by primary human microglia (Chitu et al., 2016) suggesting that inhibiting CSF1 receptor kinase activity through GW2580 may reduce phagocytosis. Assessing phagocytic activity of microglia in the current study could be carried out using immunohistochemical approaches; for example Lysosome-associated membrane protein 2, or in future studies by isolating microglia for *in vitro* functional assays or transcriptomic analysis such as single-cell RNA sequencing. The latter would provide a tremendous amount of information regarding the microglial response to cerebral hypoperfusion and treatment of GW2580, aiding our understanding of the pathophysiological mechanisms involved in the disruption of white matter. Microglial responses to hypoperfusion are exacerbated in aged mice, associated with worse cognitive performance and white matter integrity (Wolf et al., 2017), demonstrating that age and cerebrovascular disease synergistically contribute to VCI. It would be of interest to study the effect of GW2580 post-BCAS in aged mice, to interrogate if white matter disruption and spatial learning could be similarly protected. Raj et al. (2017) studied white matter microglia from aged mice and reported increases not only in pro-inflammatory gene signalling but also phagocytosis-associated genes and alterations in genes associated with lipid homeostasis.

In addition and as previously discussed, white matter hypoxia evident following cerebral hypoperfusion (Duncombe et al., 2017) enhances inflammation through increased NF-κB signalling (Eltzschig and Carmeliet, 2011). Since inflammation in turn exacerbates hypoxia by monopolising available resources (Eltzschig and Carmeliet, 2011), it is possible that inhibiting microglial proliferation via CSF1R may reduce hypoxia and contribute to the preservation of white matter and spatial learning following cerebral hypoperfusion. Early axon-glial disruption (Reimer et al., 2011) and reduced number of oligodendrocytes are evident post-BCAS, however since oligodendrocyte pools are demonstrated to have restorative potential (McQueen et

al., 2014) it is possible that GW2580 treatment by reducing inflammation allows for this response to enable white matter regeneration and prevent further damage.

5.4.8 Limitations, conclusion and future directions

The current study, while presenting encouraging results, is limited by the lack of mechanistic insight.

Firstly, as a result of our experimental design we were unable to detect microglial proliferation in either BCAS group and hence cannot conclude that GW2580 specifically inhibits or reduces microglial proliferation as reported by other groups (Gomez-Nicola et al., 2013, Olmos-Alonso et al., 2016, Martinez-Muriana et al., 2016, Gerber et al., 2018). In order to determine that this is the case also following cerebral hypoperfusion an alternative BrdU treatment regime would need to be employed.

Nonetheless, we are able to conclude that microglial upregulation via CSF1R is a driver of white matter pathology and cognitive impairment following cerebral hypoperfusion, as treatment with GW2580 successfully inhibits this increase in white matter microglia. However, whether this is driven by modulation of the inflammatory milieu, phagocytic activity or white matter hypoxia remains to be determined. Additionally, elucidating cell-to-cell interactions between microglia and astrocytes and other cell types of the neuro-gliovascular unit is essential to fully understand the pathophysiological mechanisms involving white matter disruption following cerebral hypoperfusion. Recent studies suggest that both microglia and astrocytes constitute diverse, heterogeneous populations (Grabert et al., 2016, John Lin et al., 2017, Morel et al., 2017), which display distinct ageing phenotypes such as increased inflammatory gene expression (Soreq et al., 2017, Boisvert et al., 2018). This highlights the need to study the therapeutic potential of inhibiting microglial proliferation in older animals, and to better characterise sub-cellular populations responsible for detrimental or protective pathophysiological processes. Employing newly developed cell-isolation techniques such as concurrent brain cell type acquisition (Swartzlander et al., 2018) and highly sophisticated transcriptomic and phenotypic analyses will be critical to increase our understanding of the mechanisms involved.

Tyrosine kinase inhibitors have been extensively used for the treatment of cancers which is promising for the use of GW2580 in a clinical setting, however as these are sometimes associated with adverse effect including liver injury, thought to result from inhibited oxidative metabolism and glycolysis (Mingard et al., 2018), careful study of the potential ‘off-targets’ will need to be included in future investigations.

All in all the data presented here forms a scientific basis for the use of CSF1 receptor tyrosine kinase inhibitors that target microglial proliferation as a potential treatment of chronic inflammation and white matter disruption in cerebrovascular disease and dementia.

Chapter 6

General discussion

6.1 Implications for future research

In summary, the work herein demonstrates that cerebral hypoperfusion induced by bilateral carotid artery stenosis in mice increases microglial numbers and astrogliosis, disrupts white matter and impairs cognition (Fig 6.1).

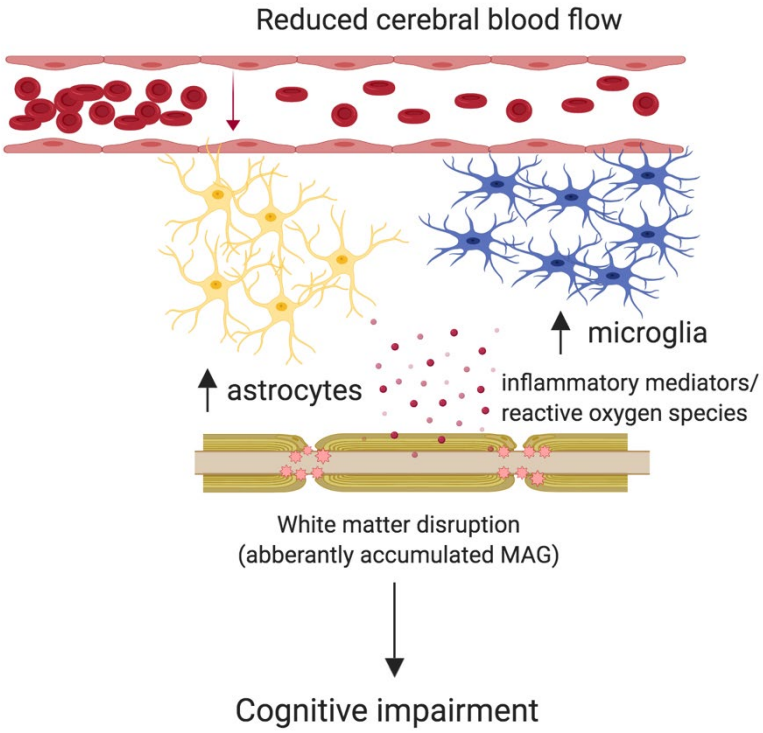

Figure 6.1 Diagram of alterations observed following reductions in cerebral blood flow. Following blood flow reductions microglial numbers increase and astrocytes become activated in the white matter leading to white matter disruption and cognitive impairment. (Diagram created with BioRender.com)

The first two chapters of this thesis utilised genetic approaches to investigate the contribution of the Nrf2 pathway in white matter pathology and cognitive impairment when cerebral blood flow is reduced. The results demonstrate that Nrf2 signalling is involved in the pathophysiological response following cerebral hypoperfusion, as white matter pathology and microgliosis are exacerbated in $Nrf2^{-/-}$ mice compared to wild types (Table 6.1). Further, astrocyte-specific overexpression of Nrf2 is associated with protection of white matter and cognitive function which is associated with reduced pro-inflammatory signalling (Table 6.1). However, the reduced/absent expression of Nrf2 did not result in a further functional impairment despite exacerbated pathology

and microgliosis, and the magnitude of protection resulting from astrocytic Nrf2 overexpression was modest. A few conclusions can be drawn from these results. One, the Nrf2 KO study was underpowered in regard to homozygous knock out mice which resulted in the failure to determine if knocking Nrf2 out had a functional outcome. Two, superior models to GFAP-Nrf2 mice may be more efficient for evaluating the therapeutic potential of Nrf2. Or three, additional/alternative mechanisms of inflammation/oxidative stress are contributing to the disruption of white matter structure and function. Additional studies comparing a larger number of $Nrf2^{-/-}$ mice to wild type mice and alternative models of activating/overexpressing Nrf2 would need to be carried out to address conclusion one and two. However, the third conclusion was explored in the final chapter of this thesis.

Table 6.1 Summary of results of BCAS and BCAS + experimental intervention

	BCAS	BCAS + $Nrf2^{-/-}$	BCAS + GFAP-Nrf2	BCAS + GW2580
WHITE MATTER MICROGLIOSIS	+	+ +	+	- -
WHITE MATTER ASTROGLIOSIS	+	+	-	- -
WHITE MATTER DISRUPTION	+	+ +	-	- -
COGNITIVE IMPAIRMENT	+	+	-	-

The final chapter details an investigation of the hypothesis that increases in microglia, a characteristic both of human VCI and cerebral hypoperfusion in mice, via CSF1R-signalling is an early driver of white matter pathology which causes subsequent cognitive impairment. In support of this hypothesis, pharmacological inhibition of CSF1R signalling using the tyrosine kinase inhibitor GW2580 protected against white matter disruption and preserved spatial learning following cerebral hypoperfusion (Table 6.1). Inhibiting the upregulation of microglia was further associated with reduced white matter astrogliosis suggesting that the overall inflammatory response was prevented. These results are encouraging as they provide robust evidence of an inflammatory mechanism involved in the disruption of white matter structure and function by cerebral hypoperfusion, which is amenable to modulation. A large number of questions remain as to how microglial increases lead to disruption of white matter, for example which specific microglial functions are responsible and what the effect and contribution of other cell types is. Cell-isolation studies should aid in answering these. One of the most important questions that needs to be answered is what the therapeutic potential of inhibiting microglial CSF1R-

signalling is when an inflammatory response is already established, as would be expected in the human condition. Further, all studies reported in this thesis were carried out using adult mice, and as previously discussed, profound changes to microglia/astrocyte transcriptomes (Grabert et al., 2016, Soreq et al., 2017, Boisvert et al., 2018) and reductions in cell-signalling such as Nrf2 (Ungvari et al., 2011a) occur with age which renders the brain more vulnerable to damage and dysfunction. It is therefore essential that future studies are carried out in older animals, especially as these have already been observed to show a more severe inflammatory response to cerebral hypoperfusion (Wolf et al., 2017).

It is also imperative to acknowledge that the results from this thesis and other cerebral hypoperfusion studies reflect only one aspect of VCI, which is in an incredible complex and heterogeneous condition. Pathological changes with are not incorporated in the model at the time points studied are blood brain barrier disruption and microhaemorrhages, both suggested to contribute to chronic inflammation and whit matter disruption. Longer-term chronic cerebral hypoperfusion lead to these changes (Holland et al., 2015), however, other mechanisms can cause this type of damage, such as hypertension or atherosclerosis which are also risk factors of VCI (Smith, 2017). Atherosclerosis for example, is associated with cerebral hypoperfusion and vascular cognitive impairment (de la Torre, 2012, Kalback et al., 2004), and inflammation is a central aspect of its pathophysiology (Geovanini and Libby, 2018). An *in vitro* study found that inflammation mediated by CSF1 promotes a proatherogenic environment which could be reduced by GW2580 (Irvine et al., 2009). Further, animal models incorporating multiple aspects of VCI are being developed, for example bilateral carotid artery stenosis in spontaneously hypertensive rats can be used to explore hypertensive and hypoperfusion mechanisms simultaneously (Choi et al., 2015). Clearly, further studies in additional experimental models should be carried out to assess the effect of GW2580 to ultimately determine its potential in the treatment of cerebrovascular disease (CVD) and VCI.

6.2 Clinical relevance

At present, available dementia treatments alleviate symptoms only and are short-lived in a subset of patients. As such, there is a desperate need for disease-modifying treatments of CVD and dementia. Pharmacological activators of the Nrf2 system are used to treat relapsing forms of MS (DMF) (Gopal et al., 2017), and ALS (Edaravone) (Hardiman and van den Berg, 2017, Liddell, 2017), both devastating fatal central nervous system disorders. Similarly, Nrf2 has been demonstrated to play an important role in preclinical models of Parkinson's disease (Chen et al., 2009), Huntington's disease (Calkins et al., 2010) and ischaemic stroke (Zhao et al., 2006). While a large body of work indicate a huge therapeutic potential of Nrf2 activation for the treatment of neurodegenerative disease, the evidence presented in this thesis and the available literature does not strongly support the use of Nrf2-activators for the treatment of hypoperfusion-induced CVD and cognitive impairment.

In contrast, results presented in this thesis suggest that the inhibition of microglial proliferation through CSF1R signalling could be an effective future treatment. While the beneficial effect of this approach was profound in a mouse model of cerebral hypoperfusion, a large amount of work will need to be carried out before it can be considered in a human setting. As mentioned in the previous section, further studies in additional experimental models of VCI need to be carried out. Due to the heterogeneity of VCI accumulating evidence from several different experimental models will be necessary. Building up a body of evidence in preclinical studies will determine whether GW2580 should be taken into a clinical trial. Previous clinical trials have been hampered by the lack of translatability between rodent models and actual human diseases. Part of this may be attributed to deficient reproducibility and robustness of results from preclinical studies using animal models, issues that could be overcome by improved study and statistical design as well as improved reporting standards (Snyder et al., 2016).

6.2.1 Considerations for targeting CSF1R signalling in humans

It is worth noting that mutations of the CSF1R in humans results in a white matter disease referred to as hereditary diffuse leukoencephalopathy with spheroids (HDLS) which is associated with behavioural and cognitive deficits including dementia (Rademakers et al., 2011). A recent study in zebrafish found that haploinsufficiency of CSF1R, resembling adult-onset leukoencephalopathy with axonal spheroids and pigmented glia (ALSP) resulted in partial depletion of microglia (Oosterhof et al.,

2018), leading the authors to urge caution before employing therapeutic strategies which target the receptor.

Importantly, and in consideration of this, treatment with GW2580 does not drastically deplete the existing microglial population, even at higher doses (Olmos-Alonso et al., 2016), but acts to inhibit its expansion, at least in mice. As a therapeutic agent this should in theory allow for treatment of the chronic inflammatory response which is detrimental to white matter integrity while preserving the established population microglial and its homeostatic function. Although further studies are warranted to ensure that GW2580 does not influence microglial phenotype, or other cell types such as neurons, in a manner which would be detrimental in the long term.

Considering this investigating the effect of GW2580 on human cells may be vital. Advances in techniques to induce pluripotent stem cells (iPSCs)(Hung et al., 2017) and complex *in vitro* systems that model the neuro-gliovascular unit including simulated perfusion (Alcendor et al., 2013) means that potential drug treatments for VCI and neurodegenerative disease can now be tested on human cells. While these models will not be able to recapitulate the human setting completely as there is no white matter present, toxicity and molecular mechanisms of the drug treatment can be investigated. Non-human primates represent an additional model which much better reflects humans, in particular for the study of VCI as primate brains contain similar proportions of white matter (Hainsworth et al., 2017). However, these studies are complicated by comparably greater life span and ethical regulations relating to primates compared to rodents.

All things considered, the road from the bench to the clinic is long and cumbersome. Nonetheless, the results presented in this thesis provide a good scientific basis for further exploration of the contribution of microglial proliferation to the disruption of white matter structure and function, and highlights the potential of inhibiting this response for the treatment of cerebrovascular disease and vascular cognitive impairment.

References

AANERUD, J., BORGHAMMER, P., CHAKRAVARTY, M. M., VANG, K., RODELL, A. B., JÓNSDOTTIR, K. Y., MØLLER, A., ASHKANIAN, M., VAFAEE, M. S., IVERSEN, P., JOHANNSEN, P. & GJEDDE, A. 2012. Brain energy metabolism and blood flow differences in healthy aging. *J Cereb Blood Flow Metab,* 32**,** 1177-87.

ABOUL-ENEIN, F., RAUSCHKA, H., KORNEK, B., STADELMANN, C., STEFFERL, A., BRUCK, W., LUCCHINETTI, C., SCHMIDBAUER, M., JELLINGER, K. & LASSMANN, H. 2003. Preferential loss of myelin-associated glycoprotein reflects hypoxia-like white matter damage in stroke and inflammatory brain diseases. *J Neuropathol Exp Neurol,* 62**,** 25-33.

AGGARWAL, S., YURLOVA, L. & SIMONS, M. 2011. Central nervous system myelin: structure, synthesis and assembly. *Trends Cell Biol,* 21**,** 585-93.

AHUJA, M., AMMAL KAIDERY, N., YANG, L., CALINGASAN, N., SMIRNOVA, N., GAISIN, A., GAISINA, I. N., GAZARYAN, I., HUSHPULIAN, D. M., KADDOUR-DJEBBAR, I., BOLLAG, W. B., MORGAN, J. C., RATAN, R. R., STARKOV, A. A., BEAL, M. F. & THOMAS, B. 2016. Distinct Nrf2 Signaling Mechanisms of Fumaric Acid Esters and Their Role in Neuroprotection against 1-Methyl-4-Phenyl-1,2,3,6-Tetrahydropyridine-Induced Experimental Parkinson's-Like Disease. *J Neurosci,* 36**,** 6332-51.

AKIGUCHI, I., TOMIMOTO, H., SUENAGA, T., WAKITA, H. & BUDKA, H. 1997. Alterations in glia and axons in the brains of Binswanger's disease patients. *Stroke,* 28**,** 1423-9.

AL-MASHHADI, S., SIMPSON, J. E., HEATH, P. R., DICKMAN, M., FORSTER, G., MATTHEWS, F. E., BRAYNE, C., INCE, P. G. & WHARTON, S. B. 2015. Oxidative Glial Cell Damage Associated with White Matter Lesions in the Aging Human Brain. *Brain Pathol,* 25**,** 565-74.

ALAWIEH, A., LANGLEY, E. F., WEBER, S., ADKINS, D. & TOMLINSON, S. 2018. Identifying the role of complement in triggering neuroinflammation after traumatic brain injury. *J Neurosci*.

ALCENDOR, D. J., BLOCK, F. E., 3RD, CLIFFEL, D. E., DANIELS, J. S., ELLACOTT, K. L., GOODWIN, C. R., HOFMEISTER, L. H., LI, D., MARKOV, D. A., MAY, J. C., MCCAWLEY, L. J., MCLAUGHLIN, B., MCLEAN, J. A., NISWENDER, K. D., PENSABENE, V., SEALE, K. T., SHERROD, S. D., SUNG, H. J., TABB, D. L., WEBB, D. J. & WIKSWO, J. P. 2013. Neurovascular unit on a chip: implications for translational applications. *Stem Cell Res Ther,* 4 Suppl 1**,** S18.

ALOSCO, M. L., GUNSTAD, J., JERSKEY, B. A., XU, X., CLARK, U. S., HASSENSTAB, J., COTE, D. M., WALSH, E. G., LABBE, D. R., HOGE, R., COHEN, R. A. & SWEET, L. H. 2013. The adverse effects of reduced cerebral perfusion on cognition and brain structure in older adults with cardiovascular disease. *Brain Behav,* 3**,** 626-36.

ANDREWS, N. C., ERDJUMENT-BROMAGE, H., DAVIDSON, M. B., TEMPST, P. & ORKIN, S. H. 1993. Erythroid transcription factor NF-E2 is a haematopoietic-specific basic-leucine zipper protein. *Nature,* 362**,** 722-8.

ANRATHER, J. & IADECOLA, C. 2016. Inflammation and Stroke: An Overview. *Neurotherapeutics,* 13**,** 661-670.

ARAQUE CABALLERO, M. A., SUAREZ-CALVET, M., DUERING, M., FRANZMEIER, N., BENZINGER, T., FAGAN, A. M., BATEMAN, R. J., JACK, C. R., LEVIN, J., DICHGANS, M., JUCKER, M., KARCH, C., MASTERS, C. L., MORRIS, J. C., WEINER, M., ROSSOR, M., FOX, N. C., LEE, J. H., SALLOWAY, S., DANEK, A., GOATE, A., YAKUSHEV, I., HASSENSTAB, J., SCHOFIELD, P. R., HAASS, C. & EWERS, M. 2018. White matter diffusion alterations precede symptom onset in autosomal dominant Alzheimer's disease. *Brain*.

ASKEW, K., LI, K., OLMOS-ALONSO, A., GARCIA-MORENO, F., LIANG, Y., RICHARDSON, P., TIPTON, T., CHAPMAN, M. A., RIECKEN, K., BECCARI, S., SIERRA, A., MOLNAR, Z., CRAGG, M. S., GARASCHUK, O., PERRY, V. H. & GOMEZ-NICOLA, D. 2017. Coupled Proliferation and Apoptosis Maintain the Rapid Turnover of Microglia in the Adult Brain. *Cell Rep,* 18**,** 391-405.

ATTWELL, D., BUCHAN, A. M., CHARPAK, S., LAURITZEN, M., MACVICAR, B. A. & NEWMAN, E. A. 2010. Glial and neuronal control of brain blood flow. *Nature,* 468**,** 232-43.

ATTWELL, D. & LAUGHLIN, S. B. 2001. An energy budget for signaling in the grey matter of the brain. *J Cereb Blood Flow Metab,* 21**,** 1133-45.

AZIZI, G., KHANNAZER, N. & MIRSHAFIEY, A. 2014. The Potential Role of Chemokines in Alzheimer's Disease Pathogenesis. *Am J Alzheimers Dis Other Demen,* 29**,** 415-25.

BACK, S. A., KROENKE, C. D., SHERMAN, L. S., LAWRENCE, G., GONG, X., TABER, E. N., SONNEN, J. A., LARSON, E. B. & MONTINE, T. J. 2011. White matter lesions defined by diffusion tensor imaging in older adults. *Ann Neurol,* 70**,** 465-76.

BALUCANI, C., VITICCHI, G., FALSETTI, L. & SILVESTRINI, M. 2012. Cerebral hemodynamics and cognitive performance in bilateral asymptomatic carotid stenosis. *Neurology,* 79**,** 1788-95.

BARKER, R., ASHBY, E. L., WELLINGTON, D., BARROW, V. M., PALMER, J. C., KEHOE, P. G., ESIRI, M. M. & LOVE, S. 2014. Pathophysiology of white matter perfusion in Alzheimer's disease and vascular dementia. *Brain,* 137**,** 1524-32.

BARKER, R., WELLINGTON, D., ESIRI, M. M. & LOVE, S. 2013. Assessing white matter ischemic damage in dementia patients by measurement of myelin proteins. *J Cereb Blood Flow Metab,* 33**,** 1050-7.

BARNES, C. A. 1979. Memory deficits associated with senescence: a neurophysiological and behavioral study in the rat. *J Comp Physiol Psychol,* 93**,** 74-104.

BARONE, F. C., GUSTAFSON, D., CRYSTAL, H. A., MORENO, H., ADAMSKI, M. G., ARAI, K., BAIRD, A. E., BALUCANI, C., BRICKMAN, A. M., CECHETTO, D., GORELICK, P., BIESSELS, G. J., KILIAAN, A., LAUNER, L., SCHNEIDER, J., SOROND, F. A., WHITMER, R., WRIGHT, C. & ZHANG, Z. G. 2016. First translational 'Think Tank' on cerebrovascular disease, cognitive impairment and dementia. *J Transl Med.* England.

BELANGER, M., ALLAMAN, I. & MAGISTRETTI, P. J. 2011. Brain energy metabolism: focus on astrocyte-neuron metabolic cooperation. *Cell Metab,* 14**,** 724-38.

BELL, K. F., AL-MUBARAK, B., FOWLER, J. H., BAXTER, P. S., GUPTA, K., TSUJITA, T., CHOWDHRY, S., PATANI, R., CHANDRAN, S., HORSBURGH, K., HAYES, J. D. & HARDINGHAM, G. E. 2011a. Mild oxidative stress activates Nrf2 in astrocytes, which contributes to neuroprotective ischemic preconditioning. *Proc Natl Acad Sci U S A.* United States.

BELL, K. F., AL-MUBARAK, B., MARTEL, M. A., MCKAY, S., WHEELAN, N., HASEL, P., MARKUS, N. M., BAXTER, P., DEIGHTON, R. F., SERIO, A., BILICAN, B., CHOWDHRY, S., MEAKIN, P. J., ASHFORD, M. L., WYLLIE, D. J., SCANNEVIN, R. H., CHANDRAN, S., HAYES, J. D. & HARDINGHAM, G. E. 2015. Neuronal development is promoted by weakened intrinsic antioxidant defences due to epigenetic repression of Nrf2. *Nat Commun,* 6**,** 7066.

BELL, K. F., FOWLER, J. H., AL-MUBARAK, B., HORSBURGH, K. & HARDINGHAM, G. E. 2011b. Activation of Nrf2-regulated glutathione pathway genes by ischemic preconditioning. *Oxid Med Cell Longev,* 2011**,** 689524.

BENDLIN, B. B., FITZGERALD, M. E., RIES, M. L., XU, G., KASTMAN, E. K., THIEL, B. W., ROWLEY, H. A., LAZAR, M., ALEXANDER, A. L. & JOHNSON, S. C. 2010. White matter in aging and cognition: a cross-sectional study of microstructure in adults aged eighteen to eighty-three. *Dev Neuropsychol,* 35**,** 257-77.

BENNETT, S., GRANT, M. M. & ALDRED, S. 2009. Oxidative stress in vascular dementia and Alzheimer's disease: a common pathology. *J Alzheimers Dis,* 17**,** 245-57.

BERNBAUM, M., MENON, B. K., FICK, G., SMITH, E. E., GOYAL, M., FRAYNE, R. & COUTTS, S. B. 2015. Reduced blood flow in normal white matter predicts development of leukoaraiosis. *J Cereb Blood Flow Metab,* 35**,** 1610-5.

BOISVERT, M. M., ERIKSON, G. A., SHOKHIREV, M. N. & ALLEN, N. J. 2018. The Aging Astrocyte Transcriptome from Multiple Regions of the Mouse Brain. *Cell Rep,* 22**,** 269-285.

BORJINI, N., FERNANDEZ, M., GIARDINO, L. & CALZA, L. 2016. Cytokine and chemokine alterations in tissue, CSF, and plasma in early presymptomatic phase of experimental allergic encephalomyelitis (EAE), in a rat model of multiple sclerosis. *J Neuroinflammation,* 13**,** 291.

BOSE, S. & CHO, J. 2013. Role of chemokine CCL2 and its receptor CCR2 in neurodegenerative diseases. *Arch Pharm Res,* 36**,** 1039-50.

BOYLE, P. A., YU, L., FLEISCHMAN, D. A., LEURGANS, S., YANG, J., WILSON, R. S., SCHNEIDER, J. A., ARVANITAKIS, Z., ARFANAKIS, K. & BENNETT, D. A. 2016. White matter hyperintensities, incident mild cognitive impairment, and cognitive decline in old age. *Ann Clin Transl Neurol,* 3**,** 791-800.

BRANCA, C., FERREIRA, E., NGUYEN, T. V., DOYLE, K., CACCAMO, A. & ODDO, S. 2017. Genetic reduction of Nrf2 exacerbates cognitive deficits in a mouse model of Alzheimer's disease. *Hum Mol Genet,* 26**,** 4823-4835.

BRICKMAN, A. M., ZAHRA, A., MURASKIN, J., STEFFENER, J., HOLLAND, C. M., HABECK, C., BOROGOVAC, A., RAMOS, M. A., BROWN, T. R., ASLLANI, I. & STERN, Y. 2009. Reduction in cerebral blood flow in areas appearing as white matter hyperintensities on magnetic resonance imaging. *Psychiatry Res,* 172**,** 117-20.

BROWN, R. E. & WONG, A. A. 2007. The influence of visual ability on learning and memory performance in 13 strains of mice. *Learn Mem,* 14**,** 134-44.

CAGNIN, A., BROOKS, D. J., KENNEDY, A. M., GUNN, R. N., MYERS, R., TURKHEIMER, F. E., JONES, T. & BANATI, R. B. 2001. In-vivo measurement of activated microglia in dementia. *Lancet,* 358**,** 461-7.

CAHOY, J. D., EMERY, B., KAUSHAL, A., FOO, L. C., ZAMANIAN, J. L., CHRISTOPHERSON, K. S., XING, Y., LUBISCHER, J. L., KRIEG, P. A., KRUPENKO, S. A., THOMPSON, W. J. & BARRES, B. A. 2008. A transcriptome database for astrocytes, neurons, and oligodendrocytes: a new resource for understanding brain development and function. *J Neurosci,* 28**,** 264-78.

CALKINS, M. J., VARGAS, M. R., JOHNSON, D. A. & JOHNSON, J. A. 2010. Astrocyte-specific overexpression of Nrf2 protects striatal neurons from mitochondrial complex II inhibition. *Toxicol Sci,* 115**,** 557-68.

CHAN, K., LU, R., CHANG, J. C. & KAN, Y. W. 1996. NRF2, a member of the NFE2 family of transcription factors, is not essential for murine erythropoiesis, growth, and development. *Proc Natl Acad Sci U S A,* 93**,** 13943-8.

CHAO, L. L., BUCKLEY, S. T., KORNAK, J., SCHUFF, N., MADISON, C., YAFFE, K., MILLER, B. L., KRAMER, J. H. & WEINER, M. W. 2010. ASL perfusion MRI predicts cognitive decline and conversion from MCI to dementia. *Alzheimer Dis Assoc Disord,* 24**,** 19-27.

CHEN, A., AKINYEMI, R. O., HASE, Y., FIRBANK, M. J., NDUNG'U, M. N., FOSTER, V., CRAGGS, L. J., WASHIDA, K., OKAMOTO, Y., THOMAS, A. J., POLVIKOSKI, T. M., ALLAN, L. M., OAKLEY, A. E., O'BRIEN, J. T., HORSBURGH, K., IHARA, M. & KALARIA, R. N. 2016. Frontal white matter hyperintensities, clasmatodendrosis and gliovascular abnormalities in ageing and post-stroke dementia. *Brain,* 139**,** 242-58.

CHEN, J. J., WIECKOWSKA, M., MEYER, E. & PIKE, G. B. 2008. Cerebral blood flow measurement using fMRI and PET: a cross-validation study. *Int J Biomed Imaging,* 2008**,** 516359.

CHEN, P. C., VARGAS, M. R., PANI, A. K., SMEYNE, R. J., JOHNSON, D. A., KAN, Y. W. & JOHNSON, J. A. 2009. Nrf2-mediated neuroprotection in the MPTP mouse model of Parkinson's disease: Critical role for the astrocyte. *Proc Natl Acad Sci U S A,* 106**,** 2933-8.

CHITU, V., GOKHAN, S., NANDI, S., MEHLER, M. F. & STANLEY, E. R. 2016. Emerging Roles for CSF-1 Receptor and its Ligands in the Nervous System. *Trends Neurosci,* 39**,** 378-393.

CHOI, J. Y., CUI, Y. & KIM, B. G. 2015. Interaction between hypertension and cerebral hypoperfusion in the development of cognitive dysfunction and white matter pathology in rats. *Neuroscience,* 303**,** 115-25.

COLTMAN, R., SPAIN, A., TSENKINA, Y., FOWLER, J. H., SMITH, J., SCULLION, G., ALLERHAND, M., SCOTT, F., KALARIA, R. N., IHARA, M., DAUMAS, S., DEARY, I. J., WOOD, E., MCCULLOCH, J. & HORSBURGH, K. 2011. Selective white matter pathology induces a specific impairment in spatial working memory. *Neurobiol Aging,* 32**,** 2324.e7-12.

CONWAY, J. G., MCDONALD, B., PARHAM, J., KEITH, B., RUSNAK, D. W., SHAW, E., JANSEN, M., LIN, P., PAYNE, A., CROSBY, R. M., JOHNSON, J. H., FRICK, L., LIN, M. H., DEPEE, S., TADEPALLI, S., VOTTA, B., JAMES, I., FULLER, K., CHAMBERS, T. J., KULL, F. C., CHAMBERLAIN, S. D. & HUTCHINS, J. T. 2005. Inhibition of colony-stimulating-factor-1 signaling in vivo with the orally bioavailable cFMS kinase inhibitor GW2580. *Proc Natl Acad Sci U S A,* 102**,** 16078-83.

CRESPO, O., KANG, S. C., DANEMAN, R., LINDSTROM, T. M., HO, P. P., SOBEL, R. A., STEINMAN, L. & ROBINSON, W. H. 2011. Tyrosine kinase inhibitors ameliorate autoimmune encephalomyelitis in a mouse model of multiple sclerosis. *J Clin Immunol,* 31**,** 1010-20.

CUADRADO, A. 2016. NRF2 in neurodegenerative diseases. *Current Opinion in Toxicology,* 1**,** 46-53.

CUADRADO, A., MARTIN-MOLDES, Z., YE, J. & LASTRES-BECKER, I. 2014. Transcription factors NRF2 and NF-kappaB are coordinated effectors of the Rho family, GTP-binding protein RAC1 during inflammation. *J Biol Chem,* 289**,** 15244-58.

CUI, Y., MA, S., ZHANG, C., LI, D., YANG, B., LV, P., XING, Q., HUANG, T., YANG, G. L., CAO, W. & GUAN, F. 2017. Pharmacological activation of the Nrf2 pathway by 3H-1, 2-dithiole-3-thione is neuroprotective in a mouse model of Alzheimer disease. *Behav Brain Res*.

DAGHER, N. N., NAJAFI, A. R., KAYALA, K. M., ELMORE, M. R., WHITE, T. E., MEDEIROS, R., WEST, B. L. & GREEN, K. N. 2015. Colony-stimulating factor 1 receptor inhibition prevents microglial plaque association and improves cognition in 3xTg-AD mice. *J Neuroinflammation,* 12**,** 139.

DE GROOT, J. C., DE LEEUW, F. E., OUDKERK, M., VAN GIJN, J., HOFMAN, A., JOLLES, J. & BRETELER, M. M. 2000. Cerebral white matter lesions and cognitive function: the Rotterdam Scan Study. *Ann Neurol,* 47**,** 145-51.

DE LA TORRE, J. C. 2012. Cardiovascular Risk Factors Promote Brain Hypoperfusion Leading to Cognitive Decline and Dementia. *Cardiovasc Psychiatry Neurol,* 2012.
DE LA TORRE, J. C. 2016. Cerebral Perfusion Enhancing Interventions: A New Strategy for the Prevention of Alzheimer Dementia. *Brain Pathol,* 26**,** 618-31.
DE PASQUALE, R., BECKHAUSER, T. F., HERNANDES, M. S. & GIORGETTI BRITTO, L. R. 2014. LTP and LTD in the visual cortex require the activation of NOX2. *J Neurosci,* 34**,** 12778-87.
DICHGANS, M. & LEYS, D. 2017. Vascular Cognitive Impairment. *Circ Res,* 120**,** 573-591.
DINKOVA-KOSTOVA, A. T., KOSTOV, R. V. & KAZANTSEV, A. G. 2018. The role of Nrf2 signaling in counteracting neurodegenerative diseases. *Febs j*.
DONG, Y. F., KATAOKA, K., TOYAMA, K., SUETA, D., KOIBUCHI, N., YAMAMOTO, E., YATA, K., TOMIMOTO, H., OGAWA, H. & KIM-MITSUYAMA, S. 2011. Attenuation of brain damage and cognitive impairment by direct renin inhibition in mice with chronic cerebral hypoperfusion. *Hypertension,* 58**,** 635-42.
DOWELL, J. A. & JOHNSON, J. A. 2013. Mechanisms of Nrf2 protection in astrocytes as identified by quantitative proteomics and siRNA screening. *PLoS One,* 8**,** e70163.
DRAHEIM, T., LIESSEM, A., SCHELD, M., WILMS, F., WEISSFLOG, M., DENECKE, B., KENSLER, T. W., ZENDEDEL, A., BEYER, C., KIPP, M., WRUCK, C. J., FRAGOULIS, A. & CLARNER, T. 2016. Activation of the astrocytic Nrf2/ARE system ameliorates the formation of demyelinating lesions in a multiple sclerosis animal model. *Glia,* 64**,** 2219-2230.
DRINGEN, R. 2000. Metabolism and functions of glutathione in brain. *Prog Neurobiol,* 62**,** 649-71.
DRUMMOND, G. R., SELEMIDIS, S., GRIENDLING, K. K. & SOBEY, C. G. 2011. Combating oxidative stress in vascular disease: NADPH oxidases as therapeutic targets. *Nat Rev Drug Discov,* 10**,** 453-71.
DU, S. Q., WANG, X. R., XIAO, L. Y., TU, J. F., ZHU, W., HE, T. & LIU, C. Z. 2016. Molecular Mechanisms of Vascular Dementia: What Can Be Learned from Animal Models of Chronic Cerebral Hypoperfusion? *Mol Neurobiol*.
DUCRUET, A. F., ZACHARIA, B. E., SOSUNOV, S. A., GIGANTE, P. R., YEH, M. L., GORSKI, J. W., OTTEN, M. L., HWANG, R. Y., DEROSA, P. A., HICKMAN, Z. L., SERGOT, P. & CONNOLLY, E. S., JR. 2012. Complement inhibition promotes endogenous neurogenesis and sustained anti-inflammatory neuroprotection following reperfused stroke. *PLoS One,* 7**,** e38664.
DUNCOMBE, J., KITAMURA, A., HASE, Y., IHARA, M., KALARIA, R. N. & HORSBURGH, K. 2017. Chronic cerebral hypoperfusion: a key mechanism leading to vascular cognitive impairment and dementia. Closing the translational gap between rodent models and human vascular cognitive impairment and dementia. *Clin Sci (Lond),* 131**,** 2451-2468.
DUNCOMBE, J., LENNEN, R. J., JANSEN, M. A., MARSHALL, I., WARDLAW, J. M. & HORSBURGH, K. 2016. Ageing causes prominent neurovascular dysfunction associated with loss of astrocytic contacts and gliosis. *Neuropathol Appl Neurobiol*.
EIKELENBOOM, P. & STAM, F. C. 1982. Immunoglobulins and complement factors in senile plaques. An immunoperoxidase study. *Acta Neuropathol,* 57**,** 239-42.
ELTZSCHIG, H. K. & CARMELIET, P. 2011. Hypoxia and inflammation. *N Engl J Med,* 364**,** 656-65.
EZZATI, A., WANG, C., LIPTON, R. B., ALTSCHUL, D., KATZ, M. J., DICKSON, D. W. & DERBY, C. A. 2017. Association Between Vascular Pathology and Rate

of Cognitive Decline Independent of Alzheimer's Disease Pathology. *J Am Geriatr Soc,* 65**,** 1836-1841.
FARACO, G., PARK, L., ANRATHER, J. & IADECOLA, C. 2017. Brain perivascular macrophages: characterization and functional roles in health and disease. *J Mol Med (Berl),* 95**,** 1143-1152.
FARKAS, E., DONKA, G., DE VOS, R. A., MIHALY, A., BARI, F. & LUITEN, P. G. 2004. Experimental cerebral hypoperfusion induces white matter injury and microglial activation in the rat brain. *Acta Neuropathol,* 108**,** 57-64.
FERNANDO, M. S., SIMPSON, J. E., MATTHEWS, F., BRAYNE, C., LEWIS, C. E., BARBER, R., KALARIA, R. N., FORSTER, G., ESTEVES, F., WHARTON, S. B., SHAW, P. J., O'BRIEN, J. T. & INCE, P. G. 2006. White matter lesions in an unselected cohort of the elderly: molecular pathology suggests origin from chronic hypoperfusion injury. *Stroke,* 37**,** 1391-8.
FILLEY, C. M. & FIELDS, R. D. 2016. White matter and cognition: making the connection. *J Neurophysiol,* 116**,** 2093-2104.
FOWLER, J. H., MCQUEEN, J., HOLLAND, P. R., MANSO, Y., MARANGONI, M., SCOTT, F., CHISHOLM, E., SCANNEVIN, R. H., HARDINGHAM, G. E. & HORSBURGH, K. 2017. Dimethyl fumarate improves white matter function following severe hypoperfusion: Involvement of microglia/macrophages and inflammatory mediators. *J Cereb Blood Flow Metab***,** 271678x17713105.
FRAGOULIS, A., SIEGL, S., FENDT, M., JANSEN, S., SOPPA, U., BRANDENBURG, L. O., PUFE, T., WEIS, J. & WRUCK, C. J. 2017. Oral administration of methysticin improves cognitive deficits in a mouse model of Alzheimer's disease. *Redox Biol,* 12**,** 843-853.
GACKOWSKI, D., ROZALSKI, R., SIOMEK, A., DZIAMAN, T., NICPON, K., KLIMARCZYK, M., ARASZKIEWICZ, A. & OLINSKI, R. 2008. Oxidative stress and oxidative DNA damage is characteristic for mixed Alzheimer disease/vascular dementia. *J Neurol Sci,* 266**,** 57-62.
GAMEIRO, I., MICHALSKA, P., TENTI, G., CORES, A., BUENDIA, I., ROJO, A. I., GEORGAKOPOULOS, N. D., HERNANDEZ-GUIJO, J. M., TERESA RAMOS, M., WELLS, G., LOPEZ, M. G., CUADRADO, A., MENENDEZ, J. C. & LEON, R. 2017. Discovery of the first dual GSK3beta inhibitor/Nrf2 inducer. A new multitarget therapeutic strategy for Alzheimer's disease. *Sci Rep,* 7**,** 45701.
GAN, L., VARGAS, M. R., JOHNSON, D. A. & JOHNSON, J. A. 2012. Astrocyte-specific overexpression of Nrf2 delays motor pathology and synuclein aggregation throughout the CNS in the alpha-synuclein mutant (A53T) mouse model. *J Neurosci,* 32**,** 17775-87.
GAO, L., ZIMMERMAN, M. C., BISWAL, S. & ZUCKER, I. H. 2017. Selective Nrf2 Gene Deletion in the Rostral Ventrolateral Medulla Evokes Hypertension and Sympathoexcitation in Mice. *Hypertension,* 69**,** 1198-1206.
GEOVANINI, G. R. & LIBBY, P. 2018. Atherosclerosis and inflammation: overview and updates. *Clin Sci (Lond),* 132**,** 1243-1252.
GERBER, Y. N., SAINT-MARTIN, G. P., BRINGUIER, C. M., BARTOLAMI, S., GOZE-BAC, C., NORISTANI, H. N. & PERRIN, F. E. 2018. CSF1R Inhibition Reduces Microglia Proliferation, Promotes Tissue Preservation and Improves Motor Recovery After Spinal Cord Injury. *Front Cell Neurosci,* 12**,** 368.
GOMEZ-NICOLA, D., FRANSEN, N. L., SUZZI, S. & PERRY, V. H. 2013. Regulation of microglial proliferation during chronic neurodegeneration. *J Neurosci,* 33**,** 2481-93.
GOPAL, S., MIKULSKIS, A., GOLD, R., FOX, R. J., DAWSON, K. T. & AMARAVADI, L. 2017. Evidence of activation of the Nrf2 pathway in multiple sclerosis patients treated with delayed-release dimethyl fumarate in the Phase 3 DEFINE and CONFIRM studies. *Mult Scler***,** 1352458517690617.

GORELICK, P. B., SCUTERI, A., BLACK, S. E., DECARLI, C., GREENBERG, S. M., IADECOLA, C., LAUNER, L. J., LAURENT, S., LOPEZ, O. L., NYENHUIS, D., PETERSEN, R. C., SCHNEIDER, J. A., TZOURIO, C., ARNETT, D. K., BENNETT, D. A., CHUI, H. C., HIGASHIDA, R. T., LINDQUIST, R., NILSSON, P. M., ROMAN, G. C., SELLKE, F. W. & SESHADRI, S. 2011. Vascular Contributions to Cognitive Impairment and Dementia. 42**,** 2672-713.

GRABERT, K., MICHOEL, T., KARAVOLOS, M. H., CLOHISEY, S., BAILLIE, J. K., STEVENS, M. P., FREEMAN, T. C., SUMMERS, K. M. & MCCOLL, B. W. 2016. Microglial brain region-dependent diversity and selective regional sensitivities to aging. *Nat Neurosci,* 19**,** 504-16.

GRANADO, N., LASTRES-BECKER, I., ARES-SANTOS, S., OLIVA, I., MARTIN, E., CUADRADO, A. & MORATALLA, R. 2011. Nrf2 deficiency potentiates methamphetamine-induced dopaminergic axonal damage and gliosis in the striatum. *Glia,* 59**,** 1850-63.

GREMMELS, H., DE JONG, O. G., HAZENBRINK, D. H., FLEDDERUS, J. O. & VERHAAR, M. C. 2017. The Transcription Factor Nrf2 Protects Angiogenic Capacity of Endothelial Colony-Forming Cells in High-Oxygen Radical Stress Conditions. *Stem Cells Int,* 2017**,** 4680612.

GUO, H., ITOH, Y., TORIUMI, H., YAMADA, S., TOMITA, Y., HOSHINO, H. & SUZUKI, N. 2011. Capillary remodeling and collateral growth without angiogenesis after unilateral common carotid artery occlusion in mice. *Microcirculation,* 18**,** 221-7.

GUO, Y., YU, S., ZHANG, C. & KONG, A. T. 2015. Epigenetic regulation of Keap1-Nrf2 signaling. *Free Radic Biol Med*.

GUSTAW-ROTHENBERG, K., KOWALCZUK, K. & STRYJECKA-ZIMMER, M. 2010. Lipids' peroxidation markers in Alzheimer's disease and vascular dementia. *Geriatr Gerontol Int,* 10**,** 161-6.

HACHINSKI, V., IADECOLA, C., PETERSEN, R. C., BRETELER, M. M., NYENHUIS, D. L., BLACK, S. E., POWERS, W. J., DECARLI, C., MERINO, J. G., KALARIA, R. N., VINTERS, H. V., HOLTZMAN, D. M., ROSENBERG, G. A., WALLIN, A., DICHGANS, M., MARLER, J. R. & LEBLANC, G. G. 2006. National Institute of Neurological Disorders and Stroke-Canadian Stroke Network vascular cognitive impairment harmonization standards. *Stroke,* 37**,** 2220-41.

HAINSWORTH, A. H., ALLAN, S. M., BOLTZE, J., CUNNINGHAM, C., FARRIS, C., HEAD, E., IHARA, M., ISAACS, J. D., KALARIA, R. N., LESNIK OBERSTEIN, S. A., MOSS, M. B., NITZSCHE, B., ROSENBERG, G. A., RUTTEN, J. W., SALKOVIC-PETRISIC, M. & TROEN, A. M. 2017. Translational models for vascular cognitive impairment: a review including larger species. *BMC Med,* 15**,** 16.

HARDIMAN, O. & VAN DEN BERG, L. H. 2017. Edaravone: a new treatment for ALS on the horizon? *Lancet Neurol,* 16**,** 490-491.

HARRIS, J. J. & ATTWELL, D. 2012. The energetics of CNS white matter. *J Neurosci,* 32**,** 356-71.

HASE, Y., HORSBURGH, K., IHARA, M. & KALARIA, R. N. 2017. White Matter Degeneration in Vascular and Other Ageing-Related Dementias. *J Neurochem*.

HATTORI, Y., ENMI, J., IGUCHI, S., SAITO, S., YAMAMOTO, Y., NAGATSUKA, K., IIDA, H. & IHARA, M. 2016. Substantial Reduction of Parenchymal Cerebral Blood Flow in Mice with Bilateral Common Carotid Artery Stenosis. *Sci Rep,* 6**,** 32179.

HATTORI, Y., ENMI, J., KITAMURA, A., YAMAMOTO, Y., SAITO, S., TAKAHASHI, Y., IGUCHI, S., TSUJI, M., YAMAHARA, K., NAGATSUKA, K., IIDA, H. &

IHARA, M. 2015. A novel mouse model of subcortical infarcts with dementia. *J Neurosci,* 35**,** 3915-28.
HEIMAN, M., KULICKE, R., FENSTER, R. J., GREENGARD, P. & HEINTZ, N. 2014. Cell type-specific mRNA purification by translating ribosome affinity purification (TRAP). *Nat Protoc,* 9**,** 1282-91.
HEISS, W. D., ROSENBERG, G. A., THIEL, A., BERLOT, R. & DE REUCK, J. 2016. Neuroimaging in vascular cognitive impairment: a state-of-the-art review. *BMC Med,* 14**,** 174.
HIRAO, K., OHNISHI, T., HIRATA, Y., YAMASHITA, F., MORI, T., MORIGUCHI, Y., MATSUDA, H., NEMOTO, K., IMABAYASHI, E., YAMADA, M., IWAMOTO, T., ARIMA, K. & ASADA, T. 2005. The prediction of rapid conversion to Alzheimer's disease in mild cognitive impairment using regional cerebral blood flow SPECT. *Neuroimage,* 28**,** 1014-21.
HOLLAND, P. R., BASTIN, M. E., JANSEN, M. A., MERRIFIELD, G. D., COLTMAN, R. B., SCOTT, F., NOWERS, H., KHALLOUT, K., MARSHALL, I., WARDLAW, J. M., DEARY, I. J., MCCULLOCH, J. & HORSBURGH, K. 2011. MRI is a sensitive marker of subtle white matter pathology in hypoperfused mice. *Neurobiol Aging,* 32**,** 2325.e1-6.
HOLLAND, P. R., SEARCY, J. L., SALVADORES, N., SCULLION, G., CHEN, G., LAWSON, G., SCOTT, F., BASTIN, M. E., IHARA, M., KALARIA, R., WOOD, E. R., SMITH, C., WARDLAW, J. M. & HORSBURGH, K. 2015. Gliovascular disruption and cognitive deficits in a mouse model with features of small vessel disease. *J Cereb Blood Flow Metab,* 35**,** 1005-14.
HOSSMANN, K. A. 2006. Pathophysiology and therapy of experimental stroke. *Cell Mol Neurobiol,* 26**,** 1057-83.
HOWELL, O. W., RUNDLE, J. L., GARG, A., KOMADA, M., BROPHY, P. J. & REYNOLDS, R. 2010. Activated microglia mediate axoglial disruption that contributes to axonal injury in multiple sclerosis. *J Neuropathol Exp Neurol,* 69**,** 1017-1033.
HUANG, Y., MAO, Y., LI, H., SHEN, G. & NAN, G. 2018. Knockdown of Nrf2 inhibits angiogenesis by downregulating VEGF expression through PI3K/Akt signaling pathway in cerebral microvascular endothelial cells under hypoxic conditions. *Biochem Cell Biol,* 96**,** 475-482.
HUBBS, A. F., BENKOVIC, S. A., MILLER, D. B., O'CALLAGHAN, J. P., BATTELLI, L., SCHWEGLER-BERRY, D. & MA, Q. 2007. Vacuolar leukoencephalopathy with widespread astrogliosis in mice lacking transcription factor Nrf2. *Am J Pathol,* 170**,** 2068-76.
HUNG, S. S. C., KHAN, S., LO, C. Y., HEWITT, A. W. & WONG, R. C. B. 2017. Drug discovery using induced pluripotent stem cell models of neurodegenerative and ocular diseases. *Pharmacol Ther,* 177**,** 32-43.
IADECOLA, C. 2013. The pathobiology of vascular dementia. *Neuron,* 80**,** 844-66.
IADECOLA, C. & NEDERGAARD, M. 2007. Glial regulation of the cerebral microvasculature. *Nat Neurosci,* 10**,** 1369-76.
IHARA, M. & TOMIMOTO, H. 2011. Lessons from a mouse model characterizing features of vascular cognitive impairment with white matter changes. *J Aging Res,* 2011**,** 978761.
INNAMORATO, N. G., JAZWA, A., ROJO, A. I., GARCIA, C., FERNANDEZ-RUIZ, J., GROCHOT-PRZECZEK, A., STACHURSKA, A., JOZKOWICZ, A., DULAK, J. & CUADRADO, A. 2010. Different susceptibility to the Parkinson's toxin MPTP in mice lacking the redox master regulator Nrf2 or its target gene heme oxygenase-1. *PLoS One,* 5**,** e11838.
INZITARI, D., PRACUCCI, G., POGGESI, A., CARLUCCI, G., BARKHOF, F., CHABRIAT, H., ERKINJUNTTI, T., FAZEKAS, F., FERRO, J. M.,

HENNERICI, M., LANGHORNE, P., O'BRIEN, J., SCHELTENS, P., VISSER, M. C., WAHLUND, L. O., WALDEMAR, G., WALLIN, A. & PANTONI, L. 2009. Changes in white matter as determinant of global functional decline in older independent outpatients: three year follow-up of LADIS (leukoaraiosis and disability) study cohort. *Bmj,* 339**,** b2477.

IRVINE, K. M., ANDREWS, M. R., FERNANDEZ-ROJO, M. A., SCHRODER, K., BURNS, C. J., SU, S., WILKS, A. F., PARTON, R. G., HUME, D. A. & SWEET, M. J. 2009. Colony-stimulating factor-1 (CSF-1) delivers a proatherogenic signal to human macrophages. *J Leukoc Biol,* 85**,** 278-88.

ISHII, T., ITOH, K., TAKAHASHI, S., SATO, H., YANAGAWA, T., KATOH, Y., BANNAI, S. & YAMAMOTO, M. 2000. Transcription factor Nrf2 coordinately regulates a group of oxidative stress-inducible genes in macrophages. *J Biol Chem,* 275**,** 16023-9.

ITOH, K., CHIBA, T., TAKAHASHI, S., ISHII, T., IGARASHI, K., KATOH, Y., OYAKE, T., HAYASHI, N., SATOH, K., HATAYAMA, I., YAMAMOTO, M. & NABESHIMA, Y. 1997. An Nrf2/small Maf heterodimer mediates the induction of phase II detoxifying enzyme genes through antioxidant response elements. *Biochem Biophys Res Commun,* 236**,** 313-22.

ITOH, K., WAKABAYASHI, N., KATOH, Y., ISHII, T., IGARASHI, K., ENGEL, J. D. & YAMAMOTO, M. 1999. Keap1 represses nuclear activation of antioxidant responsive elements by Nrf2 through binding to the amino-terminal Neh2 domain. *Genes Dev,* 13**,** 76-86.

ITOH, K., WAKABAYASHI, N., KATOH, Y., ISHII, T., O'CONNOR, T. & YAMAMOTO, M. 2003. Keap1 regulates both cytoplasmic-nuclear shuttling and degradation of Nrf2 in response to electrophiles. *Genes Cells,* 8**,** 379-91.

ITURRIA-MEDINA, Y., SOTERO, R. C., TOUSSAINT, P. J., MATEOS-PEREZ, J. M. & EVANS, A. C. 2016. Early role of vascular dysregulation on late-onset Alzheimer's disease based on multifactorial data-driven analysis. *Nat Commun,* 7**,** 11934.

JAKEL, R. J., TOWNSEND, J. A., KRAFT, A. D. & JOHNSON, J. A. 2007. Nrf2-mediated protection against 6-hydroxydopamine. *Brain Res,* 1144**,** 192-201.

JANEWAY, C. J., TRAVERS, P. & WALPORT, M. E. A. 2001. *Immunobiology: The Immune System in Health and Disease. 5th edition,* New York Garland Science.

JELLINGER, K. A. 2013. Pathology and pathogenesis of vascular cognitive impairment-a critical update. *Front Aging Neurosci,* 5**,** 17.

JI, X., WANG, H., ZHU, J., ZHU, L., PAN, H., LI, W., ZHOU, Y., CONG, Z., YAN, F. & CHEN, S. 2014. Knockdown of Nrf2 suppresses glioblastoma angiogenesis by inhibiting hypoxia-induced activation of HIF-1alpha. *Int J Cancer,* 135**,** 574-84.

JIN, W., JIA, Y., HUANG, L., WANG, T., WANG, H., DONG, Y., ZHANG, H., FAN, M. & LV, P. 2014. Lipoxin A4 methyl ester ameliorates cognitive deficits induced by chronic cerebral hypoperfusion through activating ERK/Nrf2 signaling pathway in rats. *Pharmacol Biochem Behav,* 124**,** 145-52.

JIN, W. N., SHI, S. X., LI, Z., LI, M., WOOD, K., GONZALES, R. J. & LIU, Q. 2017. Depletion of microglia exacerbates postischemic inflammation and brain injury. *J Cereb Blood Flow Metab,* 37**,** 2224-2236.

JIWA, N. S., GARRARD, P. & HAINSWORTH, A. H. 2010. Experimental models of vascular dementia and vascular cognitive impairment: a systematic review. *J Neurochem,* 115**,** 814-28.

JOHN LIN, C. C., YU, K., HATCHER, A., HUANG, T. W., LEE, H. K., CARLSON, J., WESTON, M. C., CHEN, F., ZHANG, Y., ZHU, W., MOHILA, C. A., AHMED, N., PATEL, A. J., ARENKIEL, B. R., NOEBELS, J. L., CREIGHTON, C. J. &

DENEEN, B. 2017. Identification of diverse astrocyte populations and their malignant analogs. *Nat Neurosci*.

JOHNS, T. G. & BERNARD, C. C. 1997. Binding of complement component Clq to myelin oligodendrocyte glycoprotein: a novel mechanism for regulating CNS inflammation. *Mol Immunol,* 34**,** 33-8.

JOHNSON, D. A., AMIRAHMADI, S., WARD, C., FABRY, Z. & JOHNSON, J. A. 2010. The absence of the pro-antioxidant transcription factor Nrf2 exacerbates experimental autoimmune encephalomyelitis. *Toxicol Sci,* 114**,** 237-46.

JOHNSON, D. A. & JOHNSON, J. A. 2015. Nrf2--a therapeutic target for the treatment of neurodegenerative diseases. *Free Radic Biol Med,* 88**,** 253-67.

JOSHI, G., GAN, K. A., JOHNSON, D. A. & JOHNSON, J. A. 2015. Increased Alzheimer's disease-like pathology in the APP/ PS1DeltaE9 mouse model lacking Nrf2 through modulation of autophagy. *Neurobiol Aging,* 36**,** 664-79.

JOSHI, G. & JOHNSON, J. A. 2012. The Nrf2-ARE pathway: a valuable therapeutic target for the treatment of neurodegenerative diseases. *Recent Pat CNS Drug Discov,* 7**,** 218-29.

KALBACK, W., ESH, C., CASTANO, E. M., RAHMAN, A., KOKJOHN, T., LUEHRS, D. C., SUE, L., CISNEROS, R., GERBER, F., RICHARDSON, C., BOHRMANN, B., WALKER, D. G., BEACH, T. G. & ROHER, A. E. 2004. Atherosclerosis, vascular amyloidosis and brain hypoperfusion in the pathogenesis of sporadic Alzheimer's disease. *Neurol Res,* 26**,** 525-39.

KANNINEN, K., HEIKKINEN, R., MALM, T., ROLOVA, T., KUHMONEN, S., LEINONEN, H., YLA-HERTTUALA, S., TANILA, H., LEVONEN, A. L., KOISTINAHO, M. & KOISTINAHO, J. 2009. Intrahippocampal injection of a lentiviral vector expressing Nrf2 improves spatial learning in a mouse model of Alzheimer's disease. *Proc Natl Acad Sci U S A,* 106**,** 16505-10.

KAPASI, A., DECARLI, C. & SCHNEIDER, J. A. 2017. Impact of multiple pathologies on the threshold for clinically overt dementia. *Acta Neuropathol,* 134**,** 171-186.

KILKENNY, C., BROWNE, W. J., CUTHILL, I. C., EMERSON, M. & ALTMAN, D. G. 2010. Improving bioscience research reporting: the ARRIVE guidelines for reporting animal research. *PLoS Biol,* 8**,** e1000412.

KIM, H. A., MILLER, A. A., DRUMMOND, G. R., THRIFT, A. G., ARUMUGAM, T. V., PHAN, T. G., SRIKANTH, V. K. & SOBEY, C. G. 2012. Vascular cognitive impairment and Alzheimer's disease: role of cerebral hypoperfusion and oxidative stress. *Naunyn Schmiedebergs Arch Pharmacol,* 385**,** 953-9.

KISLER, K., NELSON, A. R., MONTAGNE, A. & ZLOKOVIC, B. V. 2017. Cerebral blood flow regulation and neurovascular dysfunction in Alzheimer disease. *Nat Rev Neurosci*.

KITAMURA, A., FUJITA, Y., OISHI, N., KALARIA, R. N., WASHIDA, K., MAKI, T., OKAMOTO, Y., HASE, Y., YAMADA, M., TAKAHASHI, J., ITO, H., TOMIMOTO, H., FUKUYAMA, H., TAKAHASHI, R. & IHARA, M. 2012. Selective white matter abnormalities in a novel rat model of vascular dementia. *Neurobiol Aging,* 33**,** 1012.e25-35.

KITAMURA, A., MANSO, Y., DUNCOMBE, J., SEARCY, J., KOUDELKA, J., BINNIE, M., WEBSTER, S., LENNEN, R., JANSEN, M., MARSHALL, I., IHARA, M., KALARIA, R. N. & HORSBURGH, K. 2017. Long-term cilostazol treatment reduces gliovascular damage and memory impairment in a mouse model of chronic cerebral hypoperfusion. *Sci Rep,* 7**,** 4299.

KOBAYASHI, E. H., SUZUKI, T., FUNAYAMA, R., NAGASHIMA, T., HAYASHI, M., SEKINE, H., TANAKA, N., MORIGUCHI, T., MOTOHASHI, H., NAKAYAMA, K. & YAMAMOTO, M. 2016. Nrf2 suppresses macrophage inflammatory response by blocking proinflammatory cytokine transcription. *Nat Commun,* 7**,** 11624.

KOBAYASHI, M. & YAMAMOTO, M. 2006. Nrf2-Keap1 regulation of cellular defense mechanisms against electrophiles and reactive oxygen species. *Adv Enzyme Regul,* 46**,** 113-40.

KOIZUMI, K., HATTORI, Y., AHN, S. J., BUENDIA, I., CIACCIARELLI, A., UEKAWA, K., WANG, G., HILLER, A., ZHAO, L., VOSS, H. U., PAUL, S. M., SCHAFFER, C., PARK, L. & IADECOLA, C. 2018. Apoepsilon4 disrupts neurovascular regulation and undermines white matter integrity and cognitive function. *Nat Commun,* 9**,** 3816.

KOVAC, S., ANGELOVA, P. R., HOLMSTROM, K. M., ZHANG, Y., DINKOVA-KOSTOVA, A. T. & ABRAMOV, A. Y. 2015. Nrf2 regulates ROS production by mitochondria and NADPH oxidase. *Biochim Biophys Acta,* 1850**,** 794-801.

KRAFT, A. D., JOHNSON, D. A. & JOHNSON, J. A. 2004. Nuclear factor E2-related factor 2-dependent antioxidant response element activation by tert-butylhydroquinone and sulforaphane occurring preferentially in astrocytes conditions neurons against oxidative insult. *J Neurosci,* 24**,** 1101-12.

LAPASH DANIELS, C. M., AUSTIN, E. V., ROCKNEY, D. E., JACKA, E. M., HAGEMANN, T. L., JOHNSON, D. A., JOHNSON, J. A. & MESSING, A. 2012. Beneficial Effects of Nrf2 Overexpression in a Mouse Model of Alexander Disease. *J Neurosci,* 32**,** 10507-15.

LASTRES-BECKER, I., ULUSOY, A., INNAMORATO, N. G., SAHIN, G., RABANO, A., KIRIK, D. & CUADRADO, A. 2012. alpha-Synuclein expression and Nrf2 deficiency cooperate to aggravate protein aggregation, neuronal death and inflammation in early-stage Parkinson's disease. *Hum Mol Genet,* 21**,** 3173-92.

LAWRENCE, A. J., PATEL, B., MORRIS, R. G., MACKINNON, A. D., RICH, P. M., BARRICK, T. R. & MARKUS, H. S. 2013. Mechanisms of cognitive impairment in cerebral small vessel disease: multimodal MRI results from the St George's cognition and neuroimaging in stroke (SCANS) study. *PLoS One,* 8**,** e61014.

LAWRENCE, T. 2009. The Nuclear Factor NF-κB Pathway in Inflammation. *Cold Spring Harb Perspect Biol.*

LEE, J. M., CALKINS, M. J., CHAN, K., KAN, Y. W. & JOHNSON, J. A. 2003. Identification of the NF-E2-related factor-2-dependent genes conferring protection against oxidative stress in primary cortical astrocytes using oligonucleotide microarray analysis. *J Biol Chem,* 278**,** 12029-38.

LI, J., ZHANG, C., XING, Y., JANICKI, J. S., YAMAMOTO, M., WANG, X. L., TANG, D. Q. & CUI, T. 2011. Up-regulation of p27(kip1) contributes to Nrf2-mediated protection against angiotensin II-induced cardiac hypertrophy. *Cardiovasc Res,* 90**,** 315-24.

LI, J., ZHANG, L., CHU, Y., NAMAKA, M., DENG, B., KONG, J. & BI, X. 2016a. Astrocytes in Oligodendrocyte Lineage Development and White Matter Pathology. *Front Cell Neurosci,* 10**,** 119.

LI, L., PAN, H., WANG, H., LI, X., BU, X., WANG, Q., GAO, Y., WEN, G., ZHOU, Y., CONG, Z., YANG, Y., TANG, C. & LIU, Z. 2016b. Interplay between VEGF and Nrf2 regulates angiogenesis due to intracranial venous hypertension. *Sci Rep,* 6**,** 37338.

LI, L., WILLETS, R. S., POLIDORI, M. C., STAHL, W., NELLES, G., SIES, H. & GRIFFITHS, H. R. 2010. Oxidative LDL modification is increased in vascular dementia and is inversely associated with cognitive performance. *Free Radic Res,* 44**,** 241-8.

LIAO, J. K. 2013. Linking endothelial dysfunction with endothelial cell activation. *J Clin Invest,* 123**,** 540-1.

LIDDELL, J. R. 2017. Are Astrocytes the Predominant Cell Type for Activation of Nrf2 in Aging and Neurodegeneration? *Antioxidants (Basel),* 6.

LIDDELOW, S. A., GUTTENPLAN, K. A., CLARKE, L. E., BENNETT, F. C., BOHLEN, C. J., SCHIRMER, L., BENNETT, M. L., MUNCH, A. E., CHUNG, W. S., PETERSON, T. C., WILTON, D. K., FROUIN, A., NAPIER, B. A., PANICKER, N., KUMAR, M., BUCKWALTER, M. S., ROWITCH, D. H., DAWSON, V. L., DAWSON, T. M., STEVENS, B. & BARRES, B. A. 2017. Neurotoxic reactive astrocytes are induced by activated microglia. *Nature*.

LIN, Y. F., SMITH, A. V., ASPELUND, T., BETENSKY, R. A., SMOLLER, J. W., GUDNASON, V., LAUNER, L. J. & BLACKER, D. 2018. Genetic overlap between vascular pathologies and Alzheimer's dementia and potential causal mechanisms. *Alzheimers Dement*.

LINKER, R. A., LEE, D. H., RYAN, S., VAN DAM, A. M., CONRAD, R., BISTA, P., ZENG, W., HRONOWSKY, X., BUKO, A., CHOLLATE, S., ELLRICHMANN, G., BRUCK, W., DAWSON, K., GOELZ, S., WIESE, S., SCANNEVIN, R. H., LUKASHEV, M. & GOLD, R. 2011. Fumaric acid esters exert neuroprotective effects in neuroinflammation via activation of the Nrf2 antioxidant pathway. *Brain,* 134**,** 678-92.

LIU, H. & ZHANG, J. 2012. Cerebral hypoperfusion and cognitive impairment: the pathogenic role of vascular oxidative stress. *Int J Neurosci,* 122**,** 494-9.

LIU, H., ZHANG, J. J., LI, X., YANG, Y., XIE, X. F. & HU, K. 2015. Post-occlusion administration of sodium butyrate attenuates cognitive impairment in a rat model of chronic cerebral hypoperfusion. *Pharmacol Biochem Behav,* 135**,** 53-9.

LIU, Q., HE, S., GROYSMAN, L., SHAKED, D., RUSSIN, J., SCOTTON, T. C., CEN, S. & MACK, W. J. 2013. White matter injury due to experimental chronic cerebral hypoperfusion is associated with C5 deposition. *PLoS One,* 8**,** e84802.

LLOYD, A. F., DAVIES, C. L. & MIRON, V. E. 2017. Microglia: origins, homeostasis, and roles in myelin repair. *Curr Opin Neurobiol,* 47**,** 113-120.

LUNDGAARD, I., OSORIO, M. J., KRESS, B. T., SANGGAARD, S. & NEDERGAARD, M. 2014. White matter astrocytes in health and disease. *Neuroscience,* 276**,** 161-73.

LUO, J., ELWOOD, F., BRITSCHGI, M., VILLEDA, S., ZHANG, H., DING, Z., ZHU, L., ALABSI, H., GETACHEW, R., NARASIMHAN, R., WABL, R., FAINBERG, N., JAMES, M. L., WONG, G., RELTON, J., GAMBHIR, S. S., POLLARD, J. W. & WYSS-CORAY, T. 2013. Colony-stimulating factor 1 receptor (CSF1R) signaling in injured neurons facilitates protection and survival. *J Exp Med,* 210**,** 157-72.

MAHAD, D. H., TRAPP, B. D. & LASSMANN, H. 2015. Pathological mechanisms in progressive multiple sclerosis. *Lancet Neurol,* 14**,** 183-93.

MAKI, T., IHARA, M., FUJITA, Y., NAMBU, T., MIYASHITA, K., YAMADA, M., WASHIDA, K., NISHIO, K., ITO, H., HARADA, H., YOKOI, H., ARAI, H., ITOH, H., NAKAO, K., TAKAHASHI, R. & TOMIMOTO, H. 2011. Angiogenic and vasoprotective effects of adrenomedullin on prevention of cognitive decline after chronic cerebral hypoperfusion in mice. *Stroke,* 42**,** 1122-8.

MANSO, Y., HOLLAND, P. R., KITAMURA, A., SZYMKOWIAK, S., DUNCOMBE, J., HENNESSY, E., SEARCY, J. L., MARANGONI, M., RANDALL, A. D., BROWN, J. T., MCCOLL, B. W. & HORSBURGH, K. 2017. Minocycline reduces microgliosis and improves subcortical white matter function in a model of cerebral vascular disease. *Glia*.

MAO, L., YANG, T., LI, X., LEI, X., SUN, Y., ZHAO, Y., ZHANG, W., GAO, Y., SUN, B. & ZHANG, F. 2018. Protective effects of sulforaphane in experimental vascular cognitive impairment: Contribution of the Nrf2 pathway. *J Cereb Blood Flow Metab***,** 271678x18764083.

MARCINIAK, E., FAIVRE, E., DUTAR, P., ALVES PIRES, C., DEMEYER, D., CAILLIEREZ, R., LALOUX, C., BUEE, L., BLUM, D. & HUMEZ, S. 2015. The Chemokine MIP-1alpha/CCL3 impairs mouse hippocampal synaptic transmission, plasticity and memory. *Sci Rep,* 5**,** 15862.

MARTINEZ-MURIANA, A., MANCUSO, R., FRANCOS-QUIJORNA, I., OLMOS-ALONSO, A., OSTA, R., PERRY, V. H., NAVARRO, X., GOMEZ-NICOLA, D. & LOPEZ-VALES, R. 2016. CSF1R blockade slows the progression of amyotrophic lateral sclerosis by reducing microgliosis and invasion of macrophages into peripheral nerves. *Sci Rep,* 6**,** 25663.

MASSAAD, C. A. & KLANN, E. 2011. Reactive oxygen species in the regulation of synaptic plasticity and memory. *Antioxid Redox Signal,* 14**,** 2013-54.

MAURER, M. & VON STEBUT, E. 2004. Macrophage inflammatory protein-1. *Int J Biochem Cell Biol,* 36**,** 1882-6.

MCQUEEN, J., REIMER, M. M., HOLLAND, P. R., MANSO, Y., MCLAUGHLIN, M., FOWLER, J. H. & HORSBURGH, K. 2014. Restoration of oligodendrocyte pools in a mouse model of chronic cerebral hypoperfusion. *PLoS One,* 9**,** e87227.

MIKI, K., ISHIBASHI, S., SUN, L., XU, H., OHASHI, W., KUROIWA, T. & MIZUSAWA, H. 2009. Intensity of chronic cerebral hypoperfusion determines white/gray matter injury and cognitive/motor dysfunction in mice. *J Neurosci Res,* 87**,** 1270-81.

MILLER, D. M., WANG, J. A., BUCHANAN, A. K. & HALL, E. D. 2014. Temporal and spatial dynamics of nrf2-antioxidant response elements mediated gene targets in cortex and hippocampus after controlled cortical impact traumatic brain injury in mice. *J Neurotrauma,* 31**,** 1194-201.

MINGARD, C., PAECH, F., BOUITBIR, J. & KRAHENBUHL, S. 2018. Mechanisms of toxicity associated with six tyrosine kinase inhibitors in human hepatocyte cell lines. *J Appl Toxicol,* 38**,** 418-431.

MIYAMOTO, N., MAKI, T., PHAM, L. D., HAYAKAWA, K., SEO, J. H., MANDEVILLE, E. T., MANDEVILLE, J. B., KIM, K. W., LO, E. H. & ARAI, K. 2013. Oxidative stress interferes with white matter renewal after prolonged cerebral hypoperfusion in mice. *Stroke,* 44**,** 3516-21.

MOI, P., CHAN, K., ASUNIS, I., CAO, A. & KAN, Y. W. 1994. Isolation of NF-E2-related factor 2 (Nrf2), a NF-E2-like basic leucine zipper transcriptional activator that binds to the tandem NF-E2/AP1 repeat of the beta-globin locus control region. *Proc Natl Acad Sci U S A,* 91**,** 9926-30.

MOREL, L., CHIANG, M. S. R., HIGASHIMORI, H., SHONEYE, T., IYER, L. K., YELICK, J., TAI, A. & YANG, Y. 2017. Molecular and Functional Properties of Regional Astrocytes in the Adult Brain. *J Neurosci*.

NAKAJI, K., IHARA, M., TAKAHASHI, C., ITOHARA, S., NODA, M., TAKAHASHI, R. & TOMIMOTO, H. 2006. Matrix metalloproteinase-2 plays a critical role in the pathogenesis of white matter lesions after chronic cerebral hypoperfusion in rodents. *Stroke,* 37**,** 2816-23.

NAVE, K. A. 2010. Myelination and support of axonal integrity by glia. *Nature,* 468**,** 244-52.

NAYAK, D., ROTH, T. L. & MCGAVERN, D. B. 2014. Microglia development and function. *Annu Rev Immunol,* 32**,** 367-402.

NIMMERJAHN, A., KIRCHHOFF, F. & HELMCHEN, F. 2005. Resting microglial cells are highly dynamic surveillants of brain parenchyma in vivo. *Science,* 308**,** 1314-8.

NISHIO, K., IHARA, M., YAMASAKI, N., KALARIA, R. N., MAKI, T., FUJITA, Y., ITO, H., OISHI, N., FUKUYAMA, H., MIYAKAWA, T., TAKAHASHI, R. &

TOMIMOTO, H. 2010. A mouse model characterizing features of vascular dementia with hippocampal atrophy. *Stroke,* 41**,** 1278-84.
NISSEN, J. C., THOMPSON, K. K., WEST, B. L. & TSIRKA, S. E. 2018. Csf1R inhibition attenuates experimental autoimmune encephalomyelitis and promotes recovery. *Exp Neurol*.
NOVAK, V., LAST, D., ALSOP, D. C., ABDULJALIL, A. M., HU, K., LEPICOVSKY, L., CAVALLERANO, J. & LIPSITZ, L. A. 2006. Cerebral blood flow velocity and periventricular white matter hyperintensities in type 2 diabetes. *Diabetes Care,* 29**,** 1529-34.
O'BRIEN, J. T., ERKINJUNTTI, T., REISBERG, B., ROMAN, G., SAWADA, T., PANTONI, L., BOWLER, J. V., BALLARD, C., DECARLI, C., GORELICK, P. B., ROCKWOOD, K., BURNS, A., GAUTHIER, S. & DEKOSKY, S. T. 2003. Vascular cognitive impairment. *Lancet Neurol,* 2**,** 89-98.
O'LEARY, T. P. & BROWN, R. E. 2013. Optimization of apparatus design and behavioral measures for the assessment of visuo-spatial learning and memory of mice on the Barnes maze. *Learn Mem,* 20**,** 85-96.
OHTA, H., NISHIKAWA, H., KIMURA, H., ANAYAMA, H. & MIYAMOTO, M. 1997. Chronic cerebral hypoperfusion by permanent internal carotid ligation produces learning impairment without brain damage in rats. *Neuroscience,* 79**,** 1039-50.
OLMOS-ALONSO, A., SCHETTERS, S. T., SRI, S., ASKEW, K., MANCUSO, R., VARGAS-CABALLERO, M., HOLSCHER, C., PERRY, V. H. & GOMEZ-NICOLA, D. 2016. Pharmacological targeting of CSF1R inhibits microglial proliferation and prevents the progression of Alzheimer's-like pathology. *Brain,* 139**,** 891-907.
OLSSON, B., HERTZE, J., LAUTNER, R., ZETTERBERG, H., NAGGA, K., HOGLUND, K., BASUN, H., ANNAS, P., LANNFELT, L., ANDREASEN, N., MINTHON, L., BLENNOW, K. & HANSSON, O. 2013. Microglial markers are elevated in the prodromal phase of Alzheimer's disease and vascular dementia. *J Alzheimers Dis,* 33**,** 45-53.
OOSTERHOF, N., KUIL, L. E., VAN DER LINDE, H. C., BURM, S. M., BERDOWSKI, W., VAN IJCKEN, W. F. J., VAN SWIETEN, J. C., HOL, E. M., VERHEIJEN, M. H. G. & VAN HAM, T. J. 2018. Colony-Stimulating Factor 1 Receptor (CSF1R) Regulates Microglia Density and Distribution, but Not Microglia Differentiation In Vivo. *Cell Rep,* 24**,** 1203-1217.e6.
PAOLICELLI, R. C., BOLASCO, G., PAGANI, F., MAGGI, L., SCIANNI, M., PANZANELLI, P., GIUSTETTO, M., FERREIRA, T. A., GUIDUCCI, E., DUMAS, L., RAGOZZINO, D. & GROSS, C. T. 2011. Synaptic pruning by microglia is necessary for normal brain development. *Science,* 333**,** 1456-8.
PATTERSON, C. 2018. World Alzheimer Report 2018. The state of the art of dementia research: New frontiers. London.
PAULSON, O. 1990. Cerebral autoregulation. *Cerebrovasc Brain Metab Rev,* 2**,** 161.
PAUS, T., PESARESI, M. & FRENCH, L. 2014. White matter as a transport system. *Neuroscience,* 276**,** 117-25.
PAXINOS, G. & FRANKLIN, K. B. J. 2001. *The Mouse Brain in Stereotaxic Coordinates*, Academic Press.
PAYNE, S. J., MOHAMMAD, J., TISDALL, M. M. & TACHTSIDIS, I. 2011. Effects of arterial blood gas levels on cerebral blood flow and oxygen transport. *Biomed Opt Express,* 2**,** 966-79.

PERROTTA, M., LEMBO, G. & CARNEVALE, D. 2016. Hypertension and Dementia: Epidemiological and Experimental Evidence Revealing a Detrimental Relationship. *Int J Mol Sci,* 17**,** 347.

PIANTADOSI, C. A., WITHERS, C. M., BARTZ, R. R., MACGARVEY, N. C., FU, P., SWEENEY, T. E., WELTY-WOLF, K. E. & SULIMAN, H. B. 2011. Heme oxygenase-1 couples activation of mitochondrial biogenesis to anti-inflammatory cytokine expression. *J Biol Chem,* 286**,** 16374-85.

PIERINI, D. & BRYAN, N. S. 2015. Nitric oxide availability as a marker of oxidative stress. *Methods Mol Biol,* 1208**,** 63-71.

PIXLEY, F. J. & STANLEY, E. R. 2004. CSF-1 regulation of the wandering macrophage: complexity in action. *Trends Cell Biol,* 14**,** 628-38.

PROMJUNYAKUL, N., LAHNA, D., KAYE, J. A., DODGE, H. H., ERTEN-LYONS, D., ROONEY, W. D. & SILBERT, L. C. 2015. Characterizing the white matter hyperintensity penumbra with cerebral blood flow measures. *Neuroimage Clin,* 8**,** 224-9.

QIN, C., FAN, W. H., LIU, Q., SHANG, K., MURUGAN, M., WU, L. J., WANG, W. & TIAN, D. S. 2017. Fingolimod Protects Against Ischemic White Matter Damage by Modulating Microglia Toward M2 Polarization via STAT3 Pathway. *Stroke,* 48**,** 3336-3346.

QUARLES, R. H. 2007. Myelin-associated glycoprotein (MAG): past, present and beyond. *J Neurochem,* 100**,** 1431-48.

RADA, P., ROJO, A. I., EVRARD-TODESCHI, N., INNAMORATO, N. G., COTTE, A., JAWORSKI, T., TOBON-VELASCO, J. C., DEVIJVER, H., GARCIA-MAYORAL, M. F., VAN LEUVEN, F., HAYES, J. D., BERTHO, G. & CUADRADO, A. 2012. Structural and functional characterization of Nrf2 degradation by the glycogen synthase kinase 3/beta-TrCP axis. *Mol Cell Biol,* 32**,** 3486-99.

RADEMAKERS, R., BAKER, M., NICHOLSON, A. M., RUTHERFORD, N. J., FINCH, N., SOTO-ORTOLAZA, A., LASH, J., WIDER, C., WOJTAS, A., DEJESUS-HERNANDEZ, M., ADAMSON, J., KOURI, N., SUNDAL, C., SHUSTER, E. A., AASLY, J., MACKENZIE, J., ROEBER, S., KRETZSCHMAR, H. A., BOEVE, B. F., KNOPMAN, D. S., PETERSEN, R. C., CAIRNS, N. J., GHETTI, B., SPINA, S., GARBERN, J., TSELIS, A. C., UITTI, R., DAS, P., VAN GERPEN, J. A., MESCHIA, J. F., LEVY, S., BRODERICK, D. F., GRAFF-RADFORD, N., ROSS, O. A., MILLER, B. B., SWERDLOW, R. H., DICKSON, D. W. & WSZOLEK, Z. K. 2011. Mutations in the colony stimulating factor 1 receptor (CSF1R) gene cause hereditary diffuse leukoencephalopathy with spheroids. *Nat Genet,* 44**,** 200-5.

RAGHUNATH, A., SUNDARRAJ, K., NAGARAJAN, R., ARFUSO, F., BIAN, J., KUMAR, A. P., SETHI, G. & PERUMAL, E. 2018. Antioxidant response elements: Discovery, classes, regulation and potential applications. *Redox Biol,* 17**,** 297-314.

RAJ, D., YIN, Z., BREUR, M., DOORDUIN, J., HOLTMAN, I. R., OLAH, M., MANTINGH-OTTER, I. J., VAN DAM, D., DE DEYN, P. P., DEN DUNNEN, W., EGGEN, B. J. L., AMOR, S. & BODDEKE, E. 2017. Increased White Matter Inflammation in Aging- and Alzheimer's Disease Brain. *Front Mol Neurosci,* 10**,** 206.

RAZ, L., KNOEFEL, J. & BHASKAR, K. 2015. The neuropathology and cerebrovascular mechanisms of dementia. *J Cereb Blood Flow Metab*.

REIMER, M. M., MCQUEEN, J., SEARCY, L., SCULLION, G., ZONTA, B., DESMAZIERES, A., HOLLAND, P. R., SMITH, J., GLIDDON, C., WOOD, E. R., HERZYK, P., BROPHY, P. J., MCCULLOCH, J. & HORSBURGH, K. 2011.

Rapid disruption of axon-glial integrity in response to mild cerebral hypoperfusion. *J Neurosci,* 31**,** 18185-94.
ROJO, A. I., INNAMORATO, N. G., MARTIN-MORENO, A. M., DE CEBALLOS, M. L., YAMAMOTO, M. & CUADRADO, A. 2010. Nrf2 regulates microglial dynamics and neuroinflammation in experimental Parkinson's disease. *Glia,* 58**,** 588-98.
ROJO, A. I., PAJARES, M., GARCIA-YAGUE, A. J., BUENDIA, I., VAN LEUVEN, F., YAMAMOTO, M., LOPEZ, M. G. & CUADRADO, A. 2018. Deficiency in the transcription factor NRF2 worsens inflammatory parameters in a mouse model with combined tauopathy and amyloidopathy. *Redox Biol,* 18**,** 173-180.
ROJO, A. I., PAJARES, M., RADA, P., NUNEZ, A., NEVADO-HOLGADO, A. J., KILLIK, R., VAN LEUVEN, F., RIBE, E., LOVESTONE, S., YAMAMOTO, M. & CUADRADO, A. 2017. NRF2 deficiency replicates transcriptomic changes in Alzheimer's patients and worsens APP and TAU pathology. *Redox Biol,* 13**,** 444-451.
ROSENBERG, G. A. 2009. Inflammation and white matter damage in vascular cognitive impairment. *Stroke,* 40**,** S20-3.
ROSENBERG, G. A. 2017. Extracellular matrix inflammation in vascular cognitive impairment and dementia. *Clin Sci (Lond),* 131**,** 425-437.
ROSENBERG, G. A., SULLIVAN, N. & ESIRI, M. M. 2001. White matter damage is associated with matrix metalloproteinases in vascular dementia. *Stroke,* 32**,** 1162-8.
ROSENBERG, G. A., WALLIN, A., WARDLAW, J. M., MARKUS, H. S., MONTANER, J., WOLFSON, L., IADECOLA, C., ZLOKOVIC, B. V., JOUTEL, A., DICHGANS, M., DUERING, M., SCHMIDT, R., KORCZYN, A. D., GRINBERG, L. T., CHUI, H. C. & HACHINSKI, V. 2015. Consensus statement for diagnosis of subcortical small vessel disease. *J Cereb Blood Flow Metab*.
ROTHHAMMER, V., BORUCKI, D. M., TJON, E. C., TAKENAKA, M. C., CHAO, C. C., ARDURA-FABREGAT, A., DE LIMA, K. A., GUTIERREZ-VAZQUEZ, C., HEWSON, P., STASZEWSKI, O., BLAIN, M., HEALY, L., NEZIRAJ, T., BORIO, M., WHEELER, M., DRAGIN, L. L., LAPLAUD, D. A., ANTEL, J., ALVAREZ, J. I., PRINZ, M. & QUINTANA, F. J. 2018. Microglial control of astrocytes in response to microbial metabolites. *Nature*.
RUBERTE, J., CARRETERO, A. & NAVARRO, M. 2017. *Morphological Mouse Phenotyping, 1st Edition, Anatomy, Histology and Imaging*, Academic Press.
RUITENBERG, A., DEN HEIJER, T., BAKKER, S. L., VAN SWIETEN, J. C., KOUDSTAAL, P. J., HOFMAN, A. & BRETELER, M. M. 2005. Cerebral hypoperfusion and clinical onset of dementia: the Rotterdam Study. *Ann Neurol,* 57**,** 789-94.
RUSHMORE, T. H., MORTON, M. R. & PICKETT, C. B. 1991. The antioxidant responsive element. Activation by oxidative stress and identification of the DNA consensus sequence required for functional activity. *J Biol Chem,* 266**,** 11632-9.
SAGGU, R., SCHUMACHER, T., GERICH, F., RAKERS, C., TAI, K., DELEKATE, A. & PETZOLD, G. C. 2016. Astroglial NF-kB contributes to white matter damage and cognitive impairment in a mouse model of vascular dementia. *Acta Neuropathol Commun,* 4**,** 76.
SALTER, M. W. & STEVENS, B. 2017. Microglia emerge as central players in brain disease. *Nat Med,* 23**,** 1018-1027.
SASAKI, A. 2016. Microglia and brain macrophages: An update. *Neuropathology*.
SCHEFF, S. W., ANSARI, M. A. & MUFSON, E. J. 2016. Oxidative stress and hippocampal synaptic protein levels in elderly cognitively intact individuals with Alzheimer's disease pathology. *Neurobiol Aging,* 42**,** 1-12.

SCHMIDLIN, C. J., DODSON, M. B., MADHAVAN, L. & ZHANG, D. D. 2019. Redox regulation by NRF2 in aging and disease. *Free Radic Biol Med*.

SCHUFF, N., MATSUMOTO, S., KMIECIK, J., STUDHOLME, C., DU, A., EZEKIEL, F., MILLER, B. L., KRAMER, J. H., JAGUST, W. J., CHUI, H. C. & WEINER, M. W. 2009. Cerebral blood flow in ischemic vascular dementia and Alzheimer's disease, measured by arterial spin-labeling magnetic resonance imaging. *Alzheimers Dement,* 5**,** 454-62.

SCHULZE-TOPPHOFF, U., VARRIN-DOYER, M., PEKAREK, K., SPENCER, C. M., SHETTY, A., SAGAN, S. A., CREE, B. A., SOBEL, R. A., WIPKE, B. T., STEINMAN, L., SCANNEVIN, R. H. & ZAMVIL, S. S. 2016. Dimethyl fumarate treatment induces adaptive and innate immune modulation independent of Nrf2. *Proc Natl Acad Sci U S A,* 113**,** 4777-82.

SHARMA, S., RAKOCZY, S. & BROWN-BORG, H. 2010. Assessment of spatial memory in mice. *Life Sci,* 87**,** 521-36.

SHI, J., HE, Y., HEWETT, S. J. & HEWETT, J. A. 2016a. Interleukin 1beta Regulation of the System xc- Substrate-specific Subunit, xCT, in Primary Mouse Astrocytes Involves the RNA-binding Protein HuR. *J Biol Chem,* 291**,** 1643-51.

SHI, Q., CHOWDHURY, S., MA, R., LE, K. X., HONG, S., CALDARONE, B. J., STEVENS, B. & LEMERE, C. A. 2017. Complement C3 deficiency protects against neurodegeneration in aged plaque-rich APP/PS1 mice. *Sci Transl Med,* 9.

SHI, Y., THRIPPLETON, M. J., MAKIN, S. D., MARSHALL, I., GEERLINGS, M. I., DE CRAEN, A. J. M., VAN BUCHEM, M. A. & WARDLAW, J. M. 2016b. Cerebral blood flow in small vessel disease: A systematic review and meta-analysis. *J Cereb Blood Flow Metab,* 36**,** 1653-1667.

SHIBATA, M., OHTANI, R., IHARA, M. & TOMIMOTO, H. 2004. White matter lesions and glial activation in a novel mouse model of chronic cerebral hypoperfusion. *Stroke,* 35**,** 2598-603.

SHIBATA, M., YAMASAKI, N., MIYAKAWA, T., KALARIA, R. N., FUJITA, Y., OHTANI, R., IHARA, M., TAKAHASHI, R. & TOMIMOTO, H. 2007. Selective impairment of working memory in a mouse model of chronic cerebral hypoperfusion. *Stroke,* 38**,** 2826-32.

SHIH, A. Y., JOHNSON, D. A., WONG, G., KRAFT, A. D., JIANG, L., ERB, H., JOHNSON, J. A. & MURPHY, T. H. 2003. Coordinate regulation of glutathione biosynthesis and release by Nrf2-expressing glia potently protects neurons from oxidative stress. *J Neurosci,* 23**,** 3394-406.

SIGFRIDSSON, E., MARANGONI, M., JOHNSON, J. A., HARDINGHAM, G. E., FOWLER, J. H. & HORSBURGH, K. 2018. Astrocyte-specific overexpression of Nrf2 protects against optic tract damage and behavioural alterations in a mouse model of cerebral hypoperfusion. *Sci Rep,* 8**,** 12552.

SIMPSON, J. E., FERNANDO, M. S., CLARK, L., INCE, P. G., MATTHEWS, F., FORSTER, G., O'BRIEN, J. T., BARBER, R., KALARIA, R. N., BRAYNE, C., SHAW, P. J., LEWIS, C. E. & WHARTON, S. B. 2007a. White matter lesions in an unselected cohort of the elderly: astrocytic, microglial and oligodendrocyte precursor cell responses. *Neuropathol Appl Neurobiol,* 33**,** 410-9.

SIMPSON, J. E., HOSNY, O., WHARTON, S. B., HEATH, P. R., HOLDEN, H., FERNANDO, M. S., MATTHEWS, F., FORSTER, G., O'BRIEN, J. T., BARBER, R., KALARIA, R. N., BRAYNE, C., SHAW, P. J., LEWIS, C. E. & INCE, P. G. 2009. Microarray RNA expression analysis of cerebral white matter lesions reveals changes in multiple functional pathways. *Stroke,* 40**,** 369-75.

SIMPSON, J. E., INCE, P. G., HIGHAM, C. E., GELSTHORPE, C. H., FERNANDO, M. S., MATTHEWS, F., FORSTER, G., O'BRIEN, J. T., BARBER, R., KALARIA, R. N., BRAYNE, C., SHAW, P. J., STOEBER, K., WILLIAMS, G. H., LEWIS, C. E. & WHARTON, S. B. 2007b. Microglial activation in white matter lesions and nonlesional white matter of ageing brains. *Neuropathol Appl Neurobiol,* 33**,** 670-83.

SKROBOT, O. A., ATTEMS, J., ESIRI, M., HORTOBAGYI, T., IRONSIDE, J. W., KALARIA, R. N., KING, A., LAMMIE, G. A., MANN, D., NEAL, J., BEN-SHLOMO, Y., KEHOE, P. G. & LOVE, S. 2016. Vascular cognitive impairment neuropathology guidelines (VCING): the contribution of cerebrovascular pathology to cognitive impairment. *Brain*.

SKROBOT, O. A., BLACK, S. E., CHEN, C., DECARLI, C., ERKINJUNTTI, T., FORD, G. A., KALARIA, R. N., O'BRIEN, J., PANTONI, L., PASQUIER, F., ROMAN, G. C., WALLIN, A., SACHDEV, P., SKOOG, I., BEN-SHLOMO, Y., PASSMORE, A. P., LOVE, S. & KEHOE, P. G. 2018. Progress toward standardized diagnosis of vascular cognitive impairment: Guidelines from the Vascular Impairment of Cognition Classification Consensus Study. *Alzheimers Dement,* 14**,** 280-292.

SKROBOT, O. A., O'BRIEN, J., BLACK, S., CHEN, C., DECARLI, C., ERKINJUNTTI, T., FORD, G. A., KALARIA, R. N., PANTONI, L., PASQUIER, F., ROMAN, G. C., WALLIN, A., SACHDEV, P., SKOOG, I., BEN-SHLOMO, Y., PASSMORE, A. P., LOVE, S. & KEHOE, P. G. 2017. The Vascular Impairment of Cognition Classification Consensus Study. *Alzheimers Dement,* 13**,** 624-633.

SMITH, E. E. 2017. Clinical presentations and epidemiology of vascular dementia. *Clin Sci (Lond),* 131**,** 1059-1068.

SNOWDON, D. A., GREINER, L. H., MORTIMER, J. A., RILEY, K. P., GREINER, P. A. & MARKESBERY, W. R. 1997. Brain infarction and the clinical expression of Alzheimer disease. The Nun Study. *Jama,* 277**,** 813-7.

SNYDER, H. M., SHINEMAN, D. W., FRIEDMAN, L. G., HENDRIX, J. A., KHACHATURIAN, A., LE GUILLOU, I., PICKETT, J., REFOLO, L., SANCHO, R. M. & RIDLEY, S. H. 2016. Guidelines to improve animal study design and reproducibility for Alzheimer's disease and related dementias: For funders and researchers. *Alzheimers Dement,* 12**,** 1177-1185.

SOFRONIEW, M. V. 2014a. Astrogliosis. *Cold Spring Harb Perspect Biol,* 7**,** a020420.

SOFRONIEW, M. V. 2014b. Multiple roles for astrocytes as effectors of cytokines and inflammatory mediators. *Neuroscientist,* 20**,** 160-72.

SOFRONIEW, M. V. & VINTERS, H. V. 2010. Astrocytes: biology and pathology. *Acta Neuropathol.* Berlin/Heidelberg.

SOREQ, L., ROSE, J., SOREQ, E., HARDY, J., TRABZUNI, D., COOKSON, M. R., SMITH, C., RYTEN, M., PATANI, R. & ULE, J. 2017. Major Shifts in Glial Regional Identity Are a Transcriptional Hallmark of Human Brain Aging. *Cell Rep,* 18**,** 557-570.

SPANGENBERG, E. E., LEE, R. J., NAJAFI, A. R., RICE, R. A., ELMORE, M. R., BLURTON-JONES, M., WEST, B. L. & GREEN, K. N. 2016. Eliminating microglia in Alzheimer's mice prevents neuronal loss without modulating amyloid-beta pathology. *Brain,* 139**,** 1265-81.

SPILLER, K. J., RESTREPO, C. R., KHAN, T., DOMINIQUE, M. A., FANG, T. C., CANTER, R. G., ROBERTS, C. J., MILLER, K. R., RANSOHOFF, R. M., TROJANOWSKI, J. Q. & LEE, V. M. 2018. Microglia-mediated recovery from ALS-relevant motor neuron degeneration in a mouse model of TDP-43 proteinopathy. *Nat Neurosci,* 21**,** 329-340.

SRIVASTAVA, S., ALFIERI, A., SIOW, R. C., MANN, G. E. & FRASER, P. A. 2013. Temporal and spatial distribution of Nrf2 in rat brain following stroke:

quantification of nuclear to cytoplasmic Nrf2 content using a novel immunohistochemical technique. *J Physiol,* 591**,** 3525-38.
STASSART, R. M., MOBIUS, W., NAVE, K. A. & EDGAR, J. M. 2018. The Axon-Myelin Unit in Development and Degenerative Disease. *Front Neurosci,* 12**,** 467.
STEVENS, B., ALLEN, N. J., VAZQUEZ, L. E., HOWELL, G. R., CHRISTOPHERSON, K. S., NOURI, N., MICHEVA, K. D., MEHALOW, A. K., HUBERMAN, A. D., STAFFORD, B., SHER, A., LITKE, A. M., LAMBRIS, J. D., SMITH, S. J., JOHN, S. W. & BARRES, B. A. 2007. The classical complement cascade mediates CNS synapse elimination. *Cell,* 131**,** 1164-78.
SUNEETHA, A. & RAJA RAJESWARI, K. 2016. Role of dimethyl fumarate in oxidative stress of multiple sclerosis: A review. *J Chromatogr B Analyt Technol Biomed Life Sci,* 1019**,** 15-20.
SWARTZLANDER, D. B., PROPSON, N. E., ROY, E. R., SAITO, T., SAIDO, T., WANG, B. & ZHENG, H. 2018. Concurrent cell type-specific isolation and profiling of mouse brains in inflammation and Alzheimer's disease. *JCI Insight,* 3.
TANAKA, N., IKEDA, Y., OHTA, Y., DEGUCHI, K., TIAN, F., SHANG, J., MATSUURA, T. & ABE, K. 2011. Expression of Keap1-Nrf2 system and antioxidative proteins in mouse brain after transient middle cerebral artery occlusion. *Brain Res,* 1370**,** 246-53.
THANNICKAL, V. J. & FANBURG, B. L. 2000. Reactive oxygen species in cell signaling. *Am J Physiol Lung Cell Mol Physiol,* 279**,** L1005-28.
THIMMULAPPA, R. K., LEE, H., RANGASAMY, T., REDDY, S. P., YAMAMOTO, M., KENSLER, T. W. & BISWAL, S. 2006. Nrf2 is a critical regulator of the innate immune response and survival during experimental sepsis. *J Clin Invest,* 116**,** 984-95.
TOMIMOTO, H., AKIGUCHI, I., WAKITA, H., SUENAGA, T., NAKAMURA, S. & KIMURA, J. 1997. Regressive changes of astroglia in white matter lesions in cerebrovascular disease and Alzheimer's disease patients. *Acta Neuropathol,* 94**,** 146-52.
TOTH, P., TARANTINI, S., CSISZAR, A. & UNGVARI, Z. 2017. Functional vascular contributions to cognitive impairment and dementia: mechanisms and consequences of cerebral autoregulatory dysfunction, endothelial impairment, and neurovascular uncoupling in aging. *Am J Physiol Heart Circ Physiol,* 312**,** H1-h20.
TOTH, R. K. & WARFEL, N. A. 2017. Strange Bedfellows: Nuclear Factor, Erythroid 2-Like 2 (Nrf2) and Hypoxia-Inducible Factor 1 (HIF-1) in Tumor Hypoxia. *In:* MONDAL, D. (ed.) *Antioxidants (Basel).*
UNGVARI, Z., BAILEY-DOWNS, L., GAUTAM, T., SOSNOWSKA, D., WANG, M., MONTICONE, R. E., TELLJOHANN, R., PINTO, J. T., DE CABO, R., SONNTAG, W. E., LAKATTA, E. G. & CSISZAR, A. 2011a. Age-associated vascular oxidative stress, Nrf2 dysfunction, and NF-{kappa}B activation in the nonhuman primate Macaca mulatta. *J Gerontol A Biol Sci Med Sci,* 66**,** 866-75.
UNGVARI, Z., BAILEY-DOWNS, L., SOSNOWSKA, D., GAUTAM, T., KONCZ, P., LOSONCZY, G., BALLABH, P., DE CABO, R., SONNTAG, W. E. & CSISZAR, A. 2011b. Vascular oxidative stress in aging: a homeostatic failure due to dysregulation of NRF2-mediated antioxidant response. *Am J Physiol Heart Circ Physiol,* 301**,** H363-72.
VALCARCEL-ARES, M. N., GAUTAM, T., WARRINGTON, J. P., BAILEY-DOWNS, L., SOSNOWSKA, D., DE CABO, R., LOSONCZY, G., SONNTAG, W. E., UNGVARI, Z. & CSISZAR, A. 2012. Disruption of Nrf2 signaling impairs

angiogenic capacity of endothelial cells: implications for microvascular aging. *J Gerontol A Biol Sci Med Sci,* 67**,** 821-9.
VAN BEEK, A. H., CLAASSEN, J. A., RIKKERT, M. G. & JANSEN, R. W. 2008. Cerebral autoregulation: an overview of current concepts and methodology with special focus on the elderly. *J Cereb Blood Flow Metab,* 28**,** 1071-85.
VAN DER FLIER, W. M., SKOOG, I., SCHNEIDER, J. A., PANTONI, L., MOK, V., CHEN, C. L. H. & SCHELTENS, P. 2018. Vascular cognitive impairment. *Nat Rev Dis Primers,* 4**,** 18003.
VARGAS, M. R., BURTON, N. C., KUTZKE, J., GAN, L., JOHNSON, D. A., SCHAFER, M., WERNER, S. & JOHNSON, J. A. 2013. Absence of Nrf2 or its selective overexpression in neurons and muscle does not affect survival in ALS-linked mutant hSOD1 mouse models. *PLoS One,* 8**,** e56625.
VARGAS, M. R., JOHNSON, D. A., SIRKIS, D. W., MESSING, A. & JOHNSON, J. A. 2008. Nrf2 activation in astrocytes protects against neurodegeneration in mouse models of familial amyotrophic lateral sclerosis. *J Neurosci,* 28**,** 13574-81.
VENUGOPAL, R. & JAISWAL, A. K. 1996. Nrf1 and Nrf2 positively and c-Fos and Fra1 negatively regulate the human antioxidant response element-mediated expression of NAD(P)H:quinone oxidoreductase1 gene. *Proc Natl Acad Sci U S A,* 93**,** 14960-5.
VERKHRATSKY, A. & NEDERGAARD, M. 2018. Physiology of astroglia. *Physiological Reviews,* 98**,** 239-389
VICENTE, E., DEGERONE, D., BOHN, L., SCORNAVACA, F., PIMENTEL, A., LEITE, M. C., SWAROWSKY, A., RODRIGUES, L., NARDIN, P., DE ALMEIDA, L. M., GOTTFRIED, C., SOUZA, D. O., NETTO, C. A. & GONCALVES, C. A. 2009. Astroglial and cognitive effects of chronic cerebral hypoperfusion in the rat. *Brain Res,* 1251**,** 204-12.
VRSELJA, Z., BRKIC, H., MRDENOVIC, S., RADIC, R. & CURIC, G. 2014. Function of circle of Willis. *J Cereb Blood Flow Metab,* 34**,** 578-84.
WAKITA, H., TOMIMOTO, H., AKIGUCHI, I., MATSUO, A., LIN, J. X., IHARA, M. & MCGEER, P. L. 2002. Axonal damage and demyelination in the white matter after chronic cerebral hypoperfusion in the rat. *Brain Res,* 924**,** 63-70.
WALHOVD, K. B., JOHANSEN-BERG, H. & KARADOTTIR, R. T. 2014. Unraveling the secrets of white matter--bridging the gap between cellular, animal and human imaging studies. *Neuroscience,* 276**,** 2-13.
WANG, T., OUZOUNOV, D. G., WU, C., HORTON, N. G., ZHANG, B., WU, C. H., ZHANG, Y., SCHNITZER, M. J. & XU, C. 2018. Three-photon imaging of mouse brain structure and function through the intact skull. *Nat Methods,* 15**,** 789-792.
WARDLAW, J. M., SMITH, E. E., BIESSELS, G. J., CORDONNIER, C., FAZEKAS, F., FRAYNE, R., LINDLEY, R. I., O'BRIEN, J. T., BARKHOF, F., BENAVENTE, O. R., BLACK, S. E., BRAYNE, C., BRETELER, M., CHABRIAT, H., DECARLI, C., DE LEEUW, F. E., DOUBAL, F., DUERING, M., FOX, N. C., GREENBERG, S., HACHINSKI, V., KILIMANN, I., MOK, V., OOSTENBRUGGE, R., PANTONI, L., SPECK, O., STEPHAN, B. C., TEIPEL, S., VISWANATHAN, A., WERRING, D., CHEN, C., SMITH, C., VAN BUCHEM, M., NORRVING, B., GORELICK, P. B. & DICHGANS, M. 2013. Neuroimaging standards for research into small vessel disease and its contribution to ageing and neurodegeneration. *Lancet Neurol,* 12**,** 822-38.
WARDLAW, J. M., VALDES HERNANDEZ, M. C. & MUNOZ-MANIEGA, S. 2015. What are white matter hyperintensities made of? Relevance to vascular cognitive impairment. *J Am Heart Assoc,* 4**,** 001140.

WASHIDA, K., IHARA, M., NISHIO, K., FUJITA, Y., MAKI, T., YAMADA, M., TAKAHASHI, J., WU, X., KIHARA, T., ITO, H., TOMIMOTO, H. & TAKAHASHI, R. 2010. Nonhypotensive dose of telmisartan attenuates cognitive impairment partially due to peroxisome proliferator-activated receptor-gamma activation in mice with chronic cerebral hypoperfusion. *Stroke,* 41**,** 1798-806.

WOLF, G., LOTAN, A., LIFSCHYTZ, T., BEN-ARI, H., KREISEL MERZEL, T., TATARSKYY, P., VALITZKY, M., MERNICK, B., AVIDAN, E., KOROUKHOV, N. & LERER, B. 2017. Differentially Severe Cognitive Effects of Compromised Cerebral Blood Flow in Aged Mice: Association with Myelin Degradation and Microglia Activation. *Front Aging Neurosci,* 9**,** 191.

YAMAZAKI, H., TANJI, K., WAKABAYASHI, K., MATSUURA, S. & ITOH, K. 2015. Role of the Keap1/Nrf2 pathway in neurodegenerative diseases. *Pathol Int,* 65**,** 210-9.

YANG, G., KITAGAWA, K., MATSUSHITA, K., MABUCHI, T., YAGITA, Y., YANAGIHARA, T. & MATSUMOTO, M. 1997. C57BL/6 strain is most susceptible to cerebral ischemia following bilateral common carotid occlusion among seven mouse strains: selective neuronal death in the murine transient forebrain ischemia. *Brain Res,* 752**,** 209-18.

YANG, J., AHN, H. N., CHANG, M., NARASIMHAN, P., CHAN, P. H. & SONG, Y. S. 2013. Complement component 3 inhibition by an antioxidant is neuroprotective after cerebral ischemia and reperfusion in mice. *J Neurochem,* 124**,** 523-35.

YAO, Z. H., YAO, X. L., ZHANG, S. F., HU, J. C. & ZHANG, Y. 2019. Tripchlorolide May Improve Spatial Cognition Dysfunction and Synaptic Plasticity after Chronic Cerebral Hypoperfusion. *Neural Plast,* 2019**,** 2158285.

YOSHIZAKI, K., ADACHI, K., KATAOKA, S., WATANABE, A., TABIRA, T., TAKAHASHI, K. & WAKITA, H. 2008. Chronic cerebral hypoperfusion induced by right unilateral common carotid artery occlusion causes delayed white matter lesions and cognitive impairment in adult mice. *Exp Neurol,* 210**,** 585-91.

YUAN, B., SHI, H., ZHENG, K., SU, Z., SU, H., ZHONG, M., HE, X., ZHOU, C., CHEN, H., XIONG, Q., ZHANG, Y. & YANG, Z. 2017. MCP-1-mediated activation of microglia promotes white matter lesions and cognitive deficits by chronic cerebral hypoperfusion in mice. *Mol Cell Neurosci,* 78**,** 52-58.

YUN, S. P., KAM, T. I., PANICKER, N., KIM, S., OH, Y., PARK, J. S., KWON, S. H., PARK, Y. J., KARUPPAGOUNDER, S. S., PARK, H., OH, N., KIM, N. A., LEE, S., BRAHMACHARI, S., MAO, X., LEE, J. H., KUMAR, M., AN, D., KANG, S. U., LEE, Y., LEE, K. C., NA, D. H., KIM, D., LEE, S. H., ROSCHKE, V. V., LIDDELOW, S. A., MARI, Z., BARRES, B. A., DAWSON, V. L., DAWSON, T. M. & KO, H. S. 2018. Block of A1 astrocyte conversion by microglia is neuroprotective in models of Parkinson's disease. *Nat Med*.

ZAMANIAN, J. L., XU, L., FOO, L. C., NOURI, N., ZHOU, L., GIFFARD, R. G. & BARRES, B. A. 2012. Genomic analysis of reactive astrogliosis. *J Neurosci,* 32**,** 6391-410.

ZHANG, D., XIAO, Y., LV, P., TENG, Z., DONG, Y., QI, Q. & LIU, Z. 2017. Edaravone attenuates oxidative stress induced by chronic cerebral hypoperfusion injury: role of ERK/Nrf2/HO-1 signaling pathway. *Neurological Research*.

ZHANG, L., JOHNSON, D. & JOHNSON, J. A. 2013. Deletion of Nrf2 impairs functional recovery, reduces clearance of myelin debris and decreases axonal remyelination after peripheral nerve injury. *Neurobiol Dis,* 54**,** 329-38.

ZHANG, Y., CHEN, K., SLOAN, S. A., BENNETT, M. L., SCHOLZE, A. R., O'KEEFFE, S., PHATNANI, H. P., GUARNIERI, P., CANEDA, C.,

RUDERISCH, N., DENG, S., LIDDELOW, S. A., ZHANG, C., DANEMAN, R., MANIATIS, T., BARRES, B. A. & WU, J. Q. 2014. An RNA-sequencing transcriptome and splicing database of glia, neurons, and vascular cells of the cerebral cortex. *J Neurosci,* 34**,** 11929-47.

ZHANG, Y., SLOAN, S. A., CLARKE, L. E., CANEDA, C., PLAZA, C. A., BLUMENTHAL, P. D., VOGEL, H., STEINBERG, G. K., EDWARDS, M. S., LI, G., DUNCAN, J. A., 3RD, CHESHIER, S. H., SHUER, L. M., CHANG, E. F., GRANT, G. A., GEPHART, M. G. & BARRES, B. A. 2016. Purification and Characterization of Progenitor and Mature Human Astrocytes Reveals Transcriptional and Functional Differences with Mouse. *Neuron,* 89**,** 37-53.

ZHAO, J., KOBORI, N., ARONOWSKI, J. & DASH, P. K. 2006. Sulforaphane reduces infarct volume following focal cerebral ischemia in rodents. *Neurosci Lett,* 393**,** 108-12.

ZHAO, R., FENG, J. & HE, G. 2016. Hypoxia increases Nrf2-induced HO-1 expression via the PI3K/Akt pathway. *Front Biosci (Landmark Ed),* 21**,** 385-96.

ZHAO, S., GHOSH, A., LO, C. S., CHENIER, I., SCHOLEY, J. W., FILEP, J. G., INGELFINGER, J. R., ZHANG, S. L. & CHAN, J. S. D. 2018. Nrf2 Deficiency Upregulates Intrarenal Angiotensin-Converting Enzyme-2 and Angiotensin 1-7 Receptor Expression and Attenuates Hypertension and Nephropathy in Diabetic Mice. *Endocrinology,* 159**,** 836-852.

ZHU, J., WANG, Y., LI, J., DENG, J. & ZHOU, H. 2014. Intracranial artery stenosis and progression from mild cognitive impairment to Alzheimer disease. *Neurology,* 82**,** 842-9.

Appendix

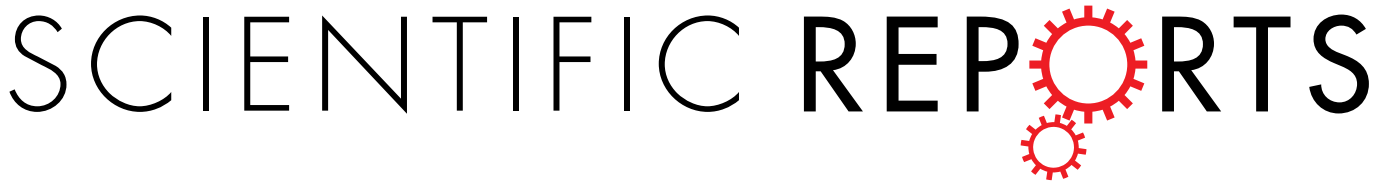

OPEN

Astrocyte-specific overexpression of Nrf2 protects against optic tract damage and behavioural alterations in a mouse model of cerebral hypoperfusion

Received: 27 September 2017
Accepted: 30 July 2018
Published online: 22 August 2018

Emma Sigfridsson[1], Martina Marangoni[1,8], Jeffrey A. Johnson[2,3,4,5], Giles E. Hardingham[1,6,7], Jill H. Fowler[1] & Karen Horsburgh[1]

Mouse models have shown that cerebral hypoperfusion causes white matter disruption and memory impairment relevant to the study of vascular cognitive impairment and dementia. The associated mechanisms include inflammation and oxidative stress are proposed to drive disruption of myelinated axons within hypoperfused white matter. The aim of this study was to determine if increased endogenous anti-oxidant and anti-inflammatory signalling in astrocytes was protective in a model of mild cerebral hypoperfusion. Transgenically altered mice overexpressing the transcription factor Nrf2 (GFAP-Nrf2) and wild type littermates were subjected to bilateral carotid artery stenosis or sham surgery. Behavioural alterations were assessed using the radial arm maze and tissue was collected for pathology and transcriptome analysis six weeks post-surgery. GFAP-Nrf2 mice showed less pronounced behavioural impairments compared to wild types following hypoperfusion, paralleled by reduced optic tract white matter disruption and astrogliosis. There was no effect of hypoperfusion on anti-oxidant gene alterations albeit the levels were increased in GFAP-Nrf2 mice. Instead, pro-inflammatory gene expression was determined to be significantly upregulated in the optic tract of hypoperfused wild type mice but differentially affected in GFAP-Nrf2 mice. In particular, complement components (C4 and C1q) were increased in wild type hypoperfused mice but expressed at levels similar to controls in hypoperfused GFAP-Nrf2 mice. This study provides evidence that overexpression of Nrf2 in astrocytes exerts beneficial effects through repression of inflammation and supports the potential use of Nrf2-activators in the amelioration of cerebrovascular-related inflammation and white matter degeneration.

Vascular cognitive impairment (VCI) is a spectrum of mild cognitive impairment to vascular dementia and is influenced by risk factors including age, hypertension and atherosclerosis. The most common form of VCI is small vessel disease which is predominantly associated with white matter changes that can be detected as hyperintense signals on FLAIR or T2-weighted magnetic resonance images[1,2]. White matter changes correlate with cognitive decline[3,4] and are closely related to reduced cerebral perfusion[5,6]. The extent and presence of white matter changes can predict development of dementia in patients with mild cognitive impairment[7,8]. Thus, understanding pathophysiology of white matter changes has important implications in the treatment of dementia.

[1]Centre for Discovery Brain Sciences, University of Edinburgh, Edinburgh, UK. [2]Division of Pharmaceutical Sciences, University of Wisconsin, Madison, USA. [3]Molecular and Environmental Toxicology Center, University of Wisconsin, Madison, USA. [4]Center for Neuroscience, University of Wisconsin, Madison, USA. [5]Waisman Center, University of Wisconsin, Madison, USA. [6]Edinburgh Medical School, University of Edinburgh, Edinburgh, UK. [7]The UK Dementia Research Institute, University of Edinburgh, Edinburgh, UK. [8]Present address: Department of Health Sciences, University of Florence, Florence, Italy. Jill H. Fowler and Karen Horsburgh jointly supervised this work. Correspondence and requests for materials should be addressed to J.H.F. (email: jill.fowler@ed.ac.uk) or K.H. (email: karen.horsburgh@ed.ac.uk)

Models of cerebral hypoperfusion have been important in providing mechanistic insight into the pathophysiology of VCI; the best characterised is the bilateral carotid artery stenosis (BCAS) model in mice[9,10]. We and others have demonstrated that cerebral hypoperfusion in mice disrupts myelinated axons within the white matter[11,12] causing impaired spatial working memory[11,13,14]. Increased inflammatory cells, particularly microglia, often parallel hypoperfusion-induced white matter damage[9,15,16]. Furthermore, there appears to be a close link between damage to white matter, microgliosis and white matter function in response to mild[17] and severe cerebral hypoperfusion[18]. Our work demonstrated that the use of a broad spectrum anti-inflammatory drug, minocycline, markedly attenuates microgliosis and improves white matter function in a mouse model of cerebral hypoperfusion[17], and has also identified activation of pro-inflammatory genes within days in hypoperfused white matter[12]. Inflammation is often accompanied by indices of oxidative stress which is also proposed as a key contributor to pathology following cerebral hypoperfusion (reviewed by[19,20]). Increased levels of the reactive species superoxide, the superoxide-producing enzyme NADPH oxidase and oxidative damage to lipids, proteins and nucleic acids is found in hypoperfused white matter[21–23]. Reduced anti-oxidant and detoxifying enzymes and/or dysfunctional mitochondria are suggested underlying mechanisms[24–26].

Deficiency of the transcription factor nuclear factor erythroid 2-related factor (Nrf2), a master regulator of endogenous cytoprotective anti-oxidant and anti-inflammatory gene pathways, is associated with white matter damage. Nrf2 knockout mice exhibit myelin pathology characterised by myelin unwinding, lipid peroxidation of the myelin sheath, and increased astrocytosis[27], as well as reduced functional recovery and remyelination following sciatic nerve crush and experimental autoimmune encephalitis (EAE)[28,29]. In contrast, activation of Nrf2 using dimethyl fumarate (DMF) has been shown to prevent myelin damage and astrocyte activation in EAE[30], and DMF has since been approved for the treatment of relapsing-remitting multiple sclerosis (reviewed by[31]). Recently we have also shown that treatment with DMF, in a severe model of cerebral hypoperfusion, ameliorates white matter functional impairment and microgliosis[18]. Nrf2 expression has been shown to be several fold higher in astrocytes compared to neurons[32] which have been shown to repress Nrf2 expression developmentally as redox-sensitive signalling pathways are important for proper maturation, and instead neurons rely on astrocytic support to prevent oxidative damage[33]. Oligodendrocytes, also highly metabolically active cells, receive anti-oxidant support from astrocytes as well[34], which may explain their comparably higher levels of Nrf2 expression. Studies using GFAP-Nrf2 mice in models of familial amytrophic lateral sclerosis, Huntington's and Parkinson's disease find increased production of glutathione and/or glutathione-related genes[35–38], similarly seen in models of cerebral ischaemia[39,40], all of which were associated with favourable outcomes.

Since astrocyte specific overexpression of Nrf2 has been shown to confer white matter protection in a number of disease models, we wished to build on this work to interrogate the effects of increased expression of astrocytic Nrf2 on white matter vulnerability and behavioural outcomes which are impaired in response to cerebral hypoperfusion. The novelty of the present study was to utlise a cell specific and genetic approach to investigate the putative protective effects of astrocytic Nrf2, unlike previous studies which have mainly used pharmacological approaches to indirectly assess the effects of Nrf2 in hypoperfusion models[41,42]. We hypothesised that overexpression of astrocytic Nrf2 would alleviate hypoperfusion induced cognitive impairment by reducing white matter disruption and inflammation, through glutathione-related mechanisms.

Results

Cortical cerebral blood flow is significantly reduced following bilateral carotid artery stenosis but is not influenced by astrocytic expression of Nrf2. Cortical cerebral blood flow (CBF) was evaluated user laser speckle imaging at baseline (before surgery) and then at 24 hours and 6 weeks after surgery to assess the temporal response to carotid artery stenosis and to determine if there was a difference between wild type and GFAP-Nrf2 mice (Fig. 1). CBF data for each animal was calculated as a percentage of its baseline CBF. Overall, there was a significant effect of time ($F_{(2,64)} = 57.02$, $p < 0.0001$) and bilateral carotid artery stenosis surgery ($F_{(1,32)} = 55.20$, $p < 0.0001$) and a significant interaction between time and surgery ($F_{(2,64)} = 32.63$, $p < 0.0001$). Post hoc analysis indicated that CBF was significantly reduced in wild type and GFAP-Nrf2 hypoperfused mice from their corresponding sham controls at 24 hours ($p < 0.001$) and 6 weeks (WT; $p < 0.001$, GFAP-Nrf2; $p = 0.03$). No overall effect of genotype was detected ($F_{(1,32)} = 0.03$, $p = 0.86$), indicating that overexpression of Nrf2 does not affect resting cortical cerebral blood flow in sham or hypoperfused mice (Fig. 1a).

Cerebral hypoperfusion causes a behavioural impairment in wild type mice which is less pronounced in GFAP-Nrf2 mice. Behaviour was assessed using an 8-arm radial arm maze which has previously been shown to be sensitive to hypoperfusion-induced disruption of frontocortical circuitry[11,13]. Sham wild type and GFAP-Nrf2 transgenic mice had different baseline performances and different patterns of learning over the trial blocks 1–8 (Fig. S1), and thus revisiting errors were analysed separately for these groups to investigate the effect of hypoperfusion over trial blocks 1–4 and 5–8. There was no significant difference in revisiting errors between wild type sham and hypoperfused mice in trials 1–4 ($F_{(1,9)} = 1.51$, $p = 0.25$) but in trials 5–8 wild type hypoperfused mice made significantly more revisiting errors than the sham controls ($F_{(1,9)} = 6.56$, $p = 0.03$) (Fig. 2a). Post hoc analysis found significant differences between wild type sham and hypoperfused animals at block 5, 6 and 7 ($p = 0.01$, 0.04, 0.04 respectively). In contrast, GFAP-Nrf2 sham animals were not significantly different from hypoperfused mice in trials 1–4 ($F_{(1,17)} = 0.33$, $p = 0.57$) and in trials 5–8 ($F_{(1,17)} = 3.81$, $p = 0.07$) (Fig. 2b). There was an overall significant effect of trial for both wild type ($F_{(2.9,25.9)} = 3.39$, $p = 0.04$) and GFAP-Nrf2 mice ($F_{(4,68.3)} = 9.47$, $p < 0.0001$) (Fig. 2a,b), indicative of learning.

To investigate whether there may be genotype differences between the groups, the fold difference of revisiting errors of hypoperfused groups was calculated to respective sham controls and then compared between wild type and GFAP-Nrf2 mice. There was an overall genotype effect ($F_{(1,13)} = 4.79$, $p = 0.048$) (Fig. 2c), a significant effect of trial ($F_{(2.5,32.4)} = 8.70$, $p < 0.0001$) and a significant interaction between trial and genotype ($F_{(2.5,32.4)} = 3.36$,

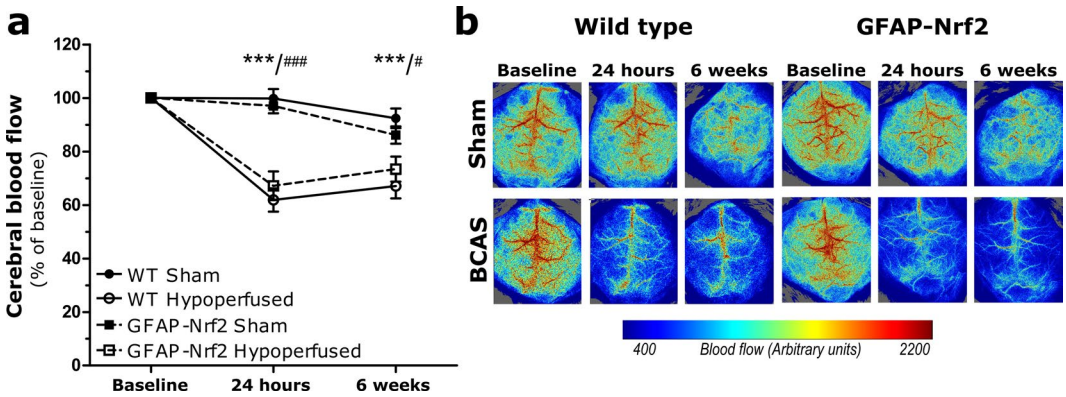

Figure 1. Resting cortical cerebral blood flow (CBF) is significantly reduced following bilateral carotid artery stenosis in wild type and GFAP-Nrf2 mice. (**a**) Resting CBF was significantly reduced by 30–40% from baseline 24 hours after bilateral carotid artery stenosis (BCAS) surgery and remained significantly reduced at 6 weeks for both groups. Effect of time $F_{(2,64)} = 57.02$, $p < 0.0001$, effect of surgery $F_{(1,32)} = 55.20$, $p < 0.0001$, no significant effect of genotype. (**b**) Representative images of laser speckle flowmetry at baseline and at 24 hr and 6weeks post-surgery. Repeated measures ANOVA with Bonferroni adjustment for post hoc analysis. Mean ± SEM. WT/GFAP-Nrf2 ***/$^{###}p < 0.001$, GFAP-Nrf2 $^{#}p = 0.03$. n = 8–10 per group.

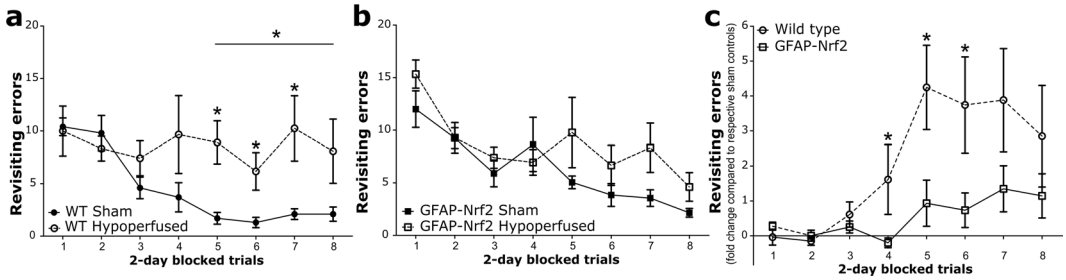

Figure 2. Cerebral hypoperfusion causes an impairment in behavioural performance in wild type mice which is less pronounced in GFAP-Nrf2 mice. Spatial behaviour was assessed by the radial arm maze as revisiting errors over consecutive trials. (**a**) Wild type (WT) hypoperfused animals committed significantly more revisiting errors than WT shams during blocks 5–8 ($F_{(1,9)} = 6.56$, $p = 0.03$). (**b**) GFAP-Nrf2 hypoperfused animals did not make significantly more revisiting errors than the GFAP-Nrf2 shams during blocks 5–8 ($F_{(1,17)} = 3.81$, $p = 0.07$) (**c**) Revisiting error fold difference compared to respective sham controls was used to investigate genotype effect and analysis revealed a significantly higher fold difference in wild type mice ($F_{(1,13)} = 4.79$, $p = 0.048$). Mean ± SEM. Repeated measures ANOVA with Bonferroni adjustment for post hoc analysis. *$p < 0.05$. n = 5–10 per group.

$p = 0.04$). Post hoc analysis identified significant differences in the fold change of revisiting errors between wild type and GFAP-Nrf2 groups at blocks 4, 5 and 6 ($p = 0.046$, 0.02, 0.03 respectively). Thus overall the data suggest a modest protective effect of Nrf2 overexpression on behavioural impairment following cerebral hypoperfusion.

Loss of optic tract white matter integrity caused by cerebral hypoperfusion is less severe in GFAP-Nrf2 mice. Behavioural performance in the radial arm maze is dependent on the integrity of myelinated axons within white matter for efficient communication. The corpus callosum, internal capsule and optic tract were immunostained for myelin associated glycoprotein (MAG) present at the axon-glial interface. The density of MAG+ immunostaining was quantified as percentage area. When the axon-glial interface is disrupted, there is an accumulation of MAG+ debris indicating a loss of white matter integrity[11].

There was no significant loss of white matter integrity as a result of hypoperfusion in the corpus callosum ($F_{(1,32)} = 2.63$, $p = 0.12$) or the internal capsule ($F_{(1,32)} = 0.08$, $p = 0.78$), and no effect of genotype ($F_{(1,32)} = 0.82$, $p = 0.37$; $F_{(1,32)} = 0.17$, $p = 0.68$ respectively) (Fig. 3a,b). However, there was a significant effect of hypoperfusion in the optic tract ($F_{(1,31)} = 13.57$, $p = 0.001$) albeit no significant effect of genotype ($F_{(1,32)} = 0.6$, $p = 0.44$). Post hoc analysis of the effect of hypoperfusion revealed a significant loss of white matter integrity in wild type hypoperfused mice compared to sham controls ($p = 0.004$), but the difference between hypoperfused GFAP-Nrf2 mice and sham controls narrowly missed accepted levels of statistical significance ($p = 0.054$) (Fig. 3c).

To investigate whether the magnitude of white matter integrity loss differs between genotypes, the fold difference of MAG+ debris compared to controls in the optic tract was calculated and compared between wild type and GFAP-Nrf2 mice (Fig. 3d). The fold difference was significantly higher in wild type mice ($p = 0.03$) (Fig. 3d), suggesting a modest protective effect of Nrf2 overexpression on white matter integrity following hypoperfusion.

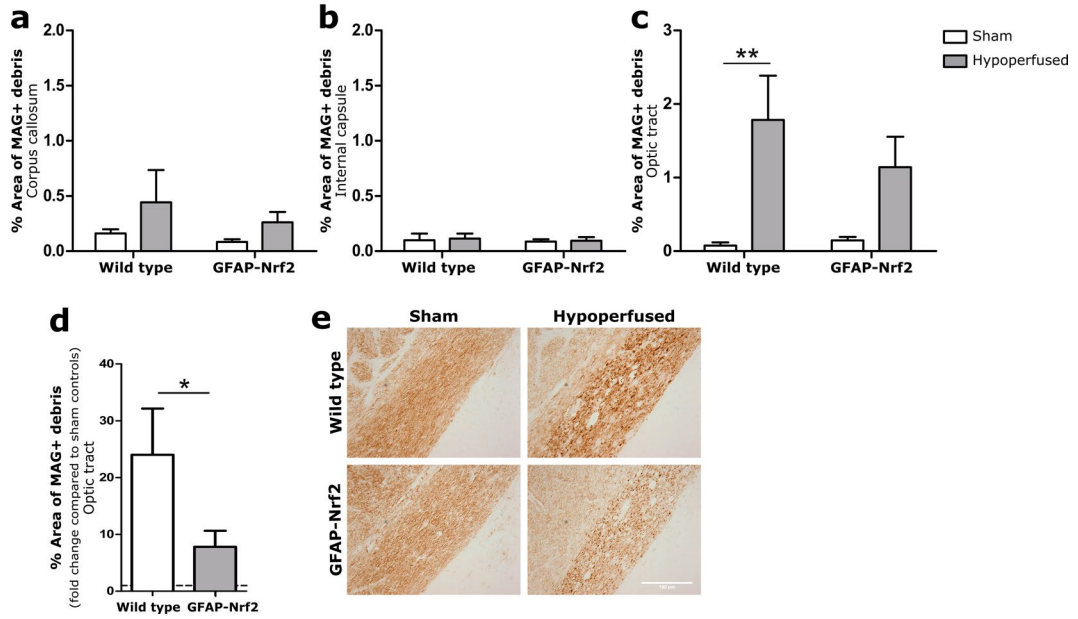

Figure 3. Loss of white matter integrity in response to hypoperfusion. (**a**) There was no significant loss of white matter integrity between groups in the corpus callosum, (**b**) nor in the internal capsule (**c**) but there was a significant effect of cerebral hypoperfusion in the optic tract ($F_{(1,31)} = 13.57$, $p = 0.001$). (**d**) Fold change of white matter integrity loss compared to respective sham controls in the optic tract showed significantly more loss in wild type animals ($p = 0.03$). Dashed line indicates average sham level. (**e**) Representative images of MAG+ staining in the optic tract. Scale bar 100 µm. Mean ± SEM. (**a**–**c**) Two-way ANOVA with Bonferroni adjustment for post hoc analysis. (**d**) Unpaired one-tailed t-test. *$p < 0.05$, ** $p < 0.01$. n = 8–10 per group.

Cerebral hypoperfusion induces micro- and astrogliosis in the optic tract, and astrogliosis is ameliorated by Nrf2-overexpression. Previously it has been shown that inflammation is a key driver of white matter disruption in cerebral hypoperfusion[17]. To assess the microglial/macrophage inflammatory response, Iba1 immunostaining was used and microglia/macrophages were quantified as Iba1+ percentage area in the main white matter tracts; corpus callosum, internal capsule and optic tract. Glial fibrillary acidic protein (GFAP) immunostaining was utilised to assess the astroglial inflammatory response; quantified as GFAP+ percentage area in the corpus callosum, internal capsule and optic tract.

Cerebral hypoperfusion had a significant effect on Iba1 expression in the optic tract ($F_{(1,32)} = 14.74$, $p = 0.001$) (Fig. 4c), but not in the corpus callosum or the internal capsule ($F_{(1,32)} = 2.41$, $p = 0.13$, $F_{(1,32)} = 2.75$, $p = 0.11$ respectively) (Fig. 4a,b). Post hoc analysis revealed significantly greater Iba1+ percentage area in both wild type and GFAP-Nrf2 hypoperfused groups compared to their controls ($p = 0.007$, $p = 0.02$, respectively). There was no effect of genotype in any region (CC-$F_{(1,32)} = 3.12$, $p = 0.09$; IC-$F_{(1,32)} = 2.23$, $p = 0.14$; OT-$F_{(1,32)} = 0.18$, $p = 0.68$).

GFAP + astrocytes were significantly affected by hypoperfusion in the optic tract ($F_{(1,32)} = 38.87$, $p < 0.0001$) (Fig. 5c) but, similar to Iba1 expression and white matter integrity, not in the corpus callosum or the internal capsule ($F_{(1,32)} = 1.43$, $p = 0.24$, $F_{(1,32)} = 2.01$, $p = 0.17$ respectively) (Fig. 5a,b). There was also no effect of genotype in these regions ($F_{(1,32)} = 1.95$, $p = 0.17$, $F_{(1,32)} = 3.34$, $p = 0.08$ respectively). However, there was an effect of genotype in the optic tract ($F_{(1,32)} = 7.45$, $p = 0.01$) and a significant interaction between hypoperfusion and genotype ($F_{(1,32)} = 7.05$, $p = 0.01$). Post hoc tests identified significantly higher GFAP+ percentage are in hypoperfused wild type ($p < 0.001$) and GFAP-Nrf2 groups ($p = 0.01$) but also a significant reduction in the GFAP-Nrf2 hypoperfused group compared to the hypoperfused wild types ($p = 0.001$) (Fig. 5c). This data indicates that astrocytic Nrf2-overexpression reduces astrogliosis induced by cerebral hypoperfusion in the optic tract.

Anti-oxidant-related genes *Slc7a11* and *Gclm* are increased by Nrf2-overexpression. Relative gene expression of *Nrf2*, *Scl7a11* (xCT; encoding the glutamate/cystine antiporter) and *Gclm*, (glutamate-cysteine ligase enzyme subunit), two Nrf2-regulated genes involved in glutathione synthesis were measured in a whole brain slice corresponding to the level of pathological assessment using qPCR and compared across groups.

There was a significant 3.5-fold increase in *Nrf2* mRNA expression in GFAP-Nrf2 animals compared to wild type ($F_{(1,32)} = 298$, $p < 0.0001$), with no effect of hypoperfusion ($F_{(1,32)} = 0.16$, $p = 0.69$) (Fig. 6a). In addition, these changes were accompanied by a ~2-fold increase in *Slc7a11* and *Gclm* in GFAP-Nrf2 mice ($F_{(1,32)} = 74.05$, $p < 0.0001$, $F_{(1,32)} = 737.5$, $p < 0.0001$ respectively), again, with no effect of hypoperfusion ($F_{(1,32)} = 0.26$, $p = 0.61$, $F_{(1,32)} = 0.08$, $p = 0.79$). These results may indicate a greater anti-oxidant capacity of GFAP-Nrf2 animals compared to wild types. Since there was no effect of hypoperfusion on the expression levels of these genes we considered whether subtle alterations in gene expression in predominantly white matter may be masked by measurements of gene expression in total brain homogenates. We therefore next investigated gene expression in white matter enriched samples.

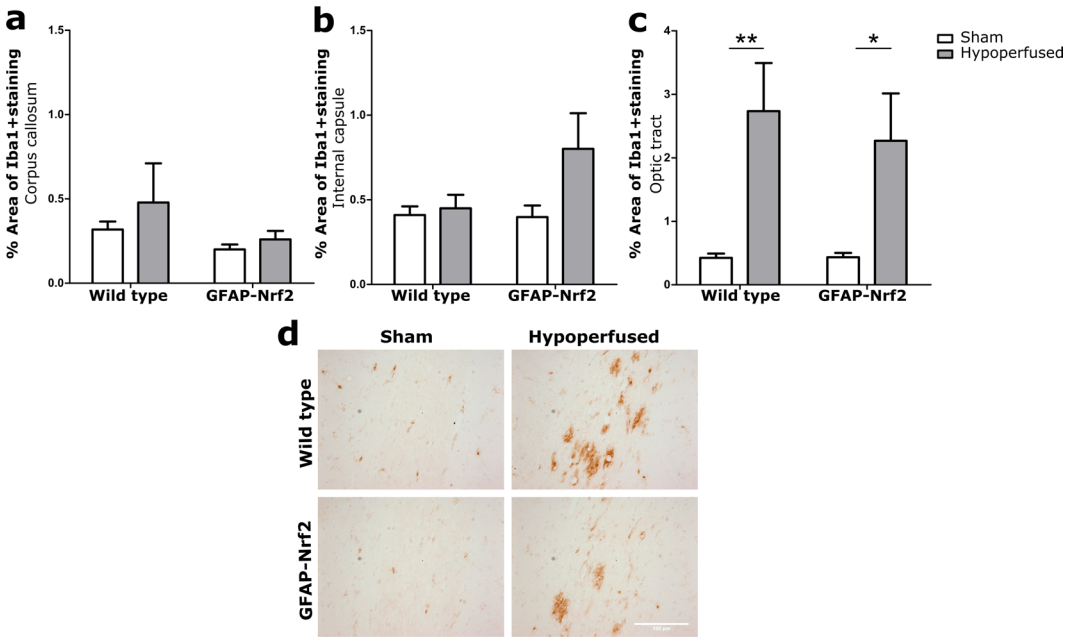

Figure 4. Increased microglia/macrophages in response to hypoperfusion. (**a**) % Area of Iba1+ staining in the corpus callosum and (**b**) internal capsule was unchanged following cerebral hypoperfusion. (**c**) % Area of Iba1+ staining in the optic tract was significantly altered by cerebral hypoperfusion ($F_{(1,32)} = 14.74$, $p = 0.001$), with no effect of genotype. (**d**) Representative images of Iba1+ staining in the optic tract. Scale bar 100 µm. Mean ± SEM. Two-way ANOVA with Bonferroni adjustment for post hoc analysis. *$p < 0.05$, ** $p < 0.01$. $n = 8–10$ per group.

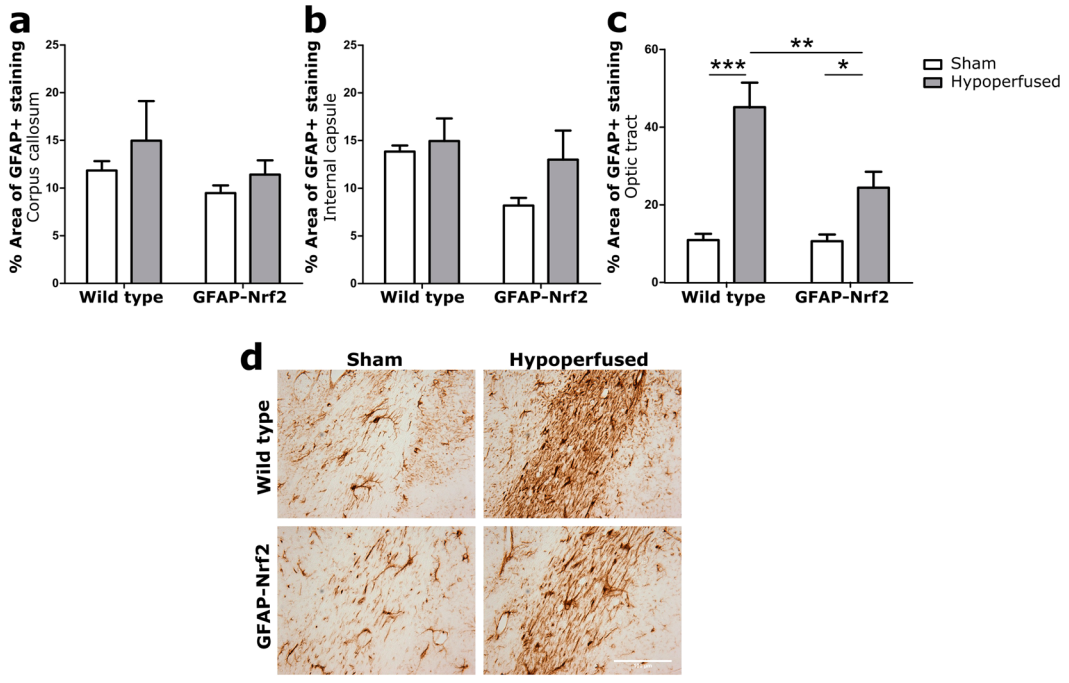

Figure 5. Astrogliosis in response to hypoperfusion was less severe in GFAP-Nrf2 animals. (**a**) % Area of GFAP+ staining in the corpus callosum and (**b**) internal capsule was unchanged following cerebral hypoperfusion. (**c**) % Area of GFAP+ staining in the optic tract was significantly increased by cerebral hypoperfusion ($F_{(1,32)} = 38.87$, $p < 0.0001$), with a significant effect of genotype ($F_{(1,32)} = 7.45$, $p = 0.01$). (**d**) Representative images of GFAP+ staining in the optic tract. Scale bar 100 µm. Mean ± SEM. Two-way ANOVA with Bonferroni adjustment for post hoc analysis. *$p < 0.05$, **$p < 0.01$, ***$p < 0.001$. $n = 8–10$ per group.

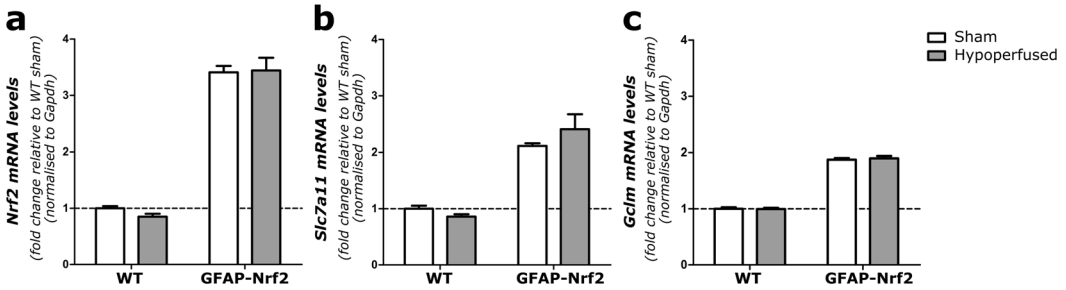

Figure 6. Nrf2, Slc7a11 and Gclm relative gene expression is higher in GFAP-Nrf2 animals with no effect of hypoperfusion. (**a**) *Nrf2*, (**b**) *Slc7a11* and **(c)** *Gclm* expression was significantly higher in GFAP-Nrf2 animals ($F_{(1,32)} = 298$, $p < 0.0001$, $F_{(1,32)} = 74.05$, $p < 0.0001$, $F_{(1,32)} = 737.5$, $p < 0.0001$; respectively), but this was not altered by hypoperfusion. Gene expression was normalised to *Gapdh* and expressed relative to WT sham controls. Dashed line indicates average WT sham level. Mean ± SEM. Two-way ANOVA. n = 8–10 per group.

Cerebral hypoperfusion induces pro-inflammatory gene expression in the optic tract and Nrf2-overexpression reduces the expression of complement component 4. Alterations in gene expression were investigated in optic tract enriched samples since we had previously determined glial alterations in this region. *Nrf2* expression in the optic tract was similar to that of the whole brain sample with an increase in GFAP-Nrf2 animals compared to wild type ($F_{(1,32)} = 116.4$, $p < 0.0001$), and no further effect of hypoperfusion ($F_{(1,32)} = 0.47$, $p = 0.5$) (Fig. 7a). To further investigate the involvement of the glutathione anti-oxidant system we measured *Gclm* expression in the optic tract enriched samples, but similarly found an effect of genotype only ($F_{(1,31)} = 49.83$, $p < 0.0001$) and no effect of hypoperfusion ($F_{(1,31)} = 0.22$, $p = 0.65$) (Fig. 7b). Collectively our results suggest that anti-oxidant gene alterations cannot explain the white matter protection conferred in hypoperfused GFAP-Nrf2 mice at this time. As an alternative, we explored the inflammatory milieu beyond the cellular responses as an alternative mechanism whereby Nrf2 may confer protection following hypoperfusion. We measured gene expression of complement component 4 and 1q (*C4, C1q*); initiators of the complement system which play an important role in the innate immune response[43]. In addition, we measured gene expression of two chemokines; *Ccl3 (Mip-1α)* and *Ccl2 (Mcp-1)*, which have previously been shown to be upregulated at the protein level following severe hypoperfusion[18].

Hypoperfusion significantly increased the expression of *C4, C1q*, and *Ccl3* expression ($F_{(1,32)} = 8.07$, $p = 0.008$, $F_{(1,32)} = 7.92$, $p = 0.008$, $F_{(1,29)} = 8.68$, $p = 0.006$; respectively) (Fig. 7c–e), whereas *Ccl2* expression was reduced by hypoperfusion ($F_{(1,31)} = 6.09$, $p = 0.02$). *C4* expression was also significantly different in GFAP-Nrf2 animals ($F_{(1,32)} = 5.66$, $p = 0.02$) and post hoc analysis found significant upregulation in wild type hypoperfused ($p = 0.005$) but not GFAP-Nrf2 hypoperfused animals ($p = 0.39$), and further that *C4* expression was significantly lower in GFAP-Nrf2 compared to wild type hypoperfused animals ($p = 0.007$). *C1q* expression followed a similar pattern, however there was no overall genotype effect ($F_{(1,32)} = 0.05$, $p = 0.83$). Post hoc tests found a significant increase of *C1q* in hypoperfused wild types compared to shams ($p = 0.02$), but found no significant difference between GFAP-Nrf2 groups ($p = 0.13$). No effect of genotype was detected on *Ccl3* and *Ccl2* expression ($F_{(1,29)} = 0.12$, $p = 0.73$, $F_{(1,31)} = 1.62$, $p = 0.21$; respectively), and post hoc analysis identified significant differences between GFAP-Nrf2 groups ($p = 0.03$, $p = 0.01$; respectively) but not between wild type groups ($p = 0.07$, $p = 0.35$; respectively). Together the data indicates that cerebral hypoperfusion increases the expression of pro-inflammatory genes and that Nrf2-overexpression in astrocytes may protect white matter integrity and behavioural performance by selectively suppressing aspects of this inflammatory response.

Discussion

The present study demonstrates that astrocytic overexpression of Nrf2 exerts beneficial effects in a mouse model of chronic cerebral hypoperfusion and alleviates loss of white matter integrity and astrogliosis in the optic tract, in parallel with improved functional impairment. These protective effects appear to be mediated via repression of specific inflammatory genes.

In agreement with previous studies, we show that bilateral carotid artery stenosis (BCAS) induces mild, sustained cerebral hypoperfusion in wild type and Nrf2-overexpressing mice[15]. The extent of CBF reduction (~30–40% at 24 hours) and gradual amelioration over 6 weeks is comparable to previously published studies[9,44,45]. Notably, we found no difference in the extent of CBF reduction between wild type and GFAP-Nrf2 mice at 24 hours and 6 weeks post-BCAS. We may have expected differences between the groups as the absence of Nrf2 has previously been shown to have vascular related effects acting to impair angiogenic capacity *in vitro*[46–48] and inhibit the upregulation of vascular endothelial growth factor (VEGF) in an *in vivo* model of venous hypertension[49]. We find increased VEGF expression and other angiogenic genes at 3 days following hypoperfusion[12], and promoting vascular remodelling is currently explored in models of hypoperfusion to establish its potential in the treatment of vascular dementia, as discussed in[50]. The current study found that astrocytic Nrf2-overexpression does not alter CBF responses following BCAS surgery, which therefore allowed us to investigate the effects of Nrf2 without confounding flow-related differences.

Consistent with previous studies, we show that hypoperfusion induces impairments in spatial behaviour as measured by the radial arm maze in wild type mice following bilateral carotid artery stenosis[11,13]. Wild type and GFAP-Nrf2 sham mice were able to learn the task with increasing trial duration but the hypoperfused mice

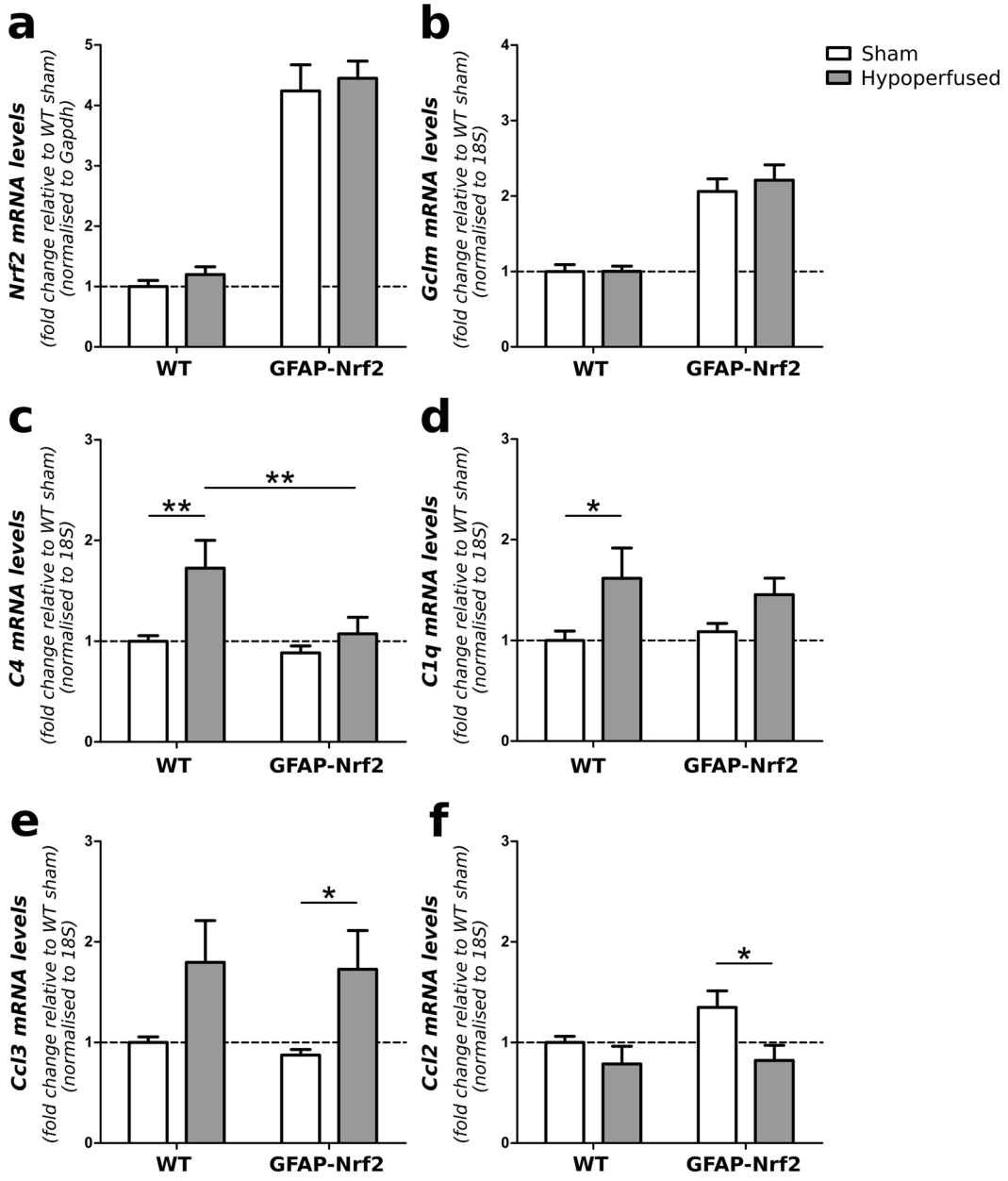

Figure 7. Cerebral hypoperfusion induces pro-inflammatory gene expression in the optic tract and Nrf2-overexpression reduces the expression of complement component 4. (**a**) *Nrf2* and (**b**) *Gclm* expression in the optic tract was significantly higher in GFAP-Nrf2 animals ($F_{(1,32)} = 116.4$, $p < 0.0001$, $F_{(1,31)} = 49.83$, $p < 0.0001$ respectively), but was not altered by hypoperfusion. (**c**) *C4* expression in the optic tract was significantly increased by hypoperfusion ($F_{(1,32)} = 8.07$, $p = 0.008$) with a significant effect of genotype ($F_{(1,32)} = 5.66$, $p = 0.02$). (**d**) Hypoperfusion significantly increased *C1q* and (**e**) *Ccl3* expression in the optic tract ($F_{(1,32)} = 7.92$, $p = 0.008$, $F_{(1,29)} = 8.68$, $p = 0.006$; respectively), but reduced the expression of *Ccl2* ($F_{(1,31)} = 6.09$, $p = 0.02$). There was no effect of genotype on the expression of *C1q*, *Ccl3* or *Ccl2*. Gene expression was normalised to *Gapdh* or *18S* and expressed relative to WT sham controls. Dashed line indicates average WT sham level. Mean ± SEM. Two-way ANOVA with Bonferroni adjustment for post hoc analysis. *$p < 0.05$, **$p < 0.01$, $n = 8$–10 per group.

in both cohorts were impaired compared to their controls. It was noted that the baseline learning pattern was different in the wild type and GFAP-Nrf2 mice. To the best of our knowledge no previously published studies using this transgenic mouse line have investigated cognitive changes, and we found no reports of altered cognition at baseline in models of Nrf2-overexpression/activation. One explanation may be a disruption in redox balance. Reactive oxygen species (ROS), albeit detrimental in excess, are cell signalling molecules[51] important for synaptic plasticity[52,53], and it is possible that Nrf2-overexpression affects spatial behaviour by excessive ROS depletion. Despite this different baseline learning pattern, GFAP-Nrf2 sham mice successfully learned the task

and the extent of impairment in spatial working memory in GFAP-Nrf2 hypoperfused mice was significantly less pronounced as compared to wild type mice. Thus the data supports our hypothesis that increased expression of Nrf2 may protect against hypoperfusion induced functional impairment.

Since the functional impairment was less pronounced in GFAP-Nrf2 mice this suggested that there may be less extensive pathological alterations. Previous studies, including ours, indicated that white matter is particularly vulnerable to cerebral hypoperfusion[9–11,54]. There is progressive axon-glial disruption,[12,15], myelin disruption[10,11,14] and reduced corpus callosal volume following cerebral hypoperfusion[55]. The current study agrees with previous findings of hypoperfusion-induced loss of white matter integrity, however only in the optic tract where the extent of pathology is more severe than previously reported. The main difference between this study and former is the background strain on which the animals were bred; FVB/C57Bl/6J F1 compared to pure C57Bl/6J. There is a possibility that the optic tract in FVB/C57Bl/6J F1 mice is more vulnerable to hypoperfusion than C57Bl/6J mice due to genetic differences. It is also reported that the cerebral vasculature of different strains is differently organised and may therefore present with different spatial distribution and severity of hypoperfusion[56]. The heightened vulnerability of the optic tract may also account for the impaired behaviour in the radial arm maze in the hypoperfused mice. Pure FVB/N mice are known to be visually impaired from an early age due to a mutation causing retinal degeneration[57]. However, it is unlikely that the mice were visually impaired since our FVB/C57 first generation cross successfully learned the visual-dependent radial arm maze task and we observed no altered behaviour indicating visual impairment in any of the mice. However, we cannot discount that disruption of the optic tract in hypoperfused mice resulted in impaired visual acuity and impaired performance on the radial arm maze task.

Protection against white matter damage using Nrf2-activating compound DMF has been reported in a mouse model of experimental autoimmune encephalitis (EAE)[30] and severe hypoperfusion[18], both of which present with substantial white matter disruption. The subtle pathology observed in this study, compared to above and previously published 1 month hypoperfusion studies[10–12,15], may have limited the ability to investigate the modulation of pathology with Nrf2-overexpression completely. Nonetheless, despite these confounds, there was an effect of GFAP-Nrf2 overexpression on the extent of white matter pathology in the optic tract and notably these mice also exhibited improved behavioural abilities. Thus the data indicate that astrocyte specific Nrf2-overexpression may alleviate behavioural impairments by preventing loss of white matter integrity in the optic tract.

We have shown previously in the hypoperfusion model that microgliosis precedes significant increases in reactive astrocytes, and associations between microgliosis and impaired white matter function suggests that microglia are important contributors to the disease process[17,18]. Other groups have shown associations between astrogliosis and impaired white matter integrity[58] and spatial working memory following cerebral hypoperfusion[59], suggestedly through activation of the pro-inflammatory transcription factor NF-κB[58] and reduced astroglial glutamate uptake[59]. In the current study, both micro- and astrogliosis were increased, however only in the optic tract of hypoperfused mice. The regional discrepancy between this study and previous may be attributed to the background strain, which as previously mentioned, may respond to hypoperfusion differently due to do variances in cerebrovascular arrangement[56]. Overexpression of Nrf2 reduced the extent of astrogliosis, but did not have an effect on microgliosis after hypoperfusion. This was somewhat unexpected as GFAP-Nrf2 mice have previously been shown to reduce both astro- and microgliosis in models of Parkinson's Disease[37,38], and Nrf2-deficiency induced robust microgliosis in a model of EAE[29]. There is conflicting evidence of the effect of Nrf2 on gliosis in other models, for example in the transgenic Alzheimer's disease mouse model APP/PS1. One study found that only astrogliosis was reduced by Nrf2[60], and another found that both astro- and microgliosis were affected[61], however both were associated with improved cognition. The differences may be accounted for by different means of Nrf2-activation; lentiviral-Nrf2 hippocampal injection[60], oral administration of the Nrf2-activating compound methysticin[61] or transgenic overexpression of Nrf2 in astrocytes[37,38]. Our contrasting results from previous studies in GFAP-Nrf2 mice may be explained by the different experimental models, and perhaps particularly by the comparably more subtle pathology. Importantly this study demonstrates that increased Nrf2 expression in astrocytes alone can have downstream beneficial effects on optic tract white matter integrity and behaviour. Together, these result further support the therapeutic potential of activating the Nrf2-pathway in cerebrovascular and neurodegenerative disease. A plethora of pharmacological compounds capable of activating the Nrf2-pathway are currently under investigation (reviewed in[62,63]).

To probe mechanisms by which Nrf2 overexpression may mediate protective effects, the levels of two glutathione-related genes; *Slc7a11* (*xCT*) and *Gclm* were measured. The glutathione system forms an important part of cellular anti-oxidant capacity[64] and has been shown previously to be upregulated by ischaemic preconditioning in an Nrf2-dependent manner[40], as well as in GFAP-Nrf2 mice in several models of neurodegenerative disease[35–37]. We found an increase in both *Slc7a11* and *Gclm* in GFAP-Nrf2 compared to wild type mice, however contrary to expectations there were no further increases in these genes with hypoperfusion. Given that hypoperfusion induces oxidative damage[23,65], we expected increased anti-oxidant gene expression also in wild type hypoperfused animals indicative of Nrf2-pathway activation. Instead, anti-oxidant enzymes were determined to be increased only in GFAP-Nrf2 animals; in line with a study in a transgenic model of Parkinsons disease[37]. Our results suggest that hypoperfusion in wild type mice is insufficient to induce Nrf2 expression and activation directly, although the constitutively higher glutathione-related gene expression in the GFAP-Nrf2 animals may indicate a higher capacity of glutathione synthesis which may provide some protection to white matter following hypoperfusion. However, we are unable to conclude this without direct measures of glutathione. A model of Alexander disease found glutathione-independent protective effects of GFAP-Nrf2 expression[66], and a proteomic study of Nrf2-overexpressing astrocytes found important roles of detoxifying and anti-inflammatory enzymes catalase, peroxiredoxin-6 and prostaglandin reductase 1[67] which could alternatively be implicated following hypoperfusion as opposed to increased glutathione synthesis. The inability to detect anti-oxidant gene expression may be explained by the lack of sensitivity of transcriptome measures in total brain homogenates but since we determined similar effects in optic-tract enriched samples, where prominent axon-glial alterations were detected, a lack of

gene alterations is unlikely due to sampling. An alternate explanation is that the protective effect seen in the study is mediated by modulation of the inflammatory environment rather than by anti-oxidant mechanisms. We investigated this by further qPCR analysis of optic tract-enriched samples of a panel of pro-inflammatory genes; *C4* and *C1q*; complement component 4 and 1q, and *Ccl3 (MIP-1α)* and *Ccl2 (MCP-1);* chemokine (C-C motif) ligand 3 and 2. The complement system is an important part of the innate immune system, aiding early responses to infection or injury. It contributes to the adaptive immune system by interacting with antigen/antibody complexes eliciting a cascade of proteolytic events which ultimately boost phagocytosis and inflammation by the recruitment of more inflammatory cells[43]. *Ccl3/Ccl2* encode pro-inflammatory chemokines involved in the recruitment of microglia and astrocytes as well as peripheral monocyts and macrophages[68,69]. Increased expression of complement components as well as pro-inflammatory chemokines has long been recognised as an indication of chronic inflammation for example in Alzheimer's disease[70–72]. Our previous work found increased expression of *C4* and a putative receptor for C1q, in white matter at 72 hours post-hypoperfusion[12] and in whole brain at 4 weeks following mild hypoperfusion in wild type mice (*unpublished obeservations*) using microarray analysis, and increased protein levels of Ccl3 and Ccl2 following severe hypoperfusion[18]. Consistent with previous work, an increase in *C4, C1q* and *Ccl3* expression following hypoperfusion was determined in wild type mice, indicative of ongoing inflammation. In Nrf2 overexpressing mice the extent of this increase in complement related genes was dampened. C1q as the initiating molecule in the classical complement pathway provides the downstream product for which C4 is a substrate[73]. Complement activation has been suggested to potentiate chronic inflammation and neurodegeneration[74,75], and has been demonstrated to trigger neuroinflammation following traumatic brain injury[76]. Since direct inhibition of complement has been neuroprotective in mouse models of Alzheimer's disease[77] and cerebral ischaemia[78,79], reduced complement activation may be a mechanism whereby Nrf2-overexpression is protective following hypoperfusion. A recently proposed hypothesis of neuroinflammation is that activated microglia release pro-inflammatory mediators (including complement C1q and C3) inducing astrocyte reactivity which in turn is detrimental to surrounding cells and tissues[74]. Our results in astrocyte-specific Nrf2-overexpressing animals find reduced astrogliosis but similar coverage of microglia as wild types, reflected also by comparable levels of expression of the chemokine *Ccl3*. If microglia are responsible for inducing astrogliosis, reduced astrogliosis in this study may result from less pro-inflammatory signalling from microglia in Nrf2-overexpressing animals. Recent evidence has demonstrated that Nrf2 not only induces the expression of cytoprotective genes, but is also able to suppress expression of pro-inflammatory genes directly[80]. Since the Nrf2-overexpression is selectively in astrocytes, another possibility is that these may also be more resistant to microglia-driven pro-inflammatory signalling as a result of increased Nrf2-signalling. In contrast to our previous work where Ccl2 protein was increased at 1 week after severe hypoperfusion,[18], *Ccl2* expression was determined to be downregulated with mild hypoperfusion at 6 weeks. The discrepancy may be due to differences in anatomical areas sampled which may display altered pro-inflammatory responses and/or the differing extent of hypoperfusion. Overall, the differential change in inflammatory gene expression likely reflects the spatial and temporal heterogeneity of inflammatory responses to hypoperfusion.

In conclusion, these results indicate that Nrf2 overexpression in astrocytes dampens aspects of hypoperfusion-induced inflammation in the optic tract, possibly by Nrf2-driven suppression of pro-inflammatory genes or by increased anti-inflammatory gene expression, ultimately reducing optic tract astrogliosis and loss of white matter integrity paralleled by improved functional outcome. This adds support to the use of Nrf2-activators as potential treatment for cerebrovascular-related inflammation and white-matter degeneration.

Methods

Animals. GFAP-Nrf2.2 mice were imported from Prof. JA Johnson, University of Wisconsin, and were on an FVB background. These mice were developed as previously described in[35] and Nrf2-overexpression in astrocytes was driven by a GFAP promoter. GFAP-Nrf2 mice were then crossed with wild type C57Bl/6J in-house. The first generation crosses including transgenic GFAP-Nrf2 and wild type littermates aged 4–5 months were utilised for the study (GFAP-Nrf2, FVB/C57Bl/6J F1). All mice used for the studies were on the same genetic background. Animals were initially group housed on a 12-hour light/dark cycle with *ad libitum* access to food and water, and assigned experimental groups by genotype then randomly assigned surgery; wild type sham (n = 8), wild type hypoperfused (n = 10), GFAP-Nrf2 sham (n = 10), GFAP-Nrf2 hypoperfused (n = 12). All mice were male. All experiments were conducted in accordance with the Animal (Scientific Procedures) Act 1986 and local ethical approval at the University of Edinburgh, and were performed under personal and project licences granted by the Home Office according to ARRIVE guidelines. Four animals tolerated surgery poorly and had to be culled. Final numbers were hence as follows; wild type sham (n = 8), wild type hypoperfused (n = 8), GFAP-Nrf2 sham (n = 10), GFAP-Nrf2 hypoperfused (n = 10). Experimenters were blind to genotype and surgery status of the mice throughout data collection and analysis.

Bilateral carotid artery stenosis. Animals underwent bilateral carotid artery stenosis (BCAS) surgery as developed by[9] under isoflurane anaesthesia using 0.18 mm internal diameter microcoils placed around both common carotid arteries. Sham surgery includes the entire procedure except for placement of the microcoils. All surgical procedures were conducted using aseptic techniques.

Laser speckle imaging. Baseline measurements of cortical cerebral perfusion were acquired prior to, 24 hours and 6 weeks post-BCAS surgery using a Moor FLPI2 laser speckle contrast imager (Moor Instruments, UK). The animal was anaesthetised using isoflurane and its' head held in position using a stereotactic frame. Body temperature was regulated using a heated pad and the skull was exposed by a midline incision and reflection of the skin of the head. Water-based gel was evenly spread on the exposed skull and a 2-min perfusion recording was acquired. The skull was then sutured and local anaesthetic applied to reduce any pain or discomfort to the animal which was then recovered in a heat regulated box.

8-arm radial arm maze to assess behavioural alterations. Animals were singly housed and food restricted (maintained at 85% of initial body weight) one week prior to, and throughout the radial arm maze test, to promote motivation (12-hour light/dark cycle, *ad libitum* access to water). Following the last trial animals were again provided food *ad libitum*. The radial arm maze test was commenced one month after hypoperfusion.

The radial arm maze comprises a central platform (20 cm in diameter) surrounded by 8 arms (47 cm long by 7 cm wide with 20 cm Plexiglas walls). Each arm has a 2-cm deep plastic well for placement of a sugar pellet and all arms can be isolated from the central platform by Plexiglas doors (remotely controlled using Any-Maze software, Stoelting, UK). Large visual cues were placed on each of the four walls surrounding the maze, and a camera mounted on the ceiling was used for data acquisition (Any-Maze software, Stoelting, UK).

Pre-training consisted of one 5 min trial of free exploration with sugar pellets scattered at random, and one where each animal was allowed to walk down each arm from the central platform to retrieve sugar pellets from the plastic cups.

The training was carried out for 16 consecutive days (1 trial/day). Each arm was baited with a sugar pellet and the animal was placed in the central platform at the start of the trial. The animal was confined to the central platform for 5 seconds between each arm choice and the trial finished when the animal had retrieved all 8 pellets or when 25 minutes had elapsed. The number of revisiting errors (visits into unbaited arms) during each trial were recorded and analysed as a measure of behaviour.

Animals that explored less than 75% of the maze during 2 of the first 4 trials were excluded from analysis due to lack of motivation resulting in skewed learning profile. That resulted in the final numbers for the behavioural analysis; wild type sham (n = 5), wild type hypoperfused (n = 6) GFAP-Nrf2 sham (n = 10), GFAP-Nrf2 hypoperfused (n = 10).

Tissue processing. Following the behavioural testing, animals were sacrificed under deep anaesthesia by transcardiac perfusion and hemi brains were snap frozen in liquid nitrogen or post-fixed in 4% paraformaldehyde for 24 hours and further processed for paraffin embedding. 6 µm thick coronal tissue sections were collected at −1.70 mm posterior of bregma according to[81] using a rotary microtome (Leica Biosystems, Germany). The corresponding level of the frozen hemi brain was used for RNA extraction and qPCR analysis. In some experiments the optic tract was identified and isolated to produce preparations enriched in optic tract for qPCR analysis.

Immunohistochemistry. Standard laboratory procedures were utilised for immunostaining. Sections were deparaffinised and endogenous peroxidase quenched in 3% H_2O_2 in methanol and antigen retrieval was carried out when required (Iba1 and GFAP) in 10 mM citric acid buffer (pH 6.0) at 95 °C for 10 min. Sections were blocked with 10% normal serum and 0.5% bovine albumin serum before overnight primary antibody incubation at 4 °C. Biotinylated secondary antibodies were incubated for 1 hour at room temperature and then further amplified; 1 hour at room temperature in Vector ABC Elite Kit (Vector Labs, UK), before visualisation of peroxidase activity using 3,3′ diaminobenzidine tetrahydrochloride (DAB, Vector Labs, UK). Primary antibodies and concentration used were as follows; Iba1 rabbit polyclonal Menarini, cat no. MP-290, 1:1000; GFAP rat monoclonal Life Technologies, cat no. 13-0300, 1:1000; MAG mouse monoclonal Abcam, cat no. ab89780, 1:15,000. Images were acquired using an Olympus BX51 microscope (x20, Olympus, UK) and analysed using ImageJ software (v1.46, NIH, Bethesda, MD, USA). The density of MAG+, Iba1+ and GFAP+ immunostaining was quantified as percentage area. The background was subtracted and a global manual threshold applied. All stains were evaluated in the corpus callosum, the internal capsule and the optic tract which were manually delineated by the experimenter.

RNA extraction, reverse transcription-PCR and quantitative (q)-PCR. RNA was extracted using the QIAGEN RNeasy Lipid Tissue Mini Kit according to manufacturer's instruction. Briefly, <100 mg fresh frozen tissue was homogenised in 1 ml QIAzol® lysis reagent using the Qiagen automated tissue lyser system and metal beads. The homogenate was transferred to fresh RNase/DNase free tubes and incubated for a couple of minutes at room temperature with 200 µl chloroform. The upper aqueous phase was collected following 15 min centrifugation at 4 °C (12,000 × *g*), and RNA was subsequently purified in mini spin columns and washed with a series of buffers before it was eluted in RNase free water. RNase-free DNase I (Thermo Scientific) was used to remove genomic DNA according to manufacturer's instruction. cDNA was synthesised from 0.1–1 µg RNA using the Roche Transcriptor First Strand cDNA Synthesis Kit, according to manufacturer's instruction. Briefly, RNA was added to reverse transcriptase (RT) reaction mix and cycled through 10 min 25 °C; 30 min 55 °C; 5 min 85 °C. NoRT control was run alongside and cDNA was diluted to the equivalent of 3 ng initial RNA per 15 µl qPCR reaction. The CFX96 Real-Time PCR Machine (Bio Rad) was used with the DyNAmo ColorFlash SYBR Green qPCR kit according to manufacturer's instructions (Thermo Scientific). cDNA template was mixed with SYBR green master mix, water and forward and reverse primer (200 nM each final concentration). Samples were run in duplicates alongside no template and no RT negative controls. Primers were validated to confirm efficiency prior to use and sequences used are as follows: *Gapdh*-F: 5′-GGGTGTGAACCACGAGAAAT-3′, *Gapdh*-R: 5′-CCTTCCACAATGCCAAAGTT-3′, *18S*-F: 5′-CCCAGTAAGTGCGGGTCAT-3′, *18S*-R: 5′-CCGAGGGCCTCACTAAACC-3′, *Nrf2*-F: 5′-CAGCTCAAGGGCACAGTGC-3′, *Nrf2*-R: 5′-GTGGCCCAAGTCTTGCTCC-3′, *Slc7a11*-F: 5′-ATACTCCAGAACACGGGCAG-3′, *Slc7a11*-R: 5′-AGTTCCACCCAGACTCGAAC-3′, *Gclm*-F: 5′-GCACAGCGAGGAGCTTC-3′, *Gclm*-R: 5′-GAGCATGCCATGTCAACTG-3′, *C4*-F: 5′-ACAACAAGGGAGACCCCCAG-3′, *C4*-R: 5′-GCTCAGAGAGCCAGAGTCCTA-3′, *C1q*-F: 5′-CAAGGACTGAAGGGCGTGAA-3′, *C1q*-R: 5′-CAAGCGTCATTGGGTTCTGC-3′, *Ccl3*-F: 5′-GCCAGGTGTCATTTTCCTGACT-3′, *Ccl3*-R: 5′-TCAGGCATTCAGTTCCAGGTC-3′, *Ccl2*-F: 5′-TCCCAAAGAAGCTGTAGTTTTTGTC-3′, *Ccl2*-R: 5′-CCCATTCCTTCTTGGGGTCA-3′.

The qPCR cycling programme was 10 min at 95 °C; 40 cycles of 30 s at 95 °C, 30 s at 65 °C (/30 s at 62.5 °C for *C1q* and *Ccl2* experiment/40 s at 60 °C for *Gclm* experiment, 62.5 °C) with detection of fluorescence, 30 s at 72 °C; 1 cycle (for dissociation curve) of 1 min at 95 °C and 30 s at 55 °C with a ramp up to 30 s at 95 °C with continuous detection of fluorescence The *C4* experiment was run at 7 min at 95 °C initially and then 40 cycles of 10 s at 95 °C, 30 s at 65 °C (/30 s at 60 °C for *Ccl3* experiment) with detection of fluorescence followed by the dissociation curve. Data was normalised to *Gapdh* or *18S* expression as reference and expressed as fold change of wild type sham expression.

Due to minute volumes of optic tract enriched RNA samples, more variation was present in these qPCR experiements. Criteria were therefore defined to exclude samples from qPCR analysis if housekeeper gene was detected >3Ct away from the mean or if gene of interest expression was 1.5 interquartile ranges less than the first quartile, or 1.5 interquartile ranges more than the third quartile for each group mean. The *Ccl3* experiment therefore had three samples exluded, and *Gclm* and *Ccl2* experiments one sample each excluded from analysis. Final numbers for these experiments were hence as follows; *Ccl3* -wild type sham (n = 7), wild type hypoperfused (n = 7) GFAP-Nrf2 sham (n = 10), GFAP-Nrf2 hypoperfused (n = 9), *Gclm* - wild type sham (n = 7), wild type hypoperfused (n = 8) GFAP-Nrf2 sham (n = 10), GFAP-Nrf2 hypoperfused (n = 10) and *Ccl2* - wild type sham (n = 8), wild type hypoperfused (n = 7) GFAP-Nrf2 sham (n = 10), GFAP-Nrf2 hypoperfused (n = 10). All other qPCR experiments included all samples.

Statistical analysis. Statistical analysis was performed using SPSS (v22, IBM Corp.) or Graphpad Prism (v5, GraphPad Software Inc, La Jolla, USA). Data are presented as mean ± SEM. Normally distributed data was analysed by analysis of variance (ANOVA). Repeated measure ANOVA was used to analyse cerebral blood flow and revisiting errors over time/trials and 2-way ANOVA was performed to test for hypoperfusion/genotype effects of immunohistochemistry and qPCR data. Bonferroni adjustment was used for post hoc analysis. Significance was determined at $p < 0.05$.

Data availability. The data sets generated during the current study are available from the corresponding authors upon reasonable request.

References

1. Wardlaw, J. M., Smith, C. & Dichgans, M. Mechanisms of sporadic cerebral small vessel disease: insights from neuroimaging. *Lancet Neurol* **12**, 483–497, https://doi.org/10.1016/s1474-4422(13)70060-7 (2013).
2. Smith, E. E. Clinical presentations and epidemiology of vascular dementia. *Clinical science (London, England: 1979)* **131**, 1059–1068, https://doi.org/10.1042/cs20160607 (2017).
3. Schmidt, R. *et al*. White matter lesion progression in LADIS: frequency, clinical effects, and sample size calculations. *Stroke; a journal of cerebral circulation* **43**, 2643–2647, https://doi.org/10.1161/strokeaha.112.662593 (2012).
4. Inzitari, D. *et al*. Changes in white matter as determinant of global functional decline in older independent outpatients: three year follow-up of LADIS (leukoaraiosis and disability) study cohort. *Bmj* **339**, b2477, https://doi.org/10.1136/bmj.b2477 (2009).
5. Fernando, M. S. *et al*. White matter lesions in an unselected cohort of the elderly: molecular pathology suggests origin from chronic hypoperfusion injury. *Stroke; a journal of cerebral circulation* **37**, 1391–1398, https://doi.org/10.1161/01.str.0000221308.94473.14 (2006).
6. Barker, R. *et al*. Pathophysiology of white matter perfusion in Alzheimer's disease and vascular dementia. *Brain: a journal of neurology* **137**, 1524–1532, https://doi.org/10.1093/brain/awu040 (2014).
7. Boyle, P. A. *et al*. White matter hyperintensities, incident mild cognitive impairment, and cognitive decline in old age. *Annals of clinical and translational neurology* **3**, 791–800, https://doi.org/10.1002/acn3.343 (2016).
8. Ruitenberg, A. *et al*. Cerebral hypoperfusion and clinical onset of dementia: the Rotterdam Study. *Annals of neurology* **57**, 789–794, https://doi.org/10.1002/ana.20493 (2005).
9. Shibata, M., Ohtani, R., Ihara, M. & Tomimoto, H. White matter lesions and glial activation in a novel mouse model of chronic cerebral hypoperfusion. *Stroke; a journal of cerebral circulation* **35**, 2598–2603, https://doi.org/10.1161/01.str.0000143725.19053.60 (2004).
10. Holland, P. R. *et al*. MRI is a sensitive marker of subtle white matter pathology in hypoperfused mice. *Neurobiol Aging* **32**, 2325.e2321–2326, https://doi.org/10.1016/j.neurobiolaging.2010.11.009 (2011).
11. Coltman, R. *et al*. Selective white matter pathology induces a specific impairment in spatial working memory. *Neurobiol Aging* **32**, 2324.e2327–2312, https://doi.org/10.1016/j.neurobiolaging.2010.09.005 (2011).
12. Reimer, M. M. *et al*. Rapid disruption of axon-glial integrity in response to mild cerebral hypoperfusion. *The Journal of neuroscience: the official journal of the Society for Neuroscience* **31**, 18185–18194, https://doi.org/10.1523/jneurosci.4936-11.2011 (2011).
13. Shibata, M. *et al*. Selective impairment of working memory in a mouse model of chronic cerebral hypoperfusion. *Stroke; a journal of cerebral circulation* **38**, 2826–2832, https://doi.org/10.1161/strokeaha.107.490151 (2007).
14. Holland, P. R. *et al*. Gliovascular disruption and cognitive deficits in a mouse model with features of small vessel disease. *Journal of cerebral blood flow and metabolism: official journal of the International Society of Cerebral Blood Flow and Metabolism* **35**, 1005–1014, https://doi.org/10.1038/jcbfm.2015.12 (2015).
15. McQueen, J. *et al*. Restoration of oligodendrocyte pools in a mouse model of chronic cerebral hypoperfusion. *PloS one* **9**, e87227, https://doi.org/10.1371/journal.pone.0087227 (2014).
16. Hase, Y. *et al*. Effects of environmental enrichment on white matter glial responses in a mouse model of chronic cerebral hypoperfusion. *Journal of neuroinflammation* **14**, 81, https://doi.org/10.1186/s12974-017-0850-5 (2017).
17. Manso, Y. *et al*. Minocycline reduces microgliosis and improves subcortical white matter function in a model of cerebral vascular disease. *Glia* https://doi.org/10.1002/glia.23190 (2017).
18. Fowler, J. H. *et al*. Dimethyl fumarate improves white matter function following severe hypoperfusion: Involvement of microglia/macrophages and inflammatory mediators. *Journal of cerebral blood flow and metabolism: official journal of the International Society of Cerebral Blood Flow and Metabolism*, 271678x17713105, https://doi.org/10.1177/0271678x17713105 (2017).
19. Kim, H. A. *et al*. Vascular cognitive impairment and Alzheimer's disease: role of cerebral hypoperfusion and oxidative stress. *Naunyn-Schmiedeberg's archives of pharmacology* **385**, 953–959, https://doi.org/10.1007/s00210-012-0790-7 (2012).
20. Daulatzai, M. A. Cerebral hypoperfusion and glucose hypometabolism: Key pathophysiological modulators promote neurodegeneration, cognitive impairment, and Alzheimer's disease. *Journal of neuroscience research* https://doi.org/10.1002/jnr.23777 (2016).
21. Kasparova, S. *et al*. Study of the oxidative stress in a rat model of chronic brain hypoperfusion. *Neurochemistry international* **46**, 601–611, https://doi.org/10.1016/j.neuint.2005.02.006 (2005).

22. Washida, K. *et al*. Nonhypotensive dose of telmisartan attenuates cognitive impairment partially due to peroxisome proliferator-activated receptor-gamma activation in mice with chronic cerebral hypoperfusion. *Stroke; a journal of cerebral circulation* **41**, 1798–1806, https://doi.org/10.1161/strokeaha.110.583948 (2010).
23. Dong, Y. F. *et al*. Attenuation of brain damage and cognitive impairment by direct renin inhibition in mice with chronic cerebral hypoperfusion. *Hypertension* **58**, 635–642, https://doi.org/10.1161/hypertensionaha.111.173534 (2011).
24. Ji, H. J. *et al*. Osthole improves chronic cerebral hypoperfusion induced cognitive deficits and neuronal damage in hippocampus. *European journal of pharmacology* **636**, 96–101, https://doi.org/10.1016/j.ejphar.2010.03.038 (2010).
25. Sayan-Ozacmak, H., Ozacmak, V. H., Barut, F. & Jakubowska-Dogru, E. Rosiglitazone treatment reduces hippocampal neuronal damage possibly through alleviating oxidative stress in chronic cerebral hypoperfusion. *Neurochemistry international* **61**, 287–290, https://doi.org/10.1016/j.neuint.2012.05.011 (2012).
26. Du, J. *et al*. Mitochondrial bioenergetic deficits in the hippocampi of rats with chronic ischemia-induced vascular dementia. *Neuroscience* **231**, 345–352, https://doi.org/10.1016/j.neuroscience.2012.11.062 (2013).
27. Hubbs, A. F. *et al*. Vacuolar leukoencephalopathy with widespread astrogliosis in mice lacking transcription factor Nrf2. *The American journal of pathology* **170**, 2068–2076, https://doi.org/10.2353/ajpath.2007.060898 (2007).
28. Zhang, L., Johnson, D. & Johnson, J. A. Deletion of Nrf2 impairs functional recovery, reduces clearance of myelin debris and decreases axonal remyelination after peripheral nerve injury. *Neurobiology of disease* **54**, 329–338, https://doi.org/10.1016/j.nbd.2013.01.003 (2013).
29. Johnson, D. A., Amirahmadi, S., Ward, C., Fabry, Z. & Johnson, J. A. The absence of the pro-antioxidant transcription factor Nrf2 exacerbates experimental autoimmune encephalomyelitis. *Toxicol Sci* **114**, 237–246, https://doi.org/10.1093/toxsci/kfp274 (2010).
30. Linker, R. A. *et al*. Fumaric acid esters exert neuroprotective effects in neuroinflammation via activation of the Nrf2 antioxidant pathway. *Brain: a journal of neurology* **134**, 678–692, https://doi.org/10.1093/brain/awq386 (2011).
31. Suneetha, A. & Raja Rajeswari, K. Role of dimethyl fumarate in oxidative stress of multiple sclerosis: A review. *Journal of chromatography. B, Analytical technologies in the biomedical and life sciences* **1019**, 15–20, https://doi.org/10.1016/j.jchromb.2016.02.010 (2016).
32. Shih, A. Y. *et al*. Coordinate regulation of glutathione biosynthesis and release by Nrf2-expressing glia potently protects neurons from oxidative stress. *The Journal of neuroscience: the official journal of the Society for Neuroscience* **23**, 3394–3406 (2003).
33. Bell, K. F. *et al*. Neuronal development is promoted by weakened intrinsic antioxidant defences due to epigenetic repression of Nrf2. *Nat Commun* **6**, 7066, https://doi.org/10.1038/ncomms8066 (2015).
34. Lundgaard, I., Osorio, M. J., Kress, B. T., Sanggaard, S. & Nedergaard, M. White matter astrocytes in health and disease. *Neuroscience* **276**, 161–173, https://doi.org/10.1016/j.neuroscience.2013.10.050 (2014).
35. Vargas, M. R., Johnson, D. A., Sirkis, D. W., Messing, A. & Johnson, J. A. Nrf2 activation in astrocytes protects against neurodegeneration in mouse models of familial amyotrophic lateral sclerosis. *The Journal of neuroscience: the official journal of the Society for Neuroscience* **28**, 13574–13581, https://doi.org/10.1523/jneurosci.4099-08.2008 (2008).
36. Calkins, M. J., Vargas, M. R., Johnson, D. A. & Johnson, J. A. Astrocyte-specific overexpression of Nrf2 protects striatal neurons from mitochondrial complex II inhibition. *Toxicol Sci* **115**, 557–568, https://doi.org/10.1093/toxsci/kfq072 (2010).
37. Gan, L., Vargas, M. R., Johnson, D. A. & Johnson, J. A. Astrocyte-specific overexpression of Nrf2 delays motor pathology and synuclein aggregation throughout the CNS in the alpha-synuclein mutant (A53T) mouse model. *The Journal of neuroscience: the official journal of the Society for Neuroscience* **32**, 17775–17787, https://doi.org/10.1523/jneurosci.3049-12.2012 (2012).
38. Chen, P. C. *et al*. Nrf2-mediated neuroprotection in the MPTP mouse model of Parkinson's disease: Critical role for the astrocyte. *Proceedings of the National Academy of Sciences of the United States of America* **106**, 2933–2938, https://doi.org/10.1073/pnas.0813361106 (2009).
39. Shih, A. Y., Li, P. & Murphy, T. H. A small-molecule-inducible Nrf2-mediated antioxidant response provides effective prophylaxis against cerebral ischemia *in vivo*. *The Journal of neuroscience: the official journal of the Society for Neuroscience* **25**, 10321–10335, https://doi.org/10.1523/jneurosci.4014-05.2005 (2005).
40. Bell, K. F., Fowler, J. H., Al-Mubarak, B., Horsburgh, K. & Hardingham, G. E. Activation of Nrf2-regulated glutathione pathway genes by ischemic preconditioning. *Oxid Med Cell Longev* **2011**, 689524, https://doi.org/10.1155/2011/689524 (2011).
41. Jin, W. *et al*. Lipoxin A4 methyl ester ameliorates cognitive deficits induced by chronic cerebral hypoperfusion through activating ERK/Nrf2 signaling pathway in rats. *Pharmacol Biochem Behav* **124**, 145–152, https://doi.org/10.1016/j.pbb.2014.05.023 (2014).
42. Liu, H. *et al*. Post-occlusion administration of sodium butyrate attenuates cognitive impairment in a rat model of chronic cerebral hypoperfusion. *Pharmacol Biochem Behav* **135**, 53–59, https://doi.org/10.1016/j.pbb.2015.05.012 (2015).
43. Janeway, C. J. Jr., Travers, P. Walport. M. & Shlomchik, M. J. *Immunobiology: The Immune System in Health and Disease. 5th edition*. 5th edn, (Garland Science, 2001).
44. Nishio, K. *et al*. A mouse model characterizing features of vascular dementia with hippocampal atrophy. *Stroke; a journal of cerebral circulation* **41**, 1278–1284, https://doi.org/10.1161/strokeaha.110.581686 (2010).
45. Maki, T. *et al*. Angiogenic and vasoprotective effects of adrenomedullin on prevention of cognitive decline after chronic cerebral hypoperfusion in mice. *Stroke; a journal of cerebral circulation* **42**, 1122–1128, https://doi.org/10.1161/strokeaha.110.603399 (2011).
46. Valcarcel-Ares, M. N. *et al*. Disruption of Nrf2 signaling impairs angiogenic capacity of endothelial cells: implications for microvascular aging. *The journals of gerontology. Series A, Biological sciences and medical sciences* **67**, 821–829, https://doi.org/10.1093/gerona/glr229 (2012).
47. Gremmels, H., de Jong, O. G., Hazenbrink, D. H., Fledderus, J. O. & Verhaar, M. C. The Transcription Factor Nrf2 Protects Angiogenic Capacity of Endothelial Colony-Forming Cells in High-Oxygen Radical Stress Conditions. *Stem cells international* **2017**, 4680612, https://doi.org/10.1155/2017/4680612 (2017).
48. Zhao, R., Feng, J. & He, G. Hypoxia increases Nrf2-induced HO-1 expression via the PI3K/Akt pathway. *Frontiers in bioscience (Landmark edition)* **21**, 385–396 (2016).
49. Li, L. *et al*. Interplay between VEGF and Nrf2 regulates angiogenesis due to intracranial venous hypertension. *Scientific reports* **6**, 37338, https://doi.org/10.1038/srep37338 (2016).
50. Du, S. Q. *et al*. Molecular Mechanisms of Vascular Dementia: What Can Be Learned from Animal Models of Chronic Cerebral Hypoperfusion? *Molecular neurobiology* https://doi.org/10.1007/s12035-016-9915-1 (2016).
51. Thannickal, V. J. & Fanburg, B. L. Reactive oxygen species in cell signaling. *American journal of physiology. Lung cellular and molecular physiology* **279**, L1005–1028 (2000).
52. Massaad, C. A. & Klann, E. Reactive oxygen species in the regulation of synaptic plasticity and memory. *Antioxidants & redox signaling* **14**, 2013–2054, https://doi.org/10.1089/ars.2010.3208 (2011).
53. De Pasquale, R., Beckhauser, T. F., Hernandes, M. S. & Giorgetti Britto, L. R. LTP and LTD in the visual cortex require the activation of NOX2. *The Journal of neuroscience: the official journal of the Society for Neuroscience* **34**, 12778–12787, https://doi.org/10.1523/jneurosci.1414-14.2014 (2014).
54. Ihara, M. & Tomimoto, H. Lessons from a mouse model characterizing features of vascular cognitive impairment with white matter changes. *Journal of aging research* **2011**, 978761, https://doi.org/10.4061/2011/978761 (2011).
55. Hase, Y. *et al*. The effects of environmental enrichment on white matter pathology in a mouse model of chronic cerebral hypoperfusion. *Journal of cerebral blood flow and metabolism: official journal of the International Society of Cerebral Blood Flow and Metabolism*, 271678x17694904 https://doi.org/10.1177/0271678x17694904 (2017).

56. Yang, G. *et al*. C57BL/6 strain is most susceptible to cerebral ischemia following bilateral common carotid occlusion among seven mouse strains: selective neuronal death in the murine transient forebrain ischemia. *Brain Res* **752**, 209–218 (1997).
57. Brown, R. E. & Wong, A. A. The influence of visual ability on learning and memory performance in 13 strains of mice. *Learning & memory (Cold Spring Harbor, N.Y.)* **14**, 134–144, https://doi.org/10.1101/lm.473907 (2007).
58. Saggu, R. *et al*. Astroglial NF-kB contributes to white matter damage and cognitive impairment in a mouse model of vascular dementia. *Acta neuropathologica communications* **4**, 76, https://doi.org/10.1186/s40478-016-0350-3 (2016).
59. Vicente, E. *et al*. Astroglial and cognitive effects of chronic cerebral hypoperfusion in the rat. *Brain Res* **1251**, 204–212, https://doi.org/10.1016/j.brainres.2008.11.032 (2009).
60. Kanninen, K. *et al*. Intrahippocampal injection of a lentiviral vector expressing Nrf2 improves spatial learning in a mouse model of Alzheimer's disease. *Proceedings of the National Academy of Sciences of the United States of America* **106**, 16505–16510, https://doi.org/10.1073/pnas.0908397106 (2009).
61. Fragoulis, A. *et al*. Oral administration of methysticin improves cognitive deficits in a mouse model of Alzheimer's disease. *Redox biology* **12**, 843–853, https://doi.org/10.1016/j.redox.2017.04.024 (2017).
62. Cuadrado, A. NRF2 in neurodegenerative diseases. *Current Opinion in Toxicology* **1**, 46–53 (2016).
63. Yamazaki, H., Tanji, K., Wakabayashi, K., Matsuura, S. & Itoh, K. Role of the Keap1/Nrf2 pathway in neurodegenerative diseases. *Pathology international* **65**, 210–219, https://doi.org/10.1111/pin.12261 (2015).
64. Dringen, R. Metabolism and functions of glutathione in brain. *Prog Neurobiol* **62**, 649–671 (2000).
65. Miyamoto, N. *et al*. Oxidative stress interferes with white matter renewal after prolonged cerebral hypoperfusion in mice. *Stroke; a journal of cerebral circulation* **44**, 3516–3521, https://doi.org/10.1161/strokeaha.113.002813 (2013).
66. LaPash Daniels, C. M. *et al*. Beneficial Effects of Nrf2 Overexpression in a Mouse Model of Alexander Disease. *The Journal of neuroscience: the official journal of the Society for Neuroscience* **32**, 10507–10515, https://doi.org/10.1523/jneurosci.1494-12.2012 (2012).
67. Dowell, J. A. & Johnson, J. A. Mechanisms of Nrf2 protection in astrocytes as identified by quantitative proteomics and siRNA screening. *PloS one* **8**, e70163, https://doi.org/10.1371/journal.pone.0070163 (2013).
68. Bose, S. & Cho, J. Role of chemokine CCL2 and its receptor CCR2 in neurodegenerative diseases. *Archives of pharmacal research* **36**, 1039–1050, https://doi.org/10.1007/s12272-013-0161-z (2013).
69. Maurer, M. & von Stebut, E. Macrophage inflammatory protein-1. *The international journal of biochemistry & cell biology* **36**, 1882–1886, https://doi.org/10.1016/j.biocel.2003.10.019 (2004).
70. Bennett, S., Grant, M. M. & Aldred, S. Oxidative stress in vascular dementia and Alzheimer's disease: a common pathology. *Journal of Alzheimer's disease: JAD* **17**, 245–257, https://doi.org/10.3233/jad-2009-1041 (2009).
71. Eikelenboom, P. & Stam, F. C. Immunoglobulins and complement factors in senile plaques. An immunoperoxidase study. *Acta neuropathologica* **57**, 239–242 (1982).
72. Azizi, G., Khannazer, N. & Mirshafiey, A. The Potential Role of Chemokines in Alzheimer's Disease Pathogenesis. *American journal of Alzheimer's disease and other dementias* **29**, 415–425, https://doi.org/10.1177/1533317513518651 (2014).
73. Akiyama, H. *et al*. Inflammation and Alzheimer's disease. *Neurobiol Aging* **21**, 383–421 (2000).
74. Liddelow, S. A. *et al*. Neurotoxic reactive astrocytes are induced by activated microglia. *Nature* https://doi.org/10.1038/nature21029 (2017).
75. Stevens, B. *et al*. The classical complement cascade mediates CNS synapse elimination. *Cell* **131**, 1164–1178, https://doi.org/10.1016/j.cell.2007.10.036 (2007).
76. Alawieh, A., Langley, E. F., Weber, S., Adkins, D. & Tomlinson, S. Identifying the role of complement in triggering neuroinflammation after traumatic brain injury. *The Journal of neuroscience: the official journal of the Society for Neuroscience* https://doi.org/10.1523/jneurosci.2197-17.2018 (2018).
77. Shi, Q. *et al*. Complement C3 deficiency protects against neurodegeneration in aged plaque-rich APP/PS1 mice. *Science translational medicine* **9** https://doi.org/10.1126/scitranslmed.aaf6295 (2017).
78. Yang, J. *et al*. Complement component 3 inhibition by an antioxidant is neuroprotective after cerebral ischemia and reperfusion in mice. *J Neurochem* **124**, 523–535, https://doi.org/10.1111/jnc.12111 (2013).
79. Ducruet, A. F. *et al*. Complement inhibition promotes endogenous neurogenesis and sustained anti-inflammatory neuroprotection following reperfused stroke. *PloS one* **7**, e38664, https://doi.org/10.1371/journal.pone.0038664 (2012).
80. Kobayashi, E. H. *et al*. Nrf2 suppresses macrophage inflammatory response by blocking proinflammatory cytokine transcription. *Nat Commun* **7**, 11624, https://doi.org/10.1038/ncomms11624 (2016).
81. Paxinos, G. & Franklin, K. B. J. *The Mouse Brain in Stereotaxic Coordinates*. 2nd edn, (Academic Press, 2001).

Acknowledgements

We gratefully acknowledge the grant support from the Alzheimer's Society (152 (PG-157); 290 (AS-PG-15b-018); 228 (AS-DTC-2014-017)), Alzheimer's Research UK (ARUK) (ART-PG2010-3; ARUK-PG2013-22; ARUK-PG2016B-6), and The University of Edinburgh Centre for Cognitive Ageing and Cognitive Epidemiology, part of the cross council Lifelong Health and Wellbeing Initiative (G0700704/84698), Biogen and The Wellcome Trust. E.S. is supported by an Alzheimer's Society Doctoral Training PhD studentship and the RS McDonald Charitable Trust, J.H.F was funded by an Alzheimer's Society Fellowship (Grant 297) and is currently supported by an ARUK Senior Fellowship (ARUK-SRF-2013-4 and ARUK-SRF2018B-005).

Author Contributions

E.S. and M.M. performed laser speckle flowmetry and behavioural testing. E.S. performed immunohistochemical, biochemical and qPCR experiments and analysis of all data, prepared figures and wrote the manuscript. J.A.J. provided the transgenic mice and provided feedback on the manuscript. G.E.H. provided feedback on the data and manuscript. J.H.F. provided input to the qPCR studies, provided feedback on the data and helped with writing the manuscript. K.H. planned, designed and supervised the studies and data analysis, performed the surgeries and wrote the manuscript.

Additional Information

Supplementary information accompanies this paper at https://doi.org/10.1038/s41598-018-30675-4.

Competing Interests: The authors declare no competing interests.

Publisher's note: Springer Nature remains neutral with regard to jurisdictional claims in published maps and institutional affiliations.